REPUBLIC OF TURKEY
BINGOL UNIVERSITY
INSTITUTE OF SCIENCE

SYNTHESIS of CHROMOPHORE GROUPS LABELED NOVEL AMINO ACID CONJUGATES and THEIR DIELECTRICAL PROPERTIES

PhD THESIS

ERAY ÇALIŞKAN

CHEMISTRY

SUPERVISOR
Prof. Dr. Ahmet ÇETİN

Co-ADVISOR
Prof. Dr. Ahmet Orhan GÖRGÜLÜ

BINGOL-2020

REPUBLIC OF TURKEY
BİNGÖL UNIVERSITY
INSTITUTE OF SCIENCE

SYNTHESIS of CHROMOPHORE GROUPS LABELED NOVEL AMINO ACID CONJUGATES and THEIR DIELECTRICAL PROPERTIES

This dissertation, created by Eray ÇALIŞKAN under supervision of Prof. Dr. Ahmet ÇETİN, was accepted as a PhD thesis in department of Chemistry by the following committee on 23/07/2020 with the vote unity.

Head of examining Committee	: Prof. Dr. Esin KAYA	*Signature* :
Member	: Prof. Dr. Ahmet ÇETİN	*Signature* :
Member	: Assoc. Prof. Dr. Sinan BAYINDIR	*Signature* :
Member	: Assoc. Prof. Dr. İ. Halil GEÇİBESLER	*Signature* :
Member	: Assoc. Prof. Dr. Gamze BARIM	*Signature* :

This result has been approved on ..... / …… /.....… with the decision of ……./…… by Board of Directors of the Science Institute.

Assoc. Prof. Dr. Zafer ŞİAR
Director of the institute

FOREWORD

I have reached the end of the thesis adventure that I started in 2015. The main subject of the thesis is the synthesis of new organic compounds and the study of electrical properties, contributing to the gap in the literature in this field.

I would like to extend my sincere thanks to my thesis supervisor Prof. Dr. Ahmet ÇETİN and co-advisor Prof. Dr. Ahmet Orhan GÖRGÜLÜ who guided me academically during the thesis research and contributed to my development with helpful discussions. I would also like to thank BUBAP, which supports my thesis research financially.

I express my gratitude to Assoc. Prof. Kenan KORAN and Dr. Fatih BİRYAN for their scientific support and useful discussions during the thesis study. I would like to extend my sincere thanks to my colleagues, Dr. Adnan AYNA, Dr. Kamuran DİLSİZ and Dr. Ekrem DARENDELİOĞLU, who have never spared their support in this difficult and long process. I would also like to thank all faculty members at the Chemistry Department at Bingol University.

Finally, I would like to extend my heartfelt thanks to my family, who always supported me in all circumstances, and especially to my dear wife, who added more happiness and positive energy to my life.

Eray ÇALIŞKAN

Bingol 2020

CONTENTS

ABBREVATIONS

AA	: Amino Acid
AC	: Alternative Current
Ala	: Alanine
BtH	: 1-*H*-benzotriazole
C	: Capacitance
CA	: Cinnamic Acid
CC	: Cyanuric chloride
CDI	: Carbonyl diimidazole
CDMT	: 2-chloro-4,6-dimethoxy-1,3,5-triazine
D	: loss factor
DC	: Direct Current
DCC	: Dcyclohexycarbodiimide
DIC	: 1,3-Diisopropylcarbodiimide
FT-IR	: Fourier Transform Infrared Spectroscopy
Gly	: Glycine
HCl	: Hydrochloric acid
HOAt	: 1-hydroxy -7-azabenzotiazole
HOBt	: 1-hydroxy benzotriazole
HOSu	: N-hydroxysuccinimide
Leu	: Leucine
MeCN	: Acetonitrile
Meth	: Methionine
NMR	: Nuclear Magnetic Resonance
R	: Resistance
V	: Voltage

TEA : Triethylamine

NNM : N-methyl morpholine

DMSO-d_6 : Deuterated Dimethylsulfoxide

$CDCl_3$-d : Deuterated Chloroform

LIST OF FIGURES

LIST OF TABLES

SYNTHESIS of CHROMOPHORE GROUPS LABELED NOVEL AMINO ACID CONJUGATES and THEIR DIELECTRICAL PROPERTIES

ABSTRACT

Amino acid conjugates are obtained by the reaction of amino acids and organic compounds with various biological and physical properties. Although the studies of these conjugates on biological activity well documented in the literature, their electrical properties have not been studied in detail. Therefore, the aim of the work described in this thesis was the synthesis of novel cinnamic acid substituted amino acid conjugate and investigation of their physical activities in terms of structure-activity relationship. In this study, 28 amino acid conjugates were synthesized using benzotriazole and triazine methods and their structures were characterized by ^{1}H, ^{13}C APT, COSY, HETCOR NMR, elemental analysis and FT-IR methods. The dielectric properties of these conjugates were studied examining their dielectric constant, dielectric loss and conductivity. The structure-activity relationship was evaluated considering the factors such as π bond conjugation, substitution, amino acid difference and electron releasing and withdrawing group effects. In parallel with the increase in the number of aromatic rings the conductivity was increased. Among para substitute conjugates 4-chloro-CA-Ala-OMe had the highest conductivity and dielectric constant (ε') 8.34. The number of amino acid in the conjugate was also observed as an important parameter level of conductivity.

Keywords: Amino acid conjugates, cinnamic acid, dielectric constant, conductivity, organic synthesis.

KROMOFOR GRUPLARI BAĞLI YENİ AMİNO ASİT KONJUGATLARININ SENTEZİ ve DİELEKTRİKSEL ÖZELLİKLERİNİN İNCELENMESİ

ÖZET

Amino asit konjugatları, amino asitlerle çeşitli biyolojik ve fiziksel özellikler gösterebilen organik bileşiklerin reaksiyonu ile elde edilen bileşiklerdir. Bu konjugatların biyolojik aktivite ile ilgili çalışmalarına literatürde daha sık rastlanırken elektriksel özelliklerine dair detaylı çalışmaya rastlanılmamıştır. Bu çalışmanın amacı sinamik asit türevlerinin bağlı olduğu yeni amino asit konjugatlarının sentezlenmesi ve yapı-aktivite ilişkisi yönünden elektriksel özelliklerinin incelenmesi üzerinedir. Bu çalışmada; benzotriazol ve triazin yöntemleri kullanılarak 28 amino asit konjugatı nihai olarak sentezlenmiş ve yapıları ^{1}H, ^{13}C APT, COSY, HETCOR NMR, elemental analiz ve FT-IR yöntemleri ile aydınlatılmıştır. Bu nihai konjügatların dielektrik sabiti, dielektrik kaybı ve iletkenlik gibi elektriksel özellikleri incelenmiştir. Sonuçlar, amino asit yapısı, π bağ konjugasyonu ve elektron salıcı-verici grup etkisi gibi faktörler dikkate alınarak yapı-aktivite ilişkisi açısından incelenmiştir. Hedef moleküllerdki aromatik halkaların sayısındaki artışa paralel olarak, ilekenliğin ve dielektrik sabitinin de arttığı tespit edilmiştir. 4-kloro-CA-Ala-OMe bileşiği para sübstitüe konjugatlar içerisinde en yüksek iletkenlik ve dielektrik sabit değerine (ε') 8.34 sahip olduğu görülmüştür. Amino asit sayısındaki artış iletkenlik seviyesinin artışında önemli bir parametre olarak gözlenmiştir.

Anahtar Kelimeler: Amino asid konjugatları, sinamik asit, dieletrik, iletkenlik, organik sentez.

1. INTRODUCTION

Amino acid conjugates are general name given to biologically or physically active compounds, usually formed by reaction between an amino acid and one or more nucleophilic/electrophilic group of active compounds some of which include vitamins, hormones, steroids, fatty acids and several heterocyclic compounds (Panda et al. 2013; Sahu et al. 2013) (Figure 1.1). The rationale behind preparation of these conjugates are to enhance the activity of these compounds for pharmacological purposes. The increasing use of amino acid / peptide conjugates in drug designs in recent years has also made synthesis of these compounds important (Ibrahim et al. 2014; Jones et al. 2014; Panda et al. 2014; Tiwari et al. 2014).

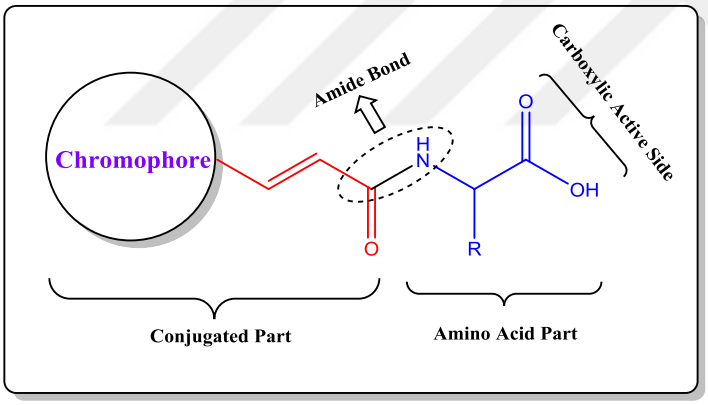

Figure 1.1. General structure for amino acid conjugates

Cinnamic acid and its common derivatives (Figure 1.2) are class of organic compounds that are mostly isolated from plants and attract attention due to the double bond present in their structure that facilitates conjugation. Cinnamic acid and its natural and synthetic derivatives have a wide range of pharmacological activities such as anti-cancer (De 2011), anti-tuberculosis (Guzman et al. 2014), anti-inflammatory (Debnath et al. 2003), anti-parasitic (Zhang et al. 2015) and anti-microbial effect (Fu et al. 2010).

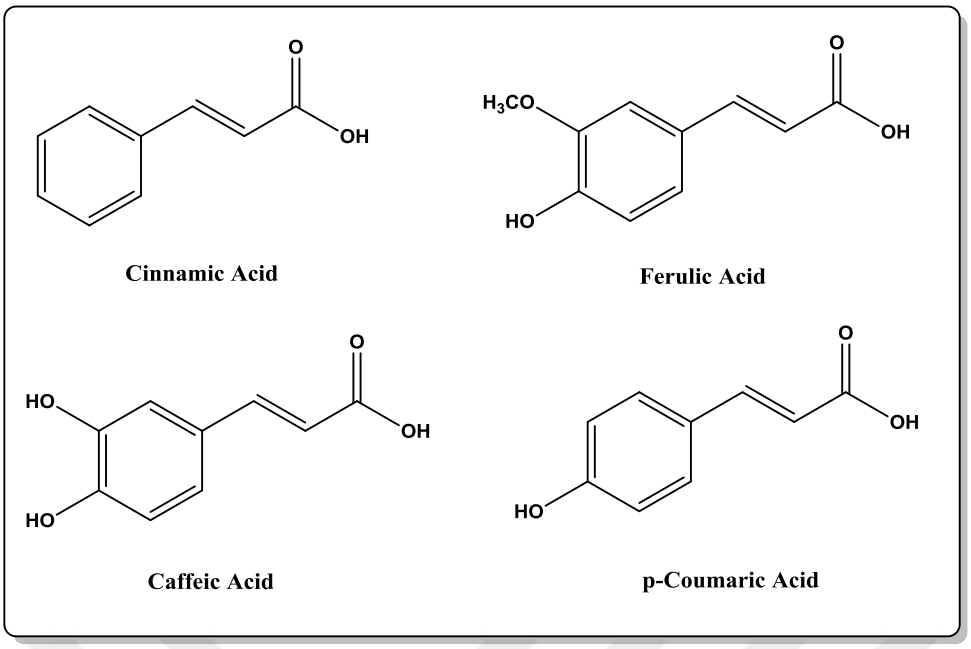

Figure 1.2. Structure of common cinnamic acid derivatives

Cinnamic acid derivatives are usually synthesized by Perkin reaction, Claisen-Schmidt condensation, Knoevenagel condensation (Knoevenagel 1898) and other methods (Fonseca et al. 2019). The double bond in its structure facilitates cis-trans isomerization under UV light.

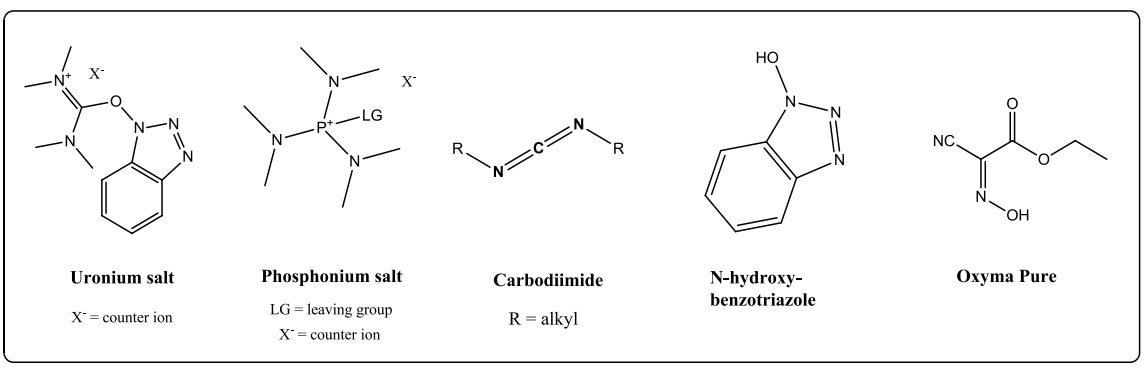

Figure 1.3. General structure representations of major coupling reagents

The main step in the synthesis of peptide / amino acid conjugates is the formation of the amide bond that is obtained after activation of the carboxylic acid by coupling reagents as shown in Figure 4. The most basic of these coupling reagents are carbodiimides, uranium salts, phosphonium salts (Figure 1.3). The use of these reagents exhibits several advantages and disadvantages in the reaction medium. For example, in the synthesis of amide, in which

coupling reagent is used, carboxylic acid is activated to react with amine, but in the absence of coupling reagent, the thermodynamically undesirable carboxylate-ammonium salt is formed instead of amide. Under standard conditions, racemization may occur with some side reactions in the formation of the peptide bond. Coupling additives come into play here, preventing both by-product formation and racemization (Belleau and Malek 1968; El-Faham and Albericio 2011; Al-Warhi et al. 2012). The most commonly used coupling additives are listed below.

- N-hydroxysuccinimide (HOSu)
- N-hydroxy-5-norbornene-2,3-dicarboximide (HONB)
- 1-hydroxy benzotriazole (HOBt)
- 6-chloro-1-hydroxy benzotriazole (6-Cl-HOBt)
- 1-hydroxy-7-azabenzotiazole (HOAt)
- 3-hydroxy-4-oxo-3,4-dihydro-1,2,3-benzotriazine (HODhbt)

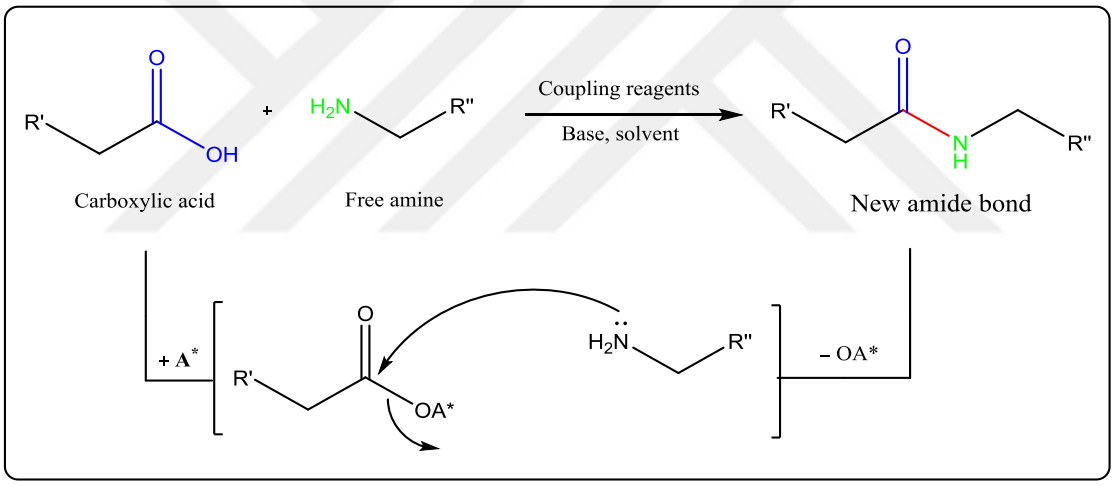

Figure 1.4. Conventional way to obtain an amide bond

König and Geiger suggested use of 1-hydroxybenzotriazole (HOBt) as an additive to prevent racemization arisen from using dicyclohexylcarbodiimide (DCC) as a coupling reagent. Although these substances (HOBt, HAt) and their derivatives are widely used as peptide coupling reagents, their explosive properties were reported during their exposure to mechanical stimuli or heat in closed containers (König and Geiger 1970).

Amino acid conjugates with methyl ester group were obtained in high purity and yield using a triazine derivative coupling reagent, 2-chloro-4,6-dimethoxy-1,3,5-triazine (CDMT). CDMT is a preferred compound in the formation of amide, ester and acid

anhydride owing to its high solubility in various organic solvents, its low cost, reactivity and its long-term stability (Figure 1.5).

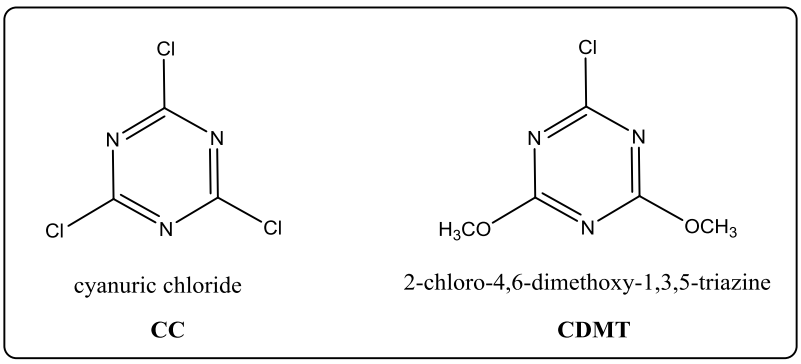

Figure 1.5. General chemical represantation of triazine based coupling reagents

The most important step in this method is the first step between the carboxylic acid and CDMT, resulting in the formation of the intermediate 2-acyloxy-4,6-dimethoxy-1,3,5-triazine. The intermediate product formed is a very effective acylating agent so that alcohols, amines, carboxylic acids, esters, amides and anhydrides can be obtained in high yield (Venkataraman and Wagle 1979, Kamiński et al. 1998; Kunishima et al. 1999). These compounds provide the suitable medium for the synthesis of substances compatible with the basic environment compared to the use of acyl chlorides in the acidic medium (Herrera et al. 2014; Kitamura et al. 2014; Braml et al. 2015). In this study, CDMT was preferred as a coupling reagent because HCl formed in traditional halogenation reactions does not occur and the suitable basic environment for acid sensitive groups is provided (Figure 1.6). In addition, the active ester formed in the CDMT method reacts with a wide variety of compounds facilitating likelihood formation of a wide range of products.

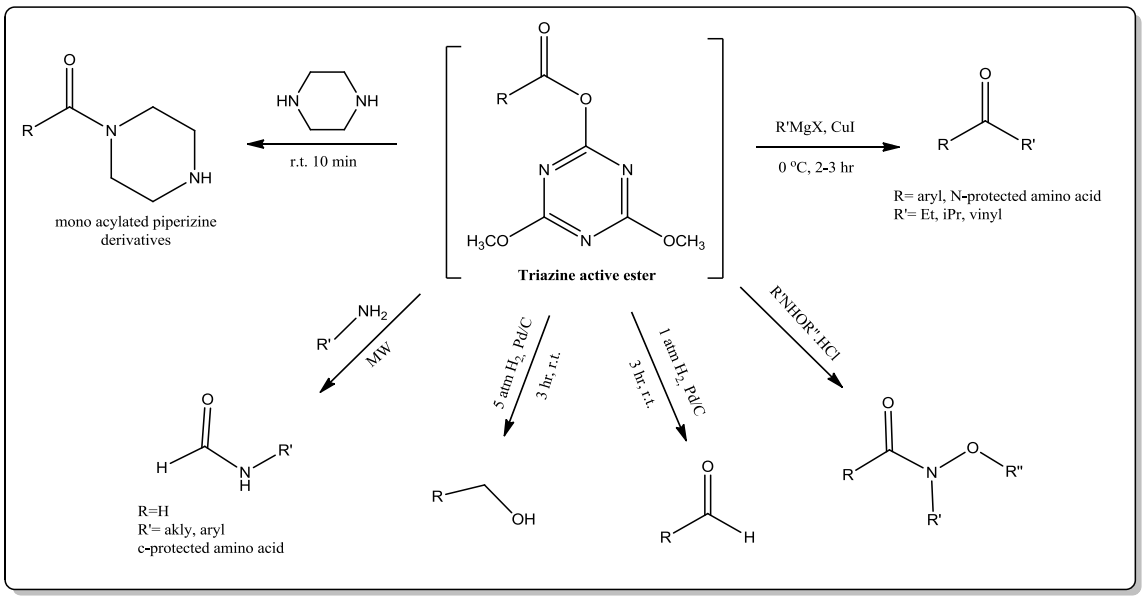

Figure 1.6. The class of compounds sythesized via CDMT method

The benzotriazole compound is a heterocyclic aromatic compound with a benzene and triazole ring (Figure 1.7). Unlike the triazole ring, the benzene ring in benzotriazole provides extra conjugation to the structure with π-π interactions (Katritzky et al. 1991; Katritzky and Rogovoy 2003). It can easily dissolve in HCl and Na_2CO_3 as it has a weak basic character thus facilitates its purification.

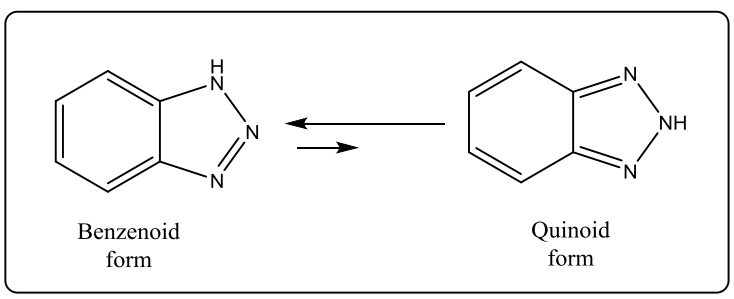

Figure 1.7. Two possible resonance structure of benzotriazole

Benzotriazole derivatives are used as corrosion inhibitors, supramolecular ligands, dyes, potential drug candidates, and fluorescent and radiochemical markers. Benzotriazole is preferred in organic synthesis due to its odorless, non-toxic, stable properties, long shelf life and solubility in various organic solvents (Katritzky et al. 2005; Katritzky et al. 2005). It is used in many organic reactions due to its following characteristics: better leaving group

than halogens, having both electron donor and electron releasing feature and stabilizing carbonations.

1.1. *N*-acylbenzotriazoles

N-acylbenzotriazole compounds are preferred due to their effectiveness in obtaining compounds of various biological properties. It is used as acylation agent in many synthesis methods. The following reactions can be give as examples;

- Amides from amines
- Esters obtained from aldehydes
- Diketone and ketosulfone from ketones and sulfones

N-acylbenzotriazoles can be obtained by the following 4 different methods (Figure 1.8);

- Carboxylic acids in the presence of methyl sulfonylbenzotriazole and TEA
- Reaction of carboxylic acids with benzotriazole and $SOCl_2$
- Reaction of N-Cl-benzotriazole with aldehydes
- Reaction of DCC and Carboxylic acids with benzotriazole

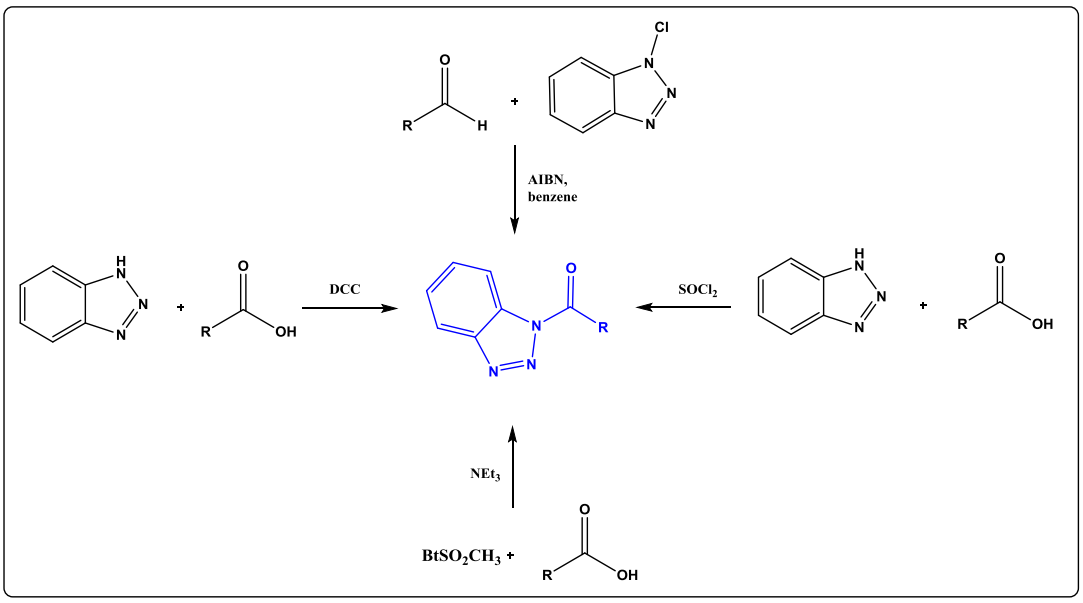

Figure 1.8. Methods for *N*-Acylbenzotriazole synthesis

The amino acid conjugates of some antibacterial drugs obtained using *N*-acylbenzotriazole showed more activity than the parent drug (Kale et al. 2010; Piccionello and Guarcello 2010; Sahu et al. 2013) (Figure 1.9).

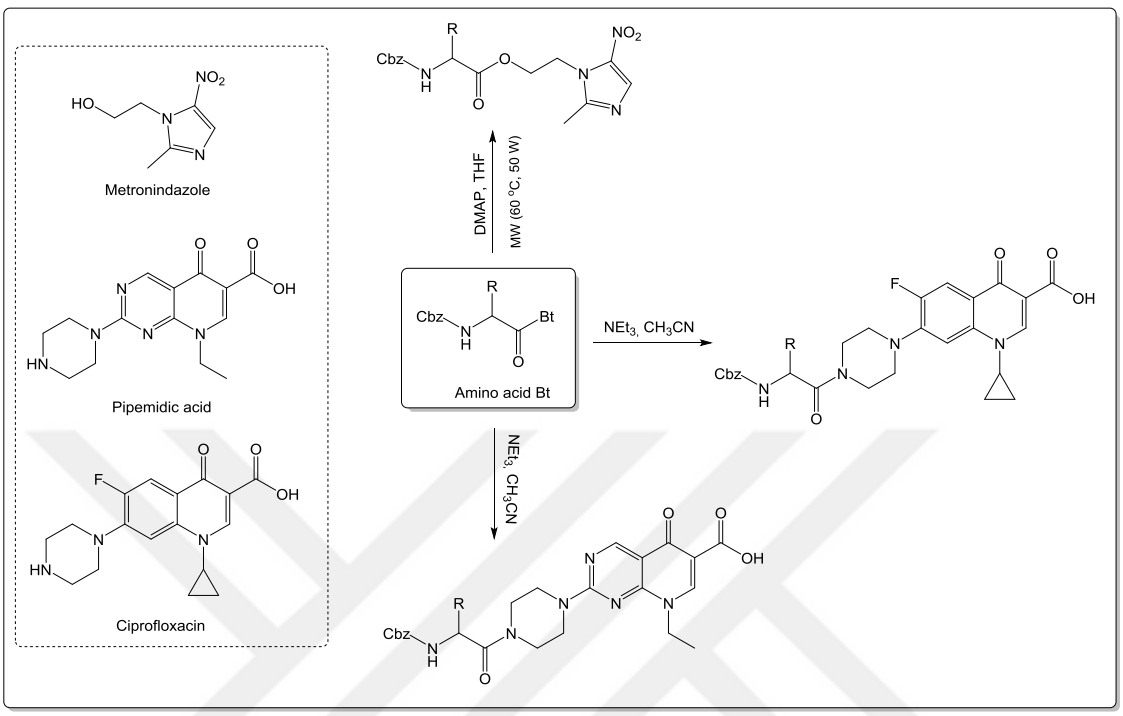

Figure 1.9. Examples of antibacterial drugs derived from *N*-acylbenzotriazole

Although the studies of the conjugates mentioned previously on biological activity well studied, their electrical properties have not been investigated in detail. Therefore, the aim of the work described in this thesis was synthesis of novel cinnamic acid substituted amino acid conjugate and investigation of their physical activities in terms of structure-activity relationship.

In this study, synthetic amino acid conjugates were synthesized by CDMT and *N*-acylbenzotriazole methods. The dielectric properties of these conjugates were studied examining their dielectric constant, dielectric loss and conductivity. The structure-activity relationship was evaluated considering the factors such as π bond conjugation, substitution, amino acid difference and electron releasing and withdrawing group effects.

1.2. Dielectric

When an external electric field is applied to the material, the molecules must rotate continuously to be able to orient with the electric field. Although these movements are possible at low frequencies, the molecules fall behind the frequency and cannot be directed as the frequency increases. The degree of orientation polarization of the material changes inversely with increasing frequency of the applied area. The situation is slightly different in electrical insulator for which the absence of free electrons in dielectric materials can be given as an example. The energy range is greater than 4ev and its specific resistance is above 104 (Ωm). They are mostly used as electrical insulators since they do not transmit electricity. However, they are affected by the applied electrical field. In the electric field effect, electrons and atoms are displaced, consequently electrical charge centers shift and electrical polarization occurs. The formed poles provide electrical charge accumulation on the material surface and are therefore used in capacitor production (Campos and Nascente 2010).

There is an electric charge accumulation on the face of the dielectric material with permanent polarization where the charge accumulation occurs automatically. When an electric field is applied to a material that does not have permanent polarization, external polarization effect and electrical charge accumulation occurs on the surface (specific resistance). In both cases, the electrical charge density on the surface is proportional to the electrical field intensity (Betova et al. 1999).

The measurement of the dielectric constant, which is one of the important properties of solids, is simpler than other analyzes because the impedance analyzer is used in this measurement and the calculation of the dielectric constant is made using C (capacitance) and D (loss factor). The dielectric constant depends on temperature and frequency (Bezgin et al. 2015).

The dielectric constant of the solid material (Figure 1.10) placed in the disc was calculated by the following equations;

$$\varepsilon = \varepsilon_0 . \varepsilon_r = \left({}^{t}/_{A}\right) . C \quad \left[\frac{F}{m}\right] \tag{1}$$

$$\varepsilon_r = \frac{t.C}{A.\varepsilon_0} = \frac{t.C}{\varepsilon_0} \quad (2)$$

In the above equation;

ε: Dielectric constant

ε_0: Dielectric constant of the cavity (8.854×10^{-12})

ε_r: Relative dielectric constant of the test device,

t: Thickness of the sample (m),

A: The area of the sample (m^2),

C: Capacitance of the sample (F),

d: Diameter of the sample (m).

Another concept used to express dielectric properties is the dielectric loss factor, also known as loss tangent.

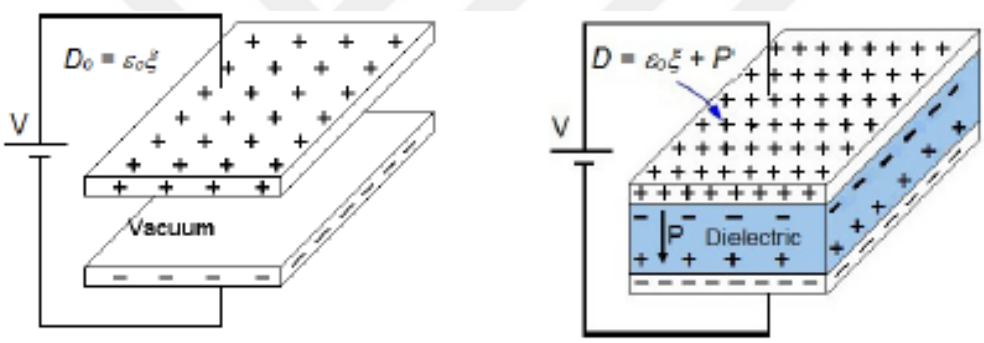

Figure 1.10. Test devices with electrode (image was reprinted from Biryan 2019)

Dielectric losses depend on the types of polarization. Dielectric losses due to surface charge polarization occur around 104 Hz, those resulting from dipole polarization occur around 108 Hz, losses due to atomic polarization occur around 1012 Hz, and dielectric losses due to electronic polarization occur around 1016 Hz. While dielectric losses increase with rising temperature (Jastrzebska et al. 1998; Singh et al. 2012), in materials with atomic and electronic polarization, the dielectric constant does not change much at low temperatures. The dielectric constant is high at high temperatures due to the high ion movement. In materials with atomic polarization, the effect of temperature and frequency is very important. The dielectric constant increases sharply at a certain temperature and increases faster with increasing temperature at low frequencies. Thus, the position of the

dielectric loss (tan δ) peaks will shift towards high temperatures, in which case the dielectric constant (ε) will decrease with increasing frequency (Park et al. 2007).

1.3. Direct Current (DC) and Alternative Current (AC) Conductivity

Conductivity, one of the electronic properties that a material can demonstrate, is especially important widely used electronic feature in technology. For example, silver has a conductivity of about 107 $ohms^{-1}m^{-1}$, while Teflon conductivity is less than 10-17 $ohms^{-1}m^{-1}$. Considering the other properties of the various materials, there is no property that shows such a significant difference. It is therefore interesting to examine electrical conductivity due to its widespread use in technology. In electrical conductivity, charge can be carried by different types or charge carriers. These different charge carriers have different masses, interact with their environment and respond differently to changes in external environments (Simpson and St.Clair 1997).

1.4. Direct Current (DC) Conductivity Measurement

The most common charge carriers in the field of physics and engineering are electrons, electron holes and ions. Direct current is a known technique for measuring electrical conductivity. Two different methods are used in this conductivity measurement, "Two probe" and "Four probe". In the "two probe" method, the two contact areas are contacted simultaneously, while in the "Four probe" method it is contacted from four different places (Figure 1.11). Although the difference between these two methods is not obvious, the 'two probe' method is more common in DC conductivity measurement. In this technique, an ammeter is used to measure the current in the circuit, a battery as a DC power source and a voltmeter to measure the potential difference.

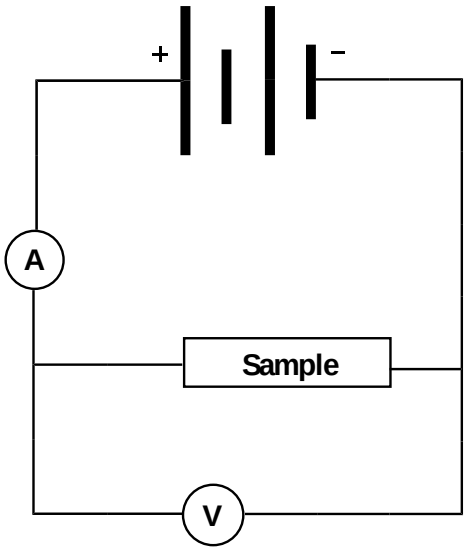

Figure 1.11. Schematic representation of two probe method

Ohm's law explains the relationship between potential difference current intensity and resistance. If the potential difference between the two ends of a conductor increases, the current intensity increases, if the potential difference decreases, the current intensity decreases. The potential difference is directly proportional to the current intensity. Since the resistance and current intensity are inversely proportional, when the resistance of a conductor increases, the current intensity shrinks because the movement of electrons becomes more difficult. When the contact areas are physically in contact with the sample, interaction between the surfaces is not flawless. Generally, thin non-conductive oxide layers are present on the surfaces and can be atomically rough even if cleaned macroscopically.

As a result, the current will start flowing from one contact surface to another when the two surfaces come into contact with each other or are connected to any electrical component by means of a wire, while facing significant resistance. This resistance is called Contact Resistance (Rc).

Applying an alternating current is a better option to measure conductivity in situations where different charge carriers are present and the flow direction of the current changes over time, and therefore the charge in the sample is forced to swing back and forth. This method, called AC conductivity measurement, can also be used for samples that transmit electrons and is a versatile technique compared to DC conductivity measurement. DC

conductivity is used as a sufficient technique as much as possible because the equipment used in this method is more expensive.

While a single data point is measured in DC measurement, in AC conductivity measurement, the properties of the signal are investigated according to different frequency ranges. Frequency varies (mHz to MHz) in AC conductivity measurement. In the AC measurement process, the sample is subjected to an amplitude AC voltage, which can be considered relatively small, the AC current corresponding to this current signal is recorded, and the change between the current and voltage is recorded as a function of time. The amplitude of the signal used in this process is very important. It must be small enough to cause the system to react linearly, but large enough to be recorded.

2. LITERATURE REVIEW

Amide bond is a very common functional group found in small or complex natural and synthetic compounds. It has a very important place in metabolism due to being involved in biological processes such as enzymatic catalysis, transport/storage, and immune protection. Since it is a pharmacologically important functional group, 25% of the known drugs have a carboxamide group (Amide bond) (Ghose et al. 1999). It owes this feature to its natural, stable structure and having both hydrogen accepting and hydrogen giving structure.

Under normal conditions, ester and amide bond formation occurs as a result of an acid's condensation reaction with alcohol or amine, respectively. While classical esterification is an equilibrium reaction, a stable salt is formed by the interaction of amine and acid in amide bond formation (Ulijn et al. 2002).

For both medicinal and synthetic chemists, the priority is to apply the most appropriate method to fight against difficult and undesirable conditions such as steric effect, poor reactivity and racemization. In general, the goal is to increase yield, reduce the amount of by-products, increase selectivity, facilitate purification and use more economical reagents. Owing to the rapid developments in coupling methods in the last two decades, it has enabled high synthesis of a wide variety of compounds in the pharmacological industry.

2.1. Amide Bond Formation Methods and Strategies

The carboxy group is activated by converting it to structures such as acyl halides, acyl azides, acylimidazoles, anhydrides, esters, acylbenzotriazole. There are many ways to combine reactive carboxy derivatives with amines (Figure 2.1);

- An acylation intermediate is obtained and isolated and then reacted with the amine.
- Interaction with the amine without isolating a reactive acylating agent from the acid

• With the addition of coupling reagent in the presence of amine in the medium with acylating agent.

Amide bond formation has problems such as low yield, racemization, degradation and difficult purification. Various types and numbers of coupling reagents have been developed to overcome these problems.

Thionyl chloride (Chu et al. 2005), oxalyl chloride (Adams and Ulich 1920; Yeung et al. 2006), phosphorous trichloride PCl_3, phosphorous pentachloride PCl_5 are the most commonly used reagents for obtaining acyl chloride.

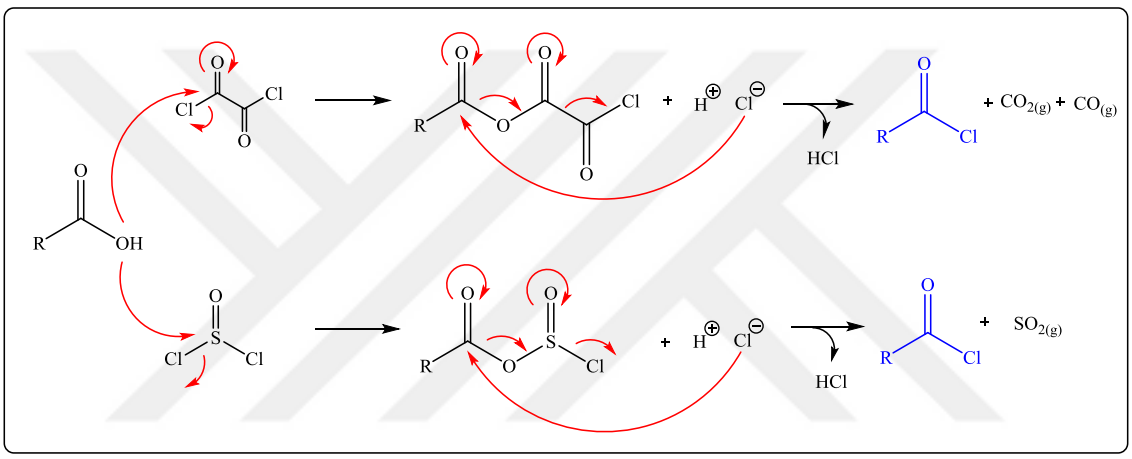

Figure 2.1. Acylchloride formation mechanism

The major disadvantage of the chlorination agents mentioned above is the formation of HCl during the reaction. Some groups are weak or sensitive to the acidic environment (such as the Boc group containing amines). Cyanuric chloride (2,4,6-trichloro-1,3,5-triazine), basic environment chlorination compound, is a reagent that provides the formation of acyl chloride in the presence of triethylamine (Venkataraman and Wagle 1979).

The pH of the reaction medium is basic with the presence of triethyl amine, the possible reaction mechanism is the formation of the active ester compound and chlorine anion as a result of the initial aromatic nucleophilic substitution reaction. The next step is to obtain the desired acyl chloride compound as a result of the nucleophilic attack of the chloride anion on the activated ester. The main advantages of this reactive are the use of 0.33

equivalent triazine, while minimizing the formation of by-product, the use of cheap inorganic base and the reaction's ability to tolerate water. After the acyl chloride is obtained, an extra base is required to retain the HCl formed in the coupling step with amine compounds. Coupling step usually takes place in the presence of dry solvents and non-nucleophilic amine bases in an inert environment. In peptide synthesis, acyl chloride shows some undesired properties such as hydrolysis, cleavage of the protecting group, racemization and side reactions (Figure 2.2).

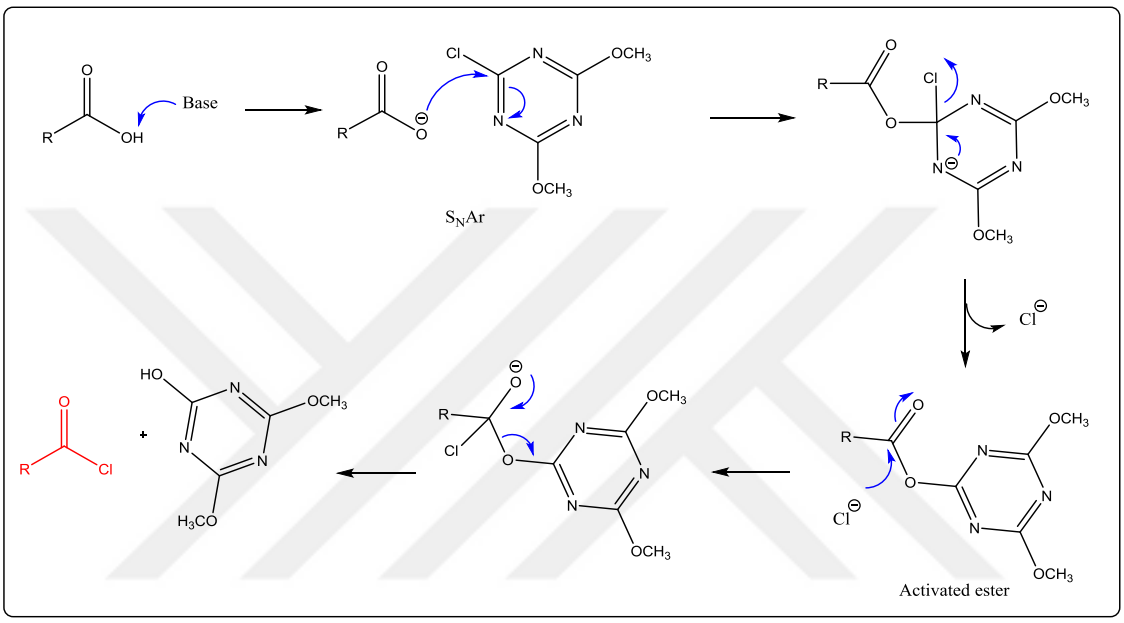

Figure 2.2. The reaction mechanism based on CDMT method

Acyl azide production is the first peptide coupling method developed by Curtius (Curtius 1902). Acyl azides are synthesized from the corresponding methyl esters in two stages. In the first step, acyl azide is obtained by nitration reaction of the compound of acyl hydrazine, which is formed by the replacement of the methoxy group with hydrazine. In the second step, the amine reacts with acyl azide intermediate (Figure 2.3). The absence of racemization makes this method very effective.

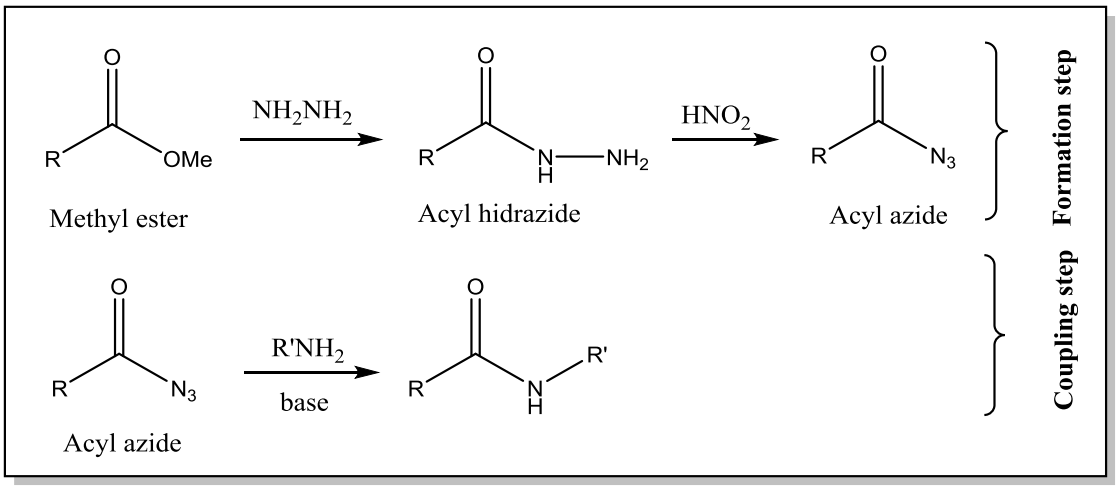

Figure 2.3. Amide formation steps via acyl azide method

Carbonyl diimidazole (CDI) reagent allows synthesis of amide bond in one pot reaction (Paul and Anderson 1960). In the first place, as soon as acyl carboxy imidazole and imidazole are formed, the acyl imidazole active intermediate is formed. In the next stage, the intermediate interacts with the amine to form an amide bond. This reaction does not need extra base and it is also suitable for reaction with the HCl salt of the amine.

Anhydrides can react with a wide range of nucleophiles such as alcohol, thiol and amine. Symmetrical anhydrides are formed by heating two related equivalent acids or reacting with DCC under mild conditions (Schlama et al. 1996). The driving force of this reaction is the formation of the urea byproduct. The anhydride then interacts with the amine to form carboxylate anion. This mild and effective coupling method is suitable for peptide synthesis (Figure 2.4). The biggest limitation for this method is that half of the acid reacts with the other half leading to acid loss.

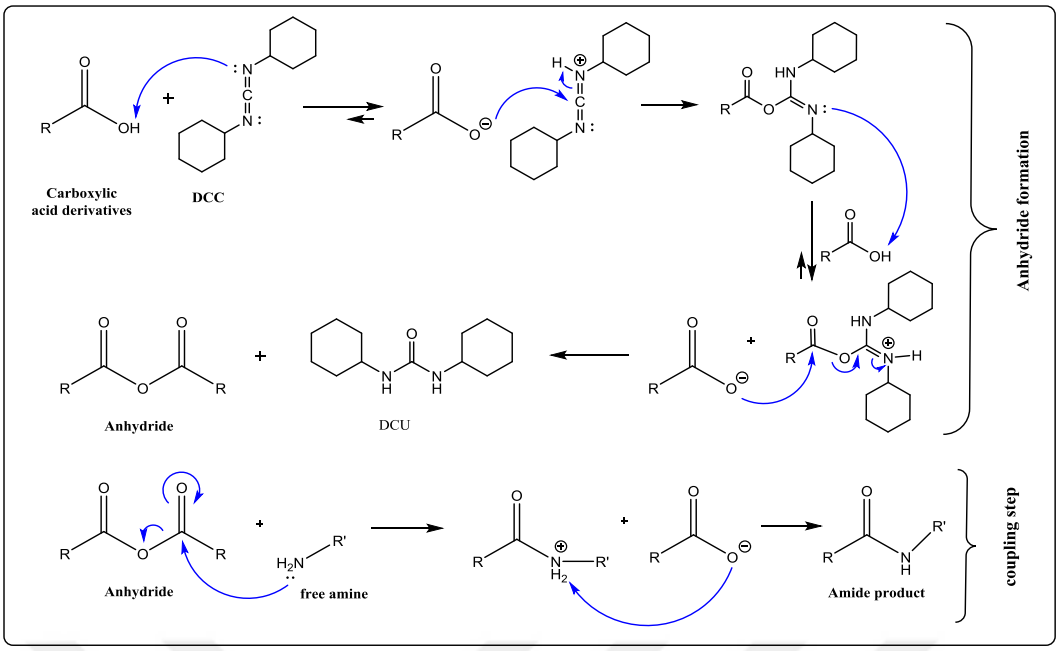

Figure 2.4. General DCC mechanism

Koenig and Geiger succeeded high efficiency and reduction in epimerization using hydroxybenzotriazole (HOBt) as additive. HOBt initially reacts with O-acylurea to form an OBt ester (Figure 2.6). The resulting activated ester is more stable and enables the amine to approach with hydrogen bond (König and Geiger 1970; König and Geiger 1970; Williams and Ibrahim 1981). In 1994, Carpino introduced the compound 1-hydroxy7-azabenzotriazole (HOAt) into the literature. This compound is a more effective additive than HOBt with both high yield rate and low epimerization (Carpino 1993; Carpino et al. 2000; Jad et al. 2015).

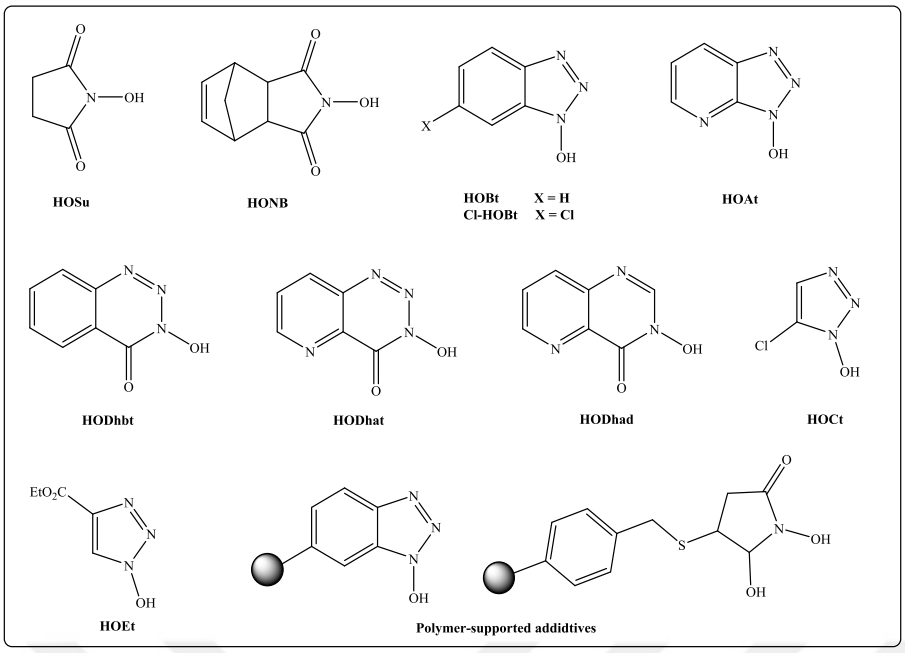

Figure 2.5. Common coupling additives

Many coupling compounds associated with benzotriazole are known as the uronium / aminium salts. These compounds react with carboxylic acid to form OAt and OBt active esters to interact with amines. As a result of the interaction of amines with the coupling reagent for this reaction, guanidinum by-product is formed according to the order of participation and timing. The most commonly used alcohols based additives in amide bond synthesis are HOBt, p-nitrophenol (PNP) and penta fluorophenol moiety (PFP) are given in Figure 2.5. (Kisfaludy et al. 1974; Gangwar et al. 1997).

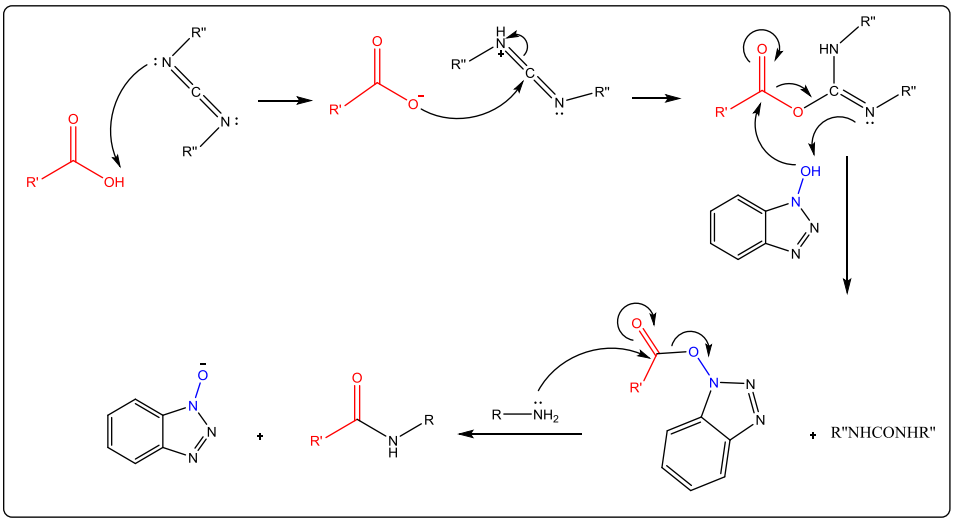

Figure 2.6. Formation of amide bond via coupling reagent and an additive HOBt

Collectively, the amide bond has a very important place in both organic chemistry and biochemistry. Several coupling compounds have been developed for amide bond synthesis, but many are not effective for a wide range of amide bond formation. Only the most commonly used coupling reagents are mentioned here.

2.2. Application of Cinnamic Acid Derivatives

Cinnamic acid has long been used by humans as a component of plant-derived flavors (Hoskins 1984). Chemically, it is an aromatic fatty acid that is usually trans-geometry and consists of an acrylic acid group and a phenyl ring, and has low toxicity. Cinnamic acid and its derivatives have an unsaturated carbonyl fragment, which can be considered an active part, the Michael acceptor, which is often used in the design of anticancer drugs (Zou al. 2006). In biological chemistry, cinnamic acid is an important intermediate in phenylpropanoid pathways, the precursor of lignin, the structural component of flavonoids and plants (Whetten et al. 1998; Boerjan et al. 2003; Edreva 2005). It is reported that chlorogenic acids (esters of kinic and cinnamic acids) are well-known antioxidants, as well as having various health benefits such as mitigating cardiovascular diseases, type 2 diabetes, and Alzheimer's disease(Kweon et al. 2001; Cos et al. 2002; Farah et al. 2008).

Cinnamic acid derivatives have been evaluated as pharmacologically active compounds due to their wide availability in plants and their low toxicity (Hoskins 1984; Clifford 1999;

Clifford 2000). Besides showing various biological activities (Saraf and Simonyan 1992; Avanesyan et al. 2009) they are often used as promising starting compounds for the development of new and highly effective drugs. Avanesyan et al. reported the antiradical activity of several cinnamic acid derivatives with different substitutions in the aromatic ring. They stated that the type and location of the substituents on the aromatic ring increase or decrease the activity, and also the cinamoil part is the determining factor on the antiradical activity. It is well known that cinnamic acid has an antimicrobial effect against pathogenic and spoilage bacteria although it restricts the use of low solubility in water (Hoskins 1984; Narasimhan et al. 2004; Truong et al. 2010). In addition to natural sources, several synthetic cinnamates have shown strong inhibitory activity against HIV-1 integrase (Serkedjieva et al. 1992; Burke et al. 1995; Lee et al. 2007).

Most of the studies in the literature are on organic, inorganic and polymer compounds. As the pure forms of these compounds show low electrical properties, it is aimed to increase the electrical properties by using carbon-based, ceramic and various metal composites as fillers as the main method. In this thesis, the electrical parameter results of chalcone compounds, which are structurally closest to the synthesized amino acid conjugates, are discussed comparatively in the result and discussion section.

The dielectric constant indicates how much energy is stored and how much is lost with the electric field applied externally to a compound (Okutan et al. 2007; Koran et al. 2016; Biryan et al. 2018). Studies on the dielectric properties of the compounds containing conjugated p electrons in its structure have increased in recent years. Koran at al. have works about various chalcone derivatives which are similar to cinnamic acid compounds structurally. In the light of these studies, conjugated chalcone compounds compounds were evaluated against increasing frequency and temperature. The obtained results showed that they can be used in various optical and electrical applications such as light emitting diode, solar cell and nano-sized electronic devices due to their conductive and semiconductor properties. Besides these works, numerous polymers have synthesized and evaluated in terms of dielectric, optoelectronic applications.

Dielectric materials continue to attract attention due to their application areas such as dielectric based capacitors, communication devices, field effect transistors (FETs) and actuators. Ceramic based dielectric materials are the most preferred in applications. Many

polymer compounds are not very suitable for dielectric applications due to their low dielectric constant (between 2 and 10). By mixing polymers with materials such as ceramic nanoparticles BaTiO3 or Pb (Zr, Ti) O_3 certain proportions have been given suitable compounds for dielectric applications (Ming et al. 2016). Huang et al. have managed to increase the dielectric constant to over 400 by forming a composite with copper atom in phthalocyanine compounds (Huang et al 2004). In another study, the dielectric constant of the compounds obtained by integrating organic photo voltaic (OPV) into semiconductors with high dielectrics was measured to around 16 (Maes et al. 2017).

In the study conducted by Burn et al. on the dielectric properties of organic semiconductors, it has been determined that the dielectric constant varies between 4 and 9 depending on the groups in the compound at low frequencies (Burn et al. 2017). In another study, graphene oxide doped poly (vinylidene fluoride) compounds with high dielectric constant and low dielectric loss were prepared (Wang et al. 2016). In the study conducted by Javed et al, glass fiber addition was applied in certain proportions to increase the dielectric parameters (Javed et al 2005).

3. MATERIALS AND METHODS

3.1. Material

Table 3.1.1. Chemical components used in the study

Chemical	**Company**	**Country**
Triethylamine (TEA)	Sigma-Aldrich	USA
Sodium hydroxide	Sigma-Aldrich	USA
Hydrochloric acid	Sigma-Aldrich	USA
1-*H*-benzotriazole (BtH)	Sigma-Aldrich	USA
Dicyclohexylcarbodiimide (DCC)	TCI	Japan
2-chloro-4,6-dimethoxy-1,3,5-triazine (CDMT)	TCI	Japan
N-methyl morpholine	Merck	Germany
Piperidine	Merck	Germany
Malonic acid	ACROSS	USA
Glycine	TCI	Japan
L-alanine	TCI	Japan
L-methionine	TCI	Japan
L-leucine	TCI	Japan
L-alanine methyl ester	TCI	Japan
Glycine methyl ester	Sigma-Aldrich	USA
2-chloro benzaldehyde	Sigma-Aldrich	USA
4-chloro benzaldehyde	Sigma-Aldrich	USA
4-nitro benzaldehyde	Sigma-Aldrich	USA
2-methyl benzaldehyde	Sigma-Aldrich	USA
3-methyl benzaldehyde	Sigma-Aldrich	USA
4-methoxy benzaldehyde	Sigma-Aldrich	USA
2,4-dimethoxy benzaldehyde	Sigma-Aldrich	USA
2,4,5-trimethoxy benzaldehyde	Sigma-Aldrich	USA
2-fluoro benzaldehyde	Sigma-Aldrich	USA
9-phenanthrenecarboxaldehyde	Sigma-Aldrich	USA
1-pyrenecarboxaldehyde	Sigma-Aldrich	USA
1-naphthaldehyde	Sigma-Aldrich	USA
Biphenyl-4-carboxaldehyde	Sigma-Aldrich	USA

Table 3.1.2. Chemical components used in the study

Chemical	**Company**	**Country**
n-hexane	Tekkim	Turkey
Chloroform	Merck	Germany
Acetonitrile	ACROSS	USA
Ethyl acetate	Sigma-Aldrich	USA
Pyridine	Merck	Germany

Table 3.1.3. Laboratory equipment used in the study

Equipment	**Company**	**Country**
pH meter	Thermo	USA
Magnetic stirrer	ISOLAB	Germany
Rotary evaporator	Buchi	Switzerland
Refrigerator	Arçelik	Turkey
400 MHz NMR	Bruker	Germany
Elemental analysis	Leco	USA
Impedance analyzer	HIOKI	Japan
FT-IR spectrometer	Thermo	USA

3.2. Experimental

^{1}H and ^{13}C APT NMR spectra were recorded on 400 MHz apparatus in $CDCl_3$ or DMSO-d_6 with using TMS as internal standard. All solvents were used without further purifications. Unprotected amino acid and ester forms were purchased from commercial sources. Cinnamic acid derivatives, *N*-acyl benzotriazoles, amino acid conjugates were prepared via literatures (Katritzky et al. 1998, Katritzky et al. 2000). FT-IR experiments carried out by using Thermo Scientific Nicolet iS5 device and Leco CHNS-932 devise were used for elemental analysis.

3.2.1. General Synthetic Procedures for Cinnamic Acid Derivatives (R-CA-OH)

The malonic acid (2.2 eq.), aromatic aldehyde (1.0 eq.), piperidine (0.2 eq.) and pyridine (5.7 eq.) as solvent was added to 250 ml reaction flask which then arranged for reflux overnight. The reaction was monitored by thin layer chromatography and after completion of the reaction, the mixture added to 600 ml baker which contained 400 ml distilled water. Initially, a precipitate was occurred. Then pH of the mixture was brought up to 5 and let the mixture stirred for couple of hours. The precipitated was filtered and the obtained solid was dried. Yields were between 85 and 95%.

3.2.1.1. (*E*)-3-(4-nitrophenyl)acrylic acid (4-nitro-CA-OH)

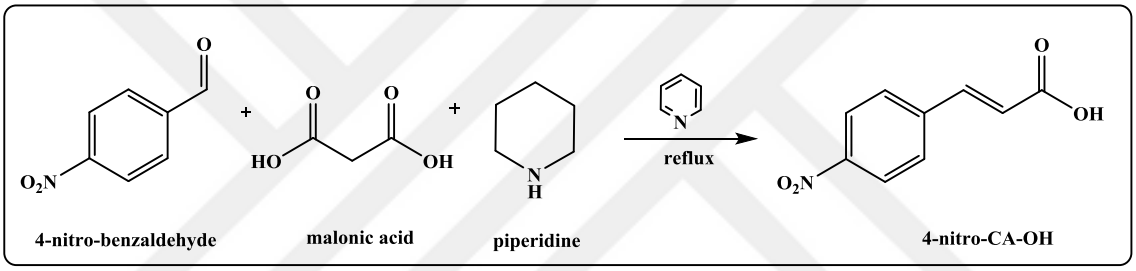

Reaction of 4-nitro benzaldehyde (1.0 g; 6.62 mmol), malonic acid (1.51 g; 14.56 mmol), and piperidine (112.7 mg; 1.32 mmol) as a catalyst in pyridine (5 ml) under reflux for 6 hours gave desired product (1.1 g; 5.69 mmol) with 86.1% yield as a white solid. Melting point: 283-287 ^{o}C, Lit: 289-290 ^{o}C . ^{1}H NMR (DMSO-d_6) δ: 12.76 (bs, CO_2H, 1H), 8.26 – 8.24 (m, =CH, AA′ part of AA′BB′ system, 2H), 8.01–7.99 (m, =CH, BB′ part of AA′BB′ system, 2H), 7.71(d, *J* = 16.0 Hz, =CH, 1H), 6.79 (d, *J* = 16.0 Hz, =CH, 1H).^{13}C-APT NMR (DMSO-d_6): 167.50, 148.43, 141.81, 141.23, 129.77, 124.40, 124. 10. Elemental analysis: $C_9H_7NO_4$ required C, 55.96; H, 3.65; N, 7.25, found C, 55.96; H, 3.67; N, 7.26. The spectroscopic results are compatible with the literature (Zhdanko et al. 2011).

3.2.1.2. (*E*)-3-(4-chlorophenyl)acrylic acid (4-chloro-CA-OH)

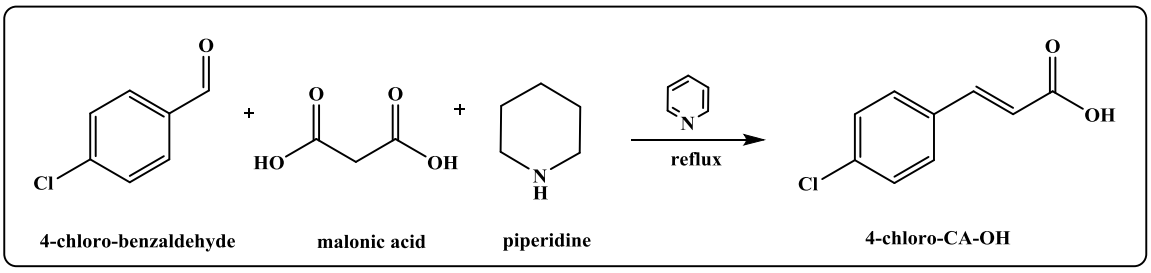

Reaction of 4-chloro benzaldehyde (3.0 g; 20.92 mmol) , malonic acid (4.89 g; 46.95 mmol), and piperidine (363.46 mg; 4.27 mmol) as a catalyst in pyridine (10 ml) under reflux for 6 hours gave desired product (3.62 g; 19.82 mmol) with 92.9% yield as a brown solid. Melting point: 238-240 ºC, lit: 242-248 ºC. ^{1}H NMR (DMSO-d_6) δ: 12.54 (bs, CO_2H, 1H), 7.76-7.74 (m, =CH, AA′ part of AA′BB′ system, 2H), 7.60 (d, *J* = 16.0 Hz, =CH, 1H), 7.50-7.48 (m, =CH, BB′ part of AA′BB′ system, 2H), 6.58 (d, *J* = 16.0 Hz, =CH, 1H).^{13}C-APT NMR (DMSO-d_6): 167.94, 142.85, 135.14, 133.73, 130.38, 129.39,120.72. The spectroscopic results are compatible with the literature (Martins et al. 2015).

3.2.1.3. (*E*)-3-(4-methoxyphenyl)acrylic acid (4-methoxy-CA-OH)

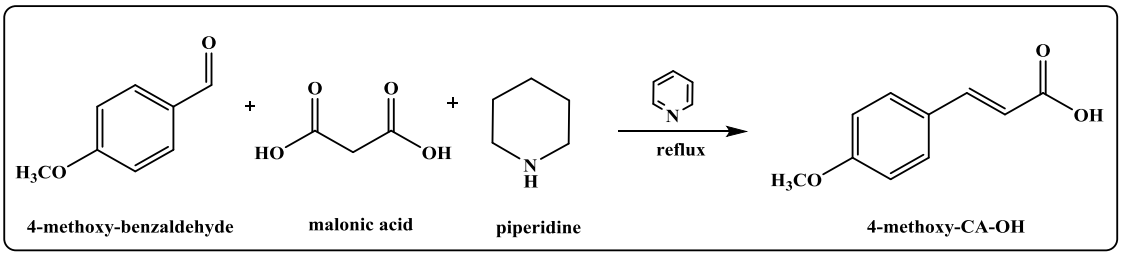

Reaction of 4-methoxy benzaldehyde (3.0 g; 22.03 mmol), malonic acid (5.04 g; 48.48 mmol), and piperidine (375.25 mg; 4.41 mmol) as a catalyst in pyridine (10 ml) under reflux for 6 hours gave desired product (3.76 g; 21.10 mmol) with 95.77% yield as a white solid. Melting point: 169-172 ºC, lit: 171-173 ºC. ^{1}H NMR (DMSO-d_6) δ: 12.21 (bs, CO_2H, 1H), 7.66-7.64 (m, =CH, AA′ part of AA′BB′ system, 2H), 7.56 (d, *J* = 16.0 Hz, =CH, 1H), 6.99-6.97 (m, =CH, BB′ part of AA′BB′ system, 2H), 6.38 (d, *J* = 16.0 Hz, =CH, 1H), 3.80 (s, OCH_3, 3H). ^{13}C-APT NMR (DMSO-d_6): 168.28, 161.42, 144.20, 130.40, 127.31,

116.99, 114.83, 55.78. The spectroscopic results are compatible with the literature (SawpathKumar et al. 1998).

3.2.1.4. (*E*)-3-(2-chlorophenyl)acrylic acid (2-chloro-CA-OH)

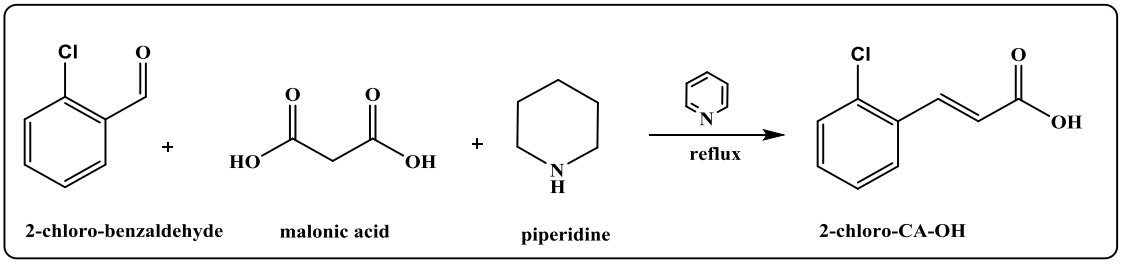

Reaction of 2-chloro benzaldehyde (3.0 g; 20.92 mmol), malonic acid (4.89 g; 46.95 mmol), and piperidine (363.46 mg; 4.27 mmol) as a catalyst in pyridine (10 ml) under reflux for 6 hours gave desired product (3.56 g; 19.50 mmol) with 91.35% yield as a white solid. Melting point: 210-212 ^{o}C, lit: 208-212 ^{o}C. ^{1}H NMR (DMSO-d_6) δ: 12.64 (bs, CO_2H, 1H), 7.95 – 7.92 (m, =CH, 1H), 7.89 (d, *J* = 16.0 Hz, =CH, 1H), 7.57–7.54 (m, =CH, 1H), 7.48–7.43 (td, *J* = 2.0 Hz, =CH, 1H), 7.42-7. 39 (td, *J* = 1.6 Hz, =CH, 1H), 6.61 (d, *J* = 16.0 Hz, =CH, 1H). ^{13}C-APT NMR (DMSO-d_6): 167.61, 139.15, 134.03, 132.35, 132.14, 130.42, 128.72, 128.24, 122.81. The spectroscopic results are compatible with the literature (Pardin et al. 2008).

3.2.1.5. (*E*)-3-(2-fluorophenyl)acrylic acid (2-fluoro-CA-OH)

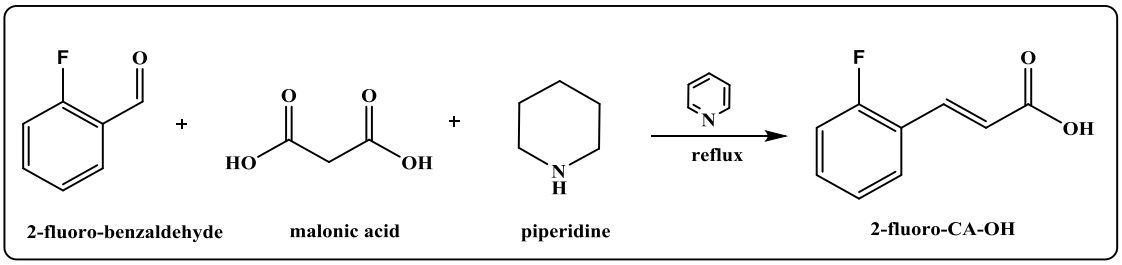

Reaction of 2-fluoro benzaldehyde (5.0 g; 40,29 mmol), malonic acid (9.22 g; 88.63 mmol), and piperidine (857.58 mg; 10.07 mmol) as a catalyst in pyridine (15 ml) under reflux for 6 hours gave desired product (6.02 g; 36.23 mmol) with 89.94 % yield as a white solid. Melting point: 170-173 ^{o}C, lit: 173-174 ^{o}C. ^{1}H NMR (DMSO-d_6) δ: 12.58 (bs, CO_2H,

1H), 7.87–7.83 (m, =CH, 1H), 7.67 (d, *J* = 16.0 Hz, =CH, 1H), 7.52–7.46 (m, =CH, 1H,), 7.32–7.29 (m, =CH, 1H), 7.27–7.25 (m, =CH, 1H), 6.61 (d, *J* = 16.0 Hz, =CH, 1H). ^{13}C-APT NMR (DMSO-d_6): 167.72, 162.22, 159.73, 136.15 – 136.12, 132.74 – 132.65, 129.73 – 129.70, 125.49 – 125.45, 122.41 – 122.35, 122.25, 116.41 – 116.41. The spectroscopic results are compatible with the literature (Szymanski et al. 2009).

3.2.1.6. (*E*)-3-(o-tolyl)acrylic acid (2-methyl-CA-OH)

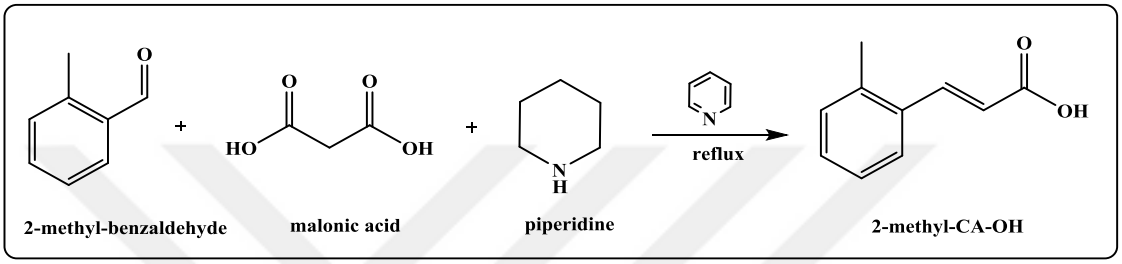

Reaction of 2-methyl benzaldehyde (5.0 g; 41.61mmol), malonic acid (8.66 g; 83.23 mmol), and piperidine (885.86 mg; 10.40 mmol) as a catalyst in pyridine (15 ml) under reflux for 6 hours gave desired product (6.25 g; 38.54 mmol) with 92.60 % yield as a white solid. Melting point: 181-183 ^{o}C, lit: 184-185 ^{o}C. ^{1}H NMR (DMSO-d_6) δ: 12.51 (bs, CO_2H, 1H), 7.83 (d, *J* = 16.0 Hz, =CH, 1H), 7.72–7.70 (m, =CH, 1H,), 7.34–7.23 (m,=CH, 3H), 6.44 (d, *J* = 16.0 Hz, =CH, 1H). ^{13}C-APT NMR (DMSO-d_6): 168.00, 141.62, 137.62, 133.39, 131.17, 130.42, 126.95, 126.89, 120.69, 19.74. The spectroscopic results are compatible with the literature (Sass et al. 2011).

3.2.1.7. (*E*)-3-(2,4-dimethoxyphenyl)acrylic acid (2,4-dimethoxy-CA-OH)

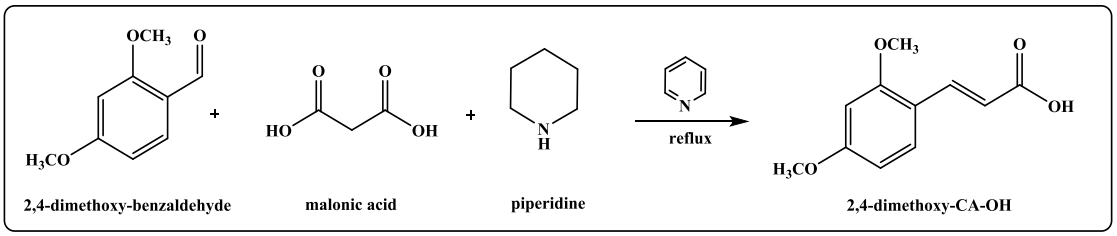

Reaction of 2,4-dimethoxy benzaldehyde (5.0 g; 30.09 mmol), malonic acid (6.89 g; 66.19 mmol), and piperidine (512.41 mg; 6.02 mmol) as a catalyst in pyridine (15 ml) under

reflux for 6 hours gave desired product (5.65 g; 27.14 mmol) with 90.19 % yield as a white solid. Melting point: 185-187 ºC, lit: 187-189 ºC. ^{1}H NMR (DMSO-d_6) δ: 12.09 ((bs, CO_2H, 1H), 7.76 (d, *J* = 16.0 Hz,=CH, 1H), 7.62 (d, *J* = 8.8 Hz, =CH, 1H), 6.63 (d, *J* = 2.4 Hz, =CH, 1H), 6.59 (d, *J* = 8.8 Hz, =CH, 1H), 6.39 (d, *J* = 16.0 Hz,=CH, 1H), 3.88 (s, OCH_3, 3H), 3.83 (s, OCH_3, 3H). ^{13}C-APT NMR (DMSO-d_6): 168.71, 162.99, 139.23, 130.40, 116.75, 155.82, 106.56, 98.77, 56.18, 55.92. The spectroscopic results are compatible with the literature (De Simone et al. 2009).

3.2.1.8. (*E*)-3-(2,4,5-trimethoxyphenyl)acrylic acid (2,4,5-trimethoxy-CA-OH)

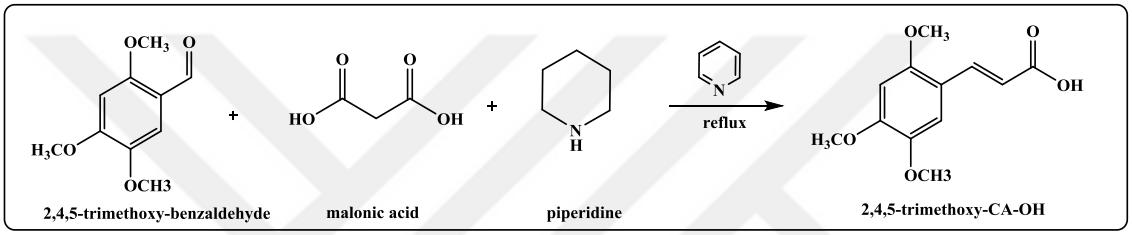

Reaction of 2,4,5-trimethoxy benzaldehyde (3.0 g; 15.29 mmol), malonic acid (3.50 g; 33.50 mmol), and piperidine (260.39 mg; 3.06 mmol) as a catalyst in pyridine (10 ml) under reflux for 6 hours gave desired product (3.11 g; 13.05 mmol) with 85.37 % yield as a light yellow solid. Melting point: 170-172 ºC, lit: 168-169 ºC. ^{1}H NMR (DMSO-d_6) δ: 12.11 (bs, CO_2H, 1H), 8.81 (d, *J* = 16.0 Hz, =CH, 1H), 7.25 (s, =CH, 1H), 6.73 (s, =CH, 1H), 6.40 (d, *J* = 16.0 Hz, =CH, 1H), 3.87 (s, OCH_3, 3H), 3.86 (s, OCH_3, 3H), 3.76 (s, OCH_3, 3H). ^{13}C-APT NMR (DMSO-d_6): 168.73, 153.71, 152.56, 143.46, 138.88, 116.55, 114.20, 111.38, 98.09, 56.81, 56.57, 56.26. The spectroscopic results are compatible with the literature (Gayam and Ravi 2017).

3.2.1.9. (*E*)-3-([1,1'-biphenyl]-4-yl)acrylic acid (phenylbenzyl-CA-OH)

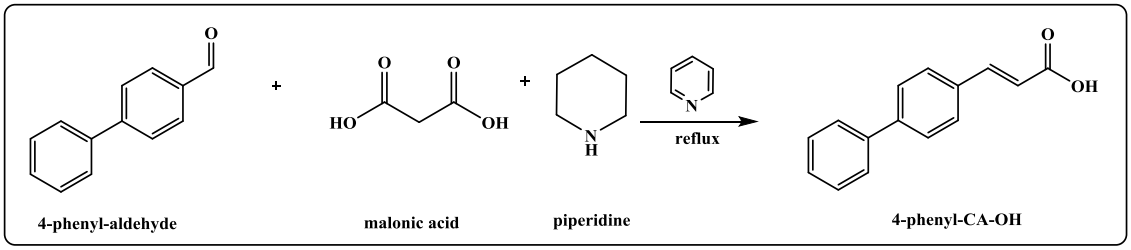

Reaction of [1,1'-biphenyl]-4-carbaldehyde (2.0 g; 10.9 mmol), malonic acid (2.51 g; 24.1 mmol), and piperidine (0.186 g; 2.19 mmol) as a catalyst in pyridine (7 ml) under reflux for 6 hours gave desired product (1.98 g; 8.83 mmol) with 80.44 % yield as a white solid. Melting point: 219-221 ^{o}C, lit: 217-223 ^{o}C. ^{1}H NMR (DMSO-d_6) δ: 7.79-7.77 (m, AA' part of AA'BB' system, =CH, 2H), 7.73-7.70 (m, BB' part of AA'BB' system, =CH, 2H), 7.72 (d, *J* = 1.2 Hz,=CH, 2H), 7.64 (d, *J* = 16.0 Hz, =CH, 1H), 7.51–7.47 (t, *J* = 7.6 Hz, =CH, 2H), 7.40 (d, *J* = 16.0 Hz, =CH, 1H). ^{13}C-APT NMR (DMSO-d_6): 168.33, 143.44, 142.08, 139.75, 133.99, 129.49, 129.25, 128.37, 127.54, 127.15, 120.27. The spectroscopic results are compatible with the literature (Gao et al. 2018).

3.2.1.10. (*E*)-3-(naphthalen-1-yl)acrylic acid (Naft-CA-OH)

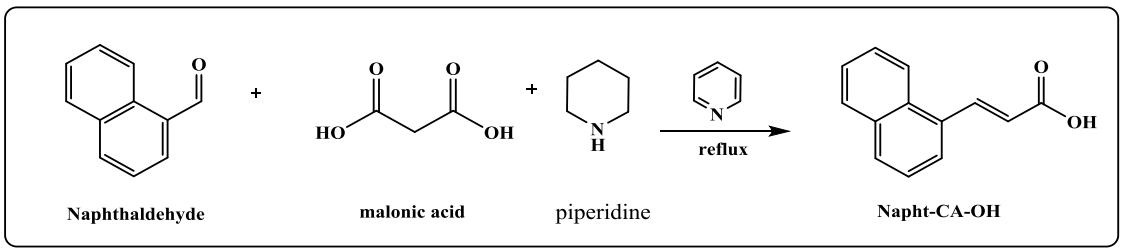

Reaction of 1-naphthaldehyde (3.0 g; 19.21 mmol), malonic acid (4.40 g; 42.26 mmol), and piperidine (327.11 mg; 3.84 mmol) as a catalyst in pyridine (5 ml) under reflux for 6 hours gave desired product (3.20 g; 16.14 mmol) with 84.05 % yield as a white solid. Melting point: 214-216 ^{o}C, lit: 210-214 ^{o}C.^{1}H NMR (DMSO-d_6) δ: 12.58 (bs, CO_2H, 1H), 8.40 (d, *J* = 15.6 Hz, =CH, 1H), 8.22 (d, *J* = 8.4 Hz, =CH, 1H), 8.04-7.95 (m, =CH, 3H), 7.67-7.56 (m, =CH, 3H), 6.62 (d, *J* = 15.6 Hz, =CH, 1H). ^{13}C-APT NMR (DMSO-d_6):

168.33, 143.44, 142.08, 139.75, 133.99, 129.49, 129.25, 128.37, 127.54, 127.15, 120.10. The spectroscopic results are compatible with the literature (Bowden and Hojatti 1990).

3.2.1.11. (*E*)-3-(phenanthren-9-yl)acrylic acid (Phenant-CA-OH)

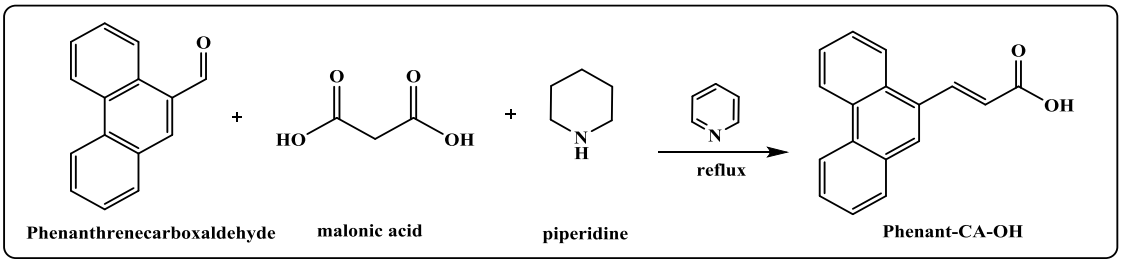

Reaction of phenanthrene-9-carbaldehyde (3.0 g; 14.55 mmol), malonic acid (3.33 g; 32,00 mmol), and piperidine (247.72 mg; 2.91 mmol) as a catalyst in pyridine (10 ml) under reflux for 6 hours gave desired product as a dark white solid (2.92 g; 11.76 mmol) with 80.85 % yield. Melting point: 228-231 ºC, lit: 230-233 ºC. ^{1}H NMR (DMSO-d$_6$) δ: 8.94–8.91 (m, =CH, 1H), 8.85 (d, *J* = 8.0 Hz, =CH, 1H), 8.40 (d, *J* = 15.6 Hz, =CH, 1H), 8.31 (s, =CH, 1H), 8.26–8.23 (m, =CH, 1H), 8.09 (d, *J* = 8.0 Hz, 1H), 7.79–7.67 (m, =CH, 4H), 6.71 (d, *J* = 15.6 Hz, =CH, 1H). ^{13}C-APT NMR (DMSO-d$_6$): 168.09, 140.87, 131.33, 130.87, 130.67, 129.95, 129.73, 128.35, 127.90, 127.70, 127.62, 126.85, 124.46, 124.06, 123.33. The spectroscopic results are compatible with the literature (Bachmann and Kloetzel 1937).

3.2.1.12. (*E*)-3-(pyren-4-yl)acrylic acid (Pyrene-CA-OH)

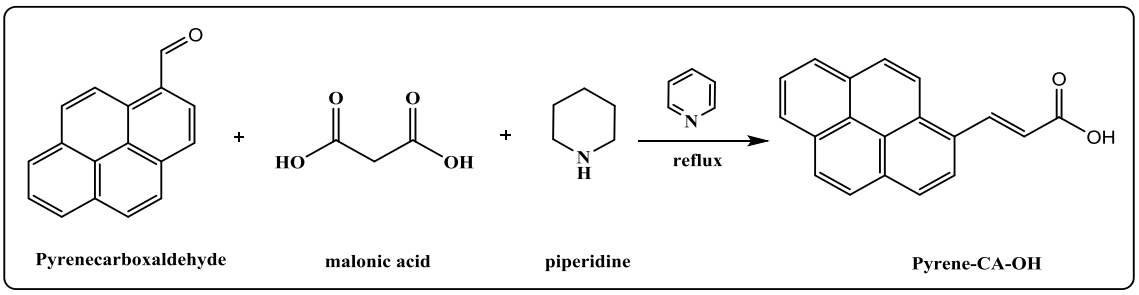

Reaction of pyrene-1-carbaldehyde (3.0 g; 13.03 mmol), malonic acid (2.98 g; 28.66 mmol), and piperidine (221.87 mg; 2.61 mmol) as a catalyst in pyridine (10 ml) under reflux for 6 hours gave desired product (2.85 g; 10.47 mmol) with 80.33 % yield as light yellow solid. Melting point: 275-278 ^{o}C, lit: 270-280 ^{o}C. ^{1}H NMR (DMSO-d_6) δ: 12.61 (s, CO_2H, 1H), 8.72 (d, *J* = 15.6 Hz, =CH, 1H), 8.57-8.53 (t, *J* = 8.4 Hz, =CH, 2H,), 8.40 (d, *J* = 3.2 Hz, =CH, 1H), 8.38 (d, *J* = 3.2 Hz, =CH, 1H), 8.34 (d, *J* = 8.8 Hz, =CH, 2H), 8.29-8.22 (m, =CH, 2H), 8.15-8.11 (t, *J* = 7.6 Hz, =CH, 1H), 6.85 (d, *J* = 15.6 Hz, =CH, 1H). ^{13}C-APT NMR (DMSO-d_6): 168.10, 140.36, 132.58, 131.32, 130.67, 129.39, 129.20, 128.96, 128.33, 127.84, 127.12, 126.61, 126.35, 125.81, 125.12, 124.51, 124.25, 122.78, 122.13. The spectroscopic results are compatible with the literature (Oh and Hong 2013).

3.2.2. General Synthetic Procedures for *N*-Acylbenzotriazol Derivatives (R-CA-Bt)

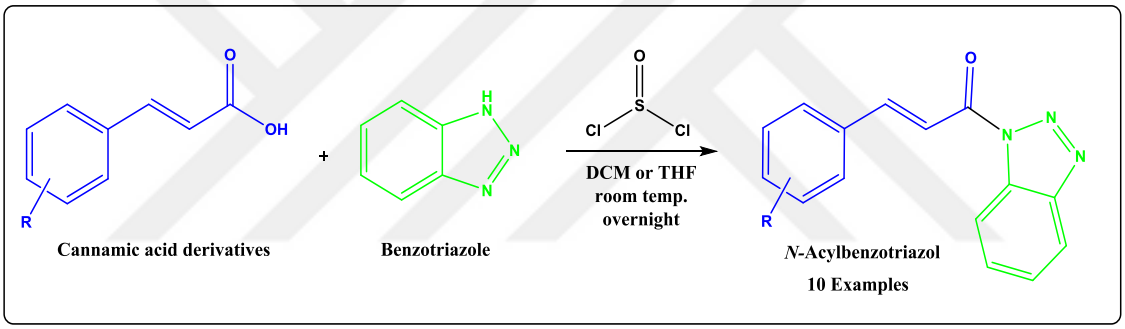

Benzotriazole (4.0 eq.) was dissolved in dichloromethane (50 ml) in 250 ml reaction flask. After became a transparent solution, thionyl chloride (1.2 eq.) was added to reaction mixture dropwise at room temperature. Yellow color was occurred and the reaction was stirred around 15 minutes. Then cinnamic acid derivative (1.0 eq.) added to reaction flask and the mixture stirred for 12 hours. After the completion of the reaction, reaction solvent was removed under pressure. The obtained solid was then added to a baker which contained 300 ml distilled water and the temperature was kept between 50 – 60 ^{o}C for 2 hours. The precipitate was filtered and dried. The desired product was obtained as solid. Yields 60 – 85%.

3.2.2.1. (*E*)-3-([1,1'-biphenyl]-4-yl)-1-(1*H*-benzo[*d*][1,2,3]triazol-1-yl)prop-2-en-1-one (phenylbenzyl-CA-Bt)

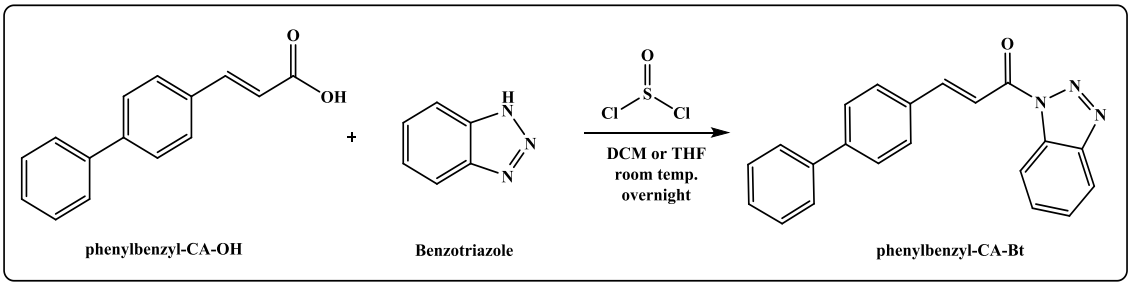

Benzotriazole (2.12 g; 17.84 mmol) and Thionyl chloride (636 mg; 5.35 mmol) were dissolved in dichloromethane (40 ml) and after 15 minutes, 4-phenybenzyl-CA-OH (1.0 g; 4.46 mmol) was added to reaction mixture. After above mentioned purification steps, desired product 4-phenybenzyl-CA-Bt was obtained as a yellow solid (1.18 g; 3.63 mmol) with yield 81.33%. Melting point: 143-146 ^{o}C. ^{1}H NMR (DMSO-d$_6$) δ: 8.37 (d, *J* = 8.0 Hz, =CH, 1H), 8.28 (d, *J* = 8.0 Hz, =CH, 1H), 8.23–8.08 (m, =CH, 3H), 8.01 (d, *J* = 8.4 Hz, =CH, 2H), 7.83 (d, *J* = 8.4 Hz, =CH, 2H), 7.77 (d, *J* = 8.0 Hz, =CH, 2H), 7.65 (t, *J* = 7.6 Hz, =CH, 1H), 7.54–7.50 (t, *J* = 7.6 Hz, =CH, 2H), 7.45–7.41 (t, *J* = 7.6 Hz, =CH, 1H). ^{13}C-APT NMR (DMSO-d$_6$): 163.99, 148.27, 146.18, 143.52, 139.49, 133.44, 131.43, 131.25, 130.37, 129.57, 128.70, 127.80, 127.30, 127.08, 120.62, 116.39, 114.84. Elemental analysis: $C_{21}H_{15}N_3O$ required C, 77.52; H, 4.65; N, 12.91, found C, 77.59; H, 4.72; N, 12.99.

3.2.2.2. (*E*)-1-(1*H*-benzo[*d*][1,2,3]triazol-1-yl)-3-(naphthalen-1-yl)prop-2-en-1-one (Naft-CA-Bt)

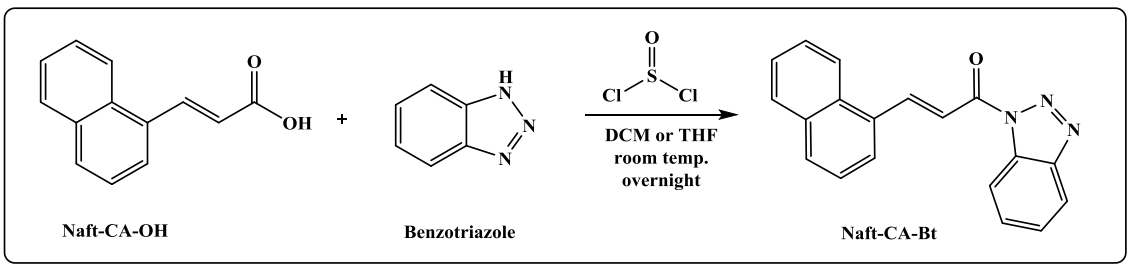

Benzotriazole (2.40 g; 20.18 mmol) and Thionyl chloride (720.16 mg; 6.05 mmol) were dissolved in dichloromethane (40 ml) and after 15 minutes, 1-napthalen-CA-OH (1.0 g; 5.04 mmol) was added to reaction mixture. After above mentioned purification steps, desired product 1-napthalen-CA-Bt was obtained as a white solid (1.26 g; 4.21 mmol) with yield 83.44%. Melting point: 138-140 ºC. ^{1}H NMR (DMSO-d_6) δ: 8.93 (d, *J* = 16.0 Hz, =CH, 1H), 8.41–8.38 (dd, *J* = 5.4 Hz, =CH, 2H), 8.31 (d, *J* = 8.0 Hz, =CH, 1H), 8.24 (d, *J* = 7.2 Hz, =CH, 1H,), 8.20–8.13 (t, *J* = 16 Hz, 8.4 Hz, =CH, 2H,), 8.06 (d, *J* = 8.0 Hz, =CH, 1H), 7.84 (d, *J* = 6.8 Hz, =CH, 1H), 7.70 (m, =CH, 3H). ^{13}C-APT NMR (DMSO-d_6): 163.80, 146.16, 144.67, 133.88, 132.34, 131.52, 131.42, 131.30, 130.96, 129.39, 128.08, 127.12, 127.03, 126.82, 126.33, 123.48, 120.65, 118.65, 114.81. Elemental analysis: $C_{19}H_{13}N_3O$ required C, 76.24; H, 4.38; N, 14.04, found C, 76.28; H, 4.45; N, 14.11. The spectroscopic results are compatible with the literature (Uraguchi, Ueki et al. 2009).

3.2.2.3. (*E*)-1-(1*H*-benzo[*d*][1,2,3]triazol-1-yl)-3-(phenanthren-9-yl)prop-2-en-1-one (Phenant-CA-Bt)

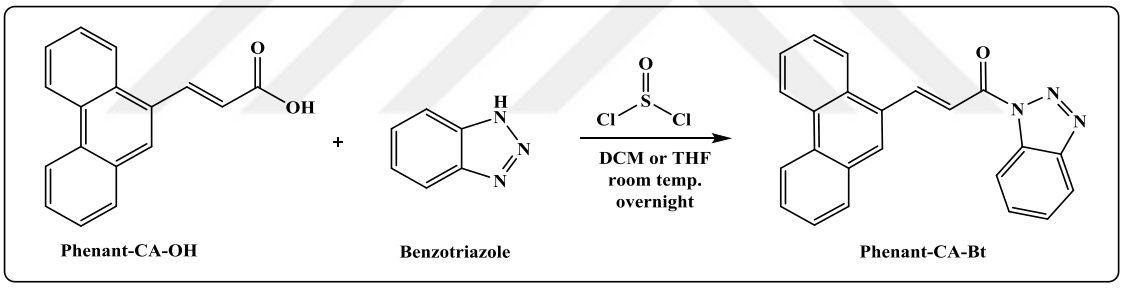

Benzotriazole (1.92 g; 16.11 mmol) and thionyl chloride (574.96 mg; 4.83 mmol) were dissolved in dichloromethane (40 ml) and after 15 minutes, phenanthrene-CA-OH (1.0 g; 4.03 mmol) was added to reaction mixture. After above mentioned purification steps, desired product phenanthrene-CA-Bt was obtained as a light yellow (1.03 g; 2.95 mmol) with yield 73.19%. Melting point: 155-157 ºC. ^{1}H NMR (DMSO-d_6) δ: 8.99 – 8.95 (dd, *J* = 5.4 Hz, =CH, 2H,), 8.90 (d, *J* = 8.4 Hz, =CH, 1H), 8.65 (s, =CH, 1H), 8.45-8.41 (m, =CH, 2H), 8.35-8.32 (m, =CH, 2H), 8.24-8.22 (dd, *J* = 1.4 Hz, =CH, 1H), 7.89-7.85 (td, *J* = 1.2 Hz, 2.4 Hz, =CH, 1H,), 7.84–7.79 (m, =CH, 3H), 7.77–7.73 (td, *J* = 0.8 Hz, 1.2 Hz, =CH, 1H,), 7.71 – 7.67 (td, *J* = 1.2 Hz, 2.0 Hz, =CH, 1H). Elemental analysis: $C_{23}H_{15}N_3O$ required C, 79.07; H, 4.33; N, 12.03, found C, 79.11; H, 4.36; N, 12.08.

3.2.2.4. (*E*)-1-(1*H*-benzo[*d*][1,2,3]triazol-1-yl)-3-(pyren-4-yl)prop-2-en-1-one (Pyrene-CA-Bt)

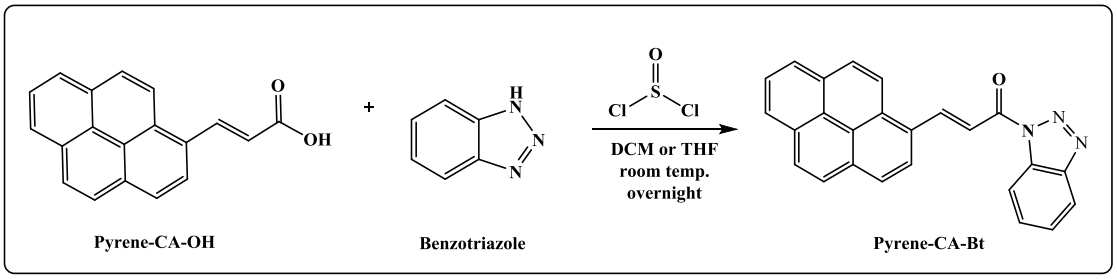

Benzotriazole (1.75 g; 14.69 mmol) and thionyl chloride (524.24 mg; 4.41 mmol) were dissolved in dichloromethane (40 ml) and after 15 minutes, pyrene-CA-OH (1.0 g; 3.67 mmol) was added to reaction mixture. After above mentioned purification steps, desired product pyrene-CA-Bt was obtained as an orange solid (856 mg; 2.29 mmol) with yield 62.42%. Melting point: 167-169 ^{o}C. ^{1}H NMR (DMSO-d_6) δ: 9.22 (d, *J* = 15.6 Hz, =CH, 1H), 8.73–8.72 (d, *J* = 3.2 Hz, =CH, 1H), 8.70–8.69 (d, *J* = 4.0 Hz, =CH, 1H), 8.43–8.39 (m, =CH, 5H), 8.34–8.33 (d, *J* = 6.8 Hz, =CH, 1H), 8.31–8.25 (m, =CH, 4H), 8.17–8.13 (t, *J* = 7.6 Hz, =CH, 1H), 7.87–7.83 (t, *J* = 7.8 Hz, =CH, 1H), 7.69–7.65 (t, *J* = 7.6 Hz, =CH, 1H). Elemental analysis: $C_{25}H_{15}N_3O$ required C, 80.41; H, 4.05; N, 11.25, found C, 80.43; H, 4.11; N, 11.27.

3.2.2.5. (*E*)-1-(1*H*-benzo[*d*][1,2,3]triazol-1-yl)-3-(2,4,5-trimethoxyphenyl)prop-2-en-1-one (2,4,5-trimethoxy-CA-Bt)

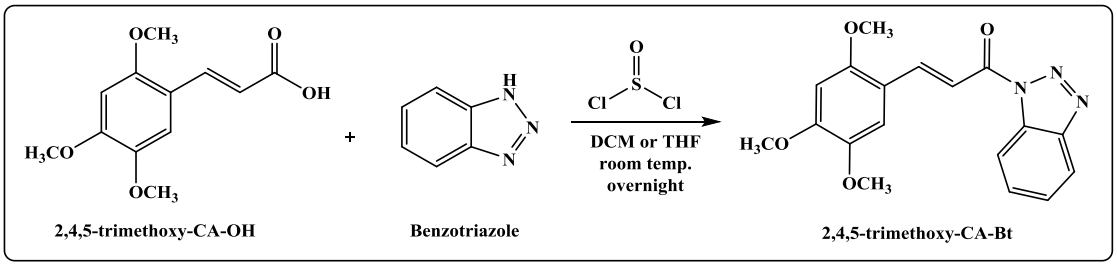

Benzotriazole (2.00 g; 16.79 mmol) and thionyl chloride (599.19 mg; 5.04 mmol) were dissolved in dichloromethane (40 ml) and after 15 minutes, 2,4,5-trimethoxy-CA-OH (1.0 g; 4.20 mmol) was added to reaction mixture. After above mentioned purification steps, desired product 2,4,5-trimethoxy-CA-Bt was obtained as a green solid (1.23 g; 3.62 mmol) with yield 86.35%. Melting point: 159-162 ^{o}C. ^{1}H NMR (DMSO-d_6) δ: 8.37-8.36 (d, *J* =

1.6 Hz, =CH, 1H), 8.34 (d, *J* = 5.2 Hz, =CH, 1H), 8.28 (d, *J* = 8.4 Hz, =CH, 1H), 8.01 (d, *J* = 15.6 Hz, =CH, 1H,), 7.82–7.78 (t, *J* = 7.8 Hz, =CH, 1H), 7.65 –7.61 (t, *J* = 7.8 Hz, =CH, 1H), 7.46 (s, =CH, 1H), 6.81 (s, =CH, 1H). ^{13}C-APT NMR (DMSO-d_6): 164.67, 155.57, 154.34, 146.11, 143.88, 143.65, 131.53, 131.03, 126.87, 120.51, 114.90, 114.05, 112.81, 112.31, 97.97, 57.03, 56.72, 56.45. Elemental analysis: $C_{18}H_{17}N_3O_4$ required C, 63.71; H, 5.05; N, 12.38, found C, 63.74; H, 5.09; N, 12.41.

3.2.2.6. (*E*)-1-(1*H*-benzo[*d*][1,2,3]triazol-1-yl)-3-(2,4-dimethoxyphenyl)prop-2-en-1-one (2,4-dimethoxy-CA-Bt)

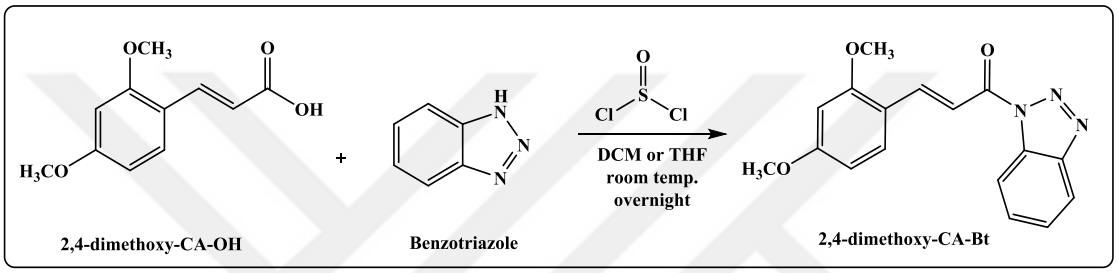

Benzotriazole (2.29 g; 19.21 mmol) and thionyl chloride (685.60 mg; 5.76 mmol) were dissolved in dichloromethane (40 ml) and after 15 minutes, 2,4-dimethoxy-CA-OH (1.0 g; 4.80 mmol) was added to reaction mixture. After above mentioned purification steps, desired product 2,4-dimethoxy-CA-Bt was obtained as a yellow solid (1.19 g; 3.85 mmol) with yield 80.10%. Melting point: 161-165 ^{o}C. ^{1}H NMR (DMSO-d_6) δ: 8.35 (d, *J* = 8.4 Hz, =CH, 1H), 8.29–8.28 (d, *J* = 5.6 Hz, =CH, 1H), 8.24 (d, *J* = 2.4 Hz, =CH, 1H), 8.01 (d, *J* = 16.0 Hz, =CH, 1H), 7.86 (d, *J* = 8.4 Hz, =CH, 1H,), 7.82–7.78 (td, *J* = 1.2 Hz, =CH, 1H), 7.65–7.61 (td, *J* = 2.4 Hz, =CH, 1H). ^{13}C-APT NMR (DMSO-d_6): 164.60, 164.46, 146.12, 144.12, 132.42, 131.49, 131.02, 126.85, 120.50, 115.84, 114.86, 113.24, 107.19, 99.00, 56.53, 56.16. Elemental analysis: $C_{17}H_{15}N_3O_3$ required C, 66.01; H, 4.89; N, 13.58, found C, 66.03; H, 4.96; N, 13.68.

3.2.2.7. (*E*)-1-(1*H*-benzo[*d*][1,2,3]triazol-1-yl)-3-(4-methoxyphenyl)prop-2-en-1-one (4-methoxy-CA-Bt)

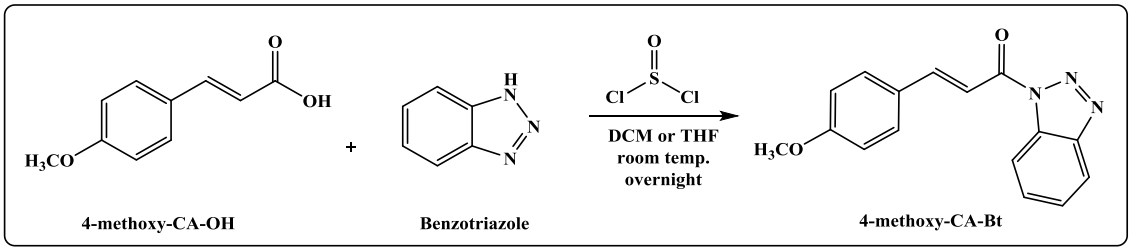

Benzotriazole (2.67 g; 22.45 mmol) and thionyl chloride (801.13 mg; 6.73 mmol) were dissolved in dichloromethane (40 ml) and after 15 minutes, 4-methoxy-CA-OH (1.0 g; 5.61 mmol) was added to reaction mixture. After above mentioned purification steps, desired product 4-methoxy-CA-Bt was obtained as a white solid (1.32 g; 4.73 mmol) with yield 84.21%. Melting point: 151-155 ^{o}C, lit: 157-159 ^{o}C. ^{1}H NMR (DMSO-d$_6$) δ: 8.36 (d, *J* = 8.2 Hz, =CH, 1H), 8.29 (d, *J* = 8.2 Hz, =CH, 1H,), 8.13 (d, *J* = 16.0 Hz, =CH, 1H), 7.96 – 7.91 (m, =CH, AA′ part of AA′BB′ system, 2H), 7.83 – 7.79 (m, =CH, 1H,), 7.66 – 7.62 (m, =CH, 1H), 7.08 (m, =CH, BB′ part of AA′BB′ system, 2H), 3.86 (s, OCH_3, 3H). ^{13}C-APT NMR (DMSO-d$_6$): 164.14, 162.67, 148.85, 146.14, 131.78, 131.45, 131.12, 127.02, 126.95, 120.56, 115.18, 114.84, 113.53, 55.99. The spectroscopic results are compatible with the literature (Xia et al. 2011).

3.2.2.8. (*E*)-1-(1*H*-benzo[*d*][1,2,3]triazol-1-yl)-3-(o-tolyl)prop-2-en-1-one (2-methyl-CA-Bt)

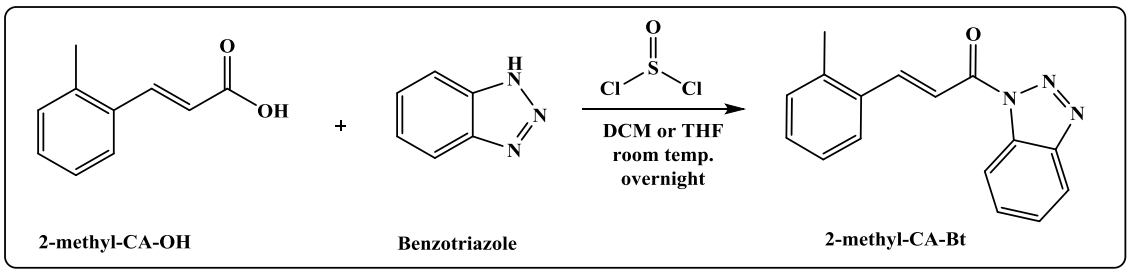

Benzotriazole (2.94 g; 24.66 mmol) and thionyl chloride (880.16 mg; 7.40 mmol) were dissolved in dichloromethane (40 ml) and after 15 minutes, 2-methyl-CA-OH (1.0 g; 6.71 mmol) was added to reaction mixture. After above mentioned purification steps, desired product 2-methyl-CA-Bt was obtained as a white solid (1.46 g; 5.55 mmol) with yield

89.93%. Melting point: 125-128 ºC, lit: 127-129 ºC. ^{1}H NMR (DMSO-d_6) δ: 8.37–8.28 (m, =CH, 3H), 8.01–7.94 (m, =CH, 2H), 7.84–7.79 (m, =CH, 1H), 7.70–7.62 (m, =CH, 1H), 7.44–7.34 (m, =CH, 3H). ^{13}C-APT NMR (DMSO-d_6): 163.92, 146.15, 145.18, 139.01, 132.96, 131.83, 131.53, 131.40, 131.25, 127.61, 127.20, 127.08, 120.62, 117.41, 114.77. 19.82. Elemental analysis: $C_{16}H_{13}N_3O$ required C, 72.99; H, 4.98; N, 15.96, found C, 73.01; H, 5.09; N, 16.02.

3.2.2.9. (*E*)-1-(1*H*-benzo[*d*][1,2,3]triazol-1-yl)-3-(2-chlorophenyl)prop-2-en-1-one (2-chloro-CA-Bt)

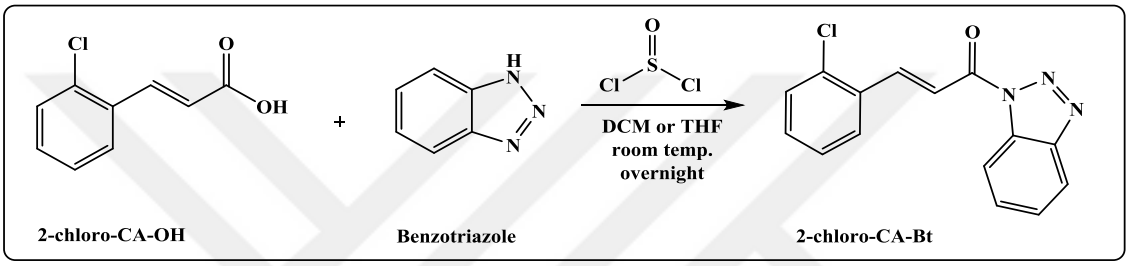

Benzotriazole (2.61 g; 21.91 mmol) and thionyl chloride (781.15 mg; 6.57 mmol) were dissolved in dichloromethane (40 ml) and after 15 minutes, 2-chloro-CA-OH (1.0 g; 5.48 mmol) was added to reaction mixture. After above mentioned purification steps, desired product 2-chloro-CA-Bt was obtained as a white solid (1.39 g; 4.90 mmol) with yield 89.46%. Melting point: 138-141 ºC, lit: 143-146 ºC. ^{1}H NMR (DMSO-d_6) δ: 8.41–8.35 (t, *J* = 16.0 Hz, 8.8 Hz, =CH, 2H), 8.31 (d, *J* = 8.0 Hz, =CH, 1H), 8.20–8.14 (t, *J* = 8.0 Hz, 16.0 Hz, =CH, 2H), 7.86–7.82 (t, *J* = 7.6 Hz, =CH, 1H,), 7.68–7.64 (t, *J* = 8.8 Hz, =CH, 2H,), 7.59–7.50 (, m, =CH, 2H). ^{13}C-APT NMR (DMSO-d_6): 163.67, 146.17, 142.18, 135.01, 133.40, 131.88, 131.36, 130.75, 129.42, 128.55, 127.20, 120.66, 119.66, 114.80. Elemental analysis: $C_{15}H_{10}ClN_3O$ required C, 63.50; H, 3.55; N, 14.81, found C, 63.58; H, 3.66; N, 14.92. The spectroscopic results are compatible with the literature (Xia et al. 2011).

3.2.2.10. (*E*)-1-(1*H*-benzo[*d*][1,2,3]triazol-1-yl)-3-(2-fluorophenyl)prop-2-en-1-one (2-fluoro-CA-Bt)

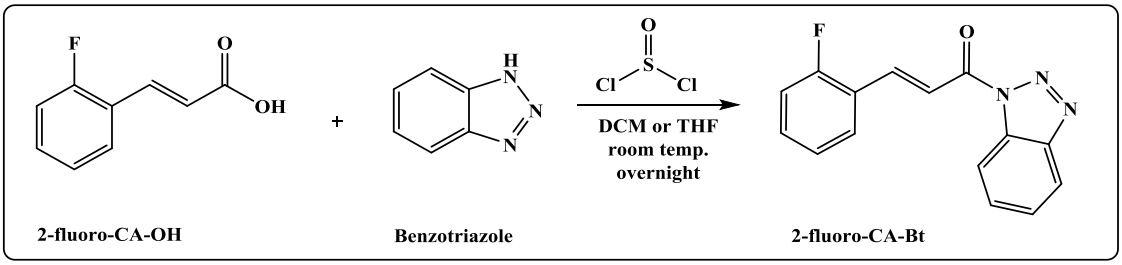

Benzotriazole (2.87 g; 24.07 mmol) and thionyl chloride (859.16 mg; 7.22 mmol) were dissolved in dichloromethane (40 ml) and after 15 minutes, 2-fluoro-CA-OH (1.0 g; 6.02 mmol) was added to reaction mixture. After above mentioned purification steps, desired product 2-fluoro-CA-Bt was obtained as a dark white (1.19 g; 4.45 mmol) with yield 73.98%. Melting point: 142-145 ^{o}C. ^{1}H NMR (DMSO-d$_6$) δ: 8.33 (d, *J* = 8.4 Hz, =CH, 1H), 8.28 (d, *J* = 8.4 Hz, =CH, 1H,), 8.14 (s, =CH, 2H), 8.07 – 8.03 (t, *J* = 8.0 Hz, =CH, 1H), 7.84-7.81 (t, *J* = 7.6 Hz, =CH, 1H), 7.60–7.59 (m, =CH, 2H), 7.42–7.34 (m, =CH, 2H). ^{13}C-APT NMR (DMSO-d$_6$): 163.83, 162.92, 160.40, 146.16, 140.49, 134.15–134.06, 131.32–131.12, 127.16, 125.81, 122.12–121.99, 120.65, 119.35–119.29, 116.95–116.73, 114.81. Elemental analysis: $C_{15}H_{10}FN_3O$ required C, 67.41; H, 3.77; N, 15.72, found C, 67.45; H, 3.85; N, 15.78.

3.2.3. General Synthesis Procedures of Amino Acid Conjugates

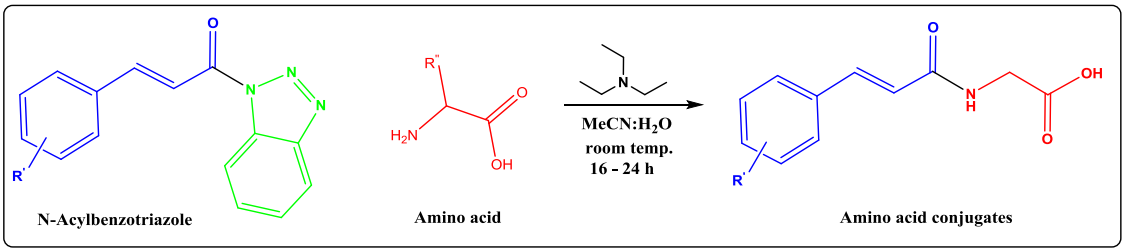

Amino acid (1.0 eq.) was dissolved in MeCN:H_2O (7:3) and then triethylamine (1.2 eq.) was added to the solution at room temperature. After 15 minutes, cinnamoyl-Bt (1.0 eq) compound was added to the mixture and stirred for overnight. The reaction was monitored via thin layer chromatography. After the completion of the reaction, all reaction solvent

was removed. The obtained crude product was precipitated in distilled water (200 ml). The obtained precipitate was filtered and dried. Yield varies between 50 - 75%.

3.2.3.1. (*E*)-(3-([1,1'-biphenyl]-4-yl)acryloyl)glycine (phenylbenzyl-CA-Gly-OH)

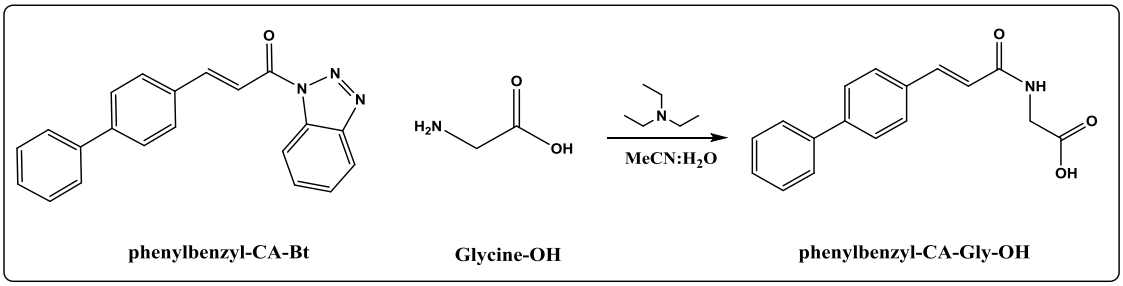

Glycine (173.03 mg; 2.31 mmol) was dissolved in MeCN:H_2O (7:3) and then triethylamine (2.77 mmol; 0.187 mL) was added to the solution at room temperature. After 15 minutes, phenylbenzyl-Bt (750.0 mg; 2.31 mmol) was added to the mixture and stirred for overnight. Ater completion of prufication steps, the desired product Phenylbenzyl-CA-Gly-OH (495.30 mg; 1.76 mmol) was obtained %76.38 yield as a white solid. Melting point: 205-208 ºC. FT-IR (ATR, cm^{-1}) υ_{N-H} 3380 cm^{-1}, $\upsilon_{=C-H}$ 3058 cm^{-1}, υ_{O-H} 3276 cm^{-1}, $\upsilon_{C=O}$ 1717 and 1652cm^{-1}, $\upsilon_{C=C}$ 1597 and 1540 cm^{-1}, υ_{C-O} 1202cm^{-1}. ^{1}H NMR (DMSO-d_6) δ: 8.14-8.12 (t, *J* = 5.0 Hz, =CH, 1H), 7.68 (d, *J* = 9.6 Hz, =CH, 6H), 7.50–7.43 (m, =CH, 3H), 7.38 (d, *J* = 7.2 Hz, =CH, 1H), 6.96 (d, *J* = 16.0 Hz, =CH, 1H), 3.81-3.80 (d, *J* = 5.2 Hz, -CH, 2H). ^{13}C-APT NMR (DMSO-d_6): 168.53, 165.24, 141.35, 139.84, 138.47, 134.64, 129.47, 128.66, 128.24, 127.56, 127.07, 122.96, 43.31. Elemental analysis: $C_{17}H_{15}NO_3$ required C, 72.58; H, 5.37; N, 4.98, found C, 72.60; H, 5.48; N, 5.08.

3.2.3.2. (*E*)-(3-([1,1'-biphenyl]-4-yl)acryloyl)alanine (phenylbenzyl-CA-Ala-OH)

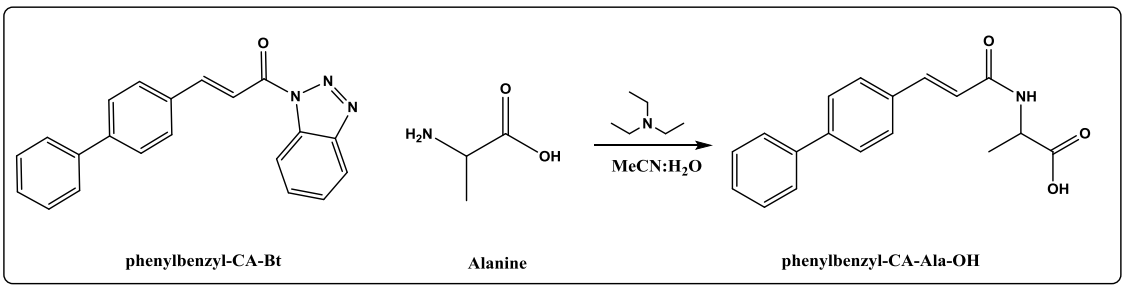

L-Alanine (136.91 mg; 1.54 mmol) was dissolved in MeCN:H_2O (7:3) and then triethylamine (257 mmL; 1.84 mmol) was added to the solution at room temperature. After 15 minutes, phenylbenzyl-Bt (500.0 mg; 1.54 mmol) was added to the mixture and stirred for overnight. Ater completion of prufication steps, desired product Phenylbenzyl-CA-Ala-OH (395.6 mg; 1.17 mmol) was obtained %76.29 yield as a light yellow. Melting point: 210-214 ^{o}C. FT-IR (ATR, cm^{-1}) υ_{N-H} 3380 cm^{-1}, $\upsilon_{=C-H}$ 3058 cm^{-1}, υ_{O-H} 3276 cm^{-1}, $\upsilon_{C=O}$ 1717 and 1652cm^{-1}, $\upsilon_{C=C}$ 1597 and 1540 cm^{-1}, υ_{C-O} 1202cm^{-1}. ^{1}H NMR (DMSO-d_6) δ: 8.30 (d, *J* = 6.8 Hz, =CH, 1H), 7.74–7.66 (m, =CH, 6H), 7.50-7.43 (m, =CH, 4H), 6.87–6.83 (d, *J* = 16.0 Hz, =CH, 1H), 4.30-4.27 (t, *J* = 7.2 Hz, -CH, 1H), 1.32 (d, *J* = 6.8 Hz, -CH_3, 3H). ^{13}C-APT NMR (DMSO-d_6): 175.45, 164.87, 141.42, 139.83, 138.68, 134.58, 129.48, 128.65, 128.26, 127.59, 127.08, 122.78, 49.03, 18.57. Elemental analysis: $C_{18}H_{17}NO_3$ required C, 73.20; H, 5.80; N, 4.74, found C, 73.26; H, 5.94; N, 4.79.

3.2.3.3. (*E*)-(3-([1,1'-biphenyl]-4-yl)acryloyl)leucine (phenylbenzyl-CA-Leu-OH)

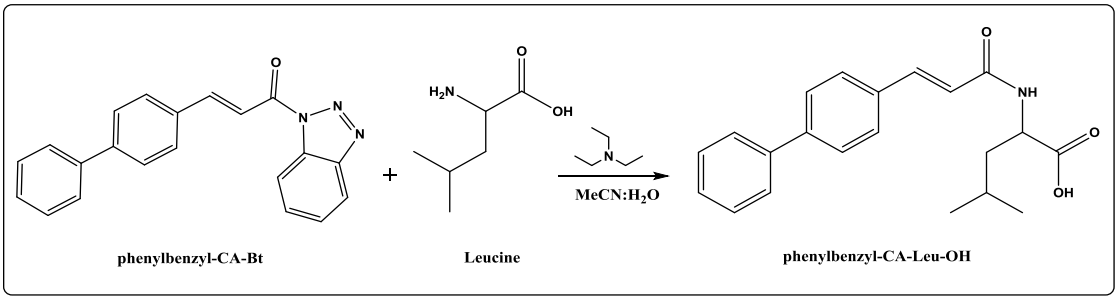

L-Leucine (201.58 mg; 1.54 mmol) was dissolved in MeCN:H_2O (7:3) and then triethylamine (257 mmL; 1.84 mmol) was added to the solution at room temperature. After 15 minutes, phenylbenzyl-Bt (500.0 mg; 1.54 mmol) was added to the mixture and stirred

for overnight. Ater completion of prufication steps, the desired product Phenylbenzyl-CA-Ala-OH (395.6 mg; 1.17 mmol) was obtained %76.29 yield as a white solid. Melting point: 215-218 ^{o}C. FT-IR (ATR, cm^{-1}) υ $_{N-H}$ 3286 cm^{-1}, υ $_{=C-H}$ 3060 cm^{-1}, υ $_{O–H}$ 3300 cm^{-1}, υ $_{C=O}$ 1716 and 1651 cm^{-1}, υ $_{C=C}$ 1602 and 1539 cm^{-1}, υ $_{C–O}$ 1207 cm^{-1}. ^{1}H NMR (DMSO-d$_6$) δ: 8.22 (d, *J* = 8.4 Hz, =CH, 1H,), 7.75–7.71 (m, =CH, 4H), 7.67 (d, *J* = 8.4 Hz, =CH, 2H), 7.51–7.46 (m, 4H), 7.41–7.38 (t, *J* = 7.2 Hz, =CH, 1H,), 4.40–4.34 (m, -CH, 1H), 1.72–1.65 (m, -CH, 1H,), 1.61–1.54 (m, -CH$_2$, 2H), 0.93 - 0.89 (dd, *J* = 6.4 Hz, -CH$_3$, 6H,). ^{13}C-APT NMR (DMSO-d$_6$): 168.36, 165.12, 141.39, 139.83, 138.67, 134.61, 129.48, 128.63, 127.59, 127.07, 122.80, 51.72, 41.47, 24.96, 23.48, 22.09. Elemental analysis: $C_{21}H_{23}NO_3$ required C, 74.75; H, 6.87; N, 4.15, found C, 74.82; H, 6.98; N, 4.29.

3.2.3.4. (*E*)-(3-(naphthalen-1-yl)acryloyl)glycine (Naft-CA-Gly-OH)

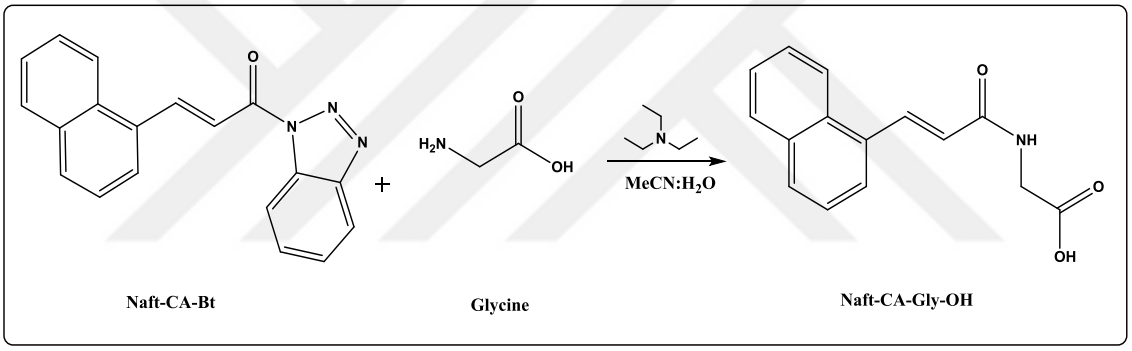

Glycine (175.55 mg; 2.34 mmol) was dissolved in MeCN:H_2O (7:3) and then triethylamine (391 mmL; 2.81 mmol) was added to the solution at room temperature. After 15 minutes, Naft-Bt (500.0 mg; 1.54 mmol) was added to the mixture and stirred for overnight. Ater completion of prufication steps, the desired product Naft-CA-Gly-OH (523.1 mg; 2.05 mmol) was obtained %87.63 yield as a dark white. Melting point: 210-215 ^{o}C. FT-IR (ATR, cm^{-1}) υ $_{N-H}$ 3360 cm^{-1}, υ $_{=C-H}$ 3060 cm^{-1}, υ $_{C=O}$ 1744 and 1649 cm^{-1}, υ $_{C=C}$ 1587 and 1542 cm^{-1}, υ $_{C–O}$ 1218 cm^{-1}. ^{1}H NMR (DMSO-d$_6$) δ: 12.69 (bs, CO_2H, 1H), 8.62 (d, -NH, 1H), 8.27–8.20 (m, =CH, 2H), 8.01 (d, *J* = 8.4 Hz, =CH, 2H,), 7.82 (d, *J* = 7.2 Hz, =CH, 1H,), 7.57–7.65 (m, =CH, 3H), 6.78-6.82 (d, *J* = 15.6 Hz, 1H), 3.95 (d, *J* = 5.6 Hz, -CH$_2$, 2H). ^{13}C-APT NMR (DMSO-d$_6$): 171.77, 165.71, 136.17, 133.82, 132.38, 131.29, 130.13, 129.15, 127.40, 126.72, 126.24, 125.15, 125.00, 123.64, 41.40. Elemental analysis: $C_{15}H_{13}NO_3$ required C, 70.58; H, 5.13; N, 5.49, found C, 70.67; H, 5.20; N, 5.55.

3.2.3.5. (*E*)-(3-(naphthalen-1-yl)acryloyl)alanine (Naft-CA-Ala-OH)

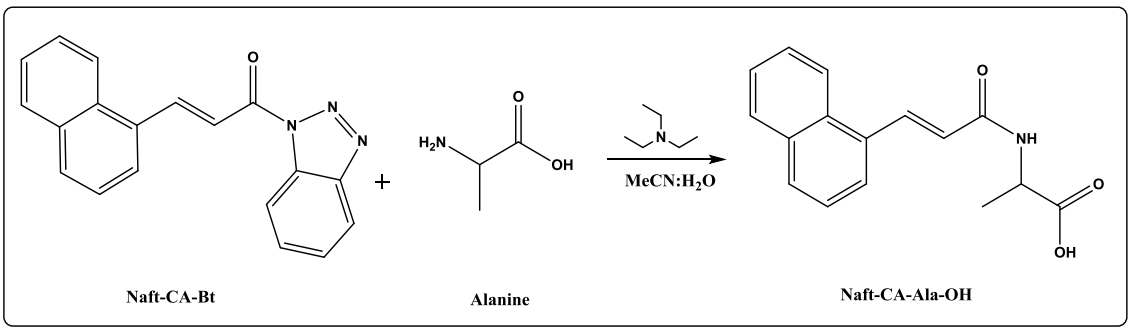

L-Alanine (148.82 mg; 1.67mmol) was dissolved in MeCN:H_2O (7:3) and then triethylamine (279 mmL; 2.00 mmol) was added to the solution at room temperature. After 15 minutes, Naft-Bt (500.0 mg; 1.67 mmol) was added to the mixture and stirred for overnight. Ater completion of prufication steps, the desired product Naft-CA-Ala-OH (321.3 mg; 1.19 mmol) was obtained %71.43 yield as a white solid. Melting point: 222-225 ^{o}C. FT-IR (ATR, cm^{-1}) υ_{N-H} 3360 cm^{-1}, $\upsilon_{=C-H}$ 3060 cm^{-1}, $\upsilon_{C=O}$ 1744 and 1649 cm^{-1}, $\upsilon_{C=C}$ 1587 and 1542 cm^{-1}, υ_{C-O} 1218 cm^{-1}. ^{1}H NMR (DMSO-d_6) δ: 8.52 (d, *J* = 7.2 Hz, -NH, 1H), 8.26–8.20 (t, *J* = 15.6 Hz, 8.0 Hz, =CH, 2H), 8.00 (d, *J* = 8.0 Hz, =CH, 2H,), 7.80 (d, *J* = 6.8 Hz, =CH, 1H), 7.65–7.57 (m, =CH, 3H), 6.80 (d, *J* = 15.6 Hz, =CH, 1H), 4.46-4.36 (m, -CH, 1H), 1.38 (d, *J* = 7.2 Hz, -CH_3, 3H). ^{13}C-APT NMR (DMSO-d_6): 174.70, 165.05, 136.11, 132.44, 131.28, 130.10, 129.15, 127.40, 126.72, 126.25, 125.27, 124.98, 123.67, 48.30, 17.90. Elemental analysis: $C_{16}H_{15}NO_3$ required C, 71.36; H, 5.61; N, 5.20, found C, 71.45; H, 5.72; N, 5.31.

3.2.3.6. (*E*)-(3-(naphthalen-1-yl)acryloyl)methionine (Naft-CA-Meth-OH)

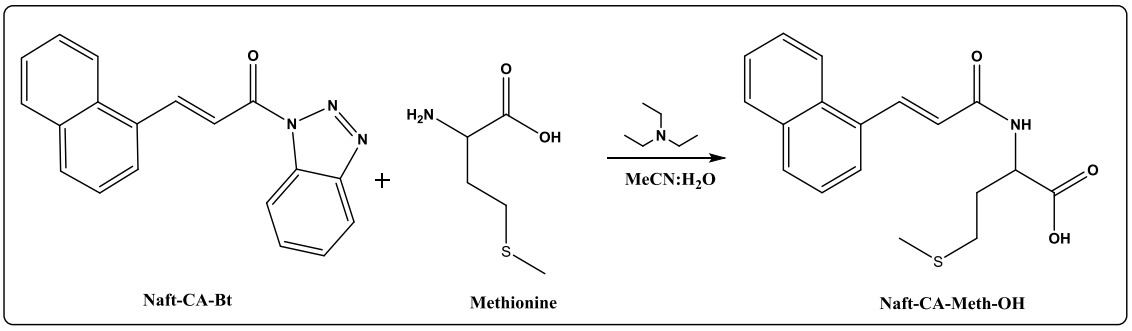

L-methionine (249.23 mg; 1.67mmol) was dissolved in MeCN:H_2O (7:3) and then triethylamine (273 mmL; 2.00 mmol) was added to the solution at room temperature. After 15 minutes, Naft-Bt (500.0 mg; 1.67 mmol) was added to the mixture and stirred for overnight. Ater completion of prufication steps, the desired product Naft-CA-Meth-OH (395.0 mg; 1.20 mmol) was obtained %71.79 yield as a white solid. Melting point: 231-236 ^oC.^1H NMR (DMSO-d_6) δ: 8.45 (d, *J* = 6.8 Hz, -NH, 1H), 8.23–8.20 (t, *J* = 6.0 Hz, =CH, 1H), 8.00–7.98 (t, *J* = 4.0 Hz, =CH, 2H), 7.83-7.80 (t, *J* = 6.4 Hz, =CH, 1H), 7.65–7.56 (m, =CH, 4H,), 6.86–6.81 (dd, *J* = 5.4 Hz, =CH, 1H), 4.51-4.51(m, -CH, 1H), 2.57 (d, *J* = 6.0 Hz, -CH_2, 2H), 2.08 (d, *J* = 6.4 Hz, -CH_3, 3H), 2.03 (m, A part of AB system -CH, 1H), 1.93-1.88 (m, B part of AB system, 1H). ^{13}C-APT NMR (DMSO-d_6): 174.36, 165.13, 136.47, 131.68, 131.42, 130.65, 130.42, 130.15, 129.48, 128.07, 127.81, 127.59, 126.35, 126.06, 124.67, 124.03, 123.34, 52.68, 32.08, 30.38, 15.12. Elemental analysis: $C_{18}H_{19}NO_3S$ required C, 65.63; H, 5.81; N, 4.25, S, 9.73 found C, 65.70; H, 5.98; N, 4.32; S, 9.69.

3.2.3.7. (*E*)-(3-(phenanthren-9-yl)acryloyl)glycine (Phenant-CA-Gly-OH)

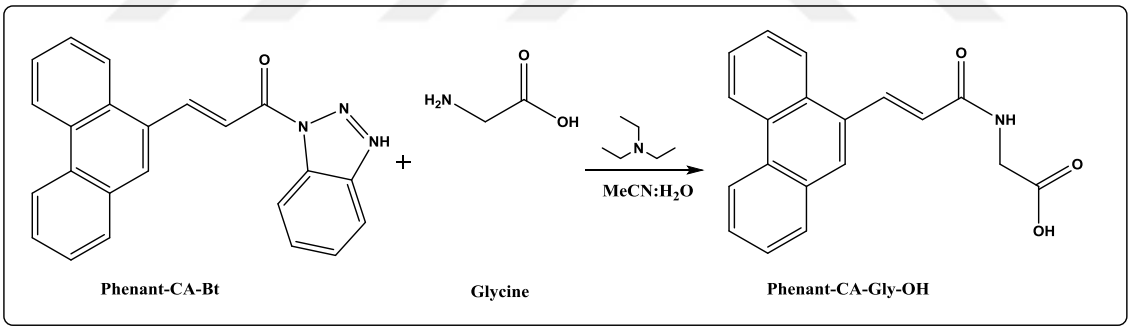

Glycine (149.95 mg; 2.00 mmol) was dissolved in MeCN:H_2O (7:3) and then triethylamine (326 mmL; 2.40 mmol) was added to the solution at room temperature. After 15 minutes, Phenant-Bt (700.0 mg; 2.00 mmol) was added to the mixture and stirred for overnight. Ater completion of prufication steps, the desired product Phenant-CA-Gly-OH (385.2. mg; 1.26 mmol) was obtained %63.15 yield as a light brown solid. Melting point: 192-195 ^oC. FT-IR (ATR, cm^{-1}) υ $_{N-H}$ 3246 cm^{-1}, υ $_{=C-H}$ 3069 cm^{-1}, υ $_{O-H}$ 3200 cm^{-1}, υ $_{C=O}$ 1749 and 1650 cm^{-1}, υ $_{C=C}$ 1613 and 1558 cm^{-1}, υ $_{C-O}$ 1208 cm^{-1}. ^1H NMR (DMSO-d_6) δ: 8.89 (d, *J* = 7.2 Hz, =CH, 1H), 8.82 (d, *J* = 8.4 Hz, =CH, 1H), 8.31 (s, =CH, 1H), 8.25– 8.22 (t, *J* = 7.8 Hz,

=CH, 2H), 8.12 (s, =CH, 1H), 8.05–8.03 (d, *J* = 7.6 Hz, =CH, 1H), 7.76–7.64 (m, =CH, 5H), 6.98–6.94 (d, *J* = 15.6 Hz, =CH, 1H), 3.89–3.88 (d, *J* = 5.2 Hz, -CH_2, 2H). ^{13}C-APT NMR (DMSO-d_6): 173.11, 165.25, 145.97, 136.22, 131.67, 131.40, 130.17, 129.47, 128.02, 127.78, 127.67, 127.56, 126.47, 125.98, 124.63, 124.01, 123.31, 43.14. Elemental analysis: $C_{19}H_{15}NO_3$ required C, 74.74; H, 4.95; N, 4.59, found C, 74.82; H, 4.99; N, 4.63.

3.2.3.8. (*E*)-(3-(phenanthren-9-yl)acryloyl)methionine (Phenant-CA-Meth-OH)

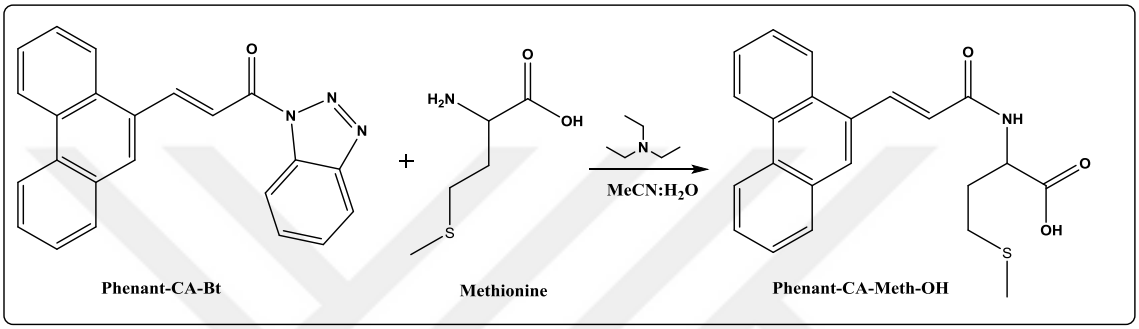

L-methionine (213.52 mg; 1.43 mmol) was dissolved in MeCN:H_2O (7:3) and then triethylamine (234 mmL; 1.72 mmol) was added to the solution at room temperature. After 15 minutes, Phenant-Bt (500.0 mg; 1.43 mmol) was added to the mixture and stirred for overnight. Ater completion of prufication steps, the desired product Phenant-CA-Meth-OH (413.2. mg; 1.09 mmol) was obtained %76.09 yield as a light yellow. Melting point: 202-205 ºC. FT-IR (ATR, cm^{-1}) υ $_{N-H}$ 3246 cm^{-1}, υ $_{=C-H}$ 3069 cm^{-1}, υ $_{O-H}$ 3200 cm^{-1}, υ $_{C=O}$ 1749 and 1650 cm^{-1}, υ $_{C=C}$ 1613 and 1558 cm^{-1}, υ $_{C-O}$ 1208 cm^{-1}. ^{1}H NMR (DMSO-d_6) δ: 8.93–8.91 (dd, *J* = 1.8 Hz, =CH, 1H), 8.85 (d, *J* = 8.4 Hz, =CH, 1H), 8.42 (d, *J* = 8.0 Hz, =CH, 1H), 8.25–8.22 (m, =CH, 2H), 8.14 (s, =CH, 1H), 8.07–8.05 (m, =CH, 1H), 7.76–7.68 (m, =CH, 5H), 6.94 (d, *J* = 15.2 Hz, =CH, 1H,), 4.47–4.45 (t, *J* = 4.0 Hz, -CH, 1H), 2.59–2.55 (t, *J* = 7.6 Hz, -CH_2, 2H), 2.08 (s, -CH_3, 3H), 2.00-1.94 (m, -CH, 1H). ^{13}C-APT NMR (DMSO-d_6): 174.36, 165.13, 136.47, 131.68, 131.42, 130.65, 130.42, 130.15, 129.48, 128.07, 127.81, 127.71, 127.59, 126,35, 126.06, 124.67, 124.03, 123.34, 52.68, 32.08, 30.38, 15.12. Elemental analysis: $C_{22}H_{21}NO_3S$ required C, 69.63; H, 5.58; N, 3.69; S, 8.45 found C, 69.71; H, 5.74; N, 3.73; S, 8.49.

3.2.3.9. (*E*)-(3-(pyren-4-yl)acryloyl)glycine (Pyrene-CA-Gly-OH)

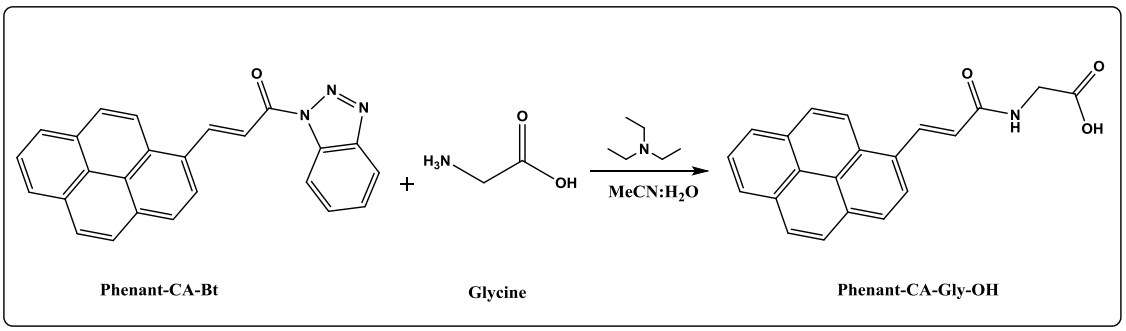

Glycine (101.86 mg; 1.34 mmol) was dissolved in MeCN:H_2O (7:3) and then triethylamine (219 mmL; 1.61 mmol) was added to the solution at room temperature. After 15 minutes, pyrene-CA-Bt (500.0 mg; 1.34 mmol) was added to the mixture and stirred for overnight. Ater completion of prufication steps, the desired product Pyrene-CA-Gly-OH (285.3 mg; 0.866 mmol) was obtained %64.69 yield as a green solid. Melting point: 221-225 ^{o}C. FT-IR (ATR, cm^{-1}) υ_{N-H} 3307 cm^{-1}, $\upsilon_{=C-H}$ 3090 and 3020 cm^{-1}, υ_{O-H} 3200 cm^{-1}, $\upsilon_{C=O}$ 1733 and 1648 cm^{-1}, υ_{C-O} 1217 cm^{-1}. ^{1}H NMR (DMSO-d_6) δ: 8.57 -8.53 (m, =CH, 3H), 8.38–8.26 (m, =CH, 5H), 8.22 (d, *J* = 8.8 Hz, =CH, 1H), 8.17–8.15 (d, *J* = 8.8 Hz, =CH, 1H), 8.11–8.08 (t, *J* = 7.6 Hz, =CH, 1H,), 7.12–7.08 (d, *J* = 15.6 Hz, =CH, 1H), 3.94 (d, *J* = 5.2 Hz, -CH_2, 2H). ^{13}C-APT NMR (DMSO-d_6): 169.03, 165.03, 145.93, 135.65, 132.03, 131.37, 130.74, 129.34, 129.13, 128.90, 128. 58, 127.82, 127.05, 126.39, 126.12, 125.83, 125.37, 124.61, 124.34, 122.97, 42.16. Elemental analysis: $C_{21}H_{15}NO_3$ required C, 76.58; H, 4.59; N, 4.25, found C, 76.65; H, 4.66; N, 4.28.

3.2.3.10. (*E*)-(3-(2,4,5-trimethoxyphenyl)acryloyl)glycine (2,4,5-trimethoxy-CA-Gly-OH)

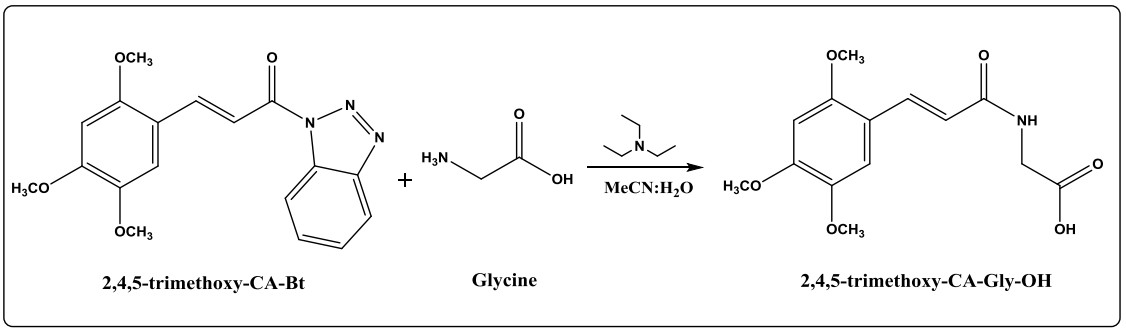

Glycine (168.13 mg; 2.21 mmol) was dissolved in MeCN:H_2O (7:3) and then triethylamine (361 mmL; 2.65 mmol) was added to the solution at room temperature. After 15 minutes, 2,4,5-trimethoxy-CA-Bt (750.0 mg; 2.21 mmol) was added to the mixture and stirred for overnight. After completion of purification steps, the desired product 2,4,5-trimethoxy-CA-Gly-OH (495.3 mg; 1.68 mmol) was obtained %75.89 yield as a yellow solid. Melting point: 182-184 ^oC. FT-IR (ATR, cm^{-1}) υ_{N-H} 3284 cm^{-1}, $\upsilon_{=C-H}$ 3056 cm^{-1}, υ_{O-H} 3200 cm^{-1}, $\upsilon_{C=O}$ 1684 and 1621 cm^{-1}, $\upsilon_{C=C}$ 1648 cm^{-1}. ^1H NMR (DMSO-d_6) δ: 12.55 (bs, CO_2H, 1H), 8.25–8.23 (t, *J* = 8.0 Hz, -NH, 1H), 7.64 (d, *J* = 16.0 Hz, =CH, 1H), 7.11 (s, =CH, 1H), 6.74 (s, =CH, 1H), 6.65–6.61 (d, *J* = 16.0 Hz, =CH, 1H), 3.92–3.91 (m, -CH_2, 2H), 3.87 (s, -OCH_3, 3H), 3.86 (s, -OCH_3, 3H), 3.76 (s, OCH_3, 3H). ^{13}C-APT NMR (DMSO-d_6): Elemental analysis: $C_{14}H_{17}NO_6$ required C, 56.95; H, 5.80; N, 4.74, found C, 56.99; H, 5.86; N, 4.83.

3.2.3.11. (*E*)-(3-(2,4-dimethoxyphenyl)acryloyl)glycine (2,4-dimethoxy-CA-Gly-OH)

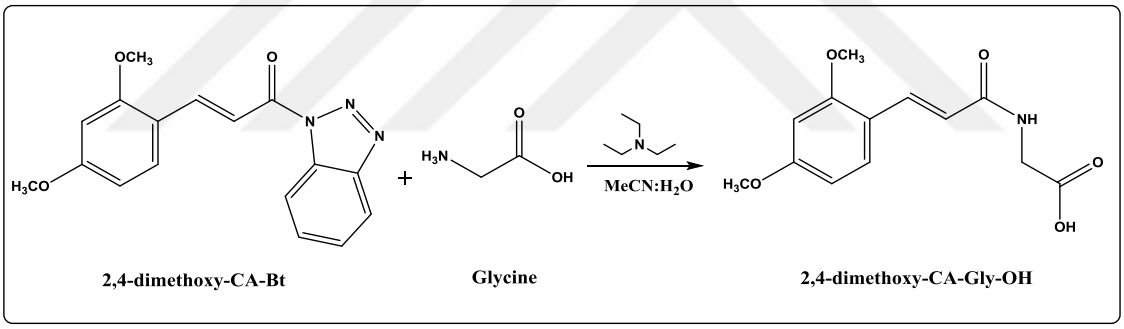

Glycine (196.75 mg; 2.59 mmol) was dissolved in MeCN:H_2O (7:3) and then triethylamine (423 mmL; 3.10 mmol) was added to the solution at room temperature. After 15 minutes, 2,4-dimethoxy-CA-Bt (800.0 mg; 2.59 mmol) was added to the mixture and stirred for overnight. After completion of purification steps, the desired product 2,4-dimethoxy-CA -Gly-OH (523.6 mg; 1.97 mmol) was obtained %76.32 yield as a yellow solid. Melting point: 170-172 ^oC. FT-IR (ATR, cm^{-1}) υ_{N-H} 3241 cm^{-1}, $\upsilon_{=C-H}$ 3062 cm^{-1}, υ_{O-H} 3270 cm^{-1}, $\upsilon_{C=O}$ 1724 and 1647 cm^{-1}, $\upsilon_{C=C}$ 1596, 1557, 1502 cm^{-1}, υ_{C-O} 1215 cm^{-1}. ^1H NMR (DMSO-d_6) δ: 12.60 (bs, CO_2H, 1H), 8.28–8.25 (t, *J* = 6.0 Hz, -NH, 1H), 7.60 (d, *J* = 16.0 Hz, =CH, 1H,), 7.48 (d, *J* = 8.4 Hz, 1H), 6.63–6.59 (m, =CH, 3H,), 3.88–3.86 (m, -CH_2 and -OCH_3 5H), 3.82 (s, OCH_3, 3H). ^{13}C-APT NMR (DMSO-d_6): 171.95, 166.49, 162.31, 159.49,

134.62, 129.67, 119.89, 116.60, 106.46, 98.96, 56.13, 55.88, 41.32. Elemental analysis: $C_{13}H_{15}NO_5$ required C, 58.86; H, 5.70; N, 5.28, found C, 58.91; H, 5.73; N, 5.33.

3.2.3.12. (*E*)-(3-(2,4-dimethoxyphenyl)acryloyl)methionine (2,4-dimethoxy-CA-Meth-OH)

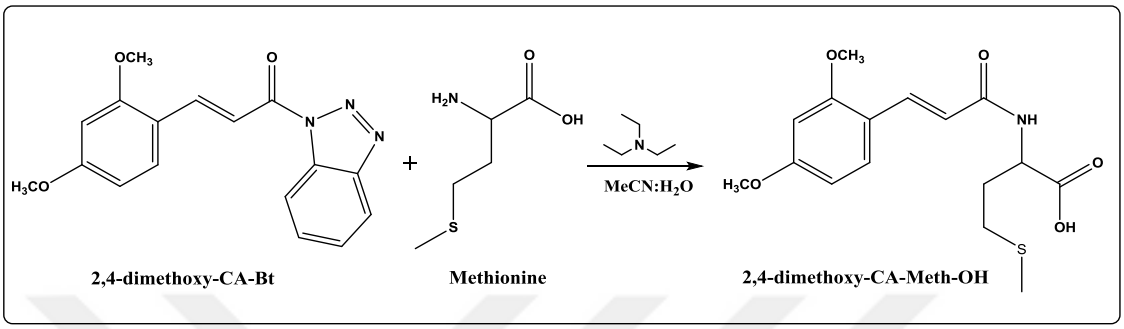

L-methionine (361.77 mg; 2.42 mmol) was dissolved in MeCN:H_2O (7:3) and then triethylamine (396 mmL; 2.91 mmol) was added to the solution at room temperature. After 15 minutes, 2,4-dimethoxy-CA-Bt (750.0 mg; 2.42 mmol) was added to the mixture and stirred for overnight. After completion of purification steps, the desired product 2,4-dimethoxy-CA -Meth-OH (665.2 mg; 1.96 mmol) was obtained %80.83 yield as a white solid. Melting point: 174-177 ^oC. FT-IR (ATR, cm^{-1}) υ_{N-H} 3288 cm^{-1}, υ_{O-H} 3200 cm^{-1}, $\upsilon_{C=O}$ 1719 and 1646 cm^{-1}, $\upsilon_{C=C}$ 1603, 1526 cm^{-1}, υ_{C-O} 1212 cm^{-1}. ^1H NMR (DMSO-d_6) δ: 12.64 (bs, CO_2H, 1H), 8.26 (d, *J* = 8.0 Hz, -NH, 1H), 7.59 (d, *J* = 16.0 Hz, =CH, 1H), 7.46 (d, *J* = 8.4 Hz, =CH, 1H), 6.65–6.59 (m, =CH, 3H), 4.47–4.41 (m, -CH, 1H), 3.87 (s, -OCH_3, 3H), 3.82 (s, -OCH_3, 3H), 2.52-2.51 (m, -CH_2, 4H), 2.06 (s, -CH_3, 3H,). ^{13}C-APT NMR (DMSO-d_6): 173.96, 166.31, 162.31, 159.53, 134.79,129.82, 119.94, 116.61, 106.44, 98.98, 56.13, 55.88, 51.60, 31.40, 30.24, 15.06. Elemental analysis: $C_{16}H_{21}NO_5S$ required C, 56.62; H, 6.24; N, 4.13, S, 9.45; found C, 56.70; H, 6.29; N, 4.18; S, 9.52.

3.2.3.13. (*E*)-(3-(4-methoxyphenyl)acryloyl)glycine (4-methoxy-CA-Gly-OH)

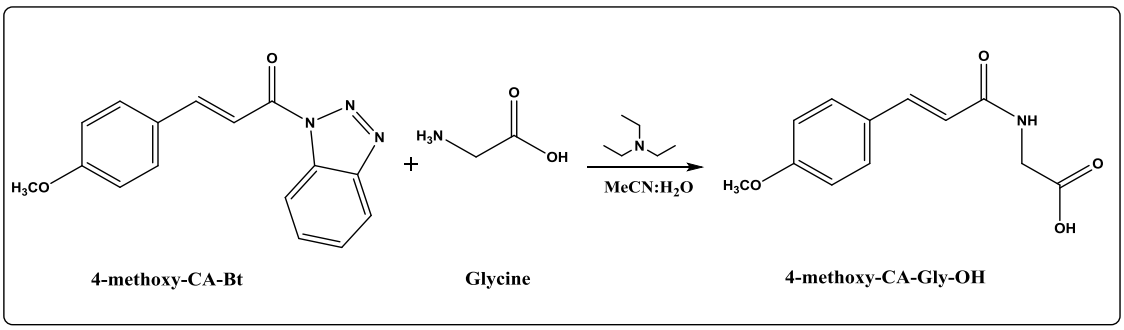

Glycine (272.38 mg; 3.58 mmol) was dissolved in MeCN:H_2O (7:3) and then triethylamine (585 mmL; 3.10 mmol) was added to the solution at room temperature. After 15 minutes, 4-methoxy-CA-Bt (1.0 g; 3.58 mmol) was added to the mixture and stirred for overnight. After completion of purification steps, the desired product 4-methoxy-CA -Gly-OH (726.3 mg; 3.07 mmol) was obtained %85.88 yield as a white solid (Acheson et al. 1960). Melting point: 162-165 ^oC, lit: 161-163 ^oC. FT-IR (ATR, cm^{-1}) υ_{N-H} 3463 cm^{-1}, $\upsilon_{=C-H}$ 3086 cm^{-1}, υ_{O-H} 3357 cm^{-1}, $\upsilon_{C=O}$ 1706 and 1657 cm^{-1}, $\upsilon_{C=C}$ 1598 cm^{-1}, υ_{C-O} 1211 cm^{-1}. ^1H NMR (DMSO-d_6) δ: 12.57 (bs, CO_2H, 1H), 8.31 (t, *J* = 6.0 Hz, -NH, 1H), 7.55–7.53 (m, =CH, AA′ part of AA′BB′ system, 2H), 7.41 (d, *J* = 16.0 Hz, =CH, 1H), 7.00–6.98 (m, =CH, BB′ part of AA′BB′ system, 2H), 6.58 (d, *J* = 16.0 Hz, =CH, 1H), 3.89 (d, *J* = 6.0 Hz, -CH_2, 2H), 3.80 (s, -OCH_3, 3H). ^{13}C-APT NMR (DMSO-d_6): 171.86, 166.05, 160.88, 139.36, 129.64, 127.64, 119.68, 114.88, 55.74, 41.28. Elemental analysis: $C_{12}H_{13}NO_4$ required C, 61.27; H, 5.57; N, 5.95, found C, 61.34; H, 5.62; N, 5.99.

3.2.3.14. (*E*)-(3-(4-methoxyphenyl)acryloyl)alanine (4-methoxy-CA-Ala-OH)

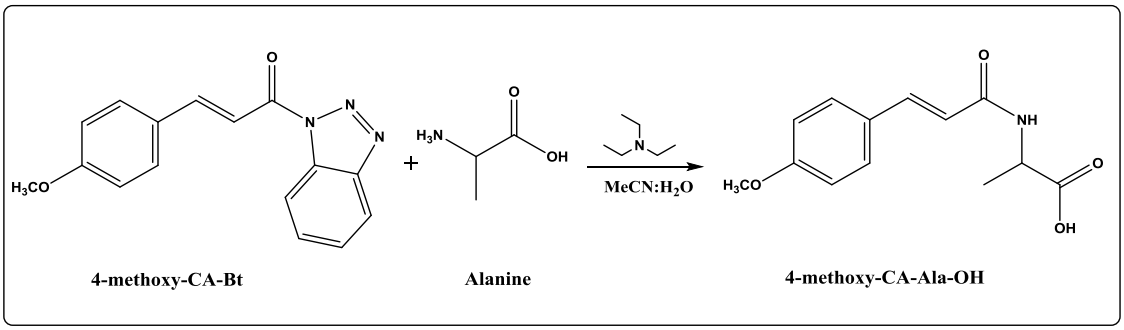

L-alanine (161.3 mg; 1.79 mmol) was dissolved in MeCN:H_2O (7:3) and then triethylamine (292 mmL; 3.10 mmol) was added to the solution at room temperature. After 15 minutes, 4-methoxy-CA-Bt (0.5 g; 1.79 mmol) was added to the mixture and stirred for overnight. After completion of purification steps, the desired product 4-methoxy-CA-Ala-OH (352.1 mg; 1.41 mmol) was obtained %78.90 yield as a yellow solid. Melting point: 167-169 ºC, lit: 162-164 ºC. FT-IR (ATR, cm^{-1}) υ $_{N-H}$ 3372 cm^{-1}, υ $_{=C-H}$ 3086 cm^{-1}, υ $_{O-H}$ 3264 cm^{-1}, υ $_{C=O}$ 1725 and 1648 cm^{-1}, υ $_{C=C}$ 1595 cm^{-1}, υ $_{C-O}$ 1208 cm^{-1}. ^{1}H NMR (DMSO-d_6) δ: 12.56 (bs, CO_2H, 1H), 8.35 (d, *J* = 7.2 Hz, -NH, 1H), 7.53-7.51 (m, =CH, AA′ part of AA′BB′ system, 2H), 7.39 (d, *J* = 15.6 Hz, =CH, 1H), 7.00-6.98 (m, =CH, BB′ part of AA′BB′ system, 2H), 6.57 (d, *J* = 15.6 Hz, =CH, 1H), 4.37-4.30 (m, =CH, 1H), 3.79 (s, OCH3, 3H), 1.32 (d, *J* = 7.6 Hz, -CH_3, 3H). ^{13}C-APT NMR (DMSO-d_6): 173.71, 165.55, 160.92, 139.64, 127.79, 119.40, 114.90, 55.74, 52.34, 48.17, 17.59. Elemental analysis: $C_{13}H_{15}NO_4$ required C, 62.64; H, 6.07; N, 5.62, found C, 62.71; H, 6.15; N, 5.69.

3.2.3.15. (*E*)-(3-(o-tolyl)acryloyl)glycine (2-methyl-CA-Gly-OH)

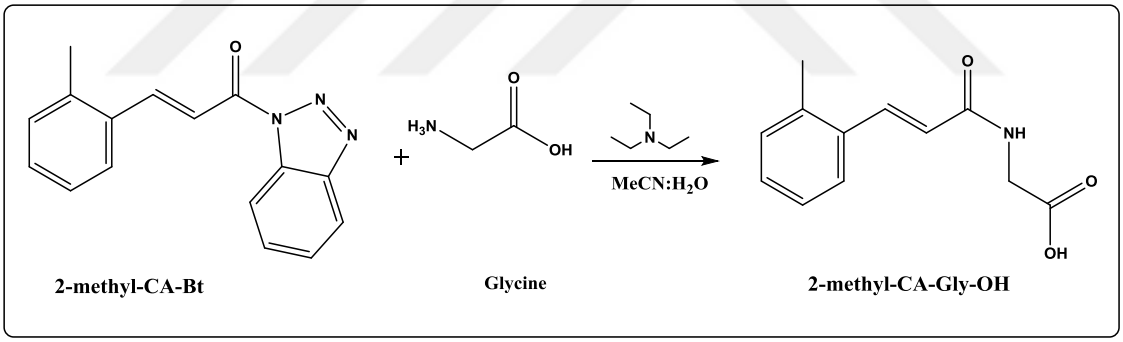

Glycine (216.70 mg; 2.85 mmol) was dissolved in MeCN:H_2O (7:3) and then triethylamine (466 mmL; 3.42 mmol) was added to the solution at room temperature. After 15 minutes, 2-methyl-CA-Bt (750.0 mg; 2.85 mmol) was added to the mixture and stirred for overnight. After completion of purification steps, the desired product 2-methyl-CA -Gly-OH (503.5 mg; 2.30 mmol) was obtained %80.62 yield as a white solid. Melting point: 127-129 ºC. FT-IR (ATR, cm^{-1}) υ $_{N-H}$ 3308 cm^{-1}, υ $_{=C-H}$ 3090 cm^{-1}, υ $_{C=O}$ 1734 and 1649 cm^{-1}, υ $_{C=C}$ 1602, 1575 cm^{-1}, υ $_{C-O}$ 1217 cm^{-1}. ^{1}H NMR (DMSO-d_6) δ: 12.65 (bs, CO_2H, 1H), 8.50–8.48 (d, *J* = 5.8 Hz, -NH, 1H), 7.69 (d, *J* = 16.0 Hz, =CH, 1H,), 7.58–7.55 (dd, *J* = 1.4 Hz, =CH, 1H), 7.28–7.27 (m, =CH, 3H), 6.63 (d, *J* = 16.0 Hz, =CH, 1H), 3.92–3.91 (d, *J* = 5.6

Hz, -CH_2, 2H,). ^{13}C-APT NMR (DMSO-d_6): 171.85, 165.78, 137.27, 137.12, 134.06, 131.18, 129.79, 126.90, 126.41, 123.26, 41.29, 19.89. Elemental analysis: $C_{12}H_{13}NO_3$ required C, 65.74; H, 5.98; N, 6.39, found C, 65.82; H, 6.06; N, 6.45.

3.2.3.16. (*E*)-(3-(2-chlorophenyl)acryloyl)glycine (2-chloro-CA-Gly-OH)

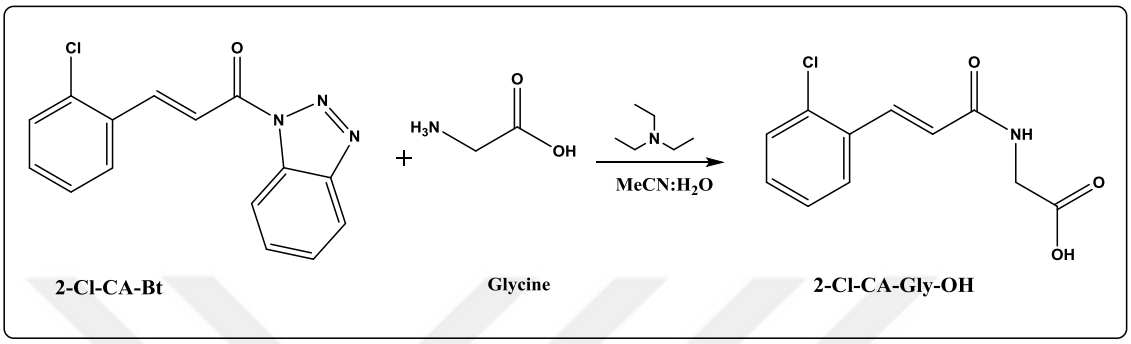

Glycine (134.07 mg; 1.76 mmol) was dissolved in MeCN:H_2O (7:3) and then triethylamine (288 mmL; 3.10 mmol) was added to the solution at room temperature. After 15 minutes, 2-chloro-CA-Bt (0.5 g; 1.76 mmol) was added to the mixture and stirred for overnight. After completion of purification steps, the desired product 2-chloro-CA -Gly-OH (356.2 mg; 1.49 mmol) was obtained %84.34 yield as light brown solid. Melting point: 173-176 ^{o}C. FT-IR (ATR, cm^{-1}) υ $_{N-H}$ 3304 cm^{-1}, υ $_{=C-H}$ 3120 cm^{-1}, υ $_{O-H}$ 3325, υ $_{C=O}$ 1736 and 1651 cm^{-1}, υ $_{C=C}$ 1606 and 1575 cm^{-1}, υ $_{C–O}$ 1215 cm^{-1}. ^{1}H NMR (DMSO-d_6) δ: 12.64 (bs, CO_2H, 1H), 8.55 – 8.52 (t, *J* = 5.8 Hz, -NH, 1H), 7.77 (d, *J* = 8.4 Hz, =CH, 1H), 7.75–7.73 (t, *J* = 3.0 Hz, =CH, 1H), 7.56–7.54 (dd, *J* = 3.6 Hz, =CH, 1H), 7.44–7.42 (dd, *J* = 3.6 Hz, =CH, 2H), 6.79 (d, *J* = 16.0 Hz, =CH, 1H), 3.92 (d, *J* = 6.0 Hz, -CH_2, 2H). ^{13}C-APT NMR (DMSO-d_6): 171.65, 165.26, 134.96, 133.80, 133.11, 131.48, 130.46, 128.27, 128.10, 125.24, 41.38. Elemental analysis: $C_{11}H_{10}ClNO_3$ required C, 55.13; H, 4.21; N, 5.84, found C, 55.15; H, 4.25; N, 5.86.

3.2.3.17. (*E*)-(3-(2-fluorophenyl)acryloyl)glycine (2-fluoro-CA-Gly-OH)

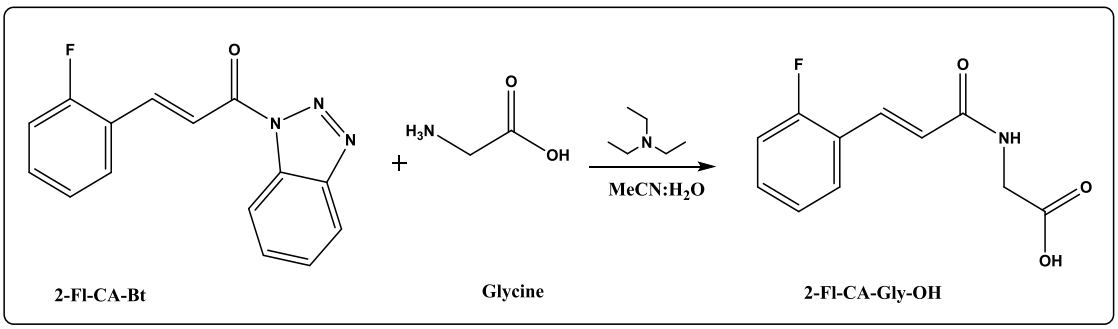

Glycine (142.32 mg; 1.87 mmol) was dissolved in MeCN: H_2O (7:3) and then triethylamine (306 mmL; 2.24 mmol) was added to the solution at room temperature. After 15 minutes, 2-fluoro-CA-Bt (500.0 mg; 1.87 mmol) was added to the mixture and stirred for overnight. After completion of purification steps, the desired product 2-fluoro-CA -Gly-OH (312.3 mg; 1.40 mmol) was obtained %74.79 yield as a light yellow. Melting point: 184-187 ^{o}C. FT-IR (ATR, cm^{-1}) υ_{N-H} 3225 cm^{-1}, $\upsilon_{=C-H}$ 3082 cm^{-1}, υ_{O-H} 3300, $\upsilon_{C=O}$ 1744 and 1647 cm^{-1}, υ_{C-O} 1194cm^{-1}. ^{1}H NMR (DMSO-d_6) δ: 12.61(bs, CO_2H, 1H), 8.56 – 8.53 (t, *J* = 6.0 Hz, -NH, 1H), 7.69 (d, *J* = 8.0 Hz, =CH, 1H), 7.53 (d, *J* = 16.0 Hz, =CH, 1H), 7.46–7.44 (m, =CH, 1H), 7.3–7.26 (m, =CH, 2H), 6.83 (d, *J* = 16.0 Hz, =CH, 1H), 3.92–3.91 (d, *J* = 6.0 Hz, -CH_2, 2H). ^{13}C-APT NMR (DMSO-d_6): 177.57, 171.68, 165.52, 162.19, 159.70, 132.00 – 131.98, 131.95 – 131.94, 129.59–129.57, 125.50–125.46, 125.01–124.98, 122.96–122.85, 116.67–116.45, 41.34. Elemental analysis: $C_{11}H_{10}FNO_3$ required C, 59.19; H, 4.52; N, 6.28, found C, 59.19; H, 4.55; N, 6.31.

3.2.4. General Synthetic Procedures for CDMT Based Amino Acid Conjugates (CA-AA-OMe)

Previously synthesized cinnamic acid derivatives (1 mmol), amino acid methyl ester (1 mmol) and 2-chloro-4,6-dimethoxy-1,3,5-triazine known as CDTM (1.05 mmol) were added to reaction flask and then asetonitrile (40 ml) was added to the mixture. The slurry stirred couple of minutes. N-Methylmorpholine (2.5 mmol if HCl salt of amino acid ester is used) was added drop wise. Reaction was monitored by tlc. After reaction completed, half of the reaction solvent was removed under rotary vacuum. Resulted mixture was added

to water and precipitate was filtered. After drying process, the target compounds were obtained. Yields (50-75 %).

3.2.4.1. Methyl (*E*)-(3-(4-nitrophenyl)acryloyl)glycinate (4-nitro-CA-Gly-OMe)

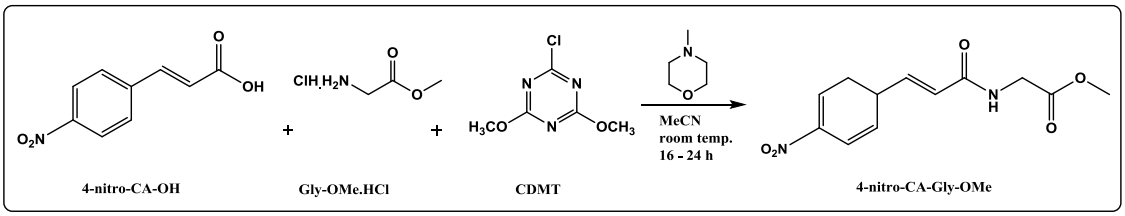

4-nitro-cinnamic acid (1.0 g; 5.18 mmol), Glycine methyl ester hydrochloride (639.56 mg; 5.18 mmol), and CDMT (1.09 g; 6.21 mmol) were taken into a reaction flask and 30 ml acetonitrile was added to the mixture then *N*-methyl morpholine added to the reaction mixture dropwise at room temperature. After the general purification steps, the desired product 4-nitro-CA-Gly-OMe (1.12 g; 4.21 mmol) was obtained in 81.25% yield as a white solid. Melting point: 128-132 ^{o}C. FT-IR (ATR, cm^{-1}) υ_{N-H} 3290 cm^{-1}, $\upsilon_{=C-H}$ 3077 cm^{-1}, $\upsilon_{C=O}$ 1741 and 1656 cm^{-1}, $\upsilon_{C=C}$ 1625 and 1511 cm^{-1}, υ_{C-O} 1212 cm^{-1}. ^{1}H NMR (DMSO-d_6) δ: 8.74–8.71 (t, *J* = 6.6 Hz, -NH, 1H), 8.29–8.27 (m, =CH, AA′ part of AA′BB′ system, 2H), 7.89–7.87 (m, =CH, BB′ part of AA′BB′ system, 2H), 7.59 (d, *J* = 15.8 Hz, =CH, 1H), 6.95–6.90 (d, *J* = 15.8 Hz, =CH, 1H), 4.03-4.02 (d, J = 5.6 Hz, -CH_2, 2H), and 3.67 (s, OCH_3, 3H). ^{13}C-APT NMR (DMSO-d_6): 170.75, 165.25, 148.07, 141.78, 137.66, 129.20, 126.05, 124.61, 52.29, 40.37. Elemental analysis: $C_{12}H_{12}N_2O_5$ required C, 54.55; H, 4.58; N, 10.60, found C, 54.58; H, 4.61; N, 10.68.

3.2.4.2. Methyl (*E*)-(3-(4-nitrophenyl)acryloyl)alaninate (4-nitro-CA-Ala-OMe)

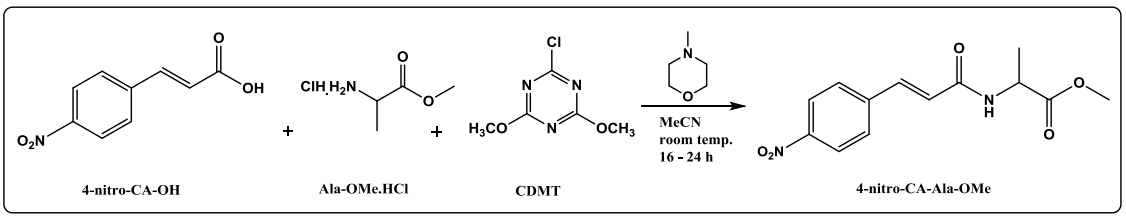

4-nitro-cinnamic acid (1.0 g; 5.18 mmol), alanine methyl ester hydrochloride (712.18 mg; 5.18 mmol), and CDMT (1.09 g; 6.21 mmol) were taken into a reaction flask and 30 ml acetonitrile was added to the mixture. Then *N*-methyl morpholine added to the reaction mixture dropwise at room temperature. After the general purification steps, the desired product 4-nitro-CA-Ala-OMe (1.23 g; 4.42 mmol) was obtained in 85.38% yield as a brown solid. Melting point: 131-133 ^{o}C. FT-IR (ATR, cm^{-1}) υ $_{N-H}$ 3272 cm^{-1}, υ $_{=C-H}$ 3075 cm^{-1}, υ $_{C=O}$ 1734 and 1653 cm^{-1}, υ $_{C=C}$ 1654, 1619, and 1547 cm^{-1}, υ $_{C–O}$ 1216 cm^{-1}. ^{1}H NMR (DMSO-d$_6$) δ: 8.74 (d, *J* = 6.8 Hz, -NH, 1H), 8.30–8.28 (m, =CH, AA′ part of AA′BB′ system, 2H), 7.88–7.55 (m, =CH, BB′ part of AA′BB′ system, 2H), 7.57 (d, *J* = 16.0 Hz, =CH, 1H), 6.91–6.87 (d, *J* = 16.0 Hz, =CH, 1H), 4.46–4.39 (m, -CH, 1H), 3.67 (s, OCH_3, 3H), 1.36 (d, *J* = 7.2 Hz, -CH_3, 3H). ^{13}C-APT NMR (DMSO-d$_6$): 173.44, 164.57, 148.09, 141.82, 137.60, 131.08, 129.14, 126.14, 124.61, 123.44, 52.44, 48.32, 17.52. Elemental analysis: $C_{13}H_{14}N_2O_5$ required C, 56.11; H, 5.07; N, 10.07, found C, 56.15; H, 5.15; N, 10.21.

3.2.4.3. Methyl (*E*)-(3-(2-chlorophenyl)acryloyl)glycinate (2-chloro-CA-Gly-OMe)

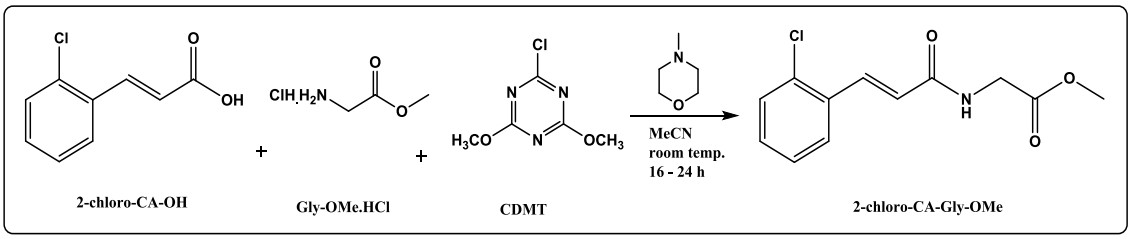

2-chloro-cinnamic acid (600.0 mg; 3.29 mmol), glycine methyl ester hydrochloride (409.23 mg; 3.29 mmol), and CDMT (692.28 g; 3.94 mmol) were taken into a reaction flask and 30 ml acetonitrile was added to the mixture. Then *N*-methyl morpholine added to

the reaction mixture dropwise at room temperature. After the general purification steps, the desired product 2-chloro-CA-Gly-OMe (586.0 mg; 2.31 mmol) was obtained in 70.30 % yield as a white solid. Melting point: 148-153 ^{o}C. FT-IR (ATR, cm^{-1}) υ $_{N-H}$ 3249 cm^{-1}, υ $_{=C-H}$ 3074 cm^{-1}, υ $_{C=O}$ 1748 and 1651 cm^{-1}, υ $_{C=C}$ 1612, and 1557 cm^{-1}, υ $_{C–O}$ 1205 cm^{-1}. ^{1}H NMR (DMSO-d_6) δ: 8.68 (d, *J* = 7.6 Hz, -NH, 1H), 7.79–7.75 (dd, *J* = 7.2 Hz, =CH, 2H), 7.57–7.53 (m, =CH, 1H), 7.47–7.42 (m, =CH, 2H), 6.78 (d, *J* = 15.6 Hz, 1H), 4.01 (d, *J* = 5.6 Hz, 2H), 3.67 (s, OCH_3, 3H). ^{13}C-APT NMR (DMSO-d_6): 170.77, 165.43, 135.21, 133.81, 133.00, 131.56, 130.47, 128.29, 128.14, 124.93, 52.25, 41.32. Elemental analysis: $C_{12}H_{12}ClNO_3$ required C, 56.82; H, 4.77; N, 5.52, found C, 56.88; H, 4.85; N, 5.58.

3.2.4.4. Methyl (*E*)-(3-(2-chlorophenyl)acryloyl)alaninate (2-chloro-CA-Ala-OMe)

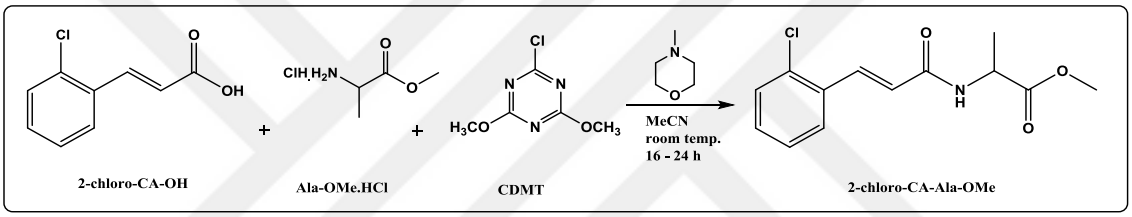

2-chloro-cinnamic acid (500.0 mg; 2.74 mmol), alanine methyl ester hydrochloride (376.67 mg; 2.74 mmol), and CDMT (528.82 mg; 3.01 mmol) were taken into a reaction flask and 30 ml acetonitrile was added to the mixture. Then *N*-methyl morpholine added to the reaction mixture dropwise at room temperature. After the general purification steps, the desired product 2-chloro-CA-Ala-OMe (532.30 mg; 1.99 mmol) was obtained in 72.62 % yield as a yellow solid. Melting point: 150-152 ^{o}C. FT-IR (ATR, cm^{-1}) υ $_{N-H}$ 3286 cm^{-1}, υ $_{=C-H}$ 3058 cm^{-1}, υ $_{C=O}$ 1731 and 1651 cm^{-1}, υ $_{C=C}$ 1611 and 1546 cm^{-1}, υ $_{C–O}$ 1214 cm^{-1}. ^{1}H NMR (DMSO-d_6) δ: 8.69-8.67 (d, *J* = 7.2 Hz, -NH, 1H), 7.78–7.72 (m, =CH, 2H), 7.55–7.54 (t, *J* = 3.6 Hz, =CH, 1H), 7.45–7.42 (m, =CH, 2H), 6.78–6.73 (dd, *J* = 1.6 Hz, =CH, 1H), 4.46–4.39 (m, -CH, 1H), 3.67 (s, -OCH_3, 3H), 1.37–1.35 (dd, *J* = 1.6 Hz, -CH_3, 3H). ^{13}C-APT NMR (DMSO-d_6): 173.50, 164.73, 135.20, 133.83, 133.03, 131.54, 130.48, 128.31, 128.09, 124.95, 52.43, 48.30, 17.53. Elemental analysis: $C_{13}H_{14}ClNO_3$ required C, 58.33; H, 5.27; N, 5.23, found C, 58.38; H, 5.29; N, 5.28.

3.2.4.5. Methyl (*E*)-(3-(o-tolyl)acryloyl)glycinate (2-methyl-CA-Gly-OMe)

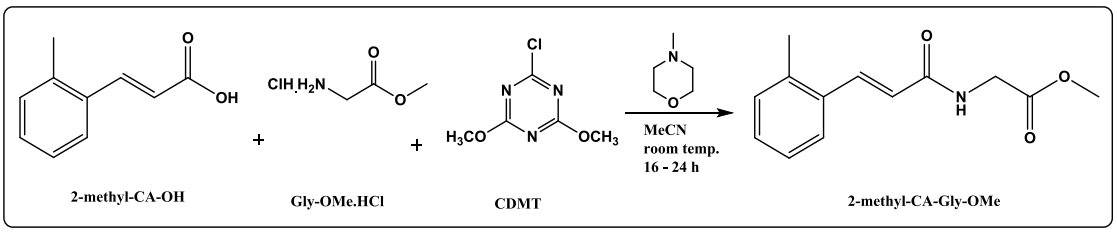

2-methyl-cinnamic acid (500.0 mg; 3.08 mmol), glycine methyl ester hydrochloride (383.95 mg; 3.08 mmol), and CDMT (595.39 mg; 3.39 mmol) were taken into a reaction flask and 20 ml acetonitrile was added to the mixture. Then *N*-methyl morpholine added to the reaction mixture dropwise at room temperature. After the general purification steps, the desired product 2-methyl-CA-Gly-OMe (625.10 mg; 2.72 mmol) was obtained in 86.91 % yield as dark white solid. Melting point: 140-142 ^{o}C. FT-IR (ATR, cm^{-1}) υ_{N-H} 3296 cm^{-1}, $\upsilon_{=C-H}$ 3062 cm^{-1}, $\upsilon_{C=O}$ 1733 and 1652 cm^{-1}, $\upsilon_{C=C}$ 1609 and 1549 cm^{-1}, υ_{C-O} 1206 cm^{-1}. ^{1}H NMR (DMSO-d_6) δ: 8.61–8.58 (d, *J* = 6.0 Hz, -NH, 1H), 7.72–7.68 (dd, *J* = 1.8 Hz, =CH, 1H), 7.58–7.56 (m, =CH, 3H), 6.65–6.60 (dd, *J* = 1.6 Hz, 2.0 Hz, =CH, 1H), 4.01–3.99 (dd, J = 1.6 Hz, -CH_2, 2H), 3.67 (s, -OCH_3, 3H), 2.39–2.38 (d, *J* = 2.0 Hz, -CH_3, 3H). ^{13}C-APT NMR (DMSO-d_6): 170.93, 165.94, 137.32, 137.32, 133.97, 131.19, 129.87, 126.91, 126.42, 122.96, 52.25, 41.26, 19.88. Elemental analysis: $C_{13}H_{15}NO_3$ required C, 66.94; H, 6.48; N, 6.00, found C, 66.95; H, 6.50; N, 6.03.

3.2.4.6. Methyl (*E*)-(3-(o-tolyl)acryloyl)alaninate (2-methyl-CA-Ala-OMe)

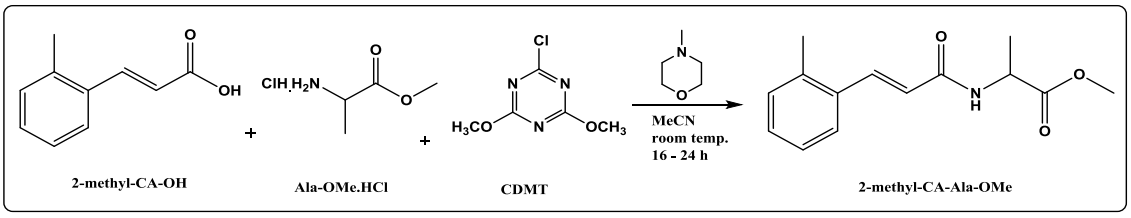

2-methyl-cinnamic acid (500.0 mg; 3.08 mmol), alanine methyl ester hydrochloride (427.19 mg; 3.08 mmol), and CDMT (595.39 mg; 3.39 mmol) were taken into a reaction flask and 20 ml acetonitrile was added to the mixture. Then *N*-methyl morpholine added to the reaction mixture dropwise at room temperature. After the general purification steps, the

desired product 2-methyl-CA-Ala-OMe (596.20 mg; 2.41 mmol) was obtained in 78.20% yield as a white solid. Melting point: 127-130 ºC. FT-IR (ATR, cm^{-1}) υ $_{N-H}$ 3296 cm^{-1}, υ $_{=C-H}$ 3062 cm^{-1}, υ $_{C=O}$ 1733 and 1652 cm^{-1}, υ $_{C=C}$ 1609 and 1549 cm^{-1}, υ $_{C–O}$ 1206 cm^{-1}. ^{1}H NMR (DMSO-d_6) δ: 8.61–8.58 (d, *J* = 3.2 Hz, -NH, 1H), 7.70–7.65 (d, *J* = 15.6 Hz, =CH, 1H), 7.55–7.54 (d, *J* = 5.2 Hz, =CH, 1H), 7.28 (m, =CH, 3H), 6.59 (d, *J* = 16.0 Hz, =CH, 1H), 4.43–4.39 (m, -CH, 1H), 3.66 (s, OCH_3, 3H), 2.38–2.37 (d, *J* = 3.2 Hz, -CH_3, 3H), 1.36 –1.33 (dd, *J* = 7.2 Hz, -CH_3, 3H). ^{13}C-APT NMR (DMSO-d_6): 173.65, 165.23, 137.35, 137.30, 134.00, 131.19, 129.82, 126.91, 126.40, 122.98, 52.40, 48.23, 19.88, 17.55. Elemental analysis: $C_{14}H_{17}NO_3$ required C, 68.00; H, 6.93; N, 5.66, found C, 68.02; H, 6.98; N, 5.70.

3.2.4.7. Methyl (*E*)-(3-(4-chlorophenyl)acryloyl)glycinate (4-chloro-CA-Gly-OMe)

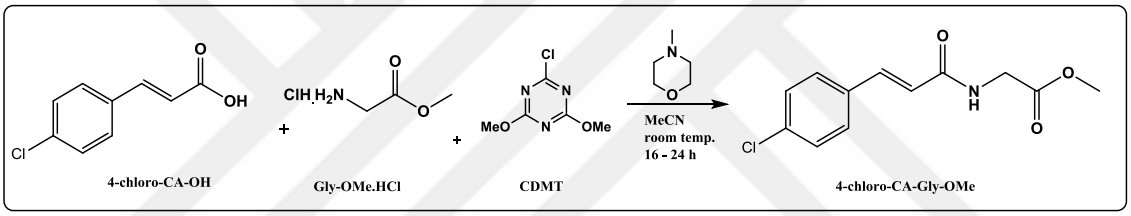

4-chloro-cinnamic acid (500.0 mg; 2.74 mmol), glycine methyl ester hydrochloride (338.26 mg; 2.74 mmol), and CDMT (528.82 mg; 3.01 mmol) were taken into a reaction flask and 20 ml acetonitrile was added to the mixture. Then *N*-methyl morpholine added to the reaction mixture dropwise at room temperature. After the general purification steps, the desired product 4-chloro-CA-Gly-OMe (612.3 mg; 2.41 mmol) was obtained in 88.15 % yield as a white solid. Melting point: 159-161 ºC. FT-IR (ATR, cm^{-1}) υ $_{N-H}$ 3225 cm^{-1}, υ $_{=C-H}$ 3062 cm^{-1}, υ $_{C=O}$ 1739 and 1654 cm^{-1}, υ $_{C–O}$ 1210 cm^{-1}. ^{1}H NMR (DMSO-d_6) δ: 8.49 (bs, -NH, 1H), 7.64–7.61 (m, =CH, AA′ part of AA′BB′ system, 2H), 7.50–7.49 (m, =CH, BB′ part of AA′BB′ system, 2H), 7.46 (d, *J* = 15.6 Hz, =CH, 1H), 6.73 (d, *J* = 15.6 Hz, =CH, 1H), 4.00–3.99 (d, *J* = 5.6 Hz, -CH_2, 2H), 3.68 (s, OCH_3, 3H). ^{13}C-APT NMR (DMSO-d_6): 170.84, 165.71, 138.59, 134.17, 129.82, 129.47, 122.68, 52.23, 41.28. Elemental analysis: $C_{12}H_{12}ClNO_3$ required C, 56.82; H, 4.77; N, 5.52, found C, 56.82; H, 4.80; N, 5.55.

3.2.4.8. Methyl (*E*)-(3-(4-chlorophenyl)acryloyl)alaninate (4-chloro-CA-Ala-OMe)

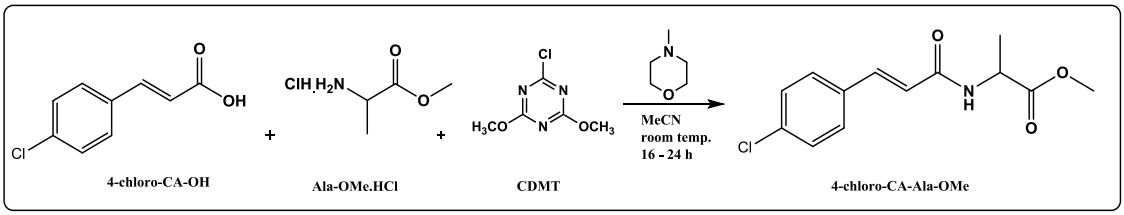

4-chloro-cinnamic acid (500.0 mg; 2.74 mmol), alanine methyl ester hydrochloride (376.67 mg; 2.74 mmol), and CDMT (525.78 mg; 3.01 mmol) were taken into a reaction flask and 20 ml acetonitrile was added to the mixture. Then *N*-methyl morpholine added to the reaction mixture dropwise at room temperature. After the general purification steps, the desired product 4-chloro-CA-Ala-OMe (525.3 mg; 1.96 mmol) was obtained in 71.66 % yield as a dark white solid. Melting point: 162-165 ^{o}C. FT-IR (ATR, cm^{-1}) υ_{N-H} 3276 cm^{-1}, $\upsilon_{=C-H}$ 3067 cm^{-1}, $\upsilon_{C=O}$ 1748 and 1652 cm^{-1}, $\upsilon_{C=C}$ 1619 and 1542 cm^{-1}, υ_{C-O} 1208 cm^{-1}. ^{1}H NMR (DMSO-d$_6$) δ: 8.55 (d, *J* = 7.2 Hz, -NH, 1H), 7.62 –7.60 (m, =CH, AA′ part of AA′BB′ system, 2H), 7.50–7.48 (m, =CH, BB′ part of AA′BB′ system, 2H), 7.44 (d, *J* = 16.0 Hz, =CH, 1H), 6.69 (d, *J* = 16 Hz, =CH, 1H,), 4.44–4.37 (m, -CH, 1H), 3.65 (s, OCH_3, 3H), 1.34 (d, *J* = 7.6 Hz, -CH_3, 3H,). ^{13}C-APT NMR (DMSO-d$_6$): 173.56, 165.03, 138.53, 134.49, 134.20, 129.75, 129.47, 122.71, 52.38, 48.22, 17.55. Elemental analysis: $C_{13}H_{14}ClNO_3$ required C, 58.33; H, 5.27; N, 5.23, found C, 58.33; H, 5.30; N, 5.25.

3.2.4.9. Methyl (*E*)-(3-(4-methoxyphenyl)acryloyl)glycinate (4-methoxy-CA-Gly-OMe)

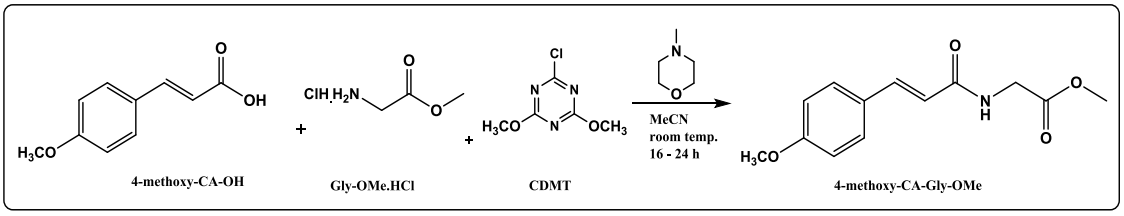

4-methoxy-cinnamic acid (500.0 mg; 2.81 mmol), glycine methyl ester hydrochloride (346.65 mg; 2.81 mmol), and CDMT (541.65 mg; 3.09 mmol) were taken into a reaction flask and 20 ml acetonitrile was added to the mixture. Then *N*-methyl morpholine added to the reaction mixture dropwise at room temperature. After the general purification steps, the

desired product 4-methoxy-CA-Gly-OMe (601.5 mg; 2.41 mmol) was obtained in 86.00 % yield as a white solid. Melting point: 132-134 ºC. FT-IR (ATR, cm^{-1}) υ $_{N-H}$ 3246 cm^{-1}, υ $_{=C-H}$ 3069 cm^{-1}, υ $_{C=O}$ 1741 and 1646 cm^{-1}, υ $_{C=C}$ 1599 and 1566 cm^{-1}. ^{1}H NMR (DMSO-d_6) δ: 8.49-8.46 (t, *J* = 6.0 Hz, -NH, 1H), 7.55 (m, =CH, AA′ part of AA′BB′ system, 2H), 7.44 -7.40 (d, *J* = 15.6 Hz, =CH, 1H), 7.00 - 6.98 (m, =CH, BB′ part of AA′BB′ system, 2H), 6.59-6.55 (, *J* = 15.6 Hz, =CH, 1H), 3.98 (d, *J* = 6.0 Hz, 2H,), 3.80 (s, OCH_3, 3H), 3.66 (, OCH_3, 3H). ^{13}C-APT NMR (DMSO-d_6): 170.98, 166.20, 160.93, 139.64, 129.70, 127.77, 119.37, 114.88, 55.74, 52.19, 41.24. Elemental analysis: $C_{13}H_{15}NO_4$ required C, 62.64; H, 6.07; N, 5.62, found C, 62.65; H, 6.13; N, 5.68.

3.2.4.10. methyl (*E*)-(3-(4-methoxyphenyl)acryloyl)alaninate (4-methoxy-CA-Ala-OMe)

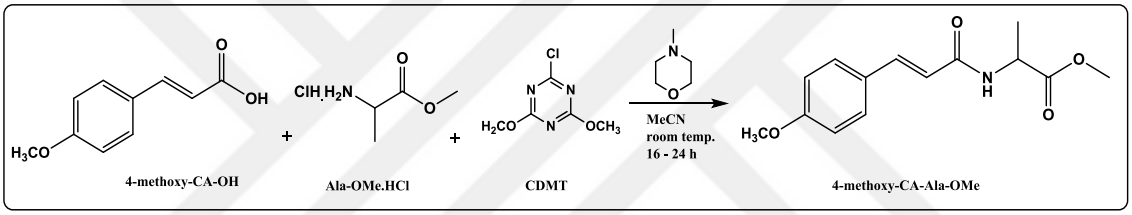

4-methoxy-cinnamic acid (500.0 mg; 2.81 mmol), alanine methyl ester hydrochloride (391.66 mg; 2.81 mmol), and CDMT (538.82 mg; 3.09 mmol) were taken into a reaction flask and 20 ml acetonitrile was added to the mixture. Then *N*-methyl morpholine added to the reaction mixture dropwise at room temperature. After the general purification steps, the desired product 4-methoxy-CA-Ala-OMe (585.2 mg; 2.22 mmol) was obtained in 79.21 % yield as a white solid (Feng et al. 2010). Melting point: 139-141 ºC. FT-IR (ATR, cm^{-1}) υ $_{N-H}$ 3299 cm^{-1}, υ $_{=C-H}$ 3022 cm^{-1}, υ $_{C=O}$ 1754 and 1648 cm^{-1}, υ $_{C=C}$ 1603 and 1617 cm^{-1}, υ $_{C-O}$ 1194 cm^{-1}. ^{1}H NMR (DMSO-d_6) δ: 8.47 (d, *J* = 7.2 Hz, -NH, 1H), 7.55-7.53 (m, =CH, AA′ part of AA′BB′ system, 2H), 7.40 (d, *J* = 15.6 Hz, =CH, 1H), 7.01- 6.98 (m, =CH, BB′ part of AA′BB′ system, 2H), 6.57-6.53 (d, *J* = 15.6 Hz, =CH, 1H), 4.41-4.38 (m, -CH, 1H), 3.80 (t, *J* = 3.2 Hz OCH_3, 3H), 3.66-3.65 (t, *J* = 2.4 Hz, -OCH_3, 3H,), 1.34 (m, -CH_3, 3H). ^{13}C-APT NMR (DMSO-d_6): 173.71, 165.55, 160.92, 139.64, 127.79, 119.40, 114.90, 55.74, 52.34, 48.17, 17.59. Elemental analysis: $C_{14}H_{17}NO_4$ required C, 63.87; H, 6.51; N, 5.32, found C, 63.88; H, 6.55; N, 5.41.

3.2.4.11. Methyl (*E*)-(3-(naphthalen-1-yl)acryloyl)glycylglycinate (Naft-CA-Gly-Gly-OMe)

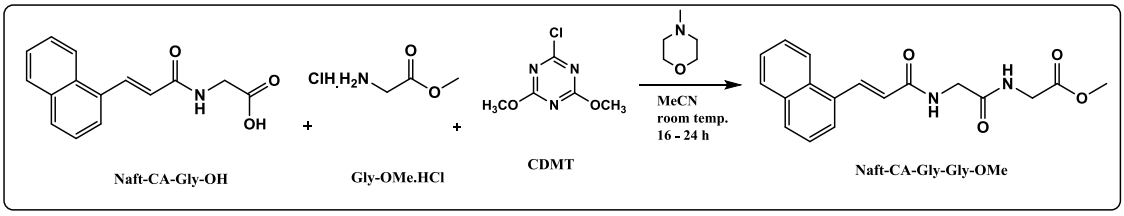

Naft-CA-Gly-OH (500.0 mg; 1.96 mmol), glycine methyl ester hydrochloride (245.92 mg; 2.81 mmol), and CDMT (378.28 mg; 2.15 mmol) were taken into a reaction flask and 20 ml acetonitrile was added to the mixture. Then *N*-methyl morpholine added to the reaction mixture dropwise at room temperature. After the general purification steps, the desired product Naft-CA-Gly-OH (426.1 mg; 1.57 mmol) was obtained in 80.21 % yield as a dark white. Melting point: 139-141 ^{o}C. FT-IR (ATR, cm^{-1}) υ_{N-H} 3282 cm^{-1}, $\upsilon_{=C-H}$ 3069 cm^{-1}, $\upsilon_{C=O}$ 1742 and 1656 cm^{-1}, $\upsilon_{C=C}$ 1615 and 1548 cm^{-1}, υ_{C-O} 1216 cm^{-1}. ^{1}H NMR (DMSO-d_6) δ: 8.61-8.60 (t, *J* = 5.6 Hz, -NH, 1H), 8.46 (d, *J* = 5.6 Hz, -NH, 1H), 8.28-8.22 (m, =CH, 2H), 8.01 (d, *J* = 1.8 Hz, =CH, 2H) 7.81 (d, *J* = 7.2 Hz, =CH, 1H), 7.65-7.58 (m, =CH, 3H), 6.82 (d, J = 15.6 Hz, =CH, 1H), 3.96-3.95 (d, *J* = 6.0 Hz, -CH_2, 2H), 3.92-3.90 (d, *J* = 6.0 Hz, -CH_2, 2H), and 3.65 (s, -OCH_3, 3H). ^{13}C-APT NMR (DMSO-d_6): 170.8, 169.9, 165.7, 135.9, 133.8, 132.4, 131.2, 130.1, 129.1, 127.4, 126.7, 126.2, 125.3, 124.9, 123.6, 52.2, 42.4, 41.0. Elemental analysis: $C_{16}H_{15}NO_3$ required C, 71.36; H, 5.61; N, 5.20, found C, 71.39; H, 5.68; N, 5.26.

4. RESULTS AND DISCUSSION

4.1. Characterization of the Synthesized Compounds

In this section, proton and carbon NMR and FT-IR spectrum evaluation for selected compounds are given in details and mechanism of the synthetic steps are discussed. In addition, structure activity relationships of the final compounds are discussed in terms of dielectric constant, dielectric loss and conductivity. The evaluation of the compounds is given in separate tables to prevent possible confusion for the readers.

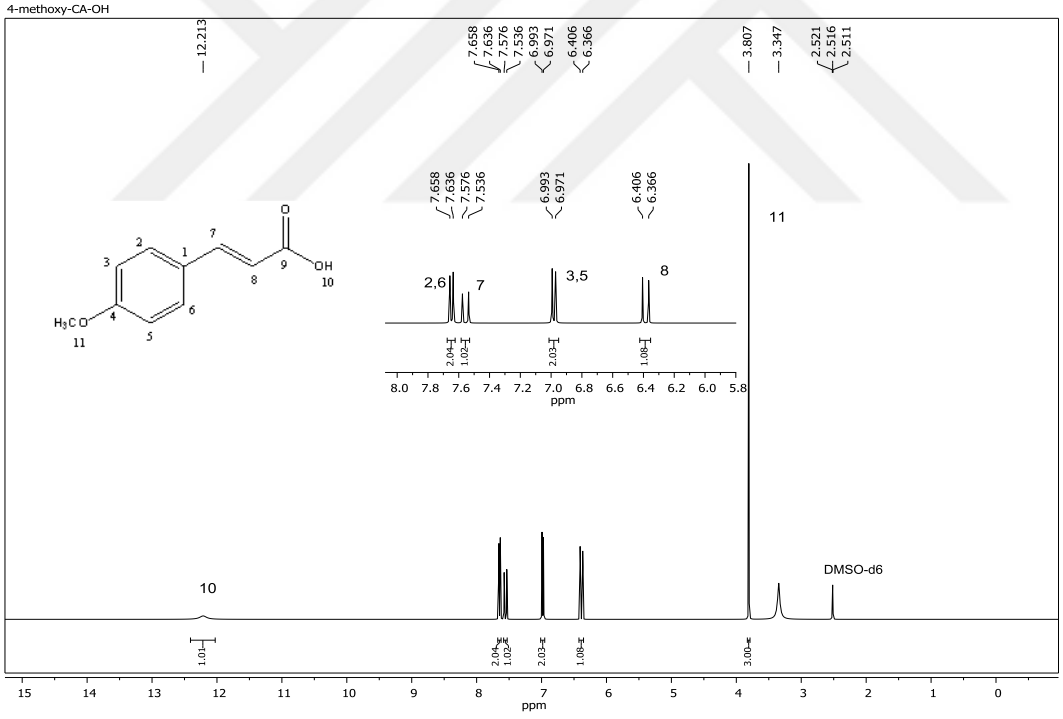

Figure 4.1.1. ^{1}H NMR spectra of 4-methoxy-CA-OH

Cinnamic acids contain aromatic, olefinic, carboxylic acid proton and aliphatic proton depending on the type of substituent. When ^{1}H NMR spectra of 4-methoxy-CA-OHcompound is examined, carboxylic acid proton at 12.21 ppm, methoxy CH_3 protons as singlet at 3.80 ppm, olefinic proton (number 7) at 7.57-7.54 ppm, and olefin proton (number 8) at 6.41-6.37 ppm were observed. Aromatic protons 2-6 resonated in a low field due to the ortho-para directing effect of the methoxy group.

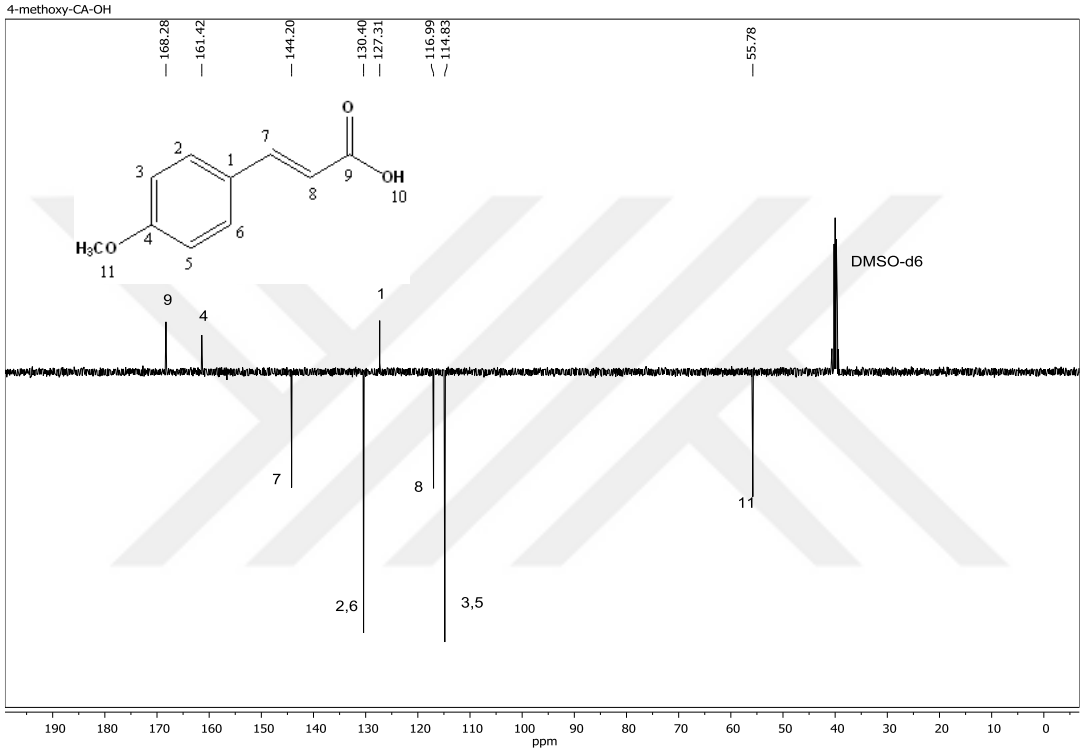

Figure 4.1.2. ^{13}C APT NMR spectra of 4-methoxy-CA-OH

When the carbon NMR spectrum is evaluated, the carboxylic acid carbon peak at 168.28 ppm, and the aromatic carbon (number 4) to which the methoxy group is bound is at 161.42 ppm, and the methoxy carbon peak at 55.78 ppm were clearly observed. In addition, aromatic =CH carbons resonate at 130.40 and 114.83 ppm. Olefinic =CH carbons are seen at 144.20 ppm and 116.99 ppm. This shows that the cinnamic acid was purely obtained.

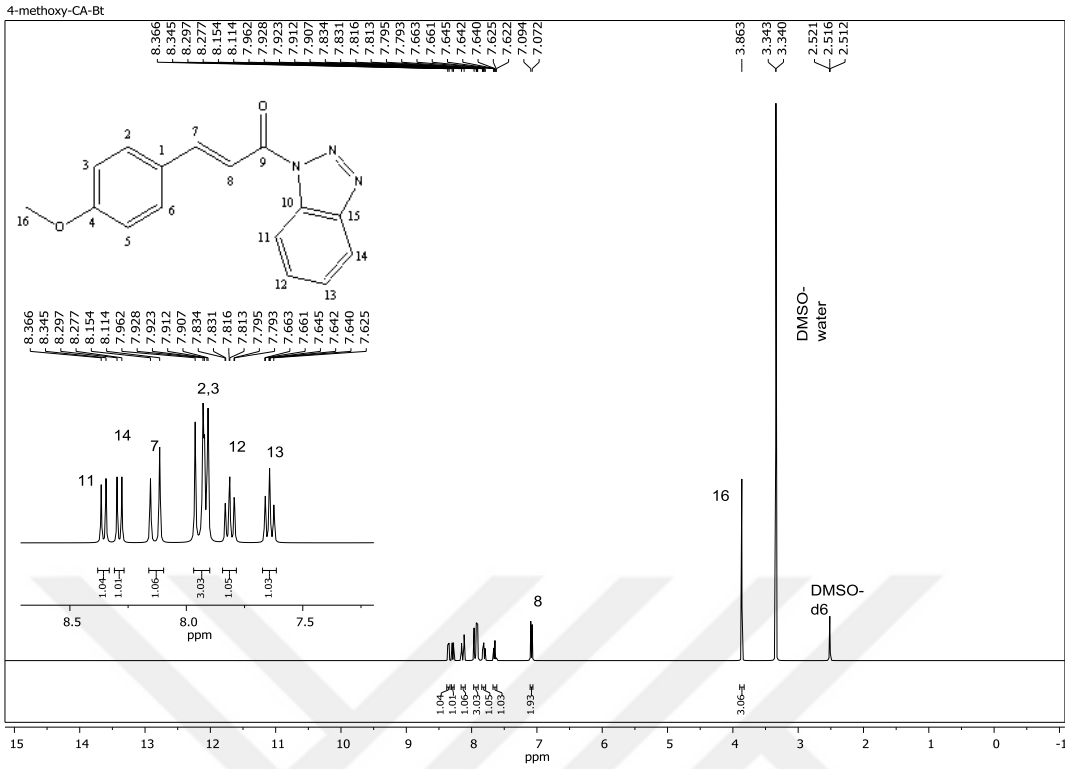

Figure 4.1.3. ^{1}H NMR spectra of 4-methoxy-CA-Bt

Compared to cinnamic acid compounds, N-Acylbenzotriazoles provided 4 extra aromatic protons with the benzene ring they carried. Two of the aromatic =CH protons of benzotriazole (number 11 and 14) resonate as two doublets between 8.36-8.11 ppm, while the other aromatic =CH protons resonated as two triplets between 7.83 and 7.62 ppm in the high field. These peaks are characteristic aromatic proton peaks of benzotriazole. The peaks of olefinic protons resonated at 7.09-7.07 ppm and 8.15-8.11 ppm, while methoxy protons resonated at 3.86 ppm.

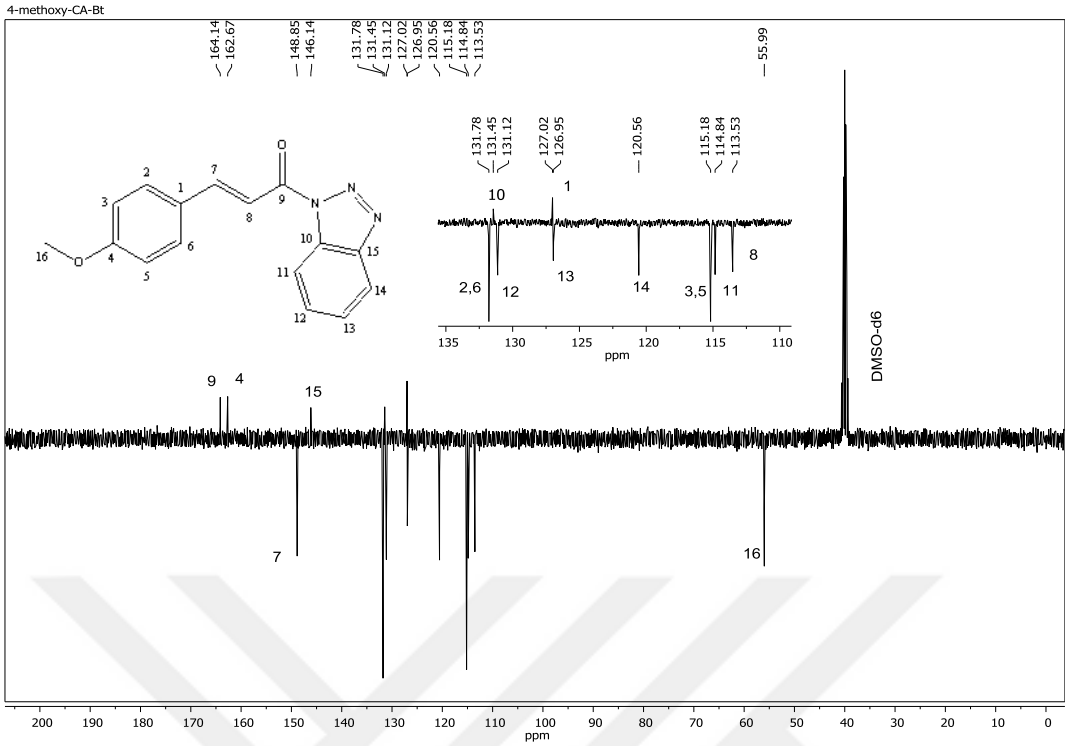

Figure 4.1.4. ^{13}C APT NMR spectra of 4-methoxy-CA-Bt

In the ^{13}C NMR spectra of *N*-acylbenzotriazole (4-methoxy-CA-Bt), there are 6 aromatic carbon peaks of benzotriazole in the spectrum. In addition, the carbonyl carbon peak has shifted to about 164.14 ppm. 2 quaternary carbon peaks of benzotriazole were resonance at 146.14 ppm and 131.45 ppm, respectively. The peak of methoxy carbon 55.99 is also clearly seen. The disappearance of carboxylic acid proton can be shown another evidence for product formation. Above mention peaks prove that amide bond was form between benzotriazole and cinnamic acid.

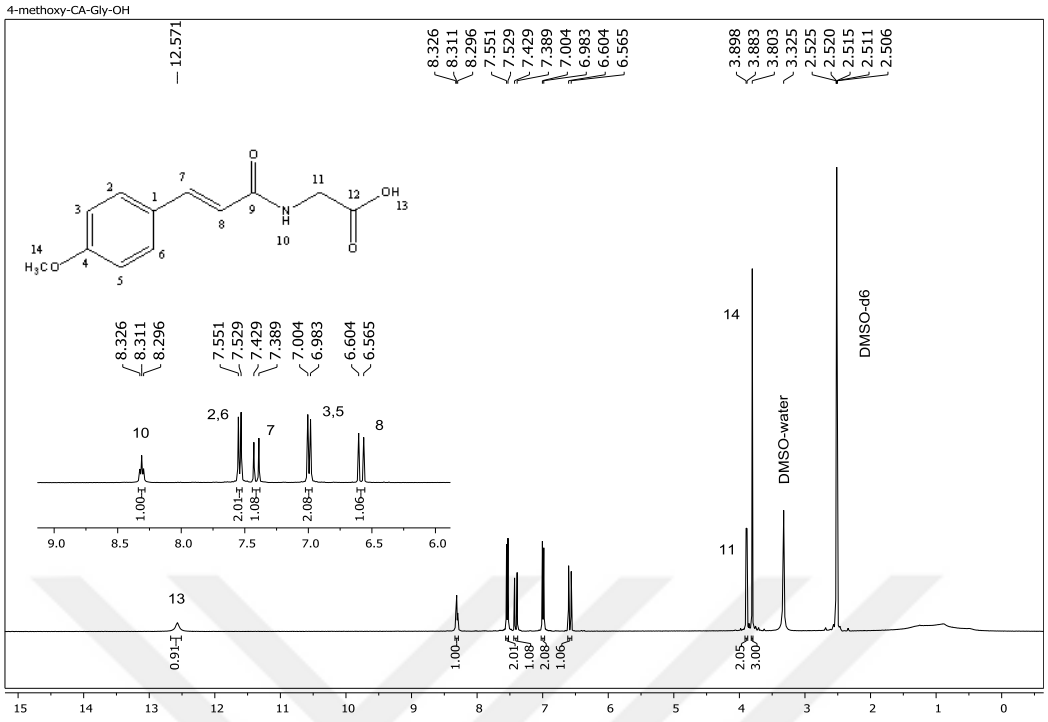

Figure 4.1.5. ^{1}H NMR spectra of 4-methoxy-CA-Gly-OH

The most important peaks to be considered in the ^{1}H NMR spectrum of analysis of amino acid conjugates containing carboxylic acid are the presence of the newly formed amide -NH proton and aliphatic protons in the side chain of the amino acid. In addition, the absence of aromatic protons of benzotriazole proves that the target compound is formed. Also, the presence of aromatic =CH protons and methoxy proton peak at 3.80 ppm from cinnamic acid can be shown as evidence. The aliphatic -CH_2 protons of glycine at 3.89-3.88 ppm as a doublet and carboxylic acid proton peak at 12.57 ppm proved that the desired product was formed.

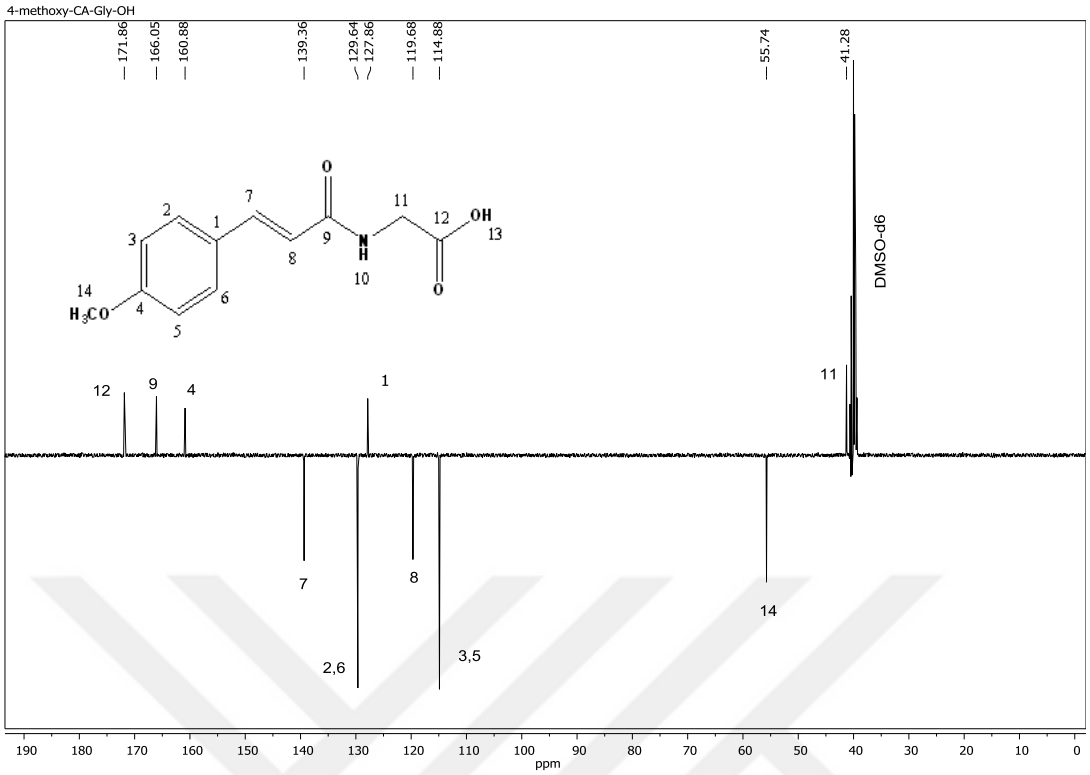

Figure 4.1.6. ^{13}C APT NMR spectra of 4-methoxy-CA-Gly-OH

Characteristic groups expected to appear in the ^{13}C NMR spectrum of amino acid conjugates; amide carbonyl and carboxylic acid carbonyl peaks of amino acid, aromatic =CH carbons, olefinic =CH carbons and aliphatic carbon peaks. When the spectrum of the 4-methoxy-CA-Gly-OH compound is examined, the presence of all the characteristic carbon peaks mentioned above is clearly visible. Carboxylic acid carbonyl carbon peak at 171.86 ppm, amide carbonyl carbon peak at 166.05 ppm, CH_2 proton peak of glycine at 41.28 ppm and olefinic carbon peaks (number 7 and 8) at 139.36 ppm and 119.68 ppm, respectively, showed that the desired amino acid conjugate was synthesized.

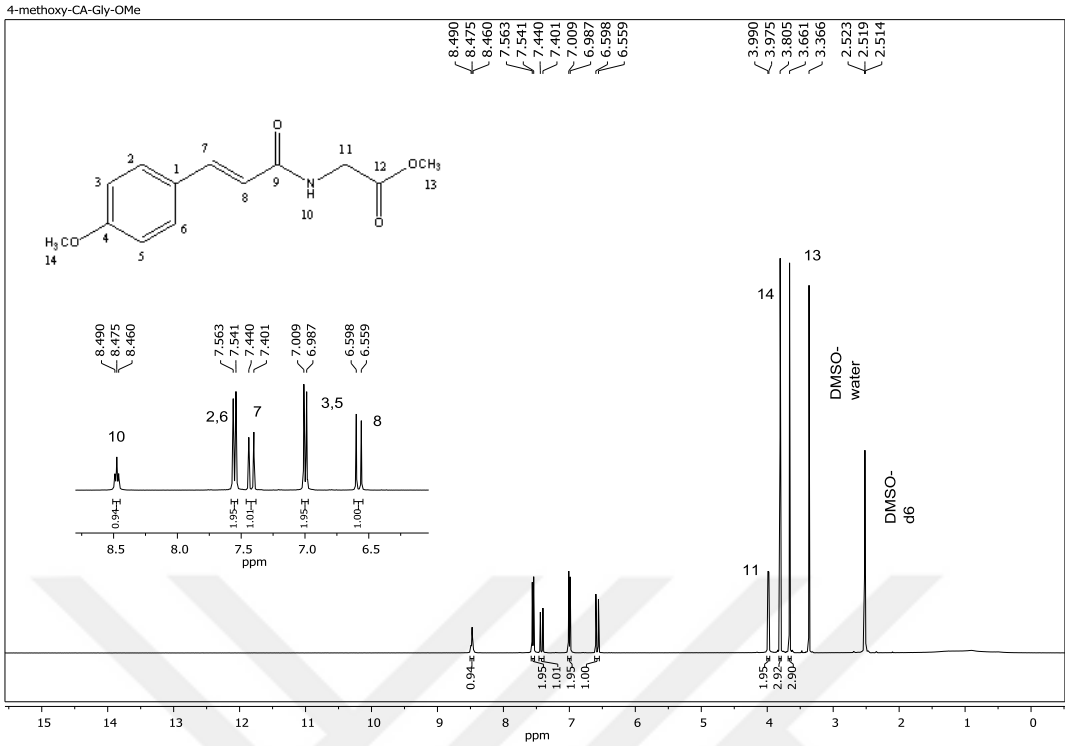

Figure 4.1.7. ^{1}H NMR spectra of 4-methoxy-CA-Gly-OMe

The main proton peaks that should be seen in the ^{1}H NMR analysis of conjugates containing ester functionality is that the methyl ester group has been replaced by the carboxylic acid group compared to the previous carboxylic acid containing conjugates. The -CH_2 proton peak (number 11) of the glycine has shifted to 3.99 ppm, and the presence of the -NH proton peak at 8.45 ppm indicates that the structure was formed. The coupling constant of olefinic protons is 15.6 Hz which proves that the structure trans positioned. The presence of olefinic =CH peaks and the presence of 2 equivalent aromatic =CH protons can also be shown as separate evidence.

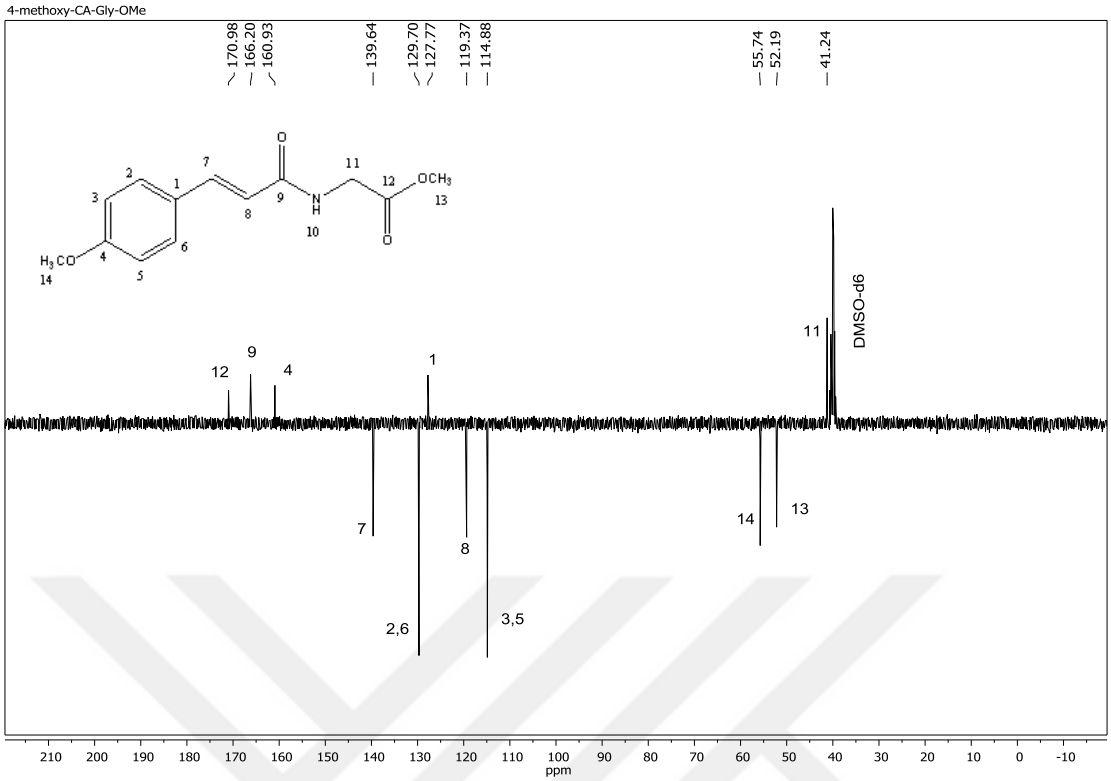

Figure. 4.1.8. ^{13}C APT NMR spectra of 4-methoxy-CA-Gly-OMe

The groups to be considered in the ^{13}C NMR analysis of amino acid conjugates containing the ester group are two carbonyl carbons, one of which belongs to the ester and the other to the amide group. Subsequently, the CH_3 methyl carbon of the methyl ester and the -OCH_3 carbons of the methoxy group can be given. The presence of olefinic carbon peaks and aromatic =CH carbons from the starting compound can also be presented as additional evidence.

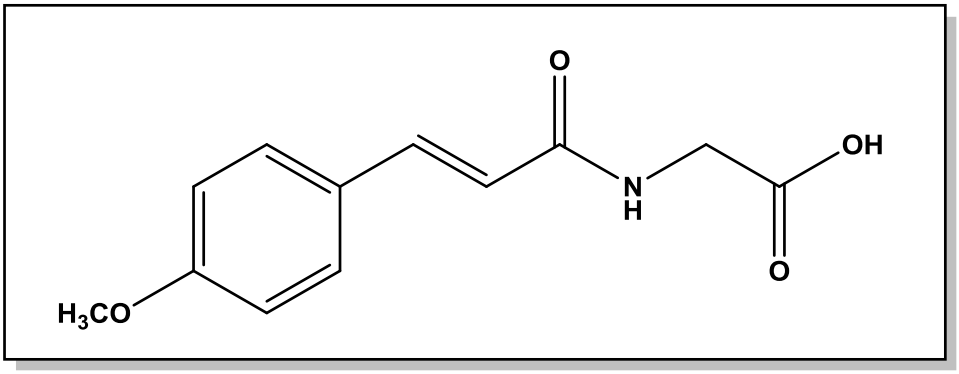

Figure 4.1.9. Chemical representation of 4-methoxy-CA-Gly-OH

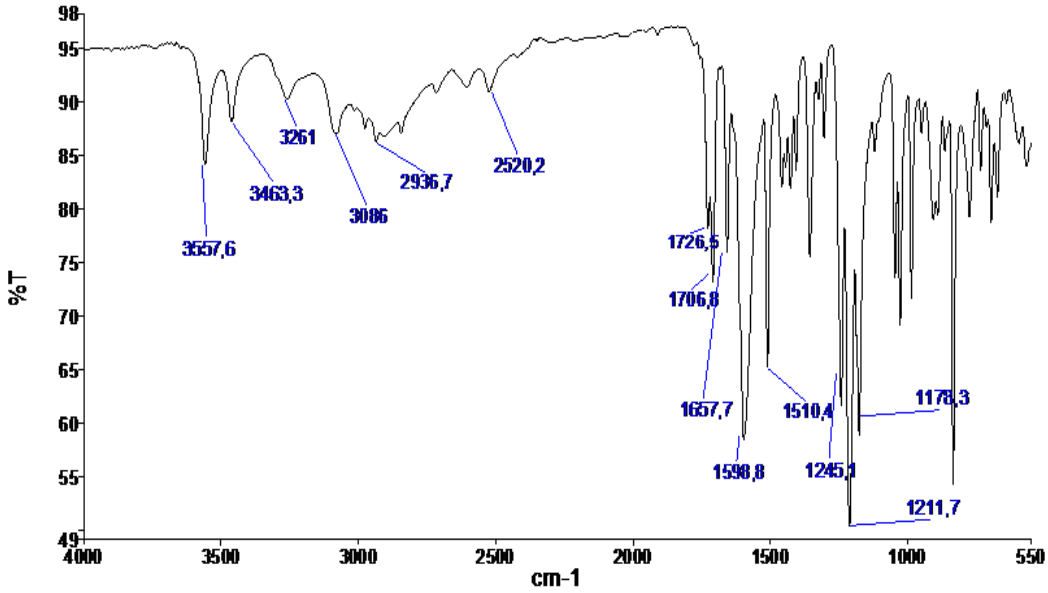

Figure 4.1.10. FT-IR spectrum of 4-methoxy-CA-Gly-OH

Amide -N-H stretching vibration at 3463 cm^{-1}, carboxylic acid -O-H stretching vibration at 3557 cm^{-1}, aromatic =C-H stretching vibration at 3086 cm-1, aliphatic -C-H stretching vibrations around 2937 cm^{-1}, carboxylic acid C=O stretching vibration at 1706 cm^{-1}, amide C=O stretching vibration at 1657 cm^{-1} and aromatic C=C bending vibrations at 1598 ve 1510 cm^{-1} can be shown as evidences that the structure have specific functional groups.

4.2. NMR Evaluation of Cinnamic Acid Derivetives

Table 4.2.1. Structural evaluation of cinnamic acid derivatives

Compounds	^{1}H NMR Interpretation	^{13}C APT NMR Interpretation
2-fluoro-CA-OH	Carboxylic acid -OH proton (number 10) shows up at 12.58 ppm as a singlet, olefinic protons (number 7and 8) show up at 7.69 – 7.65 ppm and 6.63 – 6.59 ppm with 16 Hz coupling constant which means the double bond has trans isomerization. The aromatic four protons resonance between 7.81 and 7.25 ppm show that the compound successfully obtained.	Carboxylic acid carbon (number 9) peak at 167.72 ppm, ipso carbon (number 1) peak at 122.25 ppm, fluorine attached carbon (number 2) at 162.22 ppm, olefinic carbon peaks (number 7 and 8) at 136.15 and 116.63 ppm and aromatic -CH carbons (number 3,4,5 and 6) between 132.74 and 122.35 ppm clearly show that the structure are formed.
2-chloro-CA-OH	Carboxylic acid -OH proton (number 9) shows up at 12.64 ppm as a singlet, olefinic protons (number 7and 8) show up at 7.91 – 7.87 ppm and 6.64 – 6.58 ppm with 16 Hz coupling constant which means the double bond protons are in trans position. The aromatic four protons (3,4,5, and 6) show up between 7.91 and 7.39 ppm indicate that the compound successfully formed.	Carboxylic acid carbon (number 9) peak at 167.61 ppm, ipso carbon (number 1) peak at 132.35 ppm, Chloride attached carbon (number 2) at 134.03 ppm, olefinic carbon peaks (number 7 and 8) at 139.15 and 122.81 ppm and aromatic -CH carbons (number 3,4,5 and 6) between 132.14 and 128.24 ppm clearly show the formation of the desired compound.
2-methyl-CA-OH	Carboxylic acid -OH proton peak (number 9) at 12.50 ppm as a singlet, CH3 protons (number 10) in the benzene ring at 2.40 ppm as singlet, olefinic CH protons (number 7 and 8) at 7.85 – 7.81 and 6.46 – 6.42 ppm as doublets and existence of four aromatic CH protons show that the compound are formed.	Carboxylic acid carbon (number 9) peak at 168.00 ppm, ipso carbon (number 1) peak at 133.39 ppm, methyl substituted carbon (number 2) at 137.62 ppm, olefinic carbon peaks (number 7 and 8) at 141.62 and 120.69 ppm and aromatic -CH carbons (number 3,4,5 and 6) between 131.17 and 126.89 ppm and methyl carbon peak at 19.74 ppm clearly show that the structure are formed.
3-methyl-CA-OH	Like other cinnamic acid derivatives, the carboxylic acid proton at 12.44 ppm, olefinic protons (number 7 and 8) at 7.58 – 7.54 ppm and 6.54 – 6.50 ppm with 16 Hz coupling constant showing the structure is trans isomer and the presence of 4 aromatic CH protons in total proves that the structure is obtained.	The presence of carboxylic acid carbon (number 9) at 168.04 ppm, methyl carbon (number 10) at 21.31 ppm, and quaternary carbon peaks (numbers1&3), which are the most characteristic peaks for the compound, prove that the structure was synthesized.

Table 4.2.1. Structural evaluation of cinnamic acid derivatives (continuing)

4-chloro-CA-OH	Like other cinnamic acid derivatives, the carboxylic acid proton (number 10) at 12.54 ppm, olefinic protons (number 7 and 8) at 7.62 – 7.58 ppm and 6.60 – 6.56 ppm with 16 Hz coupling constant showing the structure is trans isomer and due to the deactivating effect of chloride, protons (number 2and 6) at meta position resonance in low field, but para protons (3&5) at 7.50 – 7.48 ppm show up in high filed. In addition to these evidences, olefinic protons (number 7 and 8) at 7.62 – 7.58 and 6.60 – 6.56 ppm show that the compound were formed.	The carboxylic acid carbonyl carbon at 167.94 ppm, olefinic CH carbon peaks at 142.85 and 120.72 ppm, and existence of two symmetrical aromatic CH carbons prove that the formation of the compound.
4-methoxy-CA-OH	Characteristic proton peaks for this compound; the carboxylic acid proton (number 10) at 12.21 ppm as a broad singlet, methoxy protons (number 11) at 3.80 ppm as a singlet and olefinic protons (number 7 and 8) at 7.58 – 7.54 ppm and 6.41 – 6.37 ppm as doublets. The presence of aromatic CH protons also signifies that the structure was formed	The presence of the carboxylic acid carbon (number 9) peak at 168.28 ppm, the carbon (number 4) adjacent to the methoxy group at 161.42 ppm, and the symmetrical aromatic CH carbon peaks are evidence for product being obtained.
2,4-dimethoxy-CA-OH	A clear view of the olefinic peaks at 7.78 – 7.74 ppm and 6.40 – 6.37 ppm along with two methoxy protons (number 11 and 12) at 3.88 ppm and 3.83 ppm and carboxylic acid proton (number 10) peak specific to this compound is evidence of the compound being obtained.	Likewise, the presence of carbons belonging to methoxy groups at 56.18 ppm and 55.92 ppm and the presence of 4 quaternary carbon (number 1,2,4 and 9) peaks indicate that the structure was obtained.
2,4,5-trimethoxy-CA-OH	The characteristic three methoxy peaks (number 11,12 and 13), olefinic protons at 7.83 – 7.79 ppm and carboxylic acid proton (number 10) at 12.11 ppm clearly show that the structure was successfully synthesized.	Likewise, the presence of three methoxy carbons (number 11,12, and 13) at 56.81 ppm, 56.57 ppm and 56.26 ppm and the presence of 4 quaternary carbon of benzene ring and carbonyl carbon (number 9) at 168.73 ppm indicate that the structure was obtained.

Table 4.2.1. Structural evaluation of cinnamic acid derivatives (continuing)

Naft-CA-OH	The presence of olefinic protons at 8.42 – 8.28 and 6.64 – 6.60 ppm, carboxylic acid proton at 12.58 ppm and other aromatic protons (7 protons) indicates that this compound is obtained.	When the C NMR spectrum is examined, characteristic carbon peaks are clearly seen. Carboxylic acid carbon at 168.33 ppm, olefinic carbons at 143.44 and 120.27 ppm and other naphthalene ring carbons are observed.
Phenant-CA-OH	Total number of aromatic CH proton peak and presence of olefinic CH protons at 8.42 – 8.38 ppm and 6.73 – 6.69 ppm coherent with compound.	As with ^{1}H NMR, the clear view of the carbonyl carbon peak at 168.09 ppm and olefinic carbon (number 15) at 140.87 ppm are proofs that the compound is formed.
Pyrene-CA-OH	The presence of a total of 9 aromatic CH protons and 2 olefinic CH_2 proton peaks at 8.74 – 8.70 ppm and 6.87 – 6.83 ppm and the carboxylic acid proton peak at 12.61 ppm proves that the compound is obtained.	The ^{13}C NMR spectrum provides the total number of carbons as in the ^{1}H NMR. Carbonyl carbon peak at 168.10 ppm and olefinic carbon peaks at 140.36 ppm and 122.13 ppm can be given as examples.
Phenylbenzyl-CA-OH	Since there are many aromatic protons, splitting and peaks are intertwined, 9 clearly visible aromatic proton peaks in the spectrum are sufficient to characterize the compound, and the clear appearance of the olefinic proton (number 10) at 6.61 – 6.57 ppm as a doublet peak can be shown as another evidence.	The presence of carbonyl carbon (number 11) at 168.33 ppm, aromatic carbons and olefinic carbons (number 9 and 10) at 143.44 and 120.27 ppm are evidences for the formation of the compound.
3-methyl-CA-Bt	As evidence of benzotriazole binding of the 3-methyl-CA-OH compound, the splitting of ring protons (numbers 11 and 14) belonging to benzotriazole as doublets, as well as two triplet peakss of benzotriazole arise at in higher field. In addition, the disappearance of the carboxylic acid proton indicates that the structure was formed.	The presence of 5 quaternary carbon atom peaks (numbers 9,15,3,1 and 10) in total and the presence of 8 aromatic CH protons indicate that the structure was formed.

4.3. NMR Evaluation of N-acylbenzotriazoles

Table 4.3.1. Structural evaluation of cinnamic acid Bt derivatives

Compund Name	**^{1}H NMR Interpretation**	**^{13}C APT NMR Interpretation**
2-fluoro-CA-Bt	The spectrum provides the total amount of protons that the compound needs to have. The aromatic -CH protons of benzotriazole (number 15 and 12) appear as doublets between at 8.34 ppm and 8.27 ppm. On the other hand, cinnamoyl aromatic CH protons (number 3,4,5 and 6) arise between 7.83 ppm and 7.34 ppm. These peaks clearly show that benzotriazole successfully connected to the starting material.	When the ^{13}C NMR spectrum is examined, the presence of quaternary carbon atoms (numbers 1,2,9,10 and 15) and peaks in the range of 140.49 - 114.81 ppm of 8 aromatic CH carbon atoms prove that the structure is formed.
2-chloro-CA-Bt	8 aromatic protons from cinnamic acid and benzotriazole are present in the structure. Olefinic CH proton (number 7) arise at 8.20 – 8.14 ppm which has coupling constant value 7 Hz show that the structure has trans isomerization.	3 different quaternary carbon atoms present in the structure are seen on the upper side of the spectrum, while aromatic and olefinic CH carbons are located on the lower side. Carboxylic acid carbonic carbon (number 9) appears at 163.67 ppm, while olefinic CH carbons (number 7 and 8) appear at 133.40 and 114.80 ppm.
2-methyl-CA-Bt	Aliphatic CH3 protons (number 14) at 2.52 ppm, aromatic and olefinic 10 protons exist between 8.37 – 7.34 ppm show that the benzotriazole successfully bonded to starting compound.	Carbonyl carbon peak at 163.92 ppm, olefinic carbon peaks at 145.81 for C^{7} and 117.41 ppm for C^{8}, CH_3 carbon (number 16) at 19.82 ppm and total 8 aromatic CH carbon peaks are clearly seen in the spectrum so that it proves the formation benzotriazole intermediate.

Table 4.3.1. Structural evaluation of cinnamic acid Bt derivatives (continuing)

4-methoxy-CA-Bt	For this compound, the disappearance of the starting carboxylic acid proton and the presence of four aromatic CH protons of benzotriazole is evidence that the desired structure is obtained. In addition, the presence of two doublets of benzotriazole at 8.37 – 8.34 and 8.30 -8.28 ppm seen in the low field and two triplets at 7.83 – 7.89 and 7.66 – 7.62 ppm seen in the high field indicate that benzotriazole was successfully bound to cinnamic acid.	The presence of aromatic CH carbons of benzotriazole and cinnamic acid aromatic CH protons can be shown as evidence that the structure is formed.
2,4-dimethoxy-CA-Bt	The disappearance of the carboxylic acid proton of the starting compound and the presence of two doublets and two triplet aromatic CH proton peaks of benzotriazole indicate that benzotriazole is attached to the structure.	The presence of a total of 9 aromatic and olefinic CH carbons together with two methoxy CH_3 carbons (number 16 and 17) at 56.53 ppm and 56.16 ppm in the aliphatic region indicate that the structure is formed.
2,4,5-trimethoxy-CA-Bt	The existence of the characteristic benzotriazole ring protons two doublets in low filed and two triplet at high field and disappearance of carboxylic acid proton peaks of cinnamic acid prove that the structure was formed.	Number of carbon peaks from benzotriazole 4 -CH and 2 -C carbon peaks and existence of three methoxy carbon at aliphatic region show that the structure was obtained.
Phenylbenzyl-CA-Bt	The aromatic CH peaks (number 13,16 and 14,15) of benzotriazole appear as two doublets and two triplets, indicating that the compound was formed.	The coherence of the number of olefinic carbon peaks and aromatic CH peaks proves that the structure was obtained

4.4. NMR Evaluation of Amino acid conjugates

Table 4.4.1. Structural evaluation of amino acid conjugates

Compund Name	**^{1}H NMR Interpretation**	**^{13}C APT NMR Interpretation**
2-fluoro-CA-Gly-OH	The Carboxylic acid -OH proton (number 9) of glycine at 12.61 ppm as a singlet, the triplet of NH proton (number 7) at 8.56 – 8.53 ppm, aliphatic CH_2 protons (number 8) of glycine at 3.92 – 3.91 ppm, olefinic CH proton (number 5) at 7.55 – 7.51 ppm, the four aromatic CH protons between 8.56 – 7.26 ppm indicates the formation of the final product.	The two carbonyl carbon peaks, carboxylic acid and amide, at 171.68 and 165.52 ppm, aliphatic CH_2 carbon peak at 41.34 ppm, olefinic carbons (number 7 and 8) at 132.00 and 116.45 ppm and ipso carbon (number 1) at 122.96 ppm prove that the synthesis of the compound accomplished.
2-chloro-CA-Gly-OH	Existence of carboxylic acid -OH proton at 12.64 ppm as a singlet, olefinic protons (number 7 and 8) at 7.78 – 7.76 ppm and 6.81 – 6.77 ppm (16 Hz coupling constant indicates trans isomerism), NH proton of amide bond at 8.55 – 8.52 ppm and glycine's aliphatic CH_2 protons at 3.93 – 3.91 ppm prove the formation of product.	The structure has two carbonyl groups and carboxylic acid and amide carbonyls arise at 171.65 ppm and 165.26 ppm, respectively. In addition, aliphatic CH_2 carbon at 41.38 ppm, olefinic carbon peaks at 134.96 and 125.24 ppm and two quaternary carbon peaks at 133.80 and 133.11 ppm show that the desired compound successfully synthesized.
2-chloro-CA-Gly-OCH$_3$	CH_3 protons of methoxy group (number 11) at 3.67 ppm, CH_2 protons of glycine (number 10) at 4.02 – 4.00 as a doublet, olefinic proton (number 8) at 6.80 – 6.76 ppm as a doublet, NH proton (number 9) at 8.69 – 8.67 ppm are obvious proof of the product formation.	Ester and amide carbonyl carbon peaks at 170.77 and 165.43 ppm, methoxy carbon (number 12) at 52.25 ppm, glycine's CH_2 carbon (number 10) at 41.32 ppm and olefinic carbons (number 7 and 8) at 135.21 and 124.93 ppm prove that the desired compound obtained.

Table 4.4.1. Structural evaluation of amino acid conjugates (continuing)

2-chloro-CA-Ala-OCH$_3$	CH_3 protons of methoxy group (number 12) at 3.67 ppm, CH proton of alanine (number 10) at 4.46– 4.39 ppm, olefinic proton (number 8) at 6.78 – 6.73 ppm, CH_3 protons (number 11) of alanine at 1.37 – 1.35 ppm as doublet and NH proton (number 9) at 8.69 – 8.67 ppm are obvious proof of the product formation.	Ester and amide carbonyl carbon peaks at 173.50 and 164.73 ppm, methoxy carbon (number 12) at 52.43 ppm, olefinic carbons (number 7 and 8) at 135.21 and 124.93 ppm, alanine's CH carbon (number 10) at 48.30 ppm and CH_3 carbon (number 13) peak at 17.53 ppm proves that the desired compound obtained.
2-methyl-CA-Gly-OH	For this compound, the carboxylic acid OH proton peaked at 12.65 ppm as singlet, and olefinic CH protons (number 7 and 8) peaked at 7.71 - 7.67 ppm and 6.65 - 6.61 ppm as doublets. 15.6 Hz coupling constant of olefinic CH protons mean the structure in trans isomerization. Another characteristic peak belongs to glycine's CH2 protons (number 11) show up at 3.92 – 3.91 ppm as a doublet. Existence of NH proton peak at 8.50 – 8.48 ppm as a triplet provide us to pass judgment the amide bond successfully formed.	Two carbonyl carbon (number 12 and 9) peaks (carboxylic acid and amide) in the carbon NMR spectrum appear at 171.85 ppm and 165.78 ppm, respectively, which is proof that the free amine moiety successfully binds to the cinnamic acid compound. Moreover, CH_2 carbon (number 11) belonging to glycine and methyl carbon (number 14) bound to the aromatic ring are seen at 19.89 ppm and 41.29 ppm. Other aromatic carbon peaks are clearly visible in the aromatic region.
2-methyl-CA-Gly-OCH$_3$	Compared to the 2-methyl-CA-Gly-OH compound, the only difference between them is the disappearance of the carboxylic acid OH proton seen at 12.65 ppm and appearance of the CH_3 protons of the methyl group from the ester at 3.67 ppm. All remaining protons are compatible with the structure.	The only difference seen in the ^{13}C APT NMR is that the methyl carbon of the ester appears at 52.25 ppm. All remaining peaks are identical to 2-methyl-CA-Gly-OH with very slight shifts. This is proof that the compound is formed.

Table 4.4.1. Structural evaluation of amino acid conjugates (continuing)

2-methyl-CA-Ala-OCH_3	The difference of this compound from 2-methyl-CA-Gly-OMe is only the methyl protons of alanine, which (number 15) is observed between 1.36 and 1.33 ppm. All remaining peaks are compatible with the structure and indicate that the targeted compound are formed.	Two aliphatic methyl peaks (number 14 and 15) at 19.88 and 17.55 ppm, CH carbon of alanine at 48.23 ppm, CH3 carbon at 52.40 ppm and olefinic carbons (number 7 and 8) at 137.35 and 122.98 ppm show that the structure are formed.
3-methyl-CA-Gly-OH	The presence of the carboxylic acid proton at 12.63 ppm and aliphatic CH_2 proton peaks of the amino acid at 3.91 – 3.89 ppm, and the disappearance of aromatic protons of benzotriazole indicate that this compound has been successfully obtained.	The existence of carboxylic acid (number 12) and amide carbonyl carbon (number 9) peaks at 171.84 and 165.76 ppm, glycine's aliphatic carbon (number 11) peak at 41.29 ppm prove that the structure was formed.
4-chloro-CA-Gly-OMe	For this compound, there are several characteristic peaks such as glycine's CH2 protons at 4.00 – 3.99 ppm as a doublet, methyl protons of ester functional group at 3.68 ppm as a singlet, formation of NH protons from amide at 8.49 ppm, and disappearance of carboxylic acid proton of the starting compound exhibit that the amino acid successfully bounded to cinnamic acid compound.	Like its proton NMR evaluation, several specific peaks show that the desired product successfully obtained. These peaks are two carbonyl carbons at 170.84 and 165.71 ppm, aliphatic CH2 carbon at 41.28 ppm and two olefinic carbons at 138.59 and 122.68 ppm.
4-chloro-CA-Ala-OMe	The only difference from previous compound is that alanine's methyl protons which is at 1.35 – 1.33 ppm as a doublet due to the adjacent CH proton. The rest of the peaks of the compound are exist with slight shifts.	As in the proton NMR, the specific peaks of the methyl carbon of the alanine at 17.55 ppm and the methyl carbon of the ester group at 52.38 ppm and the two carbonyl carbons (number 12 and 9) at 173.56 and 165.03 ppm show that the compound was obtained as a result of the reaction.

Table 4.4.1. Structural evaluation of amino acid conjugates (continuing)

4-methoxy-CA-Gly-OH	For this compound, free glycine was bound to cinnamic acid by cleavage of the benzotriazole group. As such, the disappearance of aromatic CH protons of benzotriazole and the appearance of aliphatic CH_2 protons of glycine at 3.90 – 3.88 ppm can be presented as evidences.	The presence of the aliphatic CH_2 carbon at 41.28 ppm and carboxylic acid carbonyl carbon at 171.86 ppm show that the structure was formed.
4-methoxy-CA-Ala-OH	Examples of evidence showing alanine binding to the structure, as in the case of glycine, can be shown as the presence of alanine's aliphatic protons (number 11 and 15) at 3.38 ppm and 1.33 – 1.31 ppm and carboxylic acid proton at 12.56 ppm.	The presence of two carbonyl carbon peaks at 174.73 and 165.43 ppm and CH and CH_3 carbon peaks of alanine are indicative of the formation of the structure.
4-methoxy-CA-Gly-OMe	The existence of NH proton at 8.49 – 8.46 ppm as a triplet, olefinic protons (number 7 and 8) at 7.44 – 7.40 ppm and 6.59 – 6.55 ppm as doublets and aliphatic protons (methoxy and CH_2) can be shown as evidences of compound formation.	Three aliphatic carbon peaks, 2 equivalent aromatic protons and two carbonyl carbon peaks at 170.98 ppm and 166.20 ppm clearly show that the formation of amino acid conjugate successfully occurred.
4-nitro-CA-Gly-OMe	For this structure, the methyl proton peak at 3.67 ppm as a singlet, CH2 proton (number 11) peak of glycine at 4.03 – 4.02 ppm and aromatic protons (number 3,5 and 2,6) at 8.29 – 8.27 and 7.89 – 7.87 ppm are clear evidences for product formation.	Existence of two aliphatic carbons (number 11 and 13) and two carbonyl carbons (number 12 and 9) can be shown as proofs for product formation.
4-nitro-CA-Ala-OMe	Compared to the glycine conjugate, the only difference is the methyl proton (number 14) peak of alanine at 1.37 – 1.35 ppm, and all of the remaining peaks are complete with the structure.	Here, the presence of the methyl carbon (number 14) peak of the alanine at 17.52 ppm and the compatibility of the remaining peaks with the carbons in the structure shows that the compound is obtained.

Table 4.4.1. Structural evaluation of amino acid conjugates (continuing)

2,4,5-trimethoxy-CA-Gly-OH	Carboxylic acid proton (number 13) at 12.55 ppm, olefinic protons (number 7 and 8) at 7.66 – 7.62 ppm and 6.65 – 6.61 ppm and glycine's CH_2 peak at 3.92 – 3.91 ppm clearly show that the structure was formed.	
Phenylbenzyl-CA-Gly-OH	The presence of the NH proton (number 12) at 8.14 – 8.12, the olefinic proton peak (number 10) at 6.98 – 6.94 ppm and the aliphatic CH2 proton peak of the glycine at 3.81 – 3.80 ppm indicates that the structure was formed.	The glycine ch2 carbon peak at 43.31 ppm, the olefinic carbon peak at 138.47 - 122.96 ppm, is an indication that the compound is formed.
Phenylbenzyl-CA-Ala-OH	The characteristic protons for this compound are the CH_3 and CH aliphatic proton peaks at 1.33 – 1.31 ppm and 4.30 – 4.27 ppm, respectively. In addition, the existence of the NH proton peak at 8.31 – 8.29 ppm can be shown as another evidence.	the situation is similar here, and the presence of aliphatic CH_3 and CH carbon peaks at 18.57 and 49.03 ppm, two carbonyl carbons at 175.45 and 164.87 ppm and olefinic carbons at 138.68 and 122.78 ppm are indications that the structure is clearly obtained.
Phenylbenzyl-CA-Leu-OH	The presence of the NH proton peak at 8.23 – 8.21 ppm , olefinic CH proton (number 10) at 6.86 – 6.82 ppm, and the aliphatic protons can be considered sufficient as evidence of compound formation.	the presence of 4 different aliphatic carbon peaks at 22.09, 23.48, 24.96, 41.47 and 51.72 ppm from leucine and the compatibility of other carbon peaks with the structure is proof that the compound is formed.
Naft-CA-Gly-OH	Characteristic peaks for this compound; although the amino acid has a carboxylic acid proton at 12.70 ppm and aliphatic CH_2 proton peak at 3.96 - 3.95 ppm, the number of ring protons belonging to naphthalene also indicates that the compound is obtained.	The presence of two carbonyl peaks at 171.83 and 165.75 ppm and aliphatic CH_2 carbon at 41.38 ppm can be shown as clear evidence for product formation.

Table 4.4.1. Structural evaluation of amino acid conjugates (continuing)

Naft-CA-Gly-Gly-OMe	This compound contains two amino acids compared to other derivatives and ends with the ester group instead of the carboxylic acid. The methoxy proton peak of the ester at 3.66 ppm, the CH_2 proton peak of two glycine at 3.96 – 3.95 and 3.92 – 3.90 ppm and the presence of two NH proton peaks indicate that the target compound is obtained.	Three carbonyl carbon peaks at 170.77 ppm, 169.99 ppm, and 165.72 ppm, methoxy carbon of ester at 52.22 ppm and the presence of CH_2 carbon peaks of amino acids at 42.43 ppm and 41.05 ppm showed that the compound was formed.
Phenant-CA-Gly-OH	Total number of aromatic CH proton peak and presence of aliphatic CH_2 proton peak at 3.89 – 3.88 ppm coherent with compound.	Carboxylic acid carbon at 173.11 ppm, glycine's CH_2 carbon at 43.14 ppm and remaining aromatic proton peaks can be shown as evidences.
Phenant-CA-Meth-OH	Total number of aromatic and olefinic proton and aliphatic protons of methionine are in accordance with the structure.	The observation of the CH carbon at 52.68 ppm, two CH_2 carbons at 32.08 and 30.38 ppm and CH_3 carbon peak of methionine at 15.12 ppm can be given as sufficient evidence that the compound is formed.
Pyrene-CA-Gly-OH	The most characteristic peak for this compound is the CH_2 aliphatic proton peak of glycine at 3.95 – 3.93 ppm, which is the most important evidence that the structure is obtained. In addition, the spectrum supports the existence of all the remaining protons.	The presence of both aliphatic peak at 42.16 ppm and olefinic carbon peaks at 135.65 ppm and 122.96 ppm in the ^{13}C NMR spectrum is an indication that the structure is formed.

Table 4.4.1. Structural evaluation of amino acid conjugates (continuing)

2,4-dimethoxy-CA-Gly-OH	The most significant evidences showing that glycine bound to the 2,4-dimethoxy-CA-Bt compound, the presence of the glycine's CH_2 proton peak at 3.88 – 3.86 ppm and the NH proton peak at 8.28 – 8.25 ppm from the amide bond formed. The remaining peaks are compatible with other protons of the structure.	In addition to the presence of two methoxy carbons at 56.13 and 55.88 ppm with the CH_2 carbon of glycine at 41.32 ppm, the appearance of two carbonyl carbon peaks at 171.95 and 166.49 ppm can be presented as evidence that the structure is formed.
2,4-dimethoxy-CA-Meth-OH	When examining methionine amino acid containing conjugate, both the presence of aliphatic peaks of methionine (number 11,14,15 and 16) and the presence of aromatic - olefinic proton peaks of cinnamic acid indicate that the structure was formed. The mixing of some aliphatic peaks with the solvent peak complicates the interpretation, but it will have a better chance of interpretation when the carbon NMR spectrum is evaluated.	The aliphatic carbon peaks (number 11,14,15 and 16) of methionine at 51.60 ppm, 30.24 ppm, 31.40 ppm and 15.06 ppm, respectively, are clearly seen here. In addition, the presence of two different carbonyl carbon peaks at 173.96 and 166.33 ppm is another proof that the structure is formed.
Naft-CA-Ala-OH	Unlike the product containing glycine, the CH and CH3 proton peaks of the alanine at 4.46 – 4.36 and 1.39 – 1.37 ppm and the olefinic protons at 8.26 – 8.20 and 6.82 – 6.78 ppm in the spectrum prove that the compound is formed.	The presence of carbonyl carbon peaks at 174.70 and 165.05 ppm belonging to cinnamic acid and amino acid and aliphatic carbons at 48.30 and 17.90 ppm belonging to alanine clearly shows that the compound is obtained.
Naft-CA-Meth-OH	The presence of aliphatic peaks of the methionine (CH, CH2 and CH3) and the number of aromatic CH protons of naphthene are compatible with the structure.	The aliphatic carbon peaks at 52,68 ppm, 32.08 ppm, 30.38 ppm and 15.12 ppm can be shown as evidences that the structure is formed.

4.5. Mechanistic evaluation of synthesis steps

In this section, possible reaction mechanisms of cinnamic acid formation, N-acylbenzotriazole and amino acid conjugates are presented and discussed.

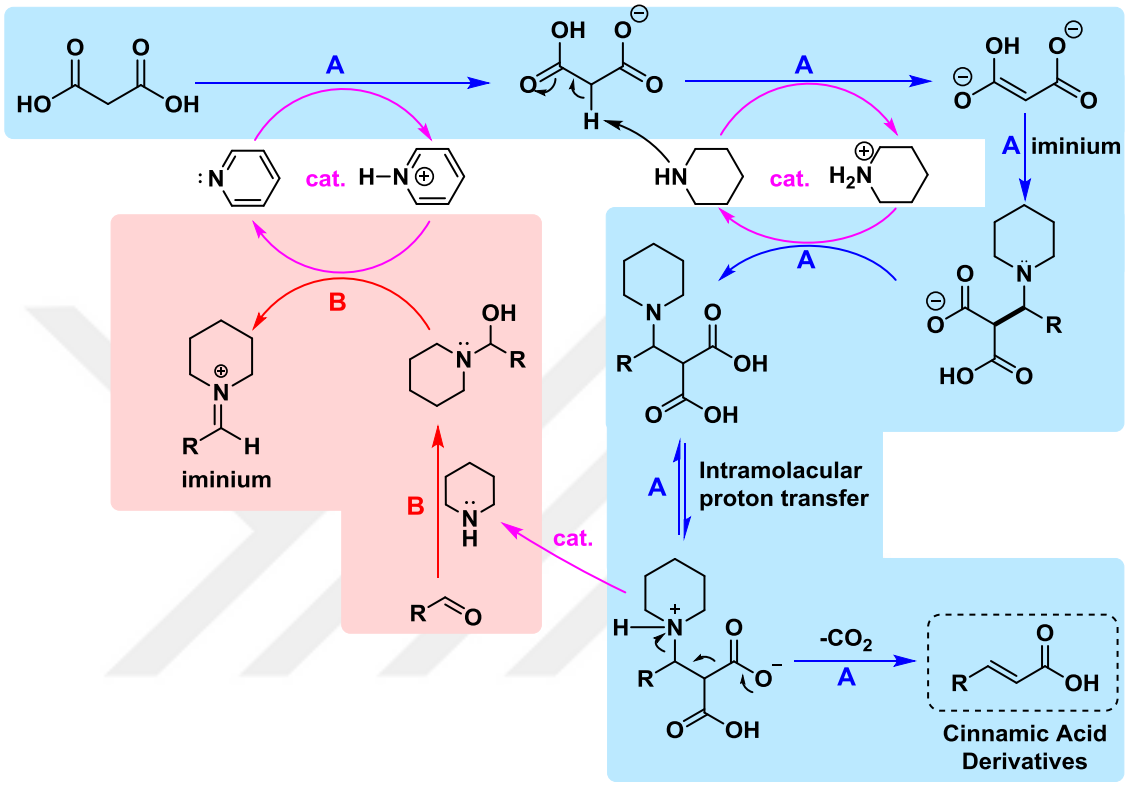

Figure 4.5.1. Proposed mechanism for cinnamic acid synthesis

As a result of the breakdown of the acid proton by pyridine, the carboxylate anion of the malonic acid is formed together with the pyridinium cation. Piperidine provides the formation of enolate by removing the acidic CH_2 proton of malonic acid, while this enolate provides a nucleophilic attack on the enamine cation formed between aldehyde and piperidine in the reaction medium. Carbon dioxide is separated from the dicarboxylate anion formed as a result of intermolecular proton transfer, and as a result of the proton rupture of the carboxylate anion from the pyridinium cation, piperidine and target product cinnamic acid derivative are formed.

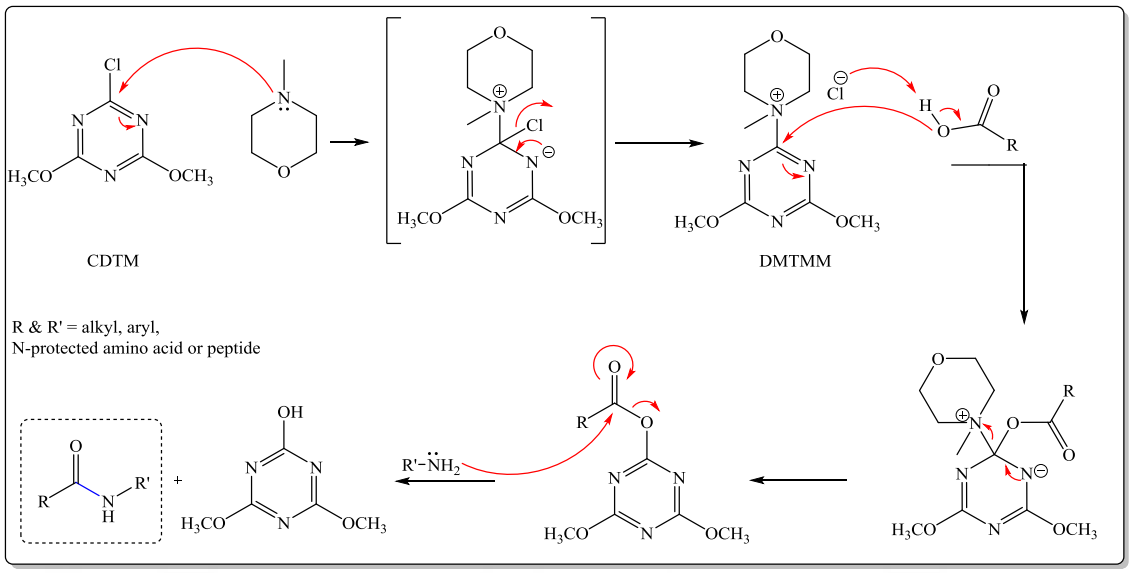

Figure 4.5.2. Proposed reaction mechanism for synthesized conjugates based on CDMT method

In this reaction (Figure 4.5.2), which can take place as one pot synthesis, the carboxylic acid derivative (amino acid / peptide) reacts with CDMT in the presence of N-methyl morpholine, giving the 2-acyloxy-4,6-dimethoxy-1,3,5-triazine compound over the DMTMM intermediate. . In the final stage, the targeted product is obtained by reacting with the free amine (amide bond) as nucleophile. The reaction takes place under cold conditions (around 0 degree of celsius), where NMM is added dropwise and solvents such as DCM or MeCN are used. Due to the weak base character of the Triazine compound, possible by-products are eliminated by using dilute acid and $NaHCO_3$ in the purification process.

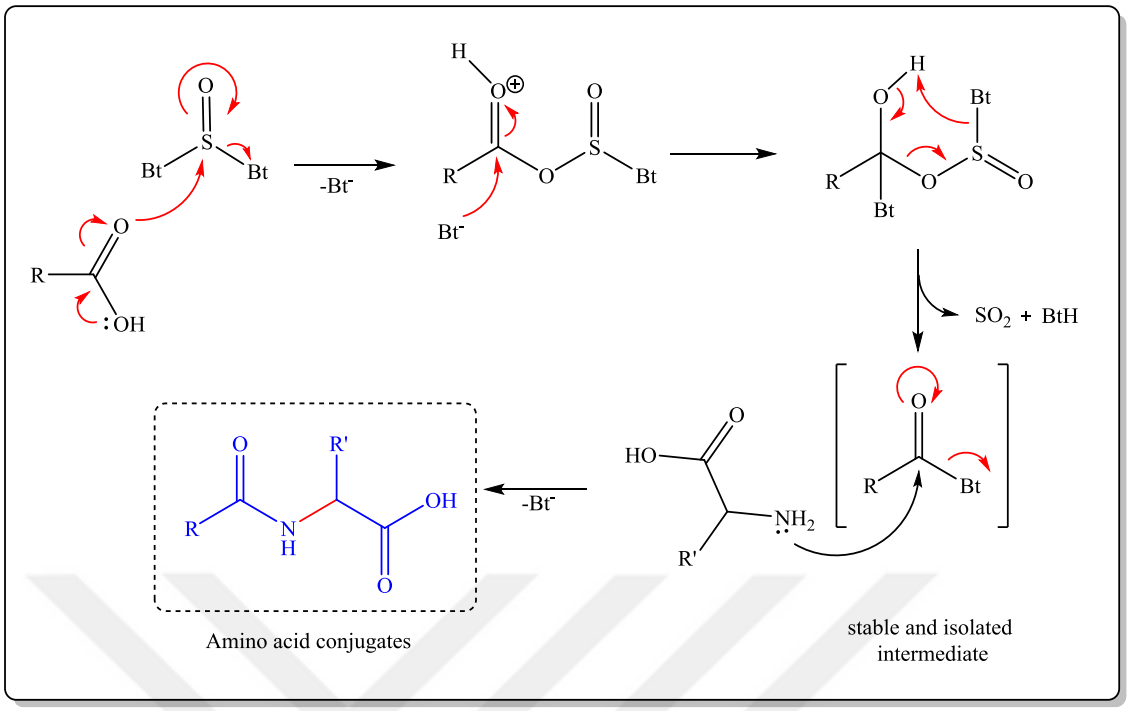

Figure 4.5.3. Proposed reaction mechanism for amino acid conjugate via *N*-acylbenzotriazole

When the conjugates are synthesized via *N*-acylbenzotriazole as shown in Figure 4.5.3., initially, two molecules of benzotriazoles is replaced by two chlorines of thionylchloride. In the next stage, carboxylic acid oxygen attacking to the sulfur atom causing the cleavage of the benzotriazole as an anion, while the possibility of attacking of the benzotriazole anion may occur in 1,2-addition. *N*-acylbenzotriazole, the stable intermediate, is formed when the benzotriazole anion causes intramolecular proton transfer and leaving of SO_2 and BtH by nucleophilic attack to the carbonyl carbon of the acid. In the final step, the amino acid conjugate is formed after a nucleophilic attack of free amino acid.

4.6. Evaluation of dielectric properties for amino acid conjugates

The conductance measurements of the compounds were analyzed at between 1 Hz and 20 kHz based on the alternating current (AC) conductivities. Tables 4.6.1.-4.6.6. show the conductivity and dielectric behavior of selected compounds versus frequency at room temperature. The conductivity values change with the frequency due to the electrical conductivity of the compounds depends on mobility of electrons or ions in their structures

Table 4.6.1. The dielectric constant (**ε'**), dielectric loss (**ε''**) and ac conductivity (σ) values in 1 kHz and at 25 ^{o}C

Compounds	**ε'**	**ε''**	**σ_{ac} (Siemens/cm)**	**log σ_{ac}**
4-nitro-CA-Gly-OMe	7,481	0,289	4.16×10^{-9}	-8,380
4-nitro-CA-Ala-OMe	8,250	0,341	4.59×10^{-9}	-8,338
4-methoxy-CA-Gly-OMe	7,938	0,317	4.41×10^{-9}	-8,354
4-methoxy-CA-Ala-Ome	7,871	0,328	4.38×10^{-9}	-8,358
4-chloro-CA-Gly-OMe	7,584	0,307	4.22×10^{-9}	-8,375
4-chloro-CA-Ala-OMe	8,337	0,339	4.64×10^{-9}	-8,333

Considering other comparisons, there is an inverse situation in para substitute conjugates in Table 4.6.1. Although the nitro group has strong electron withdrawing feature, it has been observed that the electrical values are higher because it contributes to the resonance structure of the aromatic ring and causes the electrons to dissipate more. The conjugates bearing the nitro group show a distinct difference in themselves. The hyperconjugation of the methyl group in the amino acid of alanine makes the compound electron richer than the glycine conjugate, which caused the electrical parameters to be higher. 4-chloro-CA-Ala-OMe has the highest value of dielectric constant (ε') 8.34 and conductivity (σ_{ac}) 4.64×10^{-9} and closest one is 4-nitro-CA-Ala-OMe has a value of dielectric constant (ε') 8.25 and conductivity (σ_{ac}) 4.59×10^{-9}. The conductivity values change with the frequency due to the electrical conductivity of the compounds depends on mobility of electrons or ions in their structures.

Table 4.6.2. The dielectric constant (**ε'**), dielectric loss (**ε''**) and ac conductivity (σ) values in 1 kHz and at 25 °C

Compounds	**ε'**	**ε''**	**σ_{ac} (Siemens/cm)**	**log σ_{ac}**
Naft-CA-Gly-OH	3,20	0.027	2.97×10^{-9}	-9,573
Naft-CA-Ala-OH	5,507	0,190	3.06×10^{-9}	-8,513
Naft-CA-Meth-OH	7,488	0,382	4.66×10^{-9}	-8,380
Naft-CA-Gly-Gly-OMe	9,055	0,357	$5,04 \times 10^{-9}$	-8,240
Phen-Benzyl-CA-Gly-OH	4,67	0.082	3.16×10^{-9}	-9,74
Phenylbenzyl-CA-Ala-OH	8,381	0,378	4.41×10^{-9}	-8,331

This table clearly shows how the amino acid difference in naphthalene-containing conjugates affects electrical parameters. The increase in the polarity of the group in the side chain of the amino acid was reflected in proportion to the electrical parameter results. The reason why conjugate containing methionine has the highest value is the polarity of the thio-ether group in the side chain. On the other hand, the effect of an extra amino acid added to the structure was more than the side chain effect. In the Naft-CA-Gly-Gly-OMe conjugate, the carbonyl group with a high polarity from the second amino acid contributed positively to the movements of electrons, resulting in increased electrical values.

Table 4.6.3. The dielectric constant (**ε'**) dielectric loss (**ε''**) and ac conductivity (σ) values in 1 kHz and at 25 °C

Compounds	**ε'**	**ε''**	**σ_{ac} (Siemens/cm)**	**log σ_{ac}**
2-methyl-CA-Gly-OH	7,756	0,298	4.31×10^{-9}	-8,364
2-methyl-CA-Ala-OH	8,422	0,399	4.68×10^{-9}	-8,328
3-methyl-CA-Gly-OH	8,254	2,292	4.76×10^{-9}	-8,273
2-methyl-CA-Gly-OMe	7,142	0,304	3.97×10^{-9}	-8,401

Comparison of the dielectric properties of conjugates containing methyl substituents revealed following knowledge; the conjugates with methyl group in the meta position positively contributes to the ortho position. In addition to methyl group, the amıno acid in conjugate was also found to affect conductivity in direct proportion to the growth of the side chain as in other compounds. The extra methyl group on alanine side chain donates

electrons to 2-methyl-CA-Ala-OH via hyperconjugation while 2-methyl-CA-Gly-OH did not show such effect which makes conductivity of 2-methyl-CA-Ala-OH higher than 2-methyl-CA-Gly-OH and other compounds in table 4.6.3. As with the comparison of the dielectric properties of the halogen containing compounds, the compounds containing the methyl group in the ortho and meta position in the benzene ring were compared in terms of electrical parameters. The dielectric constant of the 2-methyl-CA-Gly-OH compound in the conjugates was 7.75 and the ac conductivity value was 4.31 x 10^{-9}, while the chalcone compound with methyl in ortho position was 2.99 and 0.091 x 10^{-9}, respectively. There is a 2.5-fold difference between the dielectric constants and a 47-fold difference between the ac conductivity values. These results show that the polarization of the amino acids in the structure is higher than that of the phosphazene compound. Although a similar trend was observed when the methyl group was in the meta position, the difference between conductivity values (4.76 x 10^{-9} vs. 2.68 x 10^{-9}) were approximately 2 times higher (Koran et al. 2014).

Table 4.6.4. The dielectric constant (**ε'**) dielectric loss (**ε''**) and ac conductivity (σ) values in of 1 kHz and at 25 ºC

Compounds	**ε'**	**ε''**	**σ_{ac} (Siemens/cm)**	**log σ_{ac}**
2,4-dimethoxy-CA-Meth-OH	7,160	0,322	3.98 x 10^{-9}	-8,399
4-methoxy-CA-Gly-OH	6,784	0,279	3.77 x 10^{-9}	-8,423
4-methoxy-CA-Gly-OMe	7,938	0,317	4.41 x 10^{-9}	-8,357
4-methoxy-CA-Ala-OMe	7,871	0,328	4,38 x 10^{-9}	-8,358

In methoxy group conjugates, the ester group has a positive effect on conductivity between 4-methoxy-CA-Gly-OH with free carboxylic acid and 4-methoxy-CA-Gly-OMe conjugates with methyl ester. The amino acid side chain affected the dielectric constant positively. The more polar group the amino acid has the higher dielectric properties the conjugates has.

Table 4.6.5. The dielectric constant (**ε'**) dielectric loss (**ε''**) and ac conductivity (σ) values in 1 kHz and at 25 ^{o}C

Compounds	**ε'**	**ε''**	**σ_{ac} (Siemens/cm)**	**log σ_{ac}**
2-chloro-CA-Gly-OH	7,273	0,324	4.04×10^{-9}	-8,392
2-fluoro-CA-Gly-OH	6,982	0,280	3.88×10^{-9}	-8,410
2-chloro-CA-Gly-OMe	6,774	0,261	3.76×10^{-9}	-8,424
2-chloro-CA-Ala-OMe	6,873	0,289	3.82×10^{-9}	-8,417
4-chloro-CA-Gly-OMe	7,584	0,307	4.22×10^{-9}	-8,374
4-chloro-CA-Ala-OMe	8,338	0,339	4.64×10^{-9}	-8,333

Dielectric properties of halogen substituted conjugates are compared in Table 4.6.5. The conductivity and other electrical properties of 2-chloro-CA-Gly-OH is higher than 2-fluoro-CA-Gly-OH. This is attributed to the electronegativity differences of the halogens for which fluorine has higher value of electronegativity. Fluorine withdraws more electron from the ring than chlorine making the ring electron poor and this causes 2-fluoro-CA-Gly-OH to be less conductive. The position of the chlorine was also found to be important in defining electrical behaviors of the conjugates. The comparison of the electrical behaviors of the conjugates for which chlorine was in ortho and para position was also studied. The results demonstrated that 4-chloro-CA-Ala-OMe and 4-chloro-CA-Gly-OMe were more conductive than 2-chloro-CA-Ala-OMe and 2-chloro-CA-Gly-OMe, respectively. This was probably due to electrical conductivity of the compounds depends on distance of the electrons moved through the conjugates. The structural similarities of the chalcone compounds containing halogens in their structure obtained by Koran et al., And the amino acid conjugates synthesized in this thesis, enabled the comparison of the electrical parameters of these compounds. As a result of comparing the electrical parameters of the chalcone compound containing fluorine atom in the ortho position and the fluorine-bearing conjugate in the same position, there is an approximately 3-fold difference between the dielectric constants (6.98 vs 2.6), and the same trend is observed as a 5.3-fold difference in ac conductivity values (3.9×10^{-9} vs 7.3×10^{-10}) and this difference is thought to be due to the extra polarization provided by amino acids.

Again, according to the comparison obtained from the same study, it was seen that the comparison of compounds with chlorine atom in ortho position gave similar results to the previous comparison. It is thought that there is an approximately 2-fold difference between the dielectric constants and approximately 4.5 times ac conductivity values (7.27 vs 1.62) and this difference is due to the intramolecular polarization provided by the amino acid structures (Koran et al. 2017).

Table 4.6.6. The dielectric constant (**ε'**) dielectric loss (**ε''**) and ac conductivity (σ) values in 1 kHz and at 25 ^{o}C

Compounds	**ε'**	**ε''**	**σ_{ac} (Siemens/cm)**	**log σ_{ac}**
Phenant-CA-Gly-OH	7,84	0.170	4.45×10^{-9}	-9,56
Pyrene-CA-Gly-OH	6,72	0.088	3.86×10^{-9}	-9,50
Phenylbenzyl-CA-Gly-OH	4,67	0.082	3.16×10^{-9}	-9,74
Naft-CA-Gly-OH	3,20	0.027	2.97×10^{-9}	-9,57

Electrical properties of glycine conjugates containing extra aromatic benzene rings were examined in table 4.6.6. Among the conjugates Naft-CA-Gly-OH had the lowest conductivity while Phenant-CA-Gly-OH had the highest conductivity. The most interesting point in this comparison is that the Pyrene-CA-Gly-OH (four benzene rings) was less conductive than Phenant-CA-Gly-OH (three benzene rings) indicating that the positive effect of conjugation decreases after a point. A possible explanation for that could be the electrons localize within pyrene ring decreasing electron movement and hence conductivity.

5. CONCLUSION

The aim of the work described in this thesis was synthesis of novel cinnamic acid substituted amino acid conjugate and investigation of their physical activities in terms of structure-activity relationship. Collectively, synthesis, characterization and electrical measurements of the targeted conjugates were carried out, and a total of 28 amino acid conjugates were obtained from different cinnamic acids by benzotriazole and triazine methods. The structures of all the compounds obtained in the thesis were characterized by ^{1}H, ^{13}C APT, COSY, HETCOR NMR, FT-IR and elemental analysis methods. The electrical parameters were measured with impedance analyzer. Physical parameters such as dielectric constant, dielectric loss factor and conductivity were compared by considering structure-activity relationship. The presence of characteristic olefinic proton-carbon peaks and carboxylic acid proton seen in NMR spectra of cinnamic acids is evidence that compounds were formed. Evidence that those carrying free carboxylic acid groups from the amino acid conjugates were formed by the presence of aliphatic proton-carbon peaks and olefinic peaks from cinnamic acid seen in NMR spectra. It has been observed that as the frequency increases, there is a rapid decrease in the dielectric constant and this trend decreases towards higher frequency regions. Along with the relaxation times and electronic polarization as an explanation for this trend, another reason is that the inter-surface dipoles do not have enough time to orient themselves in the direction of the alternating current. The rapid decreases in low frequencies indicate that the charged dipoles in the molecules have a high tendency to move in the direction of the electric field applied to this frequency region. The electrical properties of the conjugates were evaluated by study of electron acceptor-donor group effect, conjugation number, amino acid differences in conjugates and effect of the ortho/meta/para positions of aromatic ring in cinnamic acid derivatives. Naft-CA-Gly-Gly-OMe had the most striking result with a conductivity value of 5.04×10^{-9} Siemens/cm. In halogenated conjugates, the 4-chloro-CA-Ala-OMe compound overrides others with a value of 4.64×10^{-9} Siemens/cm. In nutshell, the higher number of electrons

releasing group of amino acid side chain make the compounds have the higher conductivity and dielectric constant value. As the number of polarizable groups increases, the increase in the conductivity of the compound is clearly seen.

REFERENCES

Acheson RM, Booth DA, Brettle R, Harris AM (1960) The synthesis of some acylglycines and related oxazolones. Journal of the Chemical Society (Resumed)(0): 3457-3461

Adams R, Ulich LH (1920) The use of oxalyl chloride and bromidefor producing acid chlorides, acid bromides or acidanhydrides. Journal of the American Chemical Society 42(3): 599-611

Akram M, Javed A, Rizvi TZ (2005) Dielectric Properties of Industrial Polymer Composite Materials. Turkish Journal of Physics 29: 355 – 362

Al-Warhi TI, Al-Hazimi HMA, El-Faham A (2012) Recent development in peptide coupling reagents. Journal of Saudi Chemical Society 16(2): 97-116

Armin A, Stoltzfus DM, Donaghey JE, Clulow AJ, Nagiri RCR, Burn PL,. Gentle IR, Meredith P (2017) Engineering dielectric constants in organic semiconductors. Journal of Materias Chemistry C 5: 3736-3747

Avanesyan AA, Pashkov A, Simonyan NA, Simonyan AV, Myachina OV (2009) Antiradical activity of cinnamic acid derivatives. Pharmaceutical Chemistry Journal 43: 249-250

Bachmann WE, Kloetzel MC (1937) Phenanthrene Derivatives VII. The Cyclization of β-Phenanthrylpropionic Acids. Journal of the American Chemical Society 59(11): 2207-2213

Belleau B, Malek G (1968) New convenient reagent for peptide syntheses. Journal of the American Chemical Society 90(6): 1651-1652

Betova I, Bojinov M, Lankinen E, Sundholm G (1999) Studies on the redox behaviour of some polythiophene derivatives by impedance spectroscopy in symmetrical and asymmetrical configurations. Journal of Electroanalytical Chemistry 472(1): 20-32

Bezgin F, Ayaz N, Demirelli K (2015) Synthesis, characterization, and dielectric properties of polymers functionalized with coumarone and diethanolamine. Journal of Applied Polymer Science 132(26)

Biryan F, Abubakar AM, Demirelli K (2018) Product analysis, electrical and dielectric properties depending on thermal influence of poly(N-isopropyl acrylamide)/graphite-filled composite. Thermochimica Acta 669: 66-79

Biryan F (2019) Synthesis of graft copolymers carrying molecular diffusion susceptibility; investigation of the thermal, electrical and self-healing properties. PhD thesis, Chemistry, Firat University, Elazig, 15

Boerjan W, Ralph J, Baucher M (2003) Lignin Biosynthesis. Annual Review of Plant Biology 54(1): 519-546

Bowden K, Hojatti M (1990) Transmission of polar effects. Part 18. Ionisation and esterification with diazodiphenylmethane of a series of 3-(8-substituted-1-naphthyl)propiolic and (E)-3-(8-substituted-1-naphthyl)acrylic acids and the alkaline hydrolysis of the methyl esters of the former series. Journal of the Chemical Society, Perkin Transactions 2(7): 1197-1200

Braml NE, Stegbauer L, Lotsch BV, Schnick W (2015) Synthesis of Triazine-Based Materials by Functionalization with Alkynes." Chemistry – A European Journal 21(21): 7866-7873

Brebels J, Manca JV, Lutsen L, Vanderzande D, Maes W (2017) High dielectric constant conjugated materials for organic photovoltaics. Journal of Materias Chemistry A 5: 24037-24050

Burke TR, Fesen MR, Mazumder A, Wang J, Carothers AM, Grunberger D, Driscoll J, Kohn K, Pommier Y (1995) Hydroxylated aromatic inhibitors of HIV-1 integrase. Journal of Medicinal Chemistry 38(21): 4171-4178

Campos M, Nascente PAP (2010) Carrier transport properties of aluminum oxide/polypyrrole films doped with naphthalene-1,5-disulfonic acid. Synthetic Metals 160(13): 1513-1519

Carpino LA (1993) 1-Hydroxy-7-azabenzotriazole. An efficient peptide coupling additive. Journal of the American Chemical Society 115(10): 4397-4398

Carpino LA, Imazumi H, Foxman BM, Vela MJ, Henklein P, El-Faham A, Klose J, Bienert M (2000) Comparison of the Effects of 5- and 6-HOAt on Model Peptide Coupling Reactions Relative to the Cases for the 4- and 7-Isomers. Organic Letters 2(15): 2253-2256.

Cheylan S, Fraleoni-Morgera A, Puigdollers J, Voz C, Setti L, Alcubilla R, Badenes G, Costa-Bizzarri P, Lanzi M (2006) Study of a thiophene-based polymer for optoelectronic applications. Thin Solid Films 497(1): 16-19

Chu W, Tu Z, McElveen E, Xu J, Taylor M, Luedtke RR, Mach RH (2005) Synthesis and in vitro binding of N-phenyl piperazine analogs as potential dopamine D3 receptor ligands. Bioorganic & Medicinal Chemistry 13(1): 77-87

Clifford MN (1999) Chlorogenic acids and other cinnamates – nature, occurrence and dietary burden. Journal of the Science of Food and Agriculture 79(3): 362-372

Clifford MN (2000) Chlorogenic acids and other cinnamates – nature, occurrence, dietary burden, absorption and metabolism. Journal of the Science of Food and Agriculture 80(7): 1033-1043

Cos P, Rajan P, Vedernikova I, Calomme M, Pieters L, Vlietinck AJ, Augustyns K, Haemers A, Vanden Berghe D (2002) In vitro antioxidant profile of phenolic acid derivatives. Free Radic Res 36(6): 711-716

Curtius T (1902) Synthetische Versuche mit Hippurazid. Berichte der deutschen chemischen Gesellschaft 35(3): 3226-3228

Dang ZM, Zheng MS, Zha JW (2016) 1D/2D Carbon Nanomaterial-Polymer Dielectric Composites with High Permittivity for Power Energy Storage Applications. Materials Views 13: 1688-1701

De Simone F, Andrès J, Torosantucci R, Waser J (2009) Catalytic Formal Homo-Nazarov Cyclization. Organic Letters 11(4): 1023-1026

Debnath B, Samanta S, Roy K, Jha T (2003) QSAR Study on Some p-Arylthio Cinnamides as Antagonists of Biochemical ICAM-1/LFA-1 Interaction and ICAM-1/JY-8 Cell Adhesion in Relation to Anti-inflammatory Activity. Bioorganic & Medicinal Chemistry 11(8): 1615-1619

Edreva A (2005) The importance of non-photosynthetic pigments and cinnamic acid derivatives in photoprotection. Agriculture, Ecosystems & Environment 106: 135-146

El-Faham A, Albericio F (2011) Peptide Coupling Reagents, More than a Letter Soup. Chemical Reviews 111(11): 6557-6602

Farah A, Monteiro M, Donangelo CM, Lafay S (2008) Chlorogenic acids from green coffee extract are highly bioavailable in humans. Journal of Nutrition 138(12): 2309-2315

Feng C, Wang L, Yan Y, Liu J, Li S (2010) Synthesis and antitumor evaluation of some 1,3,4-oxadiazole-2(3 H)-thione and 1,2,4-triazole-5(1 H)-thione derivatives. Medicinal Chemistry Research – Med Chem Res 21

Fonseca AC, Lima MS, Sousa AF, Silvestre AJ, Coelho JFJ, Serra AC (2019) Cinnamic acid derivatives as promising building blocks for advanced polymers: synthesis, properties and applications. Polymer Chemistry 10(14): 1696-1723

Fu J, Cheng K, Zhang Z, Fang R, Zhu H (2010) Synthesis, structure and structure–activity relationship analysis of caffeic acid amides as potential antimicrobials. European Journal of Medicinal Chemistry 45(6): 2638-2643

Gangwar S, Pauletti GM, Siahaan TJ, Stella VJ, Borchardt RT (1997) Synthesis of a Novel Esterase-Sensitive Cyclic Prodrug of a Hexapeptide Using an (Acyloxy)alkoxy Promoiety. The Journal of Organic Chemistry 62(5): 1356-1362

Gao Y, Zhang P, Cui A, Ye DY, Xiang M, Chu Y (2018) Discovery and anti-inflammatory evaluation of benzothiazepinones (BTZs) as novel non-ATP competitive inhibitors of glycogen synthase kinase-3β (GSK-3β). Bioorganic & Medicinal Chemistry 26(20): 5479-5493

Gayam V, Ravi S (2017) Cinnamoylated chloroquine analogues: A new structural class of antimalarial agents. European Journal of Medicinal Chemistry 135: 382-391

Ghose AK, Viswanadhan VN, Wendoloski JJ (1999) A Knowledge-Based Approach in Designing Combinatorial or Medicinal Chemistry Libraries for Drug Discovery. 1. A Qualitative and Quantitative Characterization of Known Drug Databases. Journal of Combinatorial Chemistry 1(1): 55-68

Guzman JD, Mortazavi PN, Munshi T, Evangelopoulos D, McHugh TD, Gibbons S, Malkinson J, Bhakta S (2014) 2-Hydroxy-substituted cinnamic acids and acetanilides are selective growth inhibitors of Mycobacterium tuberculosis. MedChemComm 5(1): 47-50

Herrera A, Riaño A, Moreno R, Caso B, Pardo ZD, Fernández I, Sáez E, Molero D, Sánchez-Vázquez A, Martínez-Alvarez R (2014) One-Pot Synthesis of 1,3,5-Triazine Derivatives via Controlled Cross-Cyclotrimerization of Nitriles: A Mechanism Approach. The Journal of Organic Chemistry 79(15): 7012-7024

Hoskins JA (1984) The occurrence, metabolism and toxicity of cinnamic acid and related compounds. Journal of Appllied Toxicology 4(6): 283-292

Huang C,Su J,Zhang QM (2004) High-Dielectric-Constant All-Organic/Polymeric Composite Actuator Materials. Materials Research Society Sympousium 785: D361-D366

Ibrahim MA, Panda SS, Birs AS, Serrano JC, Gonzalez CF, Alamry KA, Katritzky AR (2014) Synthesis and antibacterial evaluation of amino acid–antibiotic conjugates. Bioorganic & Medicinal Chemistry Letters 24(7): 1856-1861

Jad YE, Acosta GA, Khattab SN, de la Torre BG, Govender T, Kruger HG, El-Faham A, Albericio F (2015) Peptide synthesis beyond DMF: THF and ACN as excellent and friendlier alternatives. Organic & Biomolecular Chemistry 13(8): 2393-2398

Jastrzebska MM, Jussila S, Isotalo H (1998) Dielectric response and a.c. conductivity of synthetic dopa-melanin polymer. Journal of Materials Science 33(16): 4023-4028

Jones RA, Thillier Y, Panda SS, Rivera Rosario N, Hall CD and Katritzky AR (2014) Synthesis and characterisation of glucosamine–NSAID bioconjugates. Organic & Biomolecular Chemistry 12(41): 8325-8335

Kale RR, Prasad V, Mohapatra PP, Tiwari VK (2010) Recent developments in benzotriazole methodology for construction of pharmacologically important heterocyclic skeletons. Monatshefte für Chemie - Chemical Monthly 141(11): 1159-1182

Kamiński ZJ, Paneth P, Rudziński J (1998) A Study on the Activation of Carboxylic Acids by Means of 2-Chloro-4,6-dimethoxy-1,3,5-triazine and 2-Chloro-4,6-diphenoxy-1,3,5-triazine. The Journal of Organic Chemistry 63(13): 4248-4255

Katritzky AR, Abdel-Fattah AAA, Vakulenko AV, Tao H (2005) N-Sulfonylbenzotriazoles as Advantageous Reagents for C-Sulfonylation. The Journal of Organic Chemistry 70(23): 9191-9197

Katritzky AR, He HY, Suzuki K (2000)N-acylbenzotriazoles: Neutral acylating reagents for the preparation of primary, secondary, and tertiary amides. Journal of Organic Chemistry 65(24): 8210-8213

Katritzky AR, Lan X, Yang JZ, Denisko OV (1998) Properties and Synthetic Utility of N-Substituted Benzotriazoles. Chemical Reviews 98(2): 409-548

Katritzky AR, Manju K, Singh SK, Meher NK (2005) Benzotriazole mediated amino-, amido- , alkoxy- and alkylthio-alkylation. Tetrahedron 61(10): 2555-2581

Katritzky AR, Rachwal S, Hitchings GJ (1991) Benzotriazole: A novel synthetic auxiliary. Tetrahedron 47(16): 2683-2732

Katritzky AR, Rogovoy BV (2003) Benzotriazole: An Ideal Synthetic Auxiliary. Chemistry – A European Journal 9(19): 4586-4593

Kisfaludy L, Schőn I, Szirtes T, Nyéki O, Lőw M (1974) A novel and rapid peptide synthesis. Tetrahedron Letters 15(19): 1785-1786

Kitamura M, Kawasaki F, Ogawa K, Nakanishi S, Tanaka H, Yamada K, Kunishima M (2014) Role of Linkers in Tertiary Amines That Mediate or Catalyze 1,3,5-Triazine-Based Amide-Forming Reactions. The Journal of Organic Chemistry 79(8): 3709-3714

Knoevenagel E (1898) Condensation von Malonsäure mit aromatischen Aldehyden durch Ammoniak und Amine. Berichte der deutschen chemischen Gesellschaft 31(3): 2596-2619

Koran K, Özen F, Torğut G, Pıhtılı G, Çil E, Görgülü AO, Arslan M (2014) Synthesis, characterization and dielectric properties of phosphazenes containing chalcones. Polyhedron 79: 2013-220

Koran K, Özen F, Biryan F, Görgülü AO (2016) Synthesis, structural characterization and dielectric behavior of new oxime-cyclotriphosphazene derivatives. Journal of Molecular Structure 1105: 135-141

Koran K, Tekin Ç, Biryan F, Tekin S, Sandal S, Görgülü AO (2017) Synthesis, structural and thermal characterizations, dielectric properties and in vitro cytotoxic activities of new 2, 2, 4, 4-tetra (4′-oxy-substituted-chalcone)-6, 6-diphenylcyclotriphosphazene derivatives. Medicinal Chemistry Research (5)26: 962-964

König W, Geiger R (1970) A new method for synthesis of peptides: activation of the carboxyl group with dicyclohexylcarbodiimide using 1-hydroxybenzotriazoles as additives. Chemische Berichte 103(3): 788-798

König W, Geiger R (1970) A new method for the synthesis of peptides: activation of the carboxy group with dicyclohexylcarbodiimide and 3-hydroxy-4-oxo-3,4-dihydro-1,2,3-benzotriazine. Chemische Berichte 103(7): 2034-2040

Kunishima M, Kawachi C, Iwasaki F, Terao K, Tani S (1999) Synthesis and characterization of 4-(4,6-dimethoxy-1,3,5-triazin-2-yl)-4-methylmorpholinium chloride. Tetrahedron Letters 40(29): 5327-5330

Kweon MH, Hwang HJ, Sung HC (2001) Identification and antioxidant activity of novel chlorogenic acid derivatives from bamboo (Phyllostachys edulis) J Agric Food Chem 49(10): 4646-4655

Lee SU, Shin CG, Lee CK, Lee YS (2007) Caffeoylglycolic and caffeoylamino acid derivatives, halfmers of l-chicoric acid, as new HIV-1 integrase inhibitors. European Journal of Medicinal Chemistry 42(10): 1309-1315

M. SawpathKumar H, Subbareddy BV, Anjaneyulu S, Yadav JS (1998) Non Solvent Reaction: Ammonium Acetate Catalyzed Highly Convenient Preparation of Trans-Cinnamic Acids. Synthetic Communications 28(20): 3811-3815

Martins GM, Zeni G, Back DF, Kaufman TS, Silveira CC (2015) Expedient Iodocyclization Approach Toward Polysubstituted 3H-Benzo[e]indoles. Advanced Synthesis & Catalysis 357(14-15): 3255-3261

Narasimhan B, Belsare D, Pharande D, Mourya V, Dhake A (2004) Esters, amides and substituted derivatives of cinnamic acid: synthesis, antimicrobial activity and QSAR investigations. European Journal of Medicinal Chemistry 39(10): 827-834

Oh J, Hong JI (2013) Discrimination of Redox-Responsible Biomolecules by a Single Molecular Sensor. Organic Letters 15(6): 1210-1213

Okutan M, Yerli Y, San SE, Yılmaz F, Günaydın O, Durak M (2007) Dielectric properties of thiophene based conducting polymers. Synthetic Metals 157(8): 368-373

De P (2011) Cinnamic Acid Derivatives as Anticancer Agents-A Review. Current Medicinal Chemistry 18: 1672-1703

Panda SS, Ibrahim MA, Küçükbay H, Meyers MJ, Sverdrup FM, El-Feky SA, Katritzky AR (2013) Synthesis and Antimalarial Bioassay of Quinine – Peptide Conjugates. Chemical Biology & Drug Design 82(4): 361-366

Panda SS, Naumov RN, Asiri AM, Katritzky AR (2014) Microwave-assisted synthesis of biotin conjugates with quinolone antibiotics via amino acids. Synthesis (Germany) 46(11): 1511-1517

Pardin C, Pelletier JN, Lubell WD, Keillor JW (2008) Cinnamoyl Inhibitors of Tissue Transglutaminase. The Journal of Organic Chemistry 73(15): 5766-5775

Park JH, Hwang DK, Lee J, Im S, Kim E (2007) Studies on poly(methyl methacrylate) dielectric layer for field effect transistor: Influence of polymer tacticity. Thin Solid Films 515(7): 4041-4044

Paul R, Anderson GW (1960) N,N'-Carbonyldiimidazole, a New Peptide Forming Reagent1. Journal of the American Chemical Society 82(17): 4596-4600

Piccionello AP, Guarcello A (2010) Bioactive compounds containing benzoxadiazole, benzothiadiazole, benzotriazole. Current Bioactive Compounds 6(4): 266-283

Rao Y, Ogitani S, Kohl P, Wong CP (2002) Novel polymer–ceramic nanocomposite based on high dielectric constant epoxy formula for embedded capacitor application. Journal of Applied Polymer Science 83(5): 1084-1090

Rout DK, Choudhary RNP, Nigam GD (1988) Optical and Dielectric Studies of Azobenzene and p-Methoxy Cinnamic Acid (p-MCA). Molecular Crystals and Liquid Crystals Incorporating Nonlinear Optics 158(2): 151-162

Sahu S, Panda SS, Asiri AM, Katritzky AR (2013) NSAID conjugates with carnosine and amino acids. Synthesis (Germany) 45(24): 3369-3374

Sakellis I, Papathanassiou AN, Grammatikakis J (2010) Pressure dependence of the dielectric loss in semi-conducting polypyrrole aged at room temperature. Synthetic Metals 160(19): 2228-2230

Saraf AS, Simonyan AV (1992) Synthesis and antiallergic activity in a series of cinnamic acid. Pharmaceutical Chemistry Journal 26(7): 598-602

Sass DC, de Lucca EC, da Silva Barbosa J,. de Oliveira KT, Constantino MG (2011) Tandem reduction + cyclization of ortho-substituted cinnamic esters. Tetrahedron Letters 52(41): 5371-5374

Schlama T, Gouverneur V, Mioskowski C (1996) A new and efficient preparation of carbodiimides from ureas using dimethylphosgeniminium chloride as a dehydrating agent. Tetrahedron Letters 37(39): 7047-7048

Serkedjieva J, Manolova N, Bankova V (1992) Anti-influenza virus effect of some propolis constituents and their analogues (esters of substituted cinnamic acids. Journal of Natural Products 55(3): 294-302

Simpson JO, St Clair AK (1997) Fundamental insight on developing low dielectric constant polyimides. Thin Solid Films 308-309: 480-485

Singh RK, Kumar A, Agarwal K, Kumar M, Singh HK, Srivastava P, Singh R (2012) DC electrical conduction and morphological behavior of counter anion-governed genesis of electrochemically synthesized polypyrrole films. Journal of Polymer Science Part B: Polymer Physics 50(5): 347-360

Szymanski W, Wu B, Weiner B, de Wildeman S, Feringa BL and Janssen DB (2009) Phenylalanine Aminomutase-Catalyzed Addition of Ammonia to Substituted Cinnamic Acids: a Route to Enantiopure α- and β-Amino Acids. The Journal of Organic Chemistry 74(23): 9152-9157

Tiwari AD, Panda SS, Girgis AS, Sahu S, George RF, Srour AM, Starza BL, Asiri AM, Hall CD, Katritzky AR (2014) Microwave assisted synthesis and QSAR study of novel NSAID acetaminophen conjugates with amino acid linkers. Organic & Biomolecular Chemistry 12(37): 7238-7249

Truong VT, Boyer RR, McKinney JM, O'Keefe SF, Williams RC (2010) Effect of alpha-cyclodextrin-cinnamic acid inclusion complexes on populations of Escherichia coli O157:H7 and Salmonella enterica in fruit juices. Journal of Food Prot 73(1): 92-96

Ulijn RV, Moore BD, Janssen AEM, Halling PJ (2002) A single aqueous reference equilibrium constant for amide synthesis–hydrolysis. Journal of the Chemical Society, Perkin Transactions 2(5): 1024-1028

Uraguchi D, Ueki Y, Ooi T (2009) Chiral Organic Ion Pair Catalysts Assembled Through a Hydrogen-Bonding Network. Science 326(5949): 120-123

Venkataraman K, Wagle DR (1979) Cyanuric chloride: a useful reagent for converting carboxylic acids into chlorides, esters, amides and peptides. Tetrahedron Letters 20(32): 3037-3040

Whetten RW, MacKay JJ, Sederoff RR (1998) Recent advances in understanding lignin biosynthesis. Annual Review Plant Physiology Plant Molecular Biology 49: 585-609

Williams A, Ibrahim IT (1981) Carbodiimide chemistry: recent advances. Chemical Reviews 81(6): 589-636

Xia Z, Lv X, Wang W, Wang X (2011) Regioselective addition of thiophenol to α,β-unsaturated N-acylbenzotriazoles. Tetrahedron Letters 52(38): 4906-4910

Xu X, Yang C, Yang J, Huang T, Zhang N, Wang Y, Zhou Z (2016) Excellent dielectric properties of poly(vinylidene fluoride) composites based on partially reduced graphene oxide. Composites Part B 109(15): 91-100

Yeung Hong S, Corey EJ (2006) A Short Enantioselective Pathway for the Synthesis of the Anti-Influenza Neuramidase Inhibitor Oseltamivir from 1,3-Butadiene and Acrylic Acid. Journal of the American Chemical Society 128(19): 6310-6311

Zhang B, Lv C, Li W, Cui Z, Chen D, Cao F, Miao F, Zhou L (2015) Ethyl Cinnamate Derivatives as Promising High-Efficient Acaricides against iPsoroptes cuniculii: Synthesis, Bioactivity and Structure–Activity Relationship. Chemical and Pharmaceutical Bulletin 63(4): 255-262

Zhdanko A, Schmauder A, Ma CI, Sibley LD, Sept D, Sasse F, Maier ME (2011) Synthesis of Chondramide A Analogues with Modified β-Tyrosine and Their Biological Evaluation. Chemistry – A European Journal 17(47): 13349-13357

Zou H.B, Dong SY, Zhou CX, Hu LH, Wu YH, Li HB, Gong JX, Sun LL, Wu XM, Bai H, Zhao Y (2006) Design, synthesis, and SAR analysis of cytotoxic sinapyl alcohol derivatives. Bioorganic Medicinal Chemistry 14(6): 2060-2071

APPENDIX

A.1. NMR spectrum of cinnamic acid derivatives

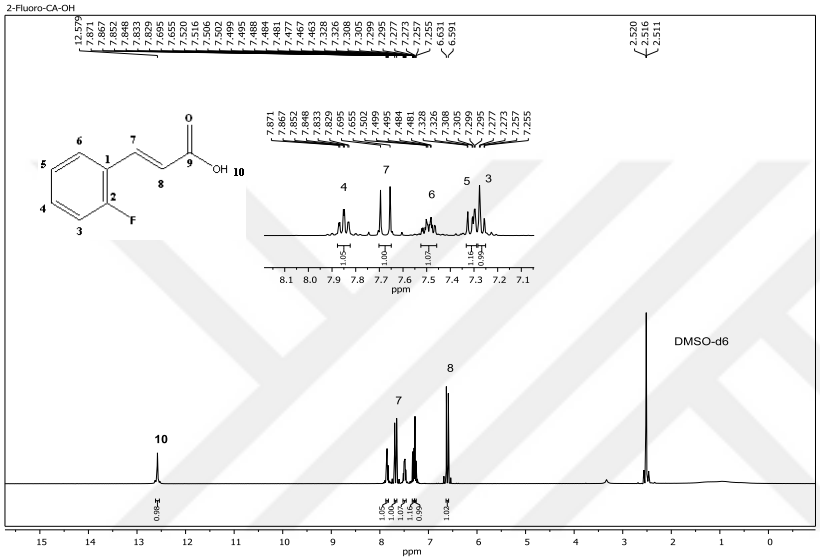

Appx. 1.1. ^{1}H NMR spectra of 2-fluoro-CA-OH

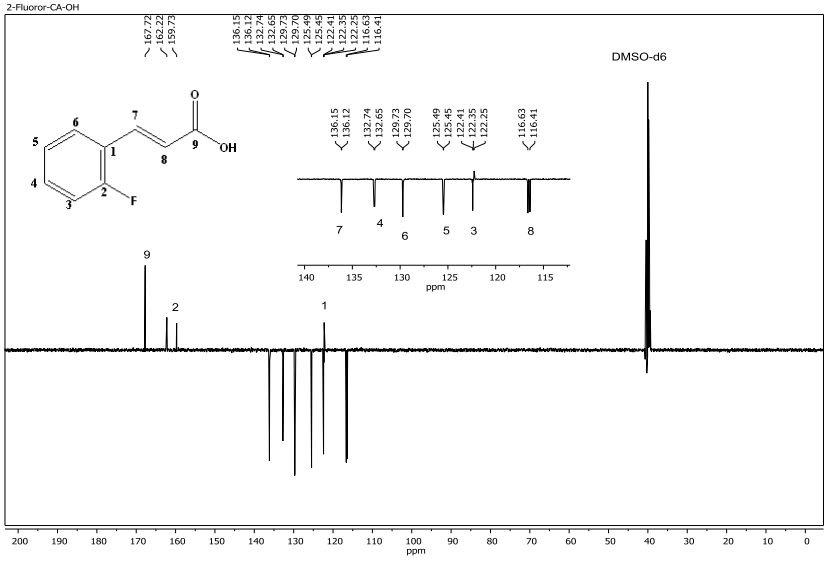

Appx. 1.2. ^{13}C APT NMR spectra of 2-fluoro-CA-OH

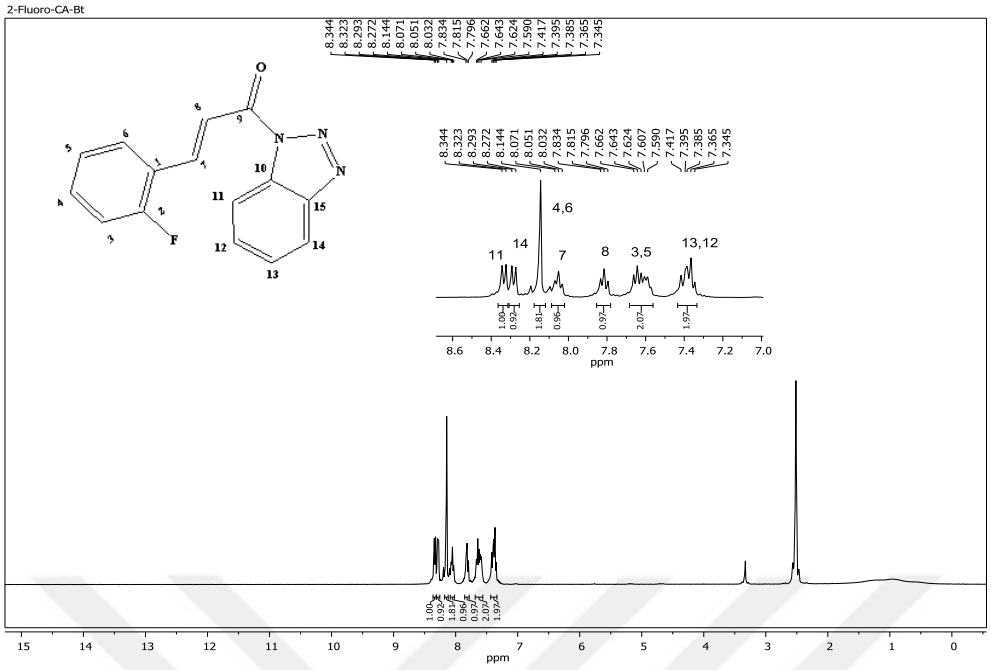

Appx. 1.3. ^{1}H NMR spectra of 2-fluoro-CA-Bt

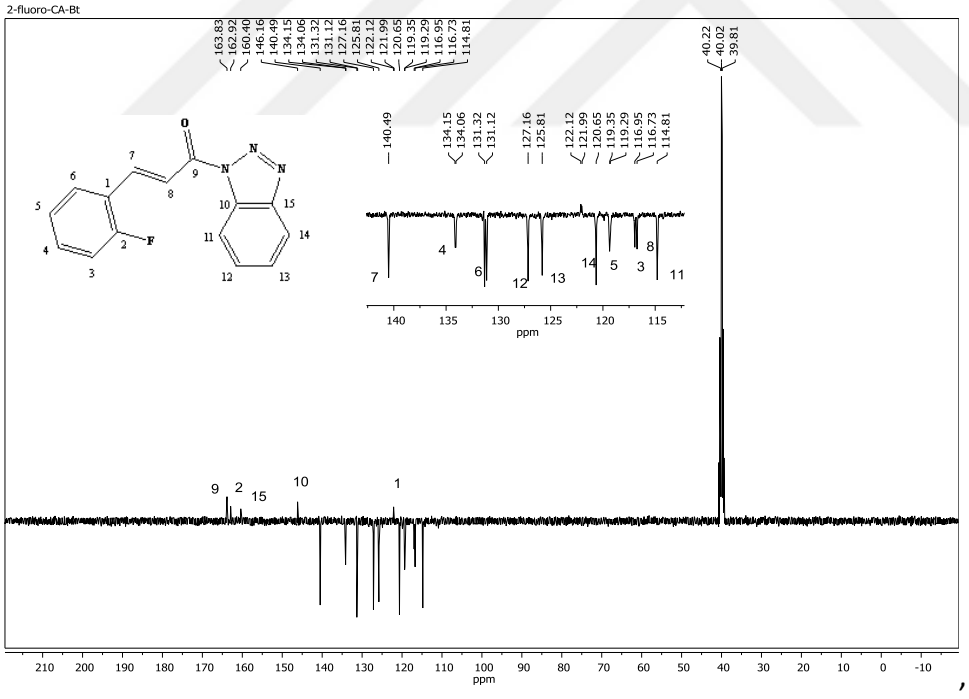

Appx. 1.4. ^{13}C APT NMR spectra of 2-fluoro-CA-Bt

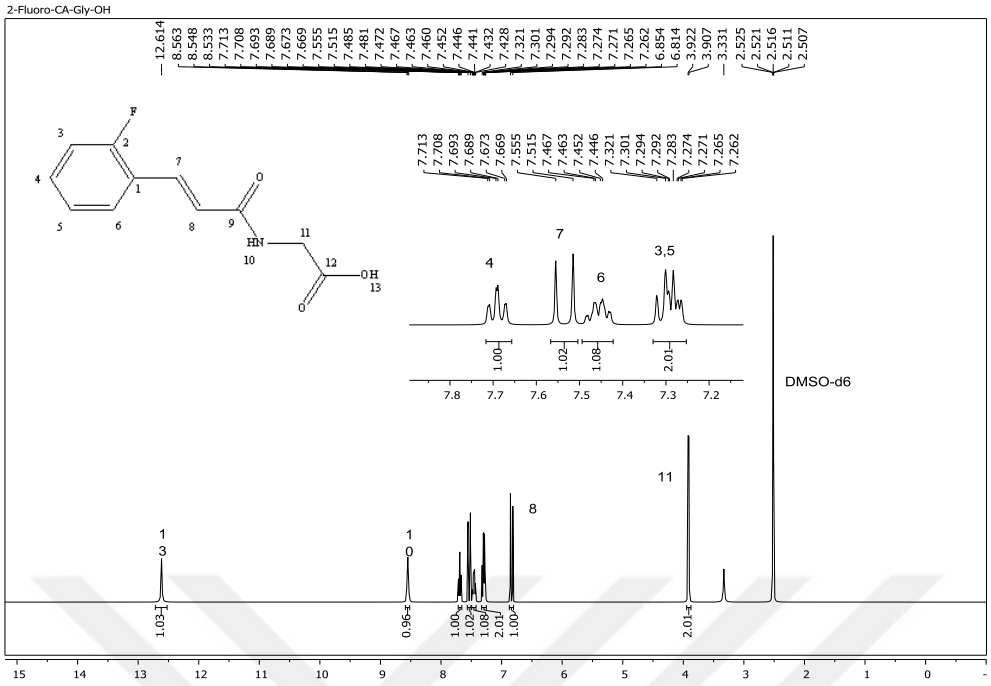

Appx. 1.5. ^{1}H NMR spectra of 2-fluoro-CA-Gly-OH

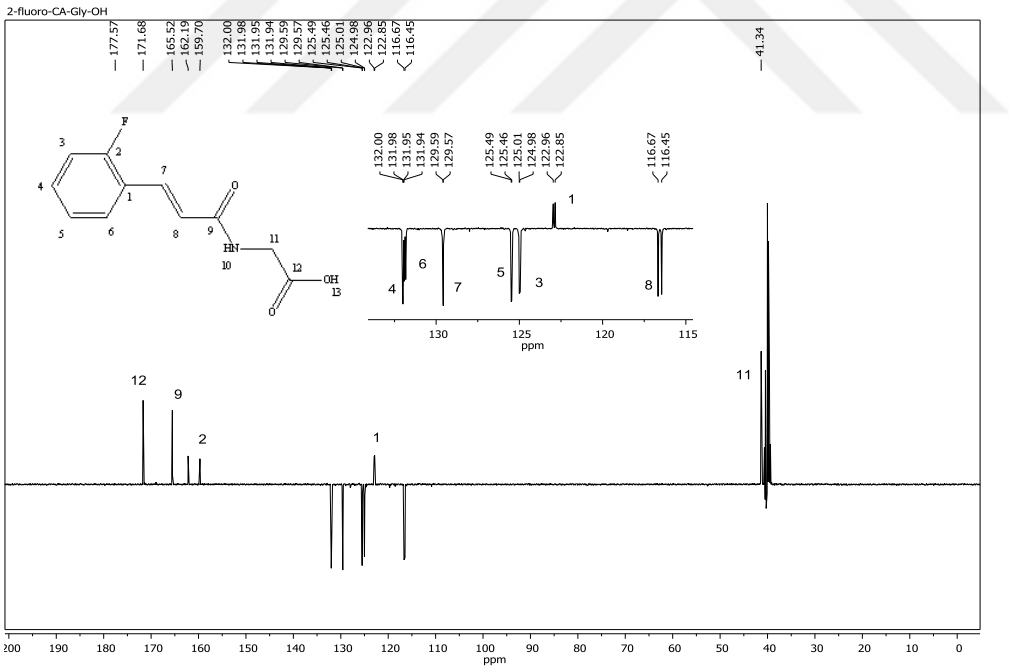

Appx. 1.6. ^{13}C APT NMR spectra of 2-fluoro-CA- Gly-OH

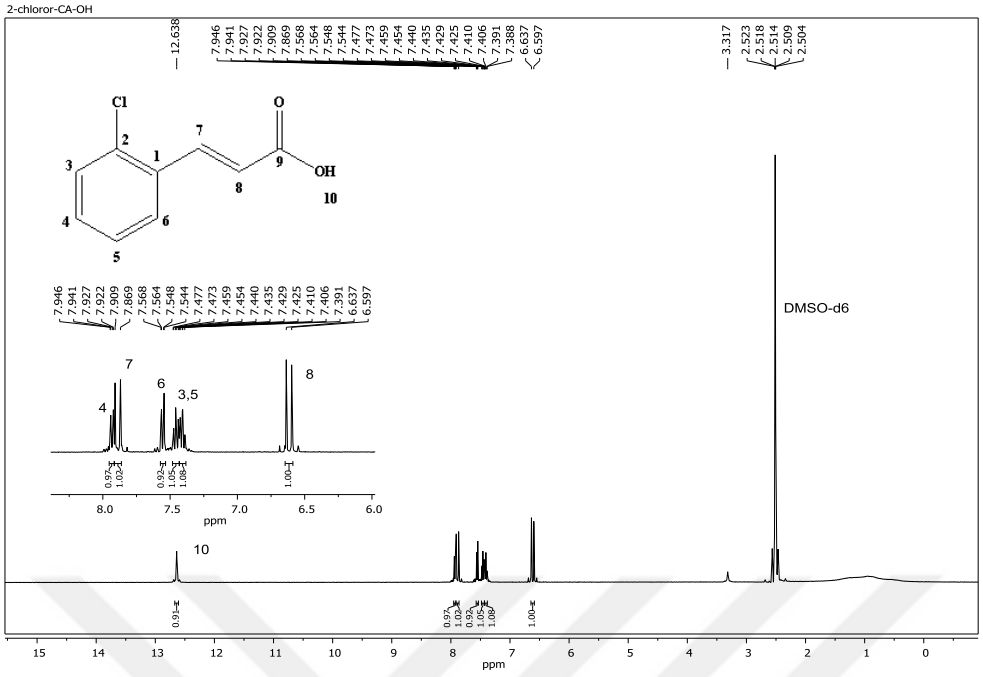

Appx. 1.7. ^{1}H NMR spectra of 2-chloro-CA-OH

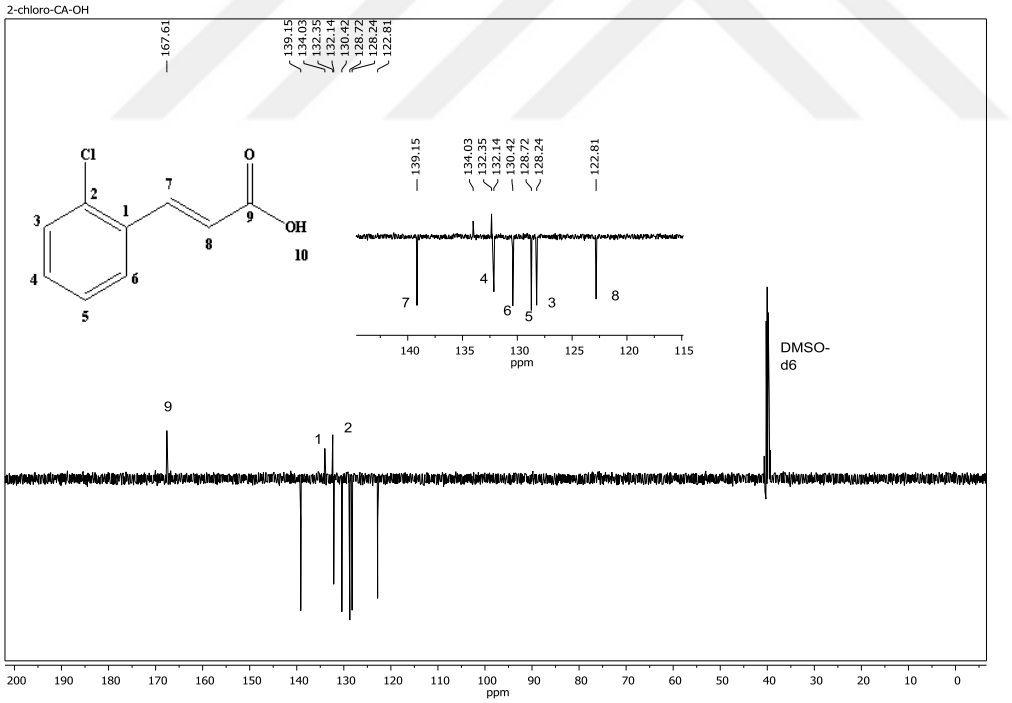

Appx. 1.8. ^{13}C APT NMR spectra of 2-chloro-CA-OH

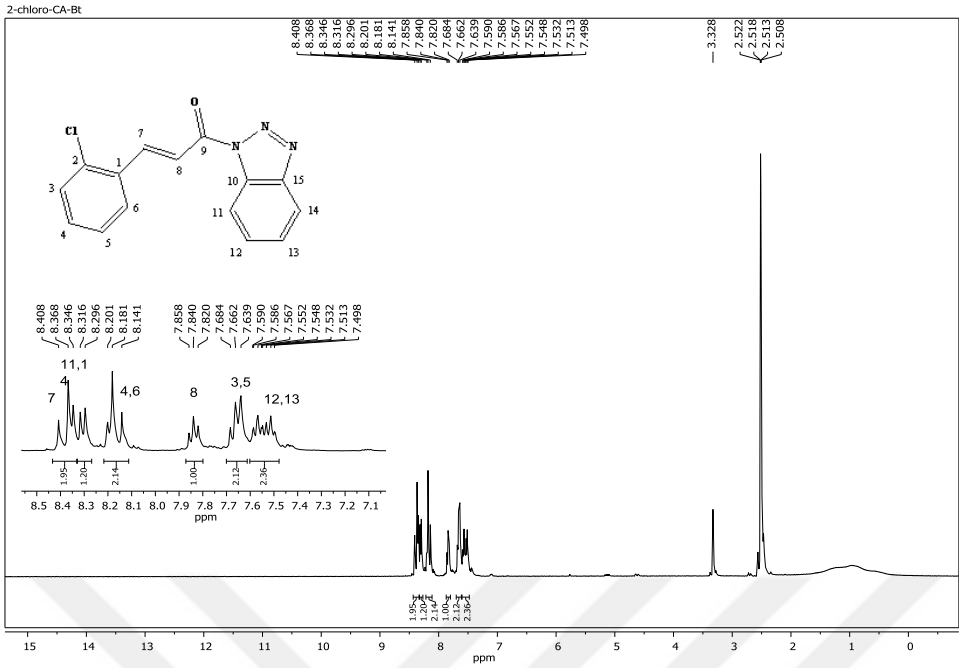

Appx. 1.9. ^{1}H NMR spectra of 2-chloro-CA-Bt

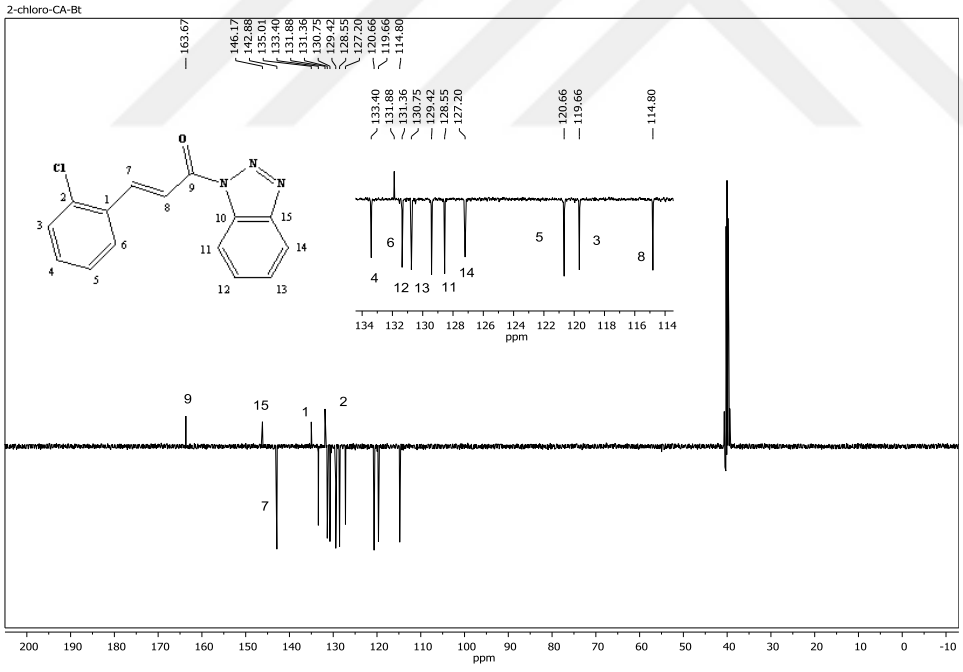

Appx. 1.10. ^{13}C APT NMR spectra of 2-chloro-CA-Bt

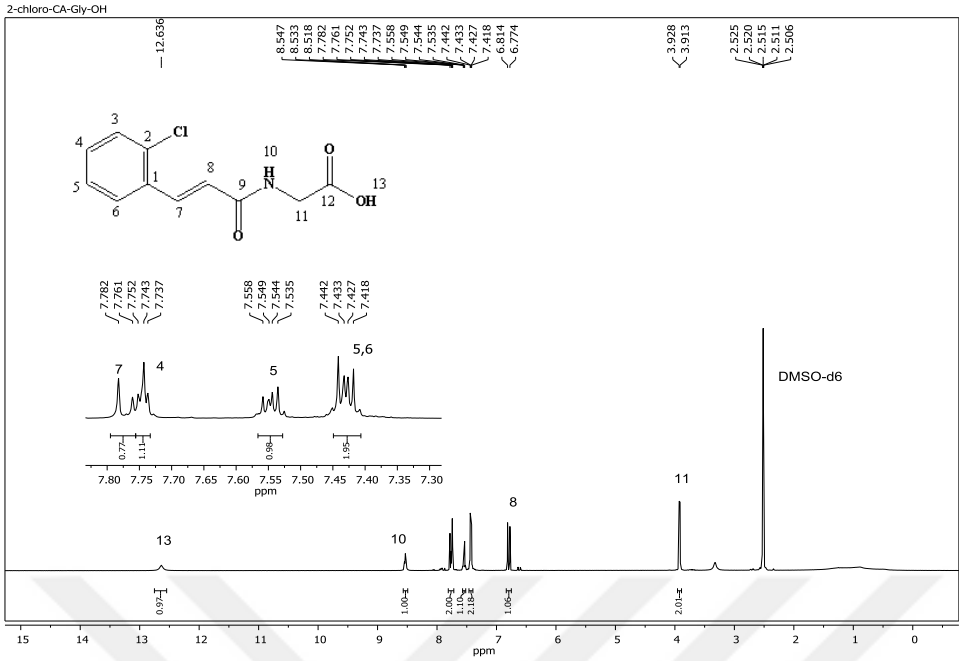

Appx. 1.11. ^{1}H NMR spectra of 2-chloro-CA-Gly-OH

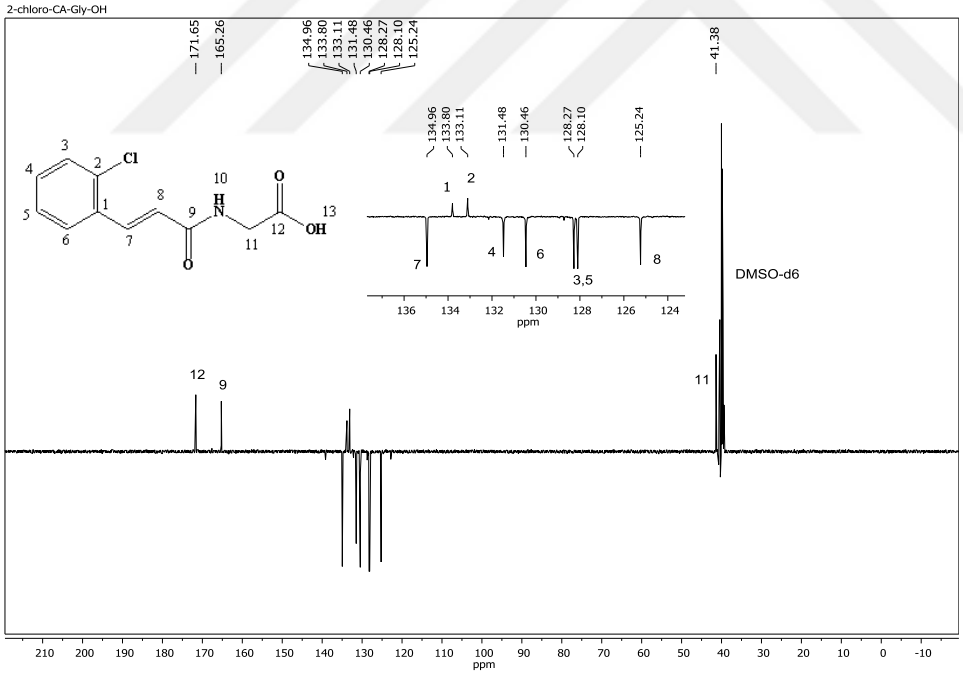

Appx. 1.12. ^{13}C APT NMR spectra of 2-chloro-CA-Gly-OH

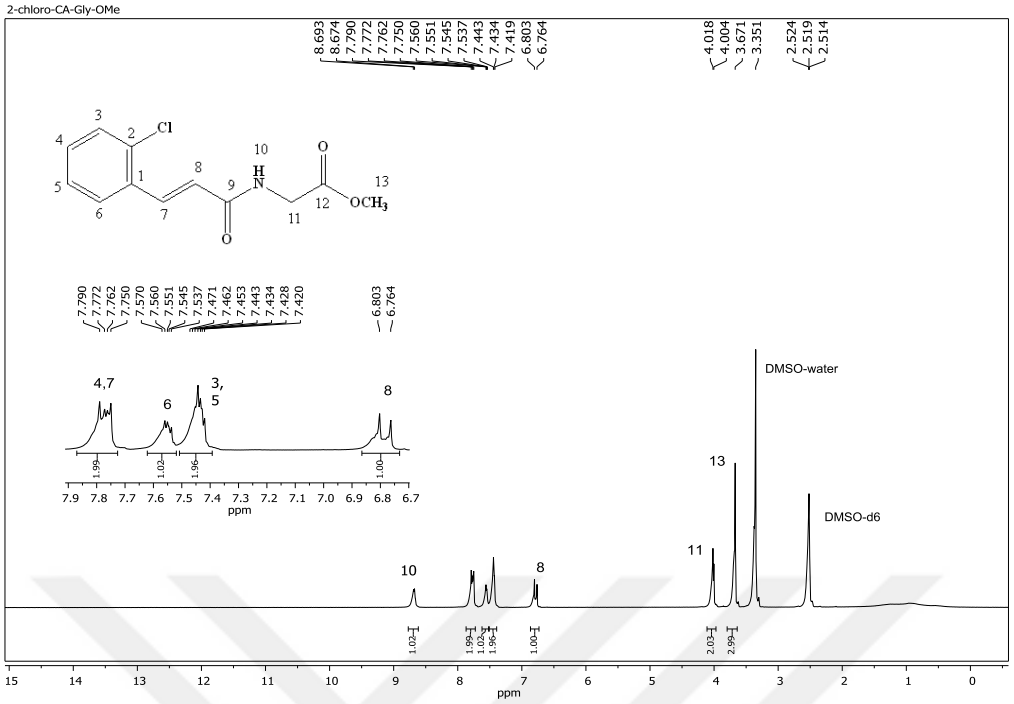

Appx. 1.13. ^{1}H NMR spectra of 2-chloro-CA-Gly-OMe

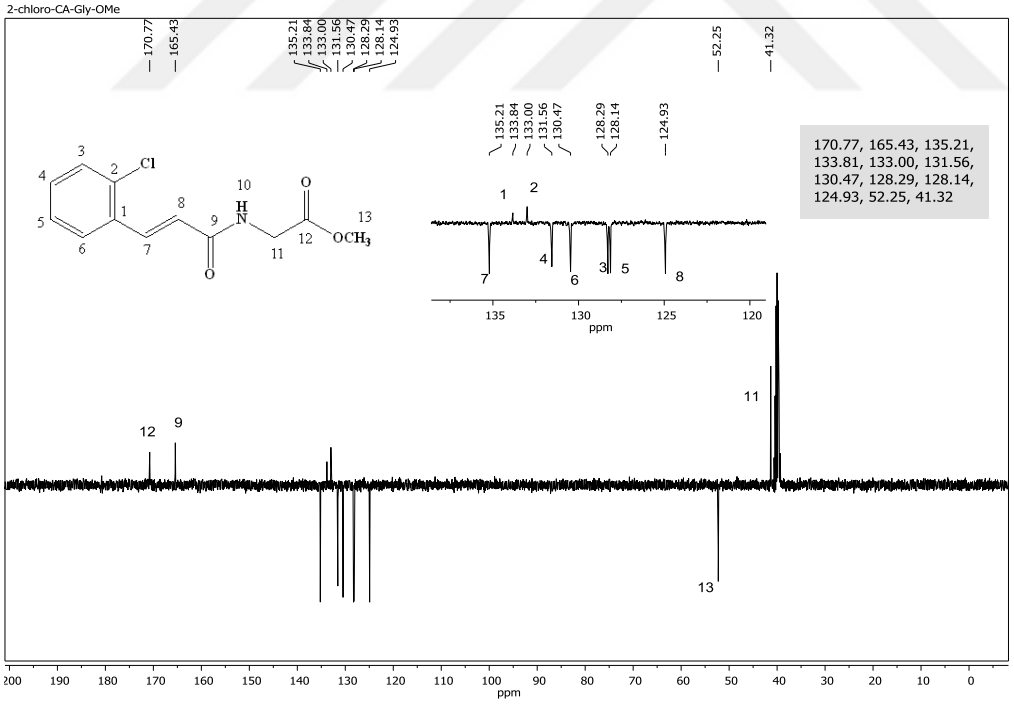

Appx. 1.14. ^{13}C APT NMR spectra of 2-chloro-CA-Gly-OMe

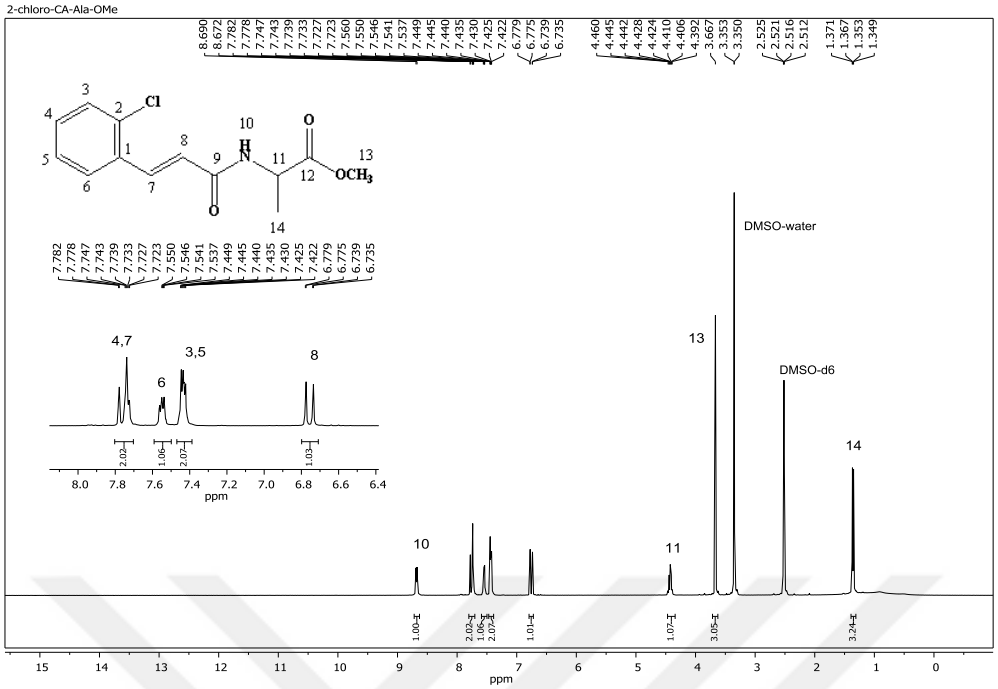

Appx. 1.15. ^{1}H NMR spectra of 2-chloro-CA-Ala-OMe

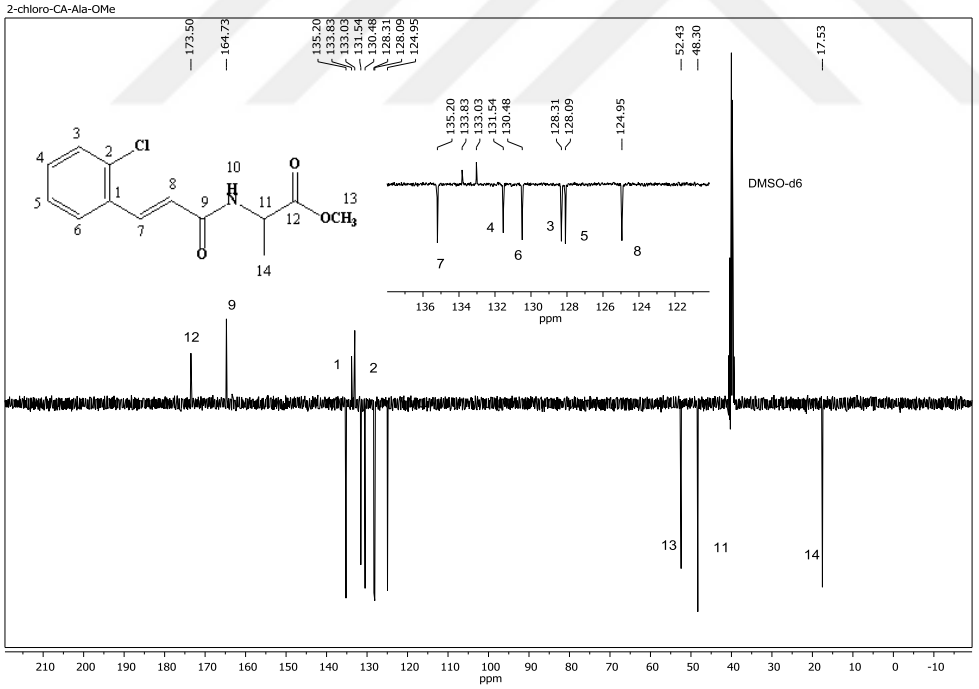

Appx. 1.16. ^{13}C APT NMR spectra of 2-chloro-CA-Ala-OMe

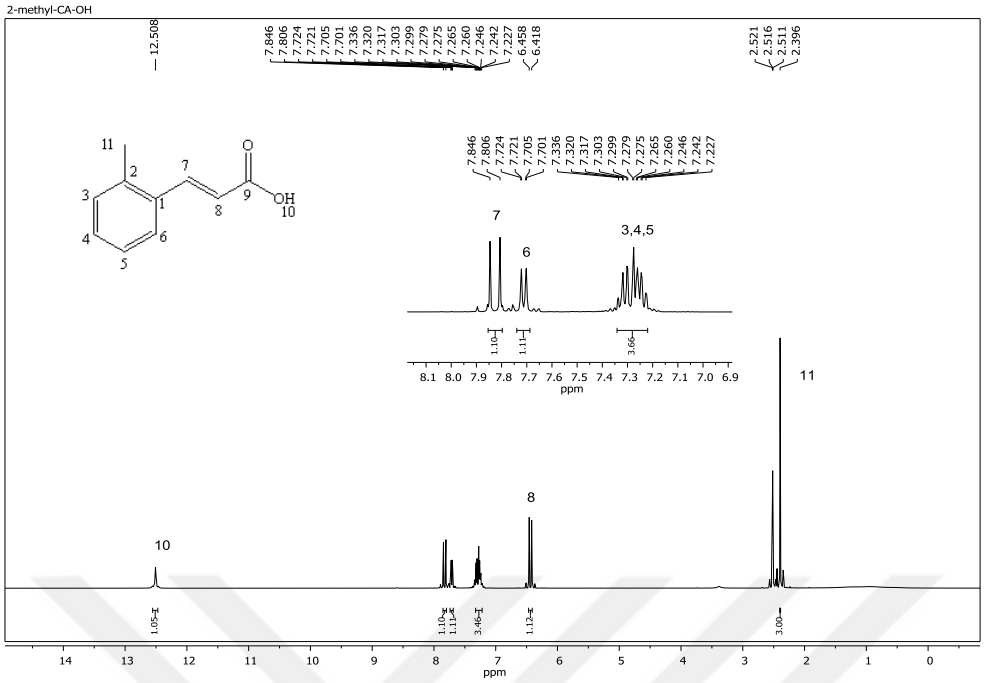

Appx. 1.17. ^{1}H NMR spectra of 2-methyl-CA-OH

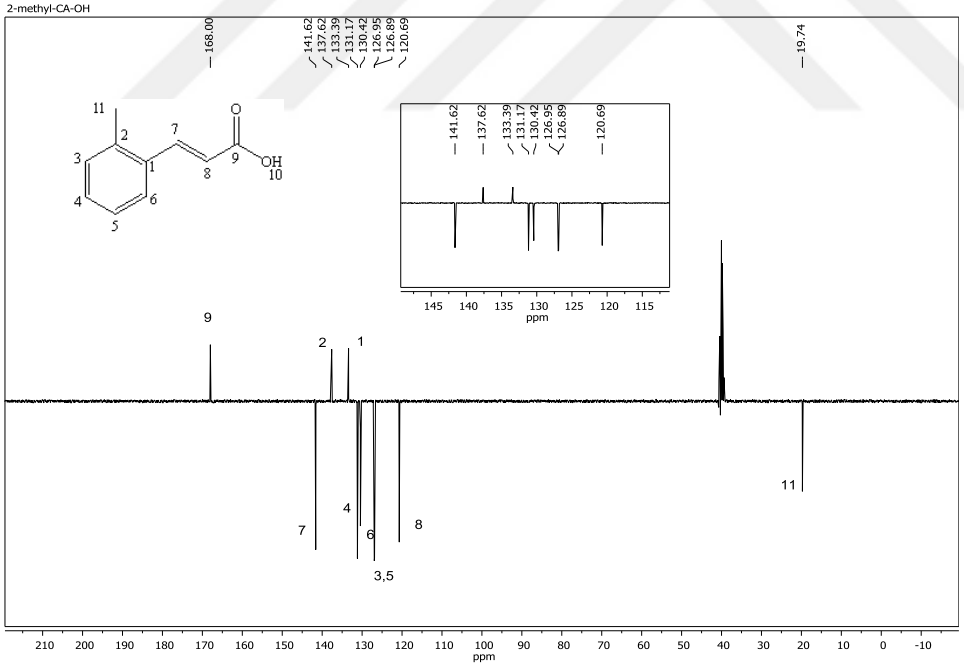

Appx. 1.18. ^{13}C APT NMR spectra of 2-methyl-CA-OH

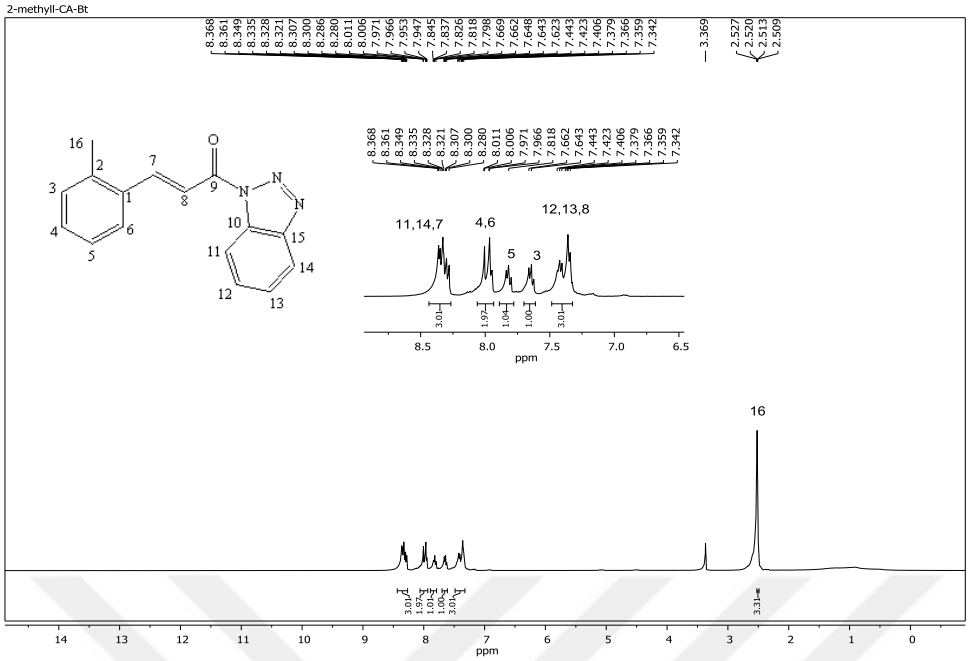

Appx. 1.19. ^{1}H NMR spectra of 2-methyl-CA-Bt

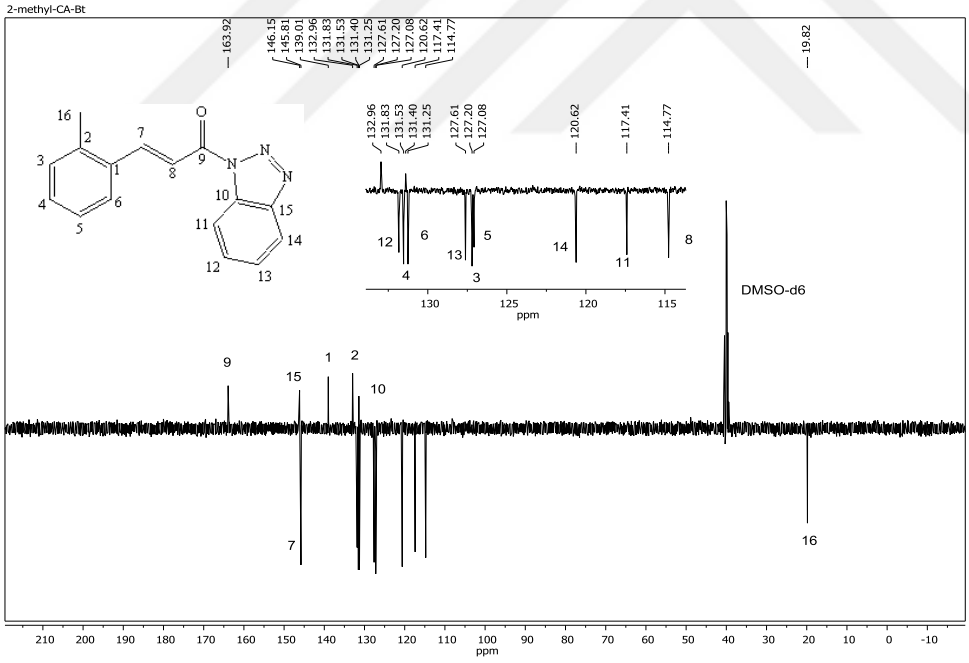

Appx. 1.20. ^{13}C APT NMR spectra of 2-methyl-CA-Bt

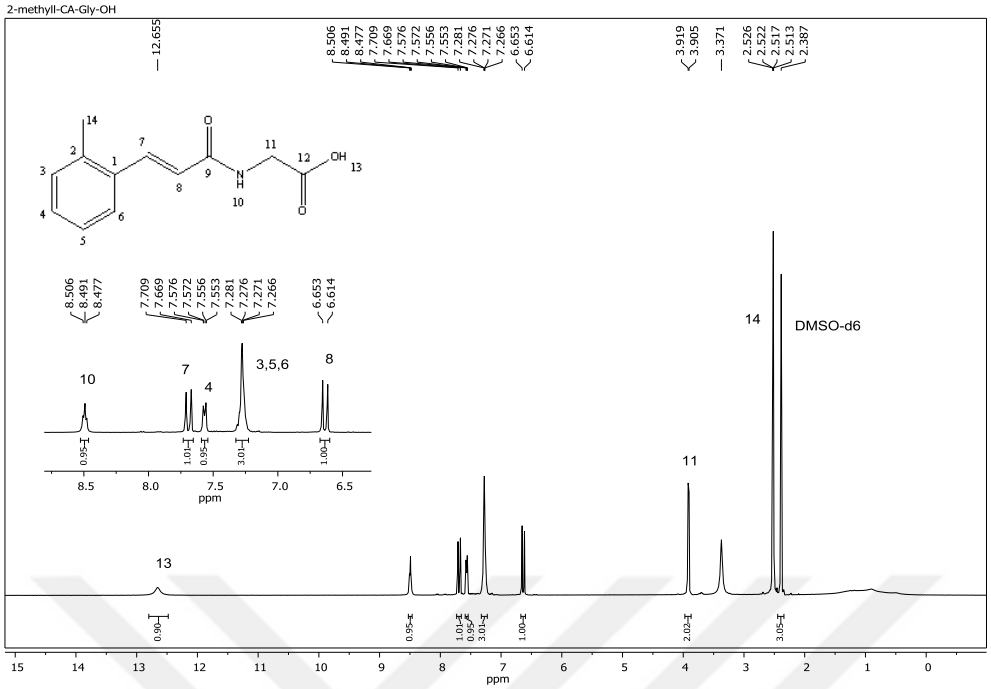

Appx. 1.21. ^{1}H NMR spectra of 2-methyl-CA-Gly-OH

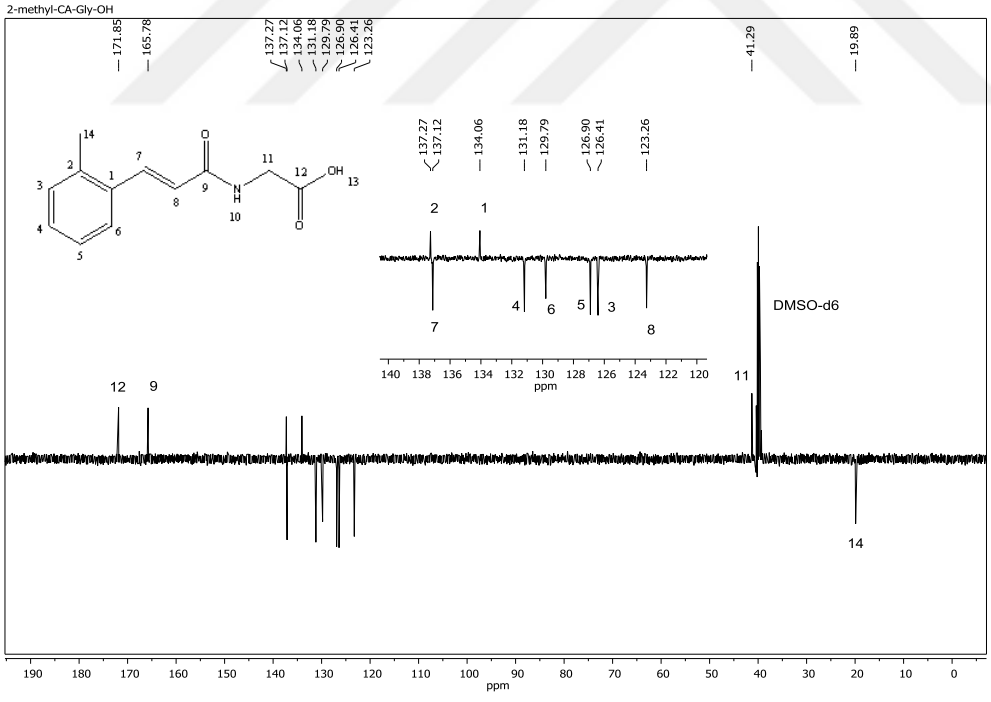

Appx. 1.22. ^{13}C APT NMR spectra of 2-methyl-CA-Gly-OH

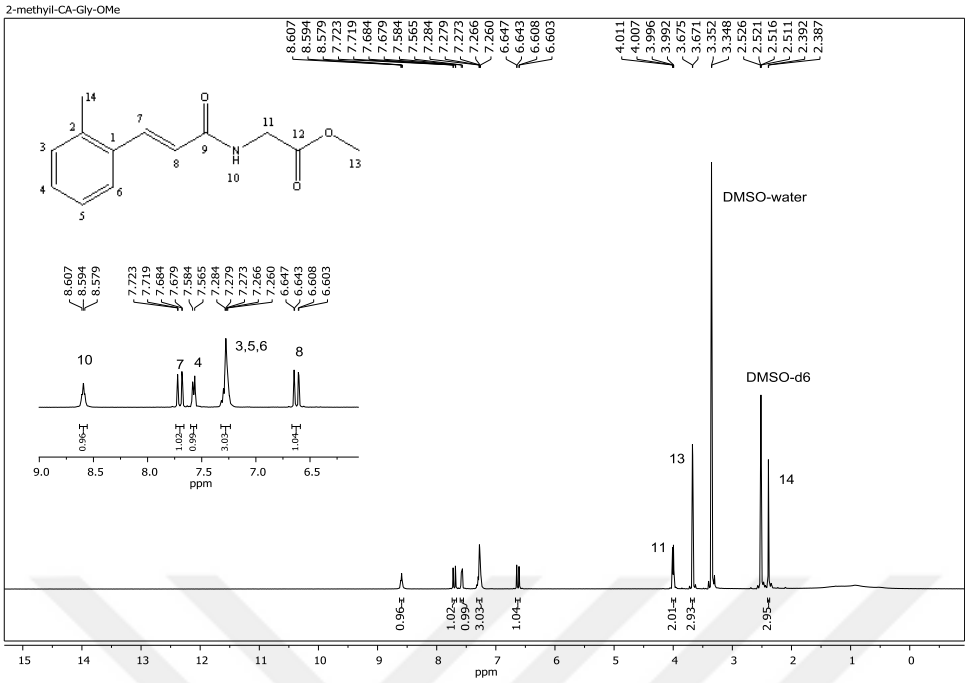

Appx. 1.23. ^{1}H NMR spectra of 2-methyl-CA-Gly-OMe

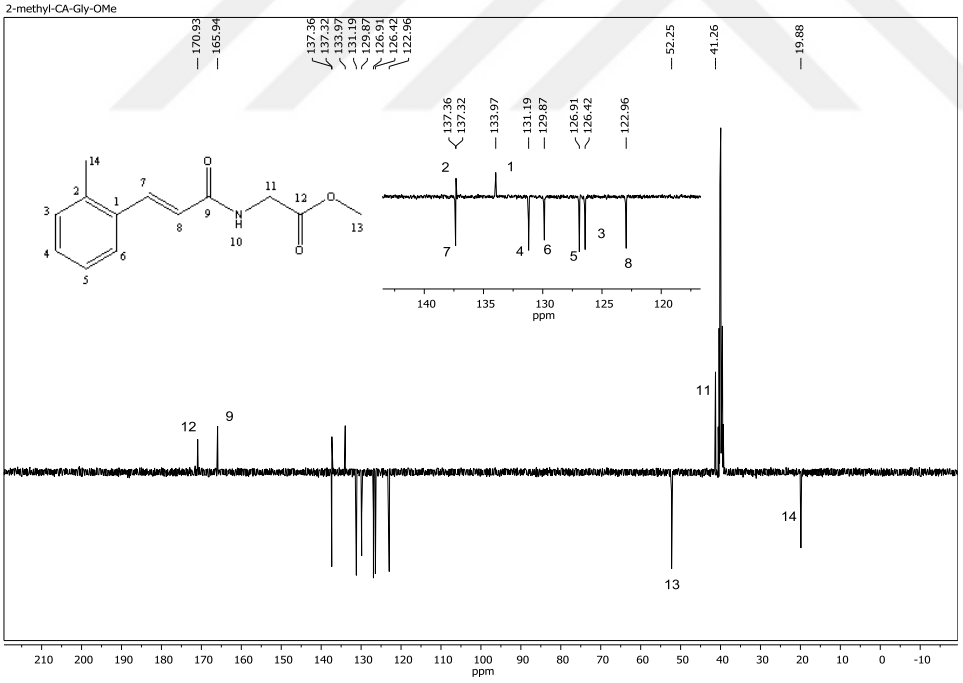

Appx. 1.24. ^{13}C APT NMR spectra of 2-methyl-CA-Gly-OMe

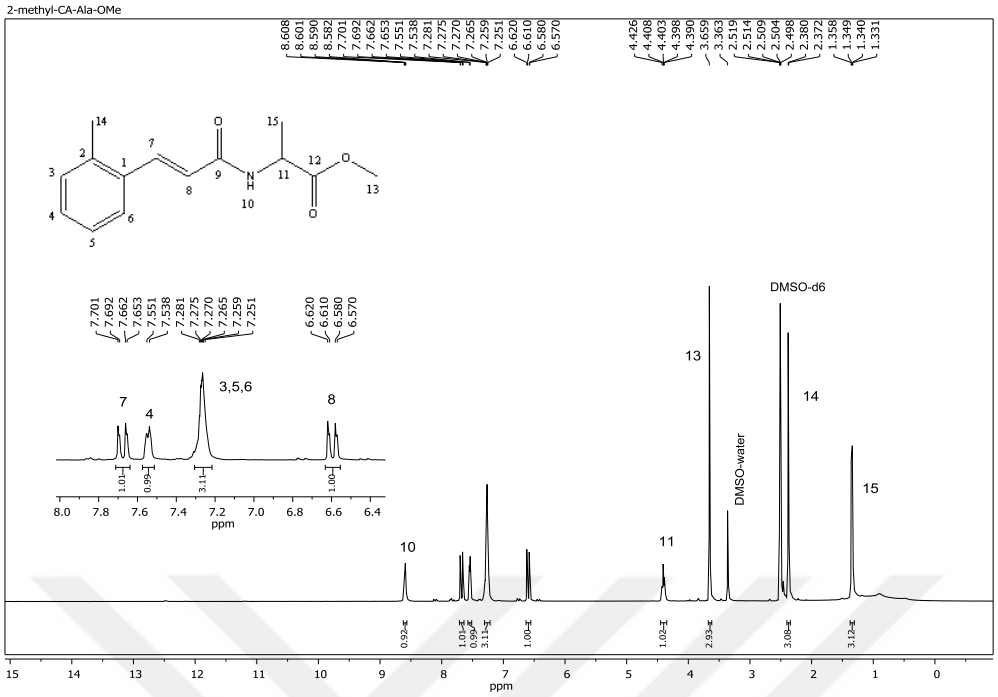

Appx. 1.25. ^{1}H NMR spectra of 2-methyl-CA-Ala-OMe

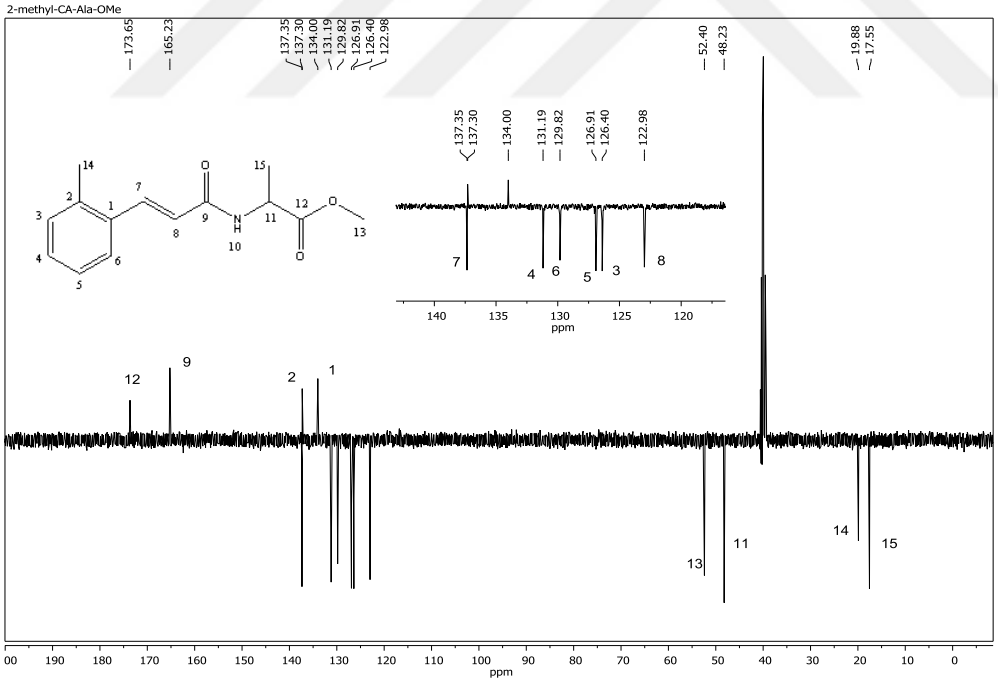

Appx. 1.26. ^{13}C APT NMR spectra of 2-methyl-CA-Ala-OMe

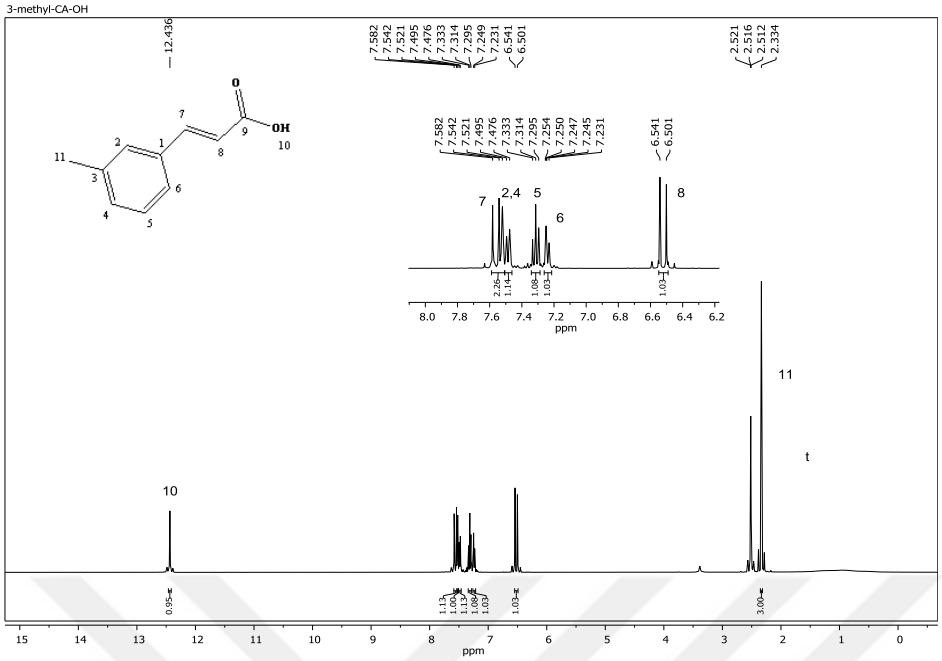

Appx. 1.27. ^{1}H NMR spectra of 3-methyl-CA-OH

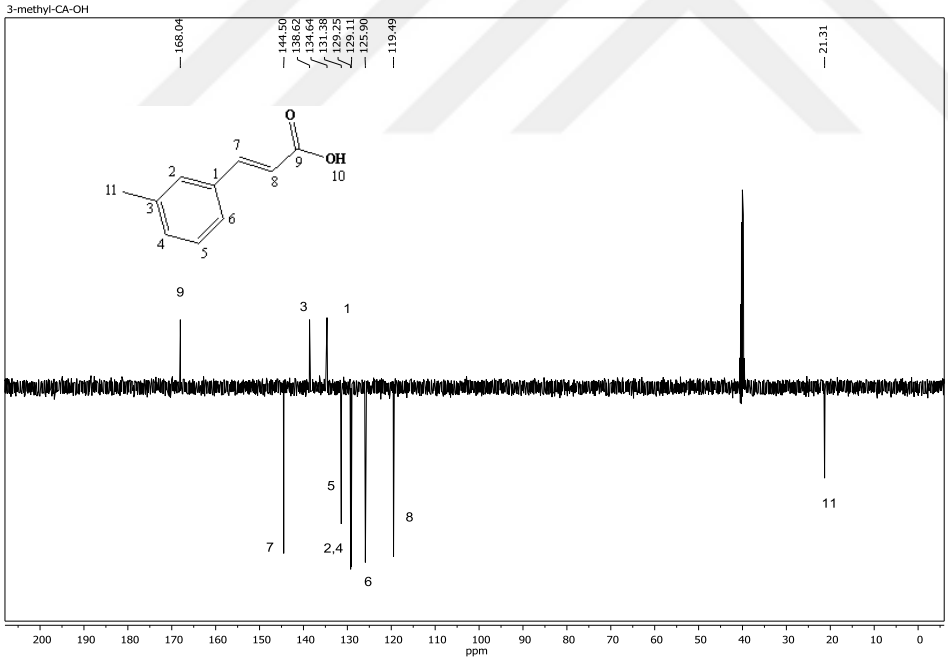

Appx. 1.28. ^{13}C APT NMR spectra of 3-methyl-CA-OH

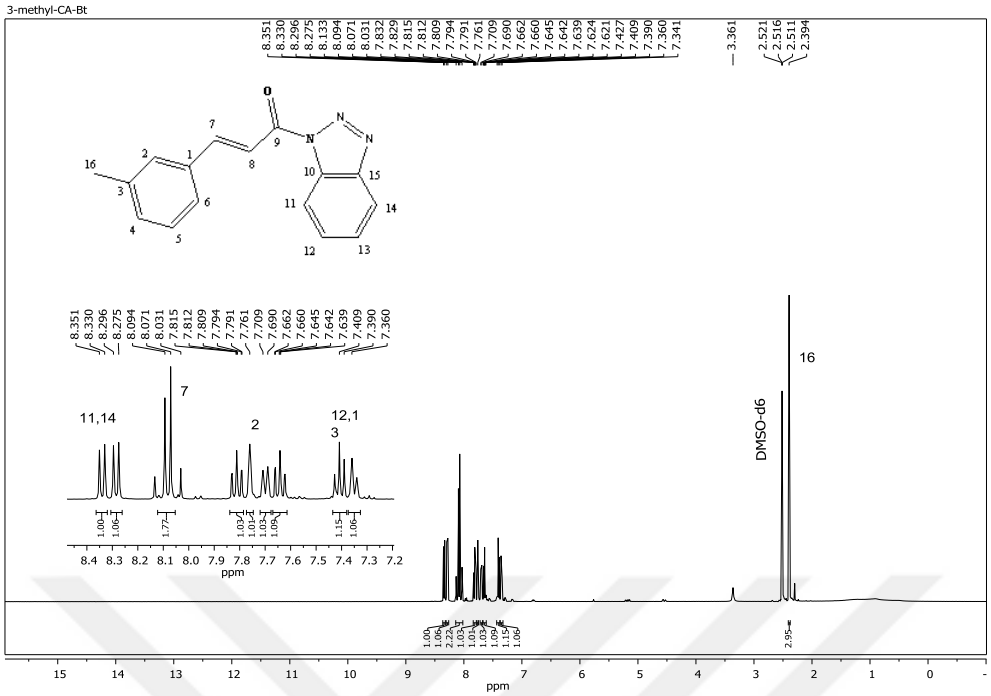

Appx. 1.29. ^{1}H NMR spectra of 3-methyl-CA-Bt

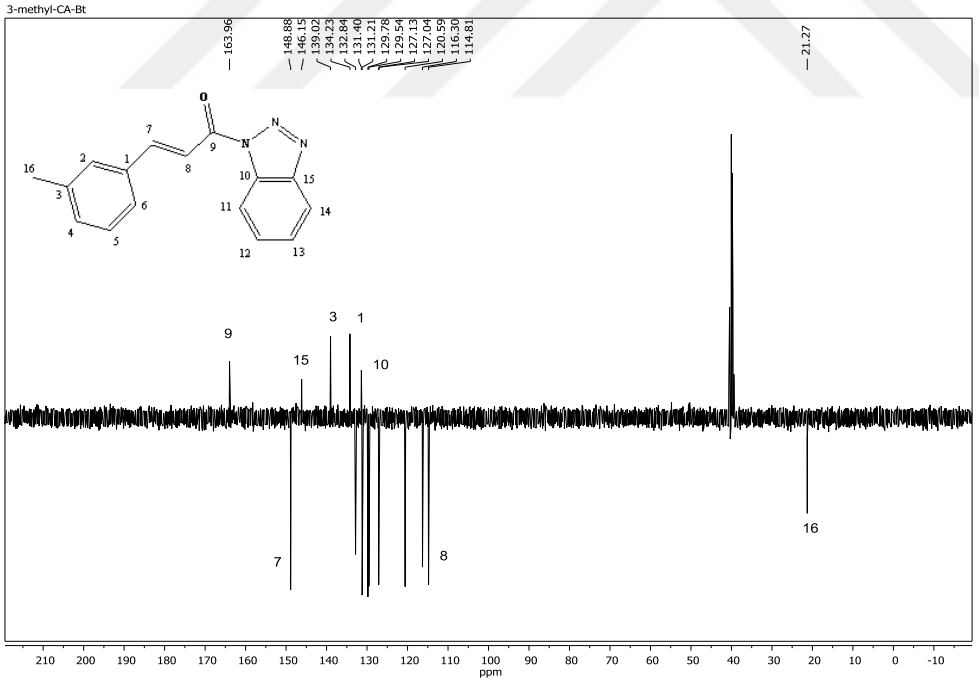

Appx. 1.30. ^{13}C APT NMR spectra of 3-methyl-CA-Bt

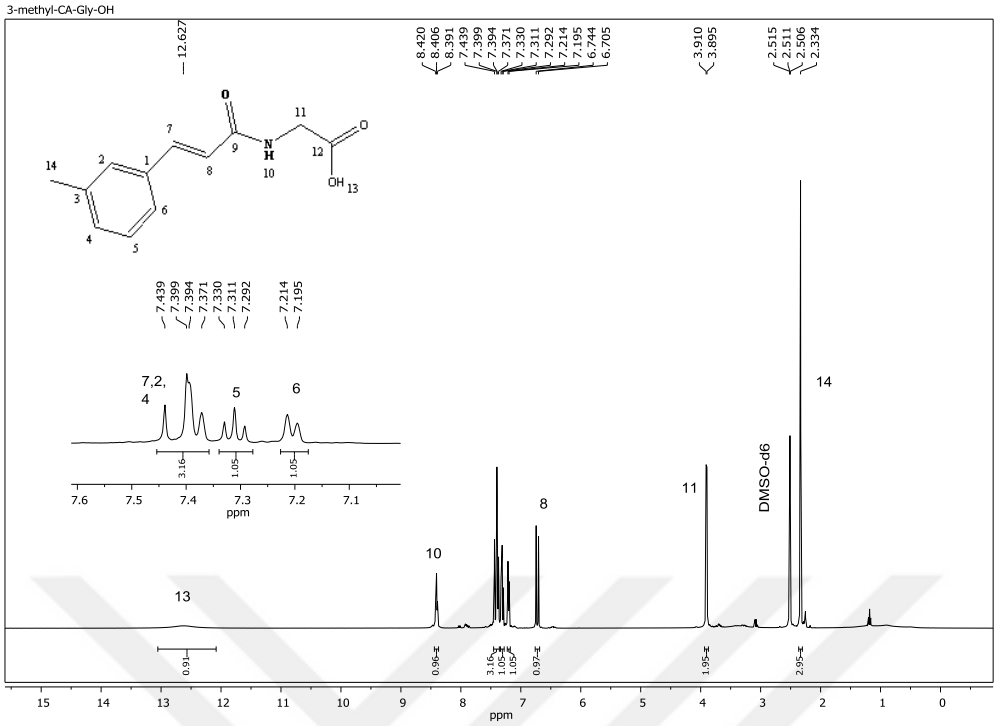

Appx. 1.31. ^{1}H NMR spectra of 3-methyl-CA-Gly-OH

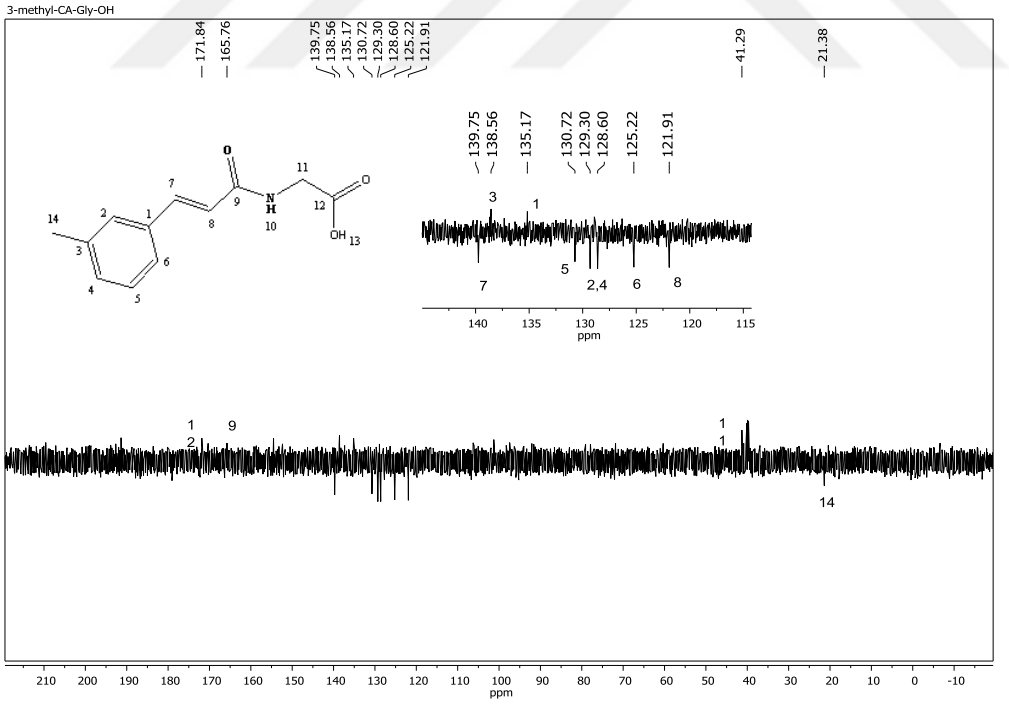

Appx. 1.32. ^{13}C APT NMR spectra of 3-methyl-CA-Gly-OH

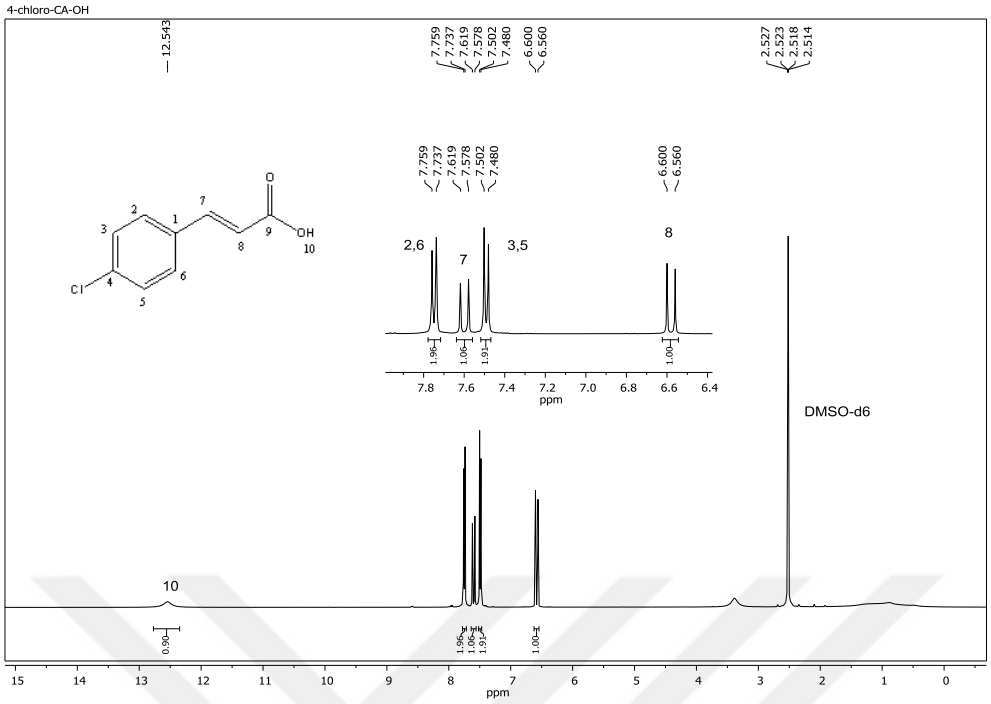

Appx. 1.33. ^{1}H NMR spectra of 2-chloro-CA-OH

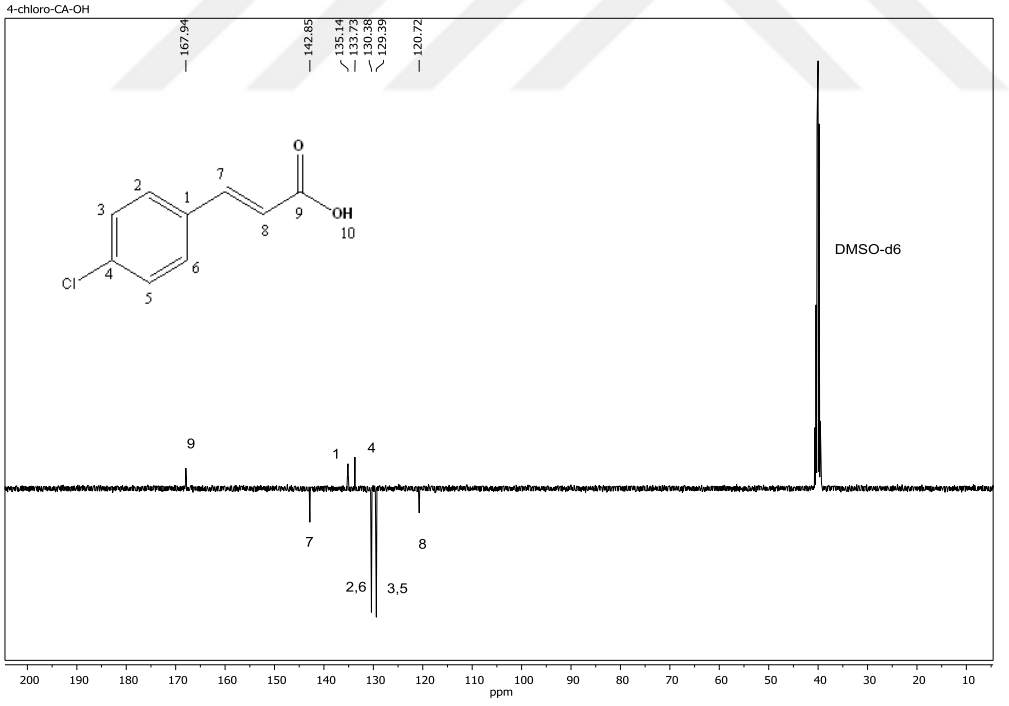

Appx. 1.34. ^{13}C APT NMR spectra of 2-chloro-CA-OH

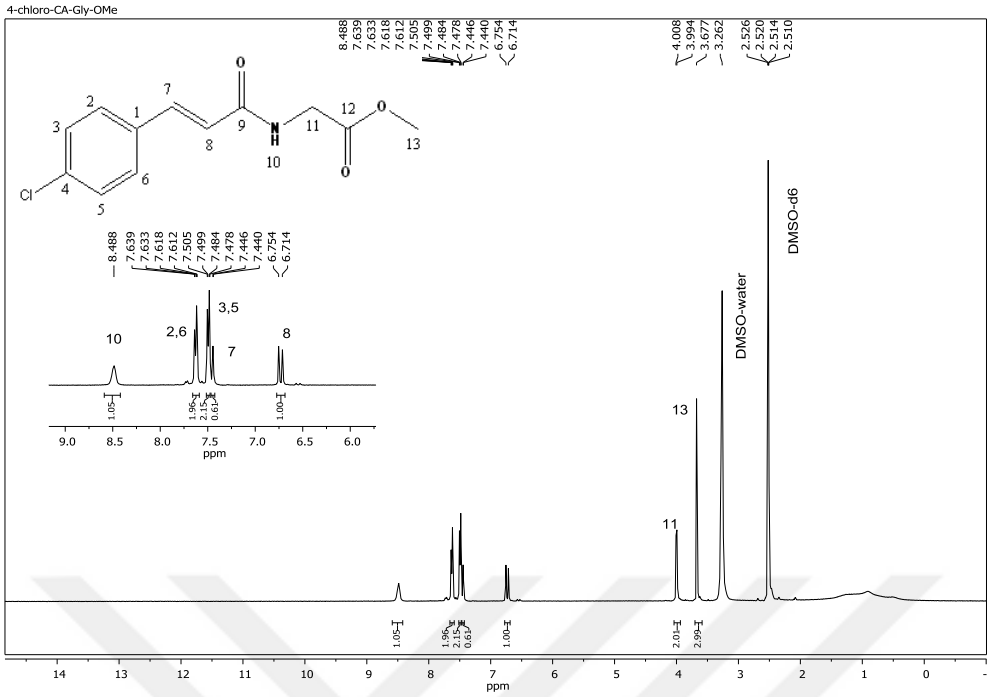

Appx. 1.35. ^{1}H NMR spectra of 2-chloro-CA-Gly-OMe

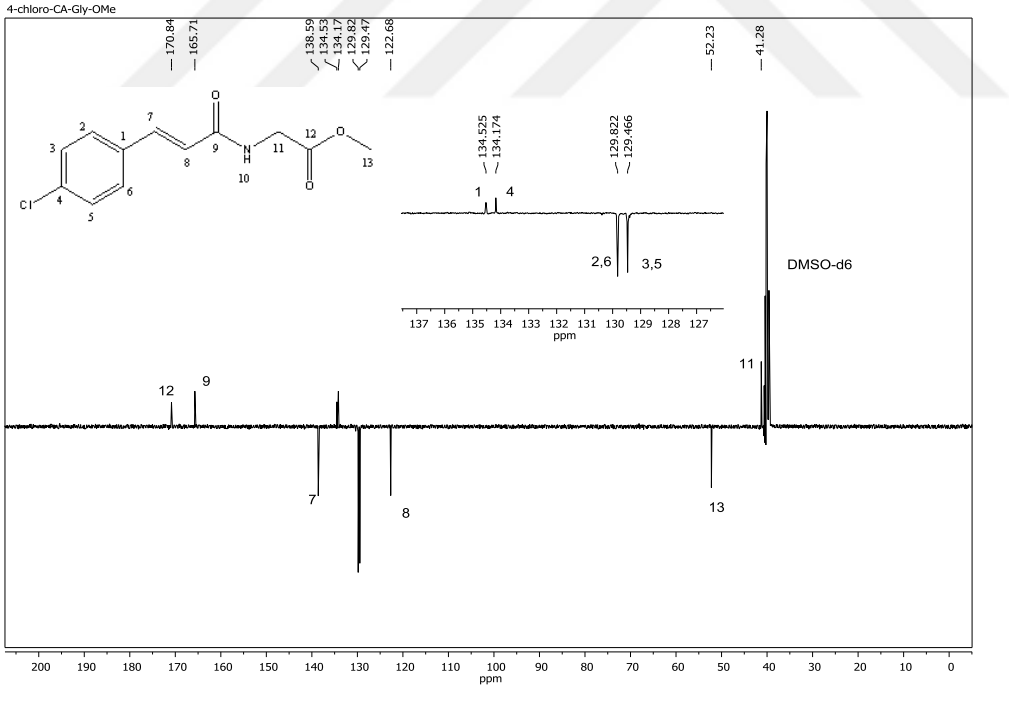

Appx. 1.36. ^{13}C APT NMR spectra of 2-chloro-CA-Gly-OMe

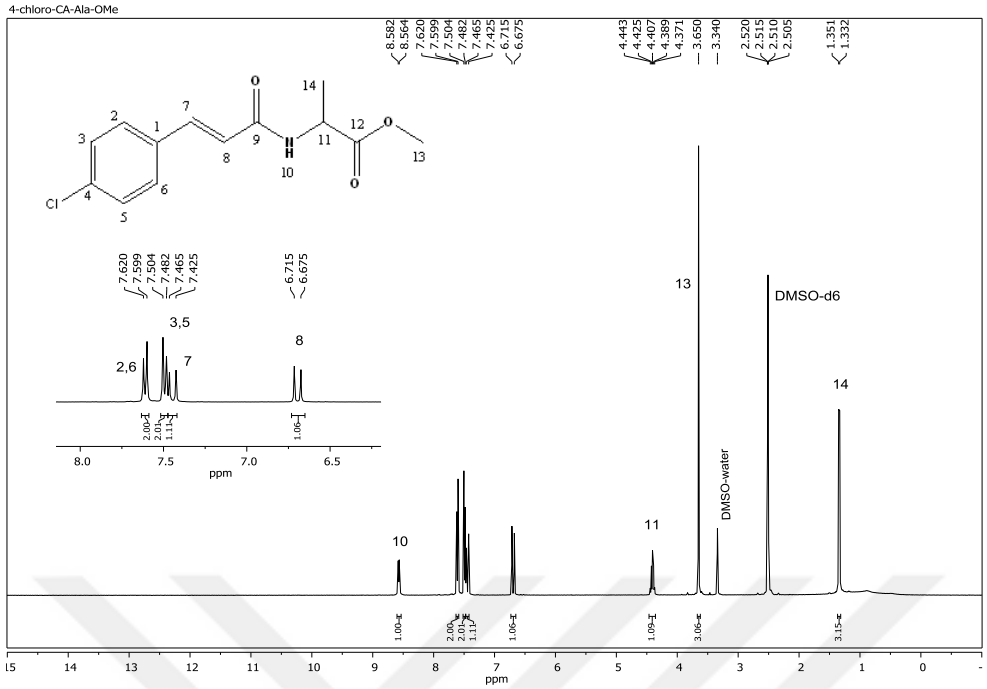

Appx. 1.37. ^{1}H NMR spectra of 2-chloro-CA-Ala-OMe

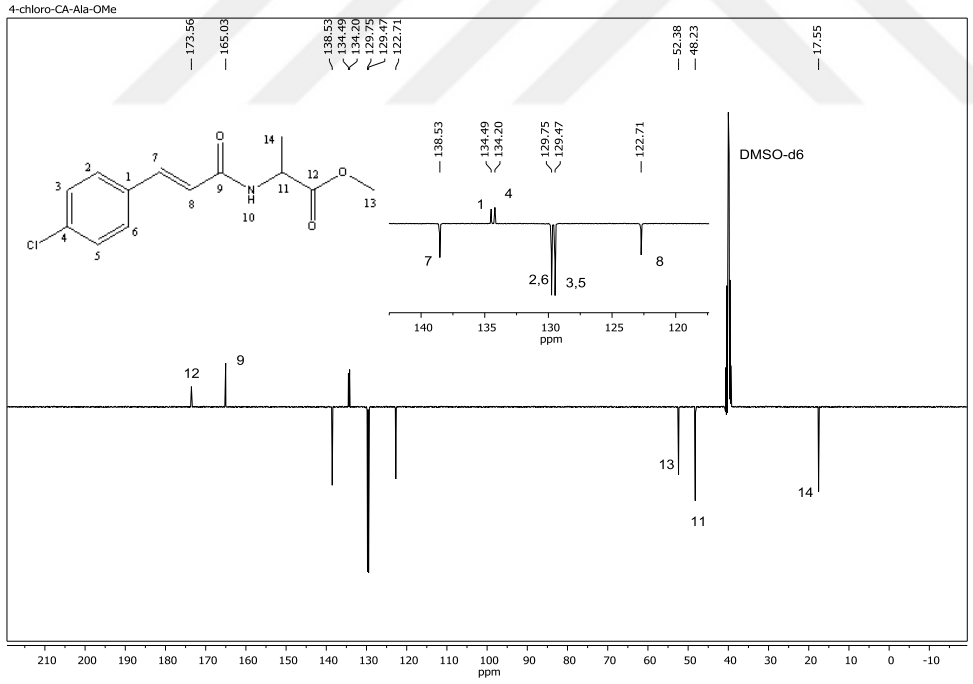

Appx. 1.38. ^{13}C APT NMR spectra of 2-chloro-CA-Ala-OMe

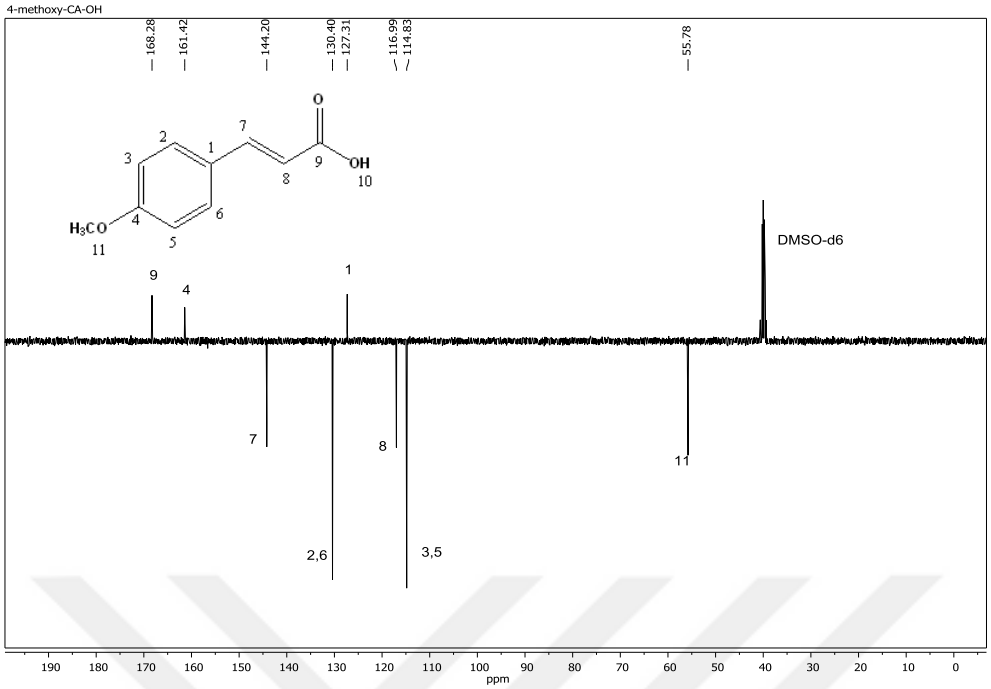

Appx. 1.39. ^{13}C APT NMR spectra of 4-methoxy-CA-OH

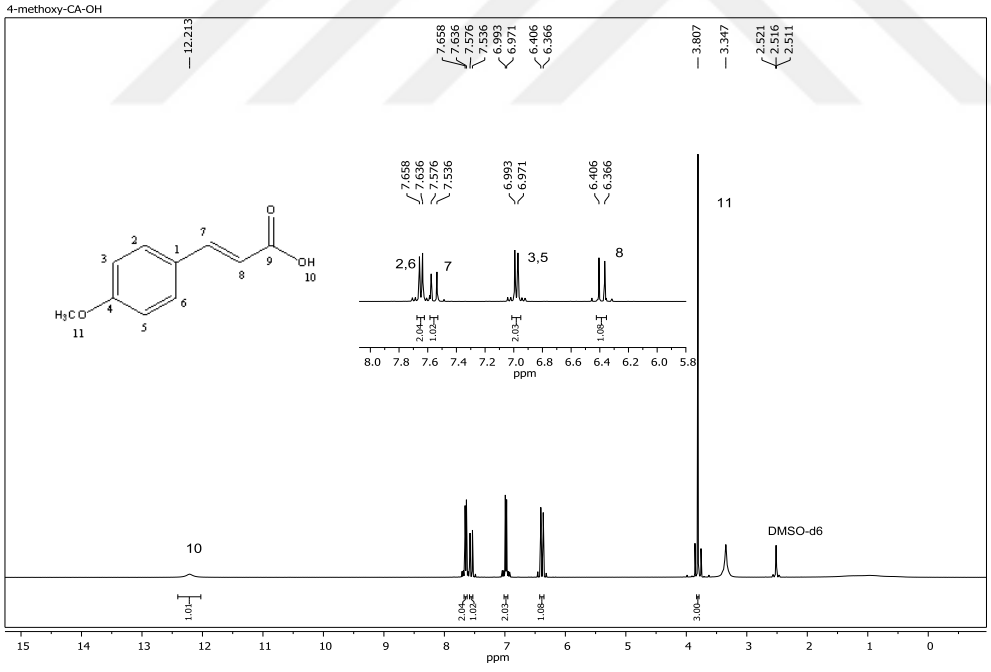

Appx. 1.40. ^{1}H NMR spectra of 4-methoxy-CA-OH

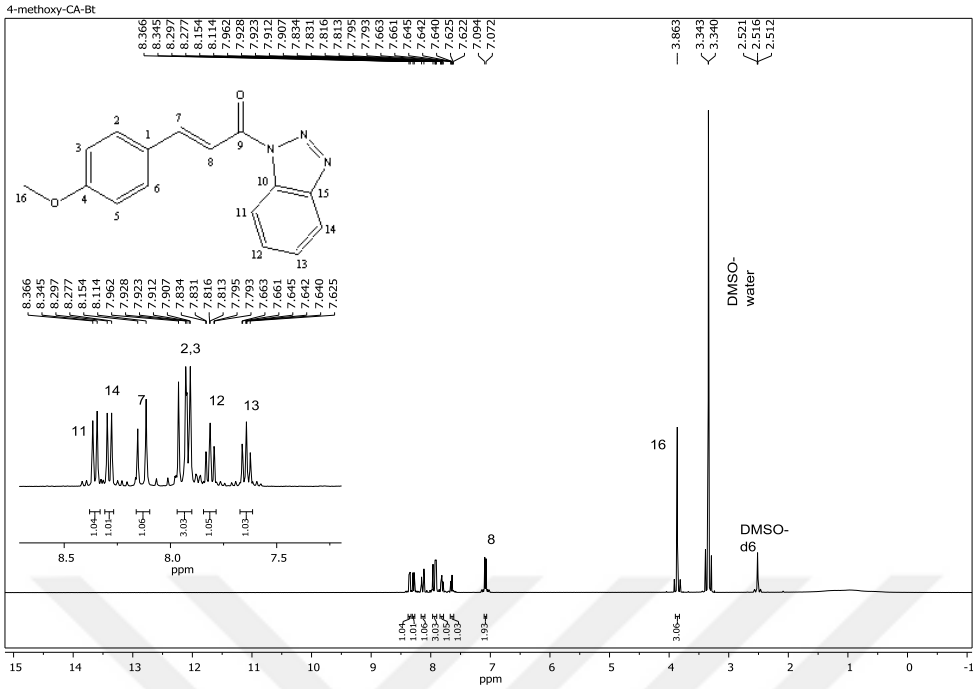

Appx. 1.41. ^{1}H NMR spectra of 4-methoxy-CA-Bt

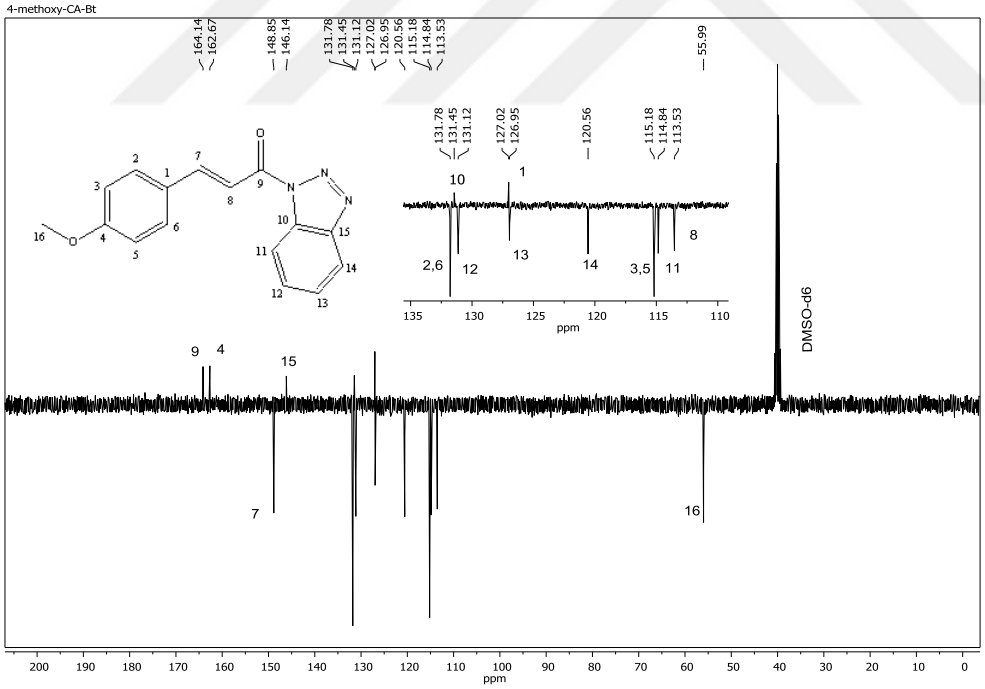

Appx. 1.42. ^{13}C APT NMR spectra of 4-methoxy-CA-Bt

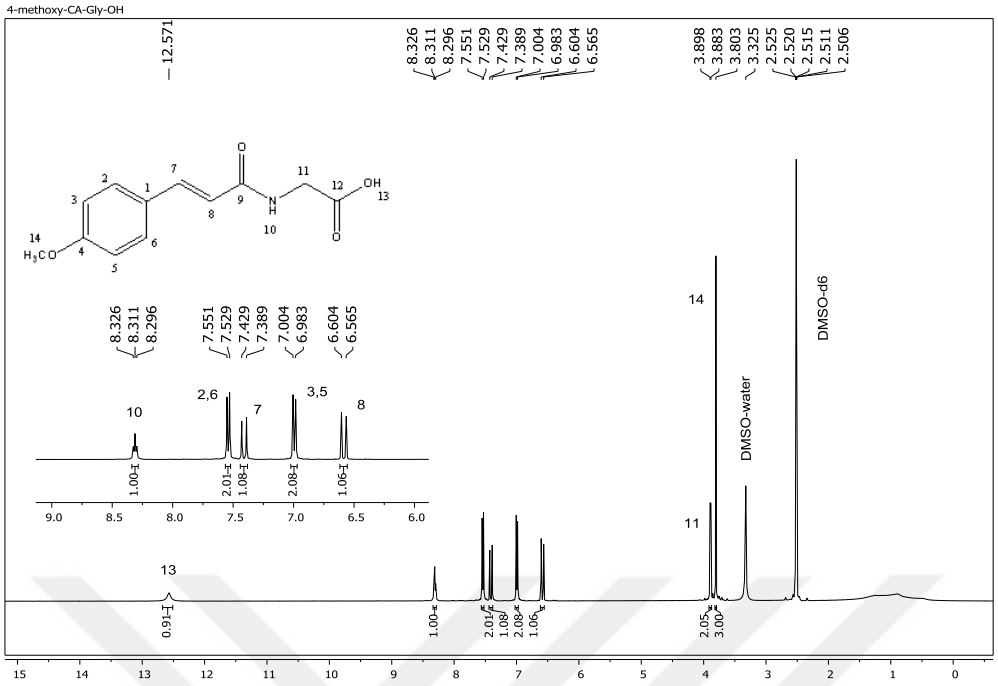

Appx. 1.43. ^{1}H NMR spectra of 4-methoxy-CA-Gly-OH

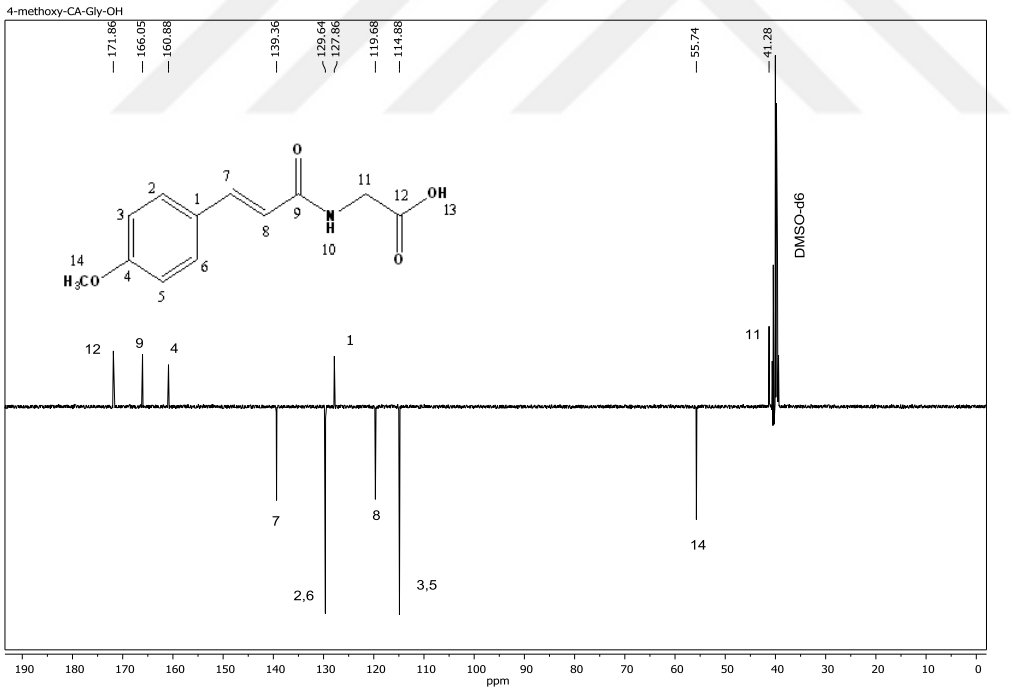

Appx. 1.44. ^{13}C APT NMR spectra of 4-methoxy-CA-Gly-OH

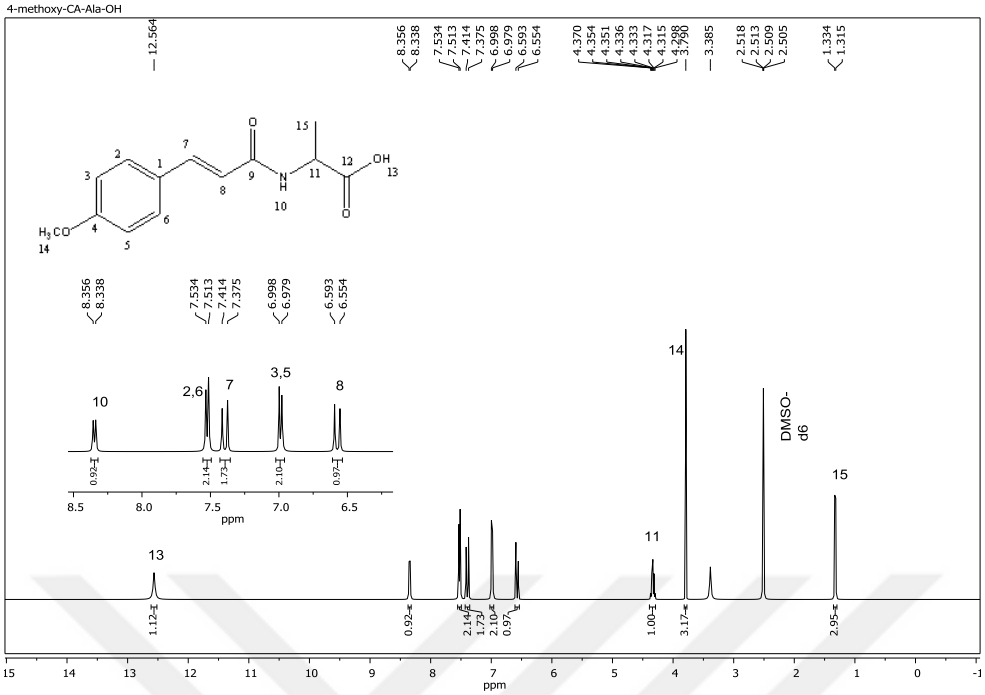

Appx. 1.45. ^{1}H NMR spectra of 4-methoxy-CA-Ala-OH

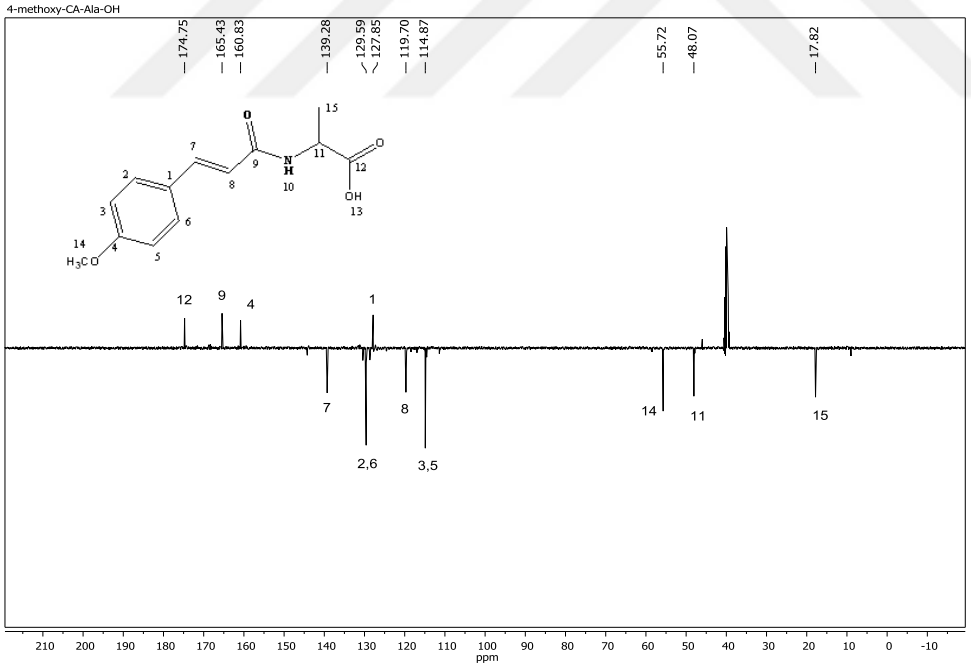

Appx. 1.46. ^{13}C APT NMR spectra of 4-methoxy-CA-Ala-OH

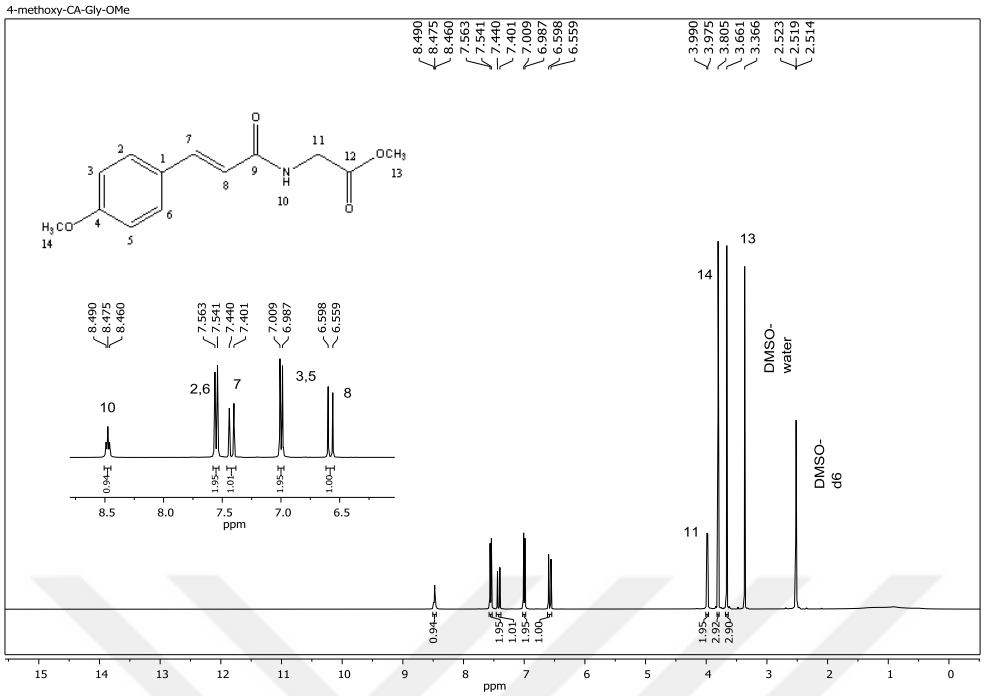

Appx. 1.47. ^{1}H NMR spectra of 4-methoxy-CA-Gly-OMe

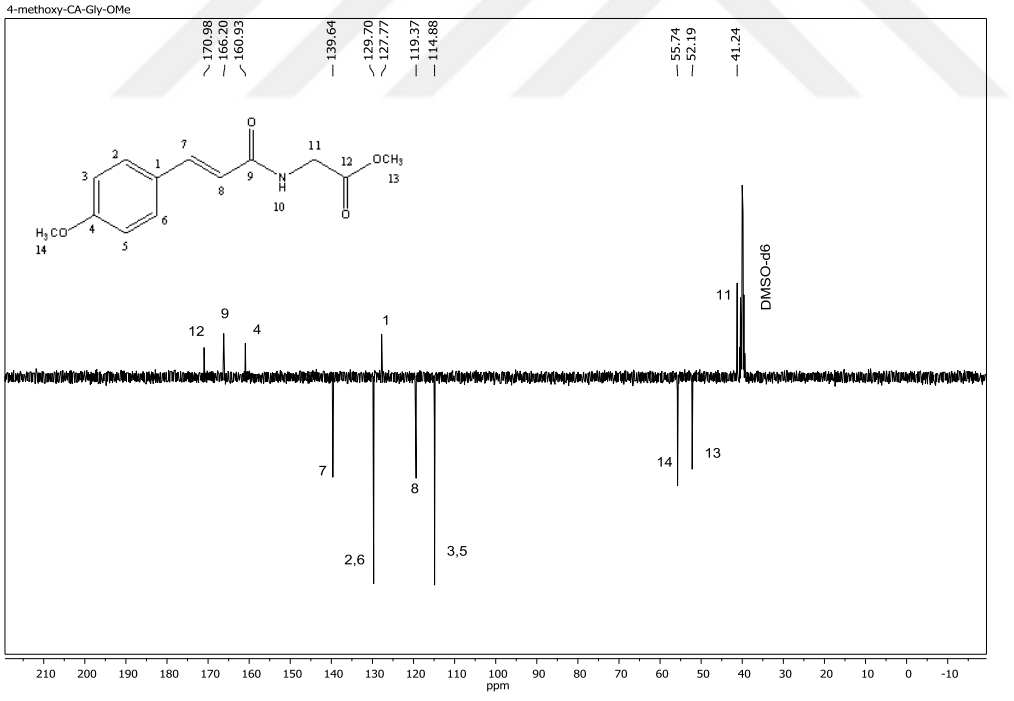

Appx. 1.48. ^{13}C APT NMR spectra of 4-methoxy-CA-Gly-OMe

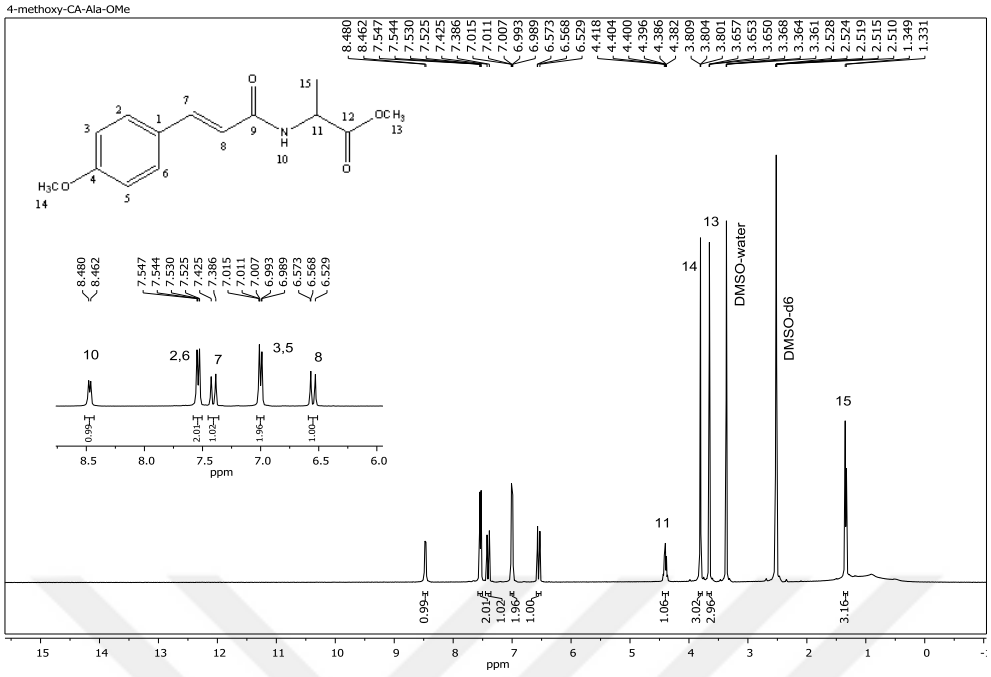

Appx. 1.49. ^{1}H NMR spectra of 4-methoxy-CA-Ala-OMe

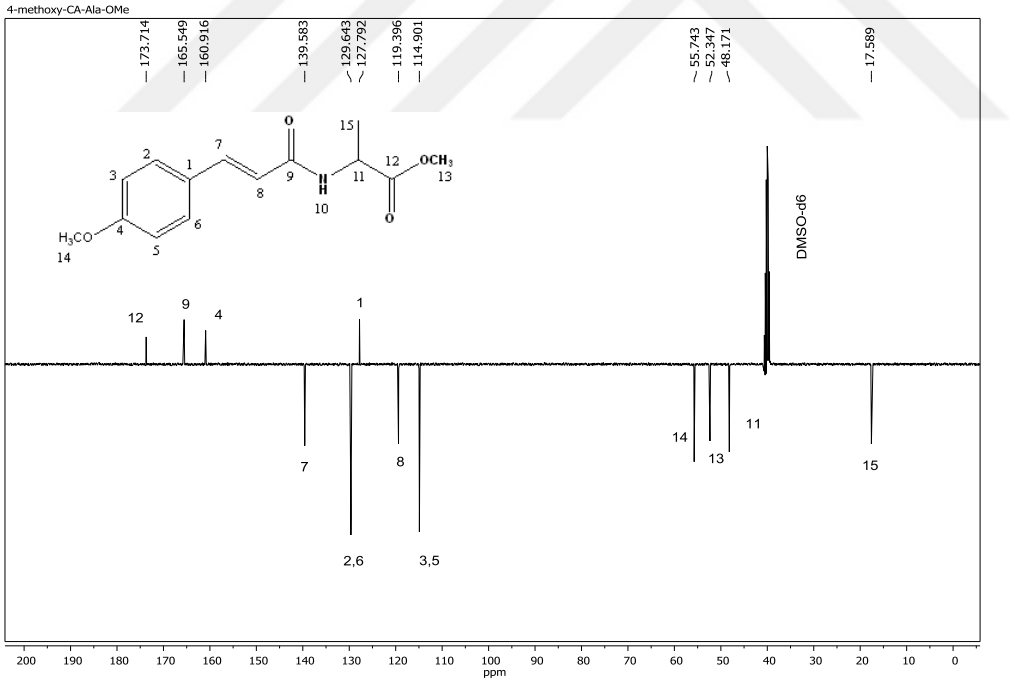

Appx. 1.50. ^{13}C APT NMR spectra of 4-methoxy-CA-Ala-OMe

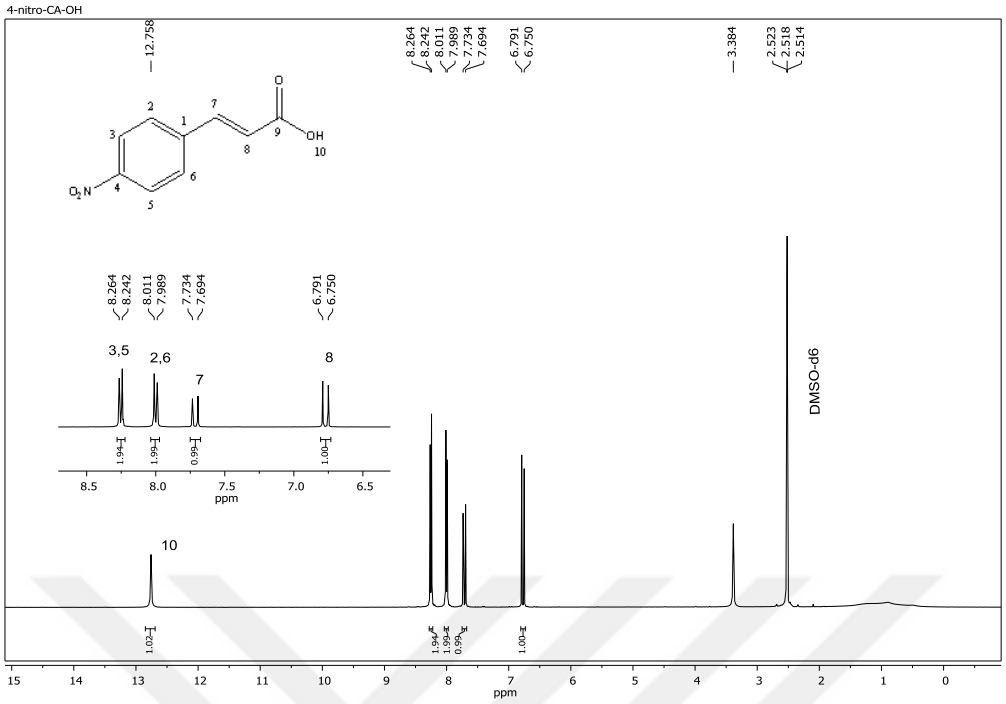

Appx. 1.51. ^{1}H NMR spectra of 4-nitro-CA-OH

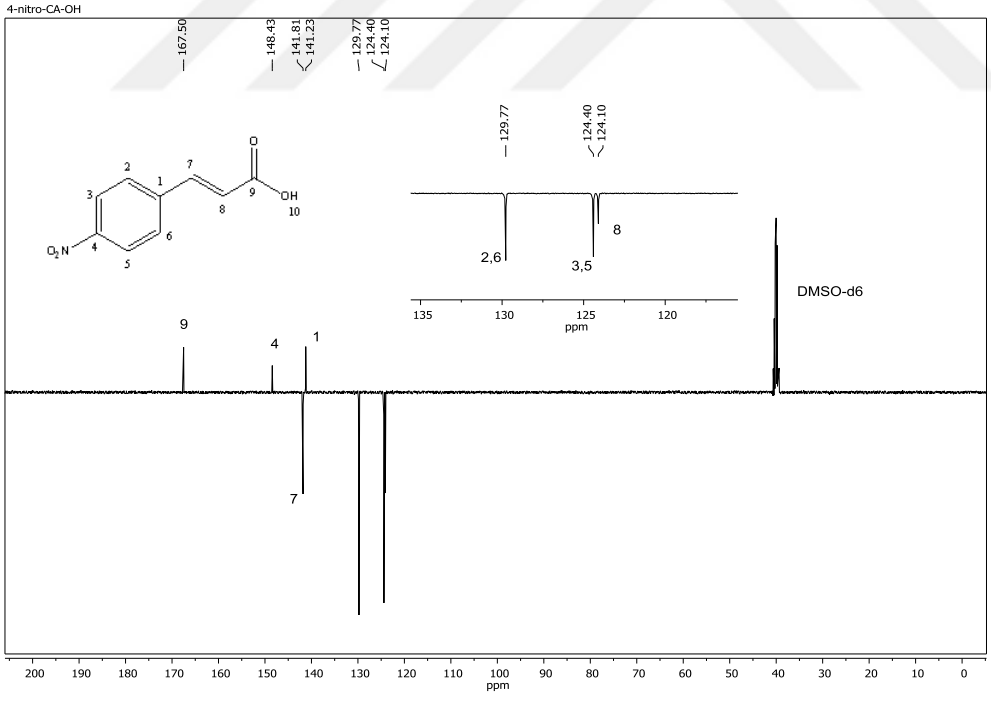

Appx. 1.52. ^{13}C APT NMR spectra of 4-nitro-CA-OH

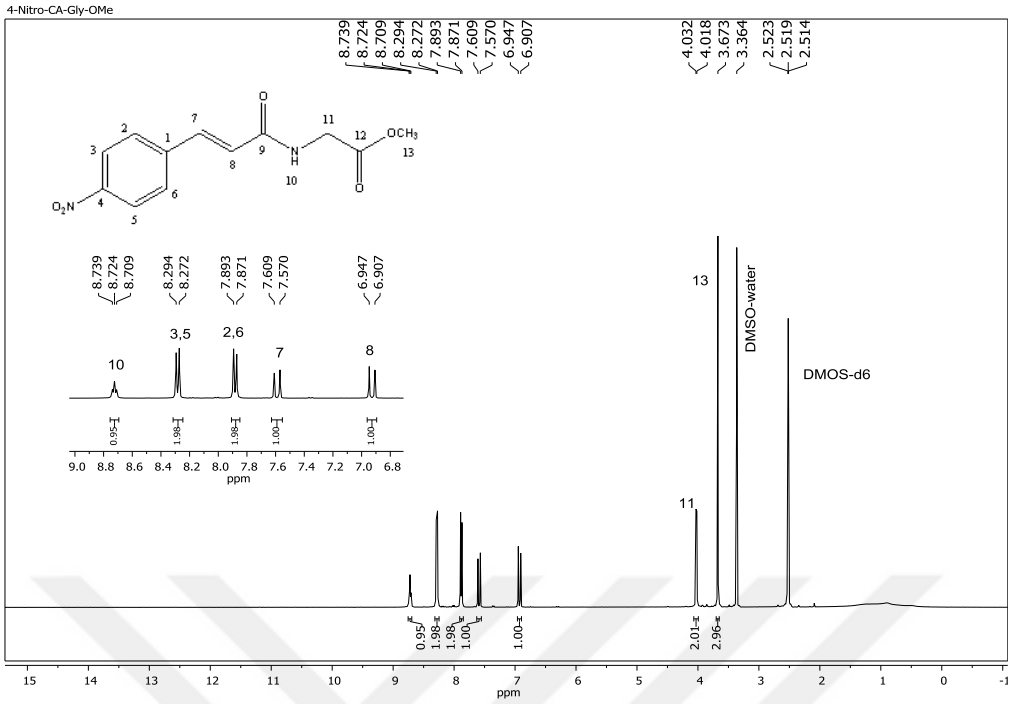

Appx. 1.53. ^{1}H NMR spectra of 4-nitro-CA-Gly-OMe

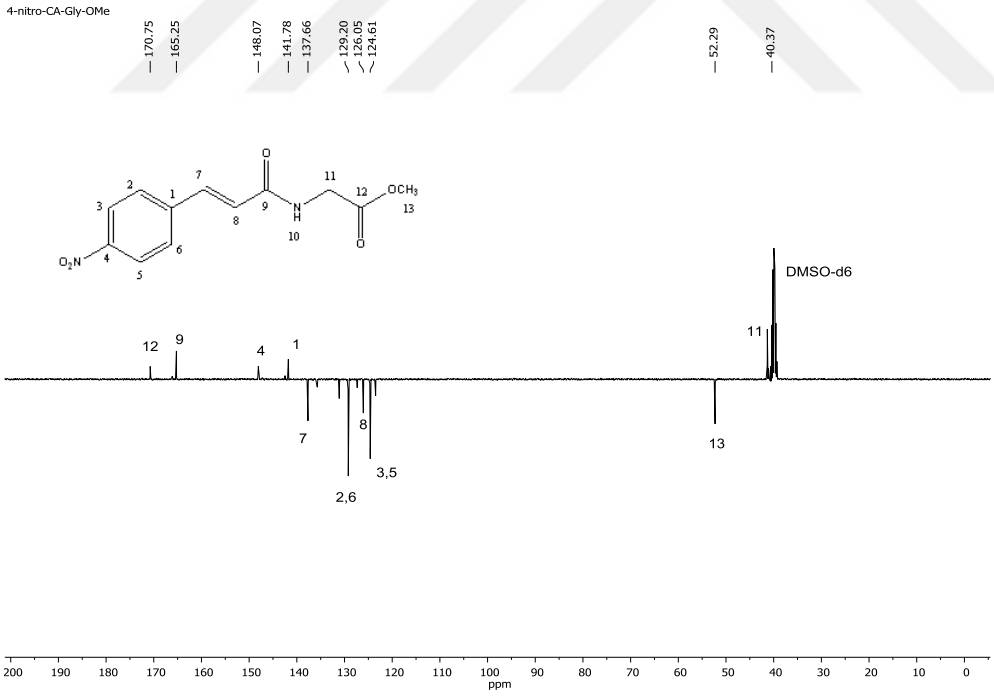

Appx. 1.54. ^{13}C APT NMR spectra of 4-nitro-CA-Gly-OMe

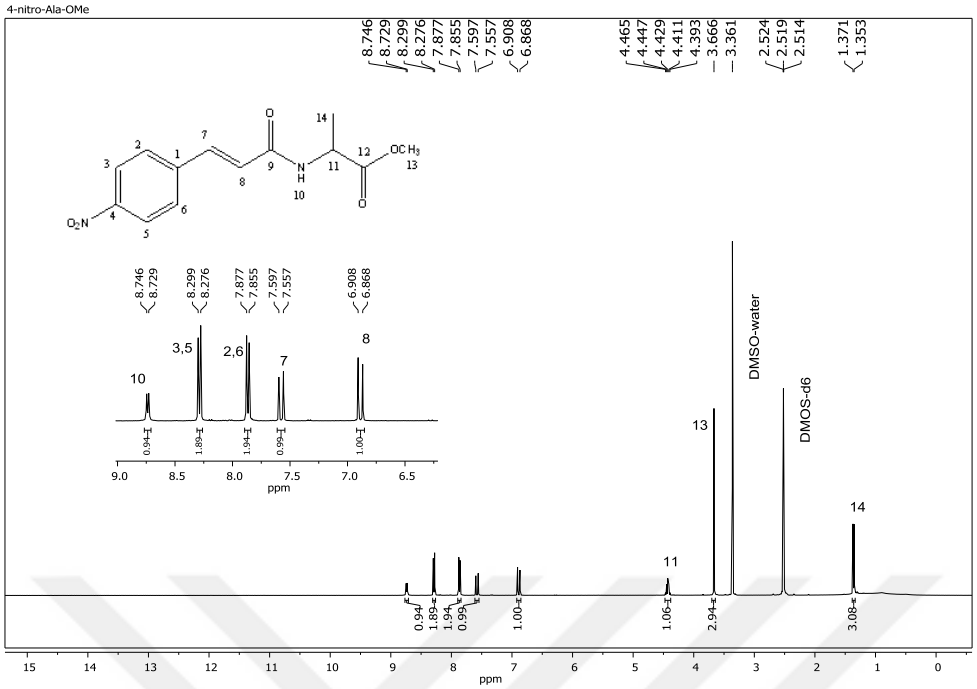

Appx. 1.55. ^{1}H NMR spectra of 4-nitro-CA-Ala-OMe

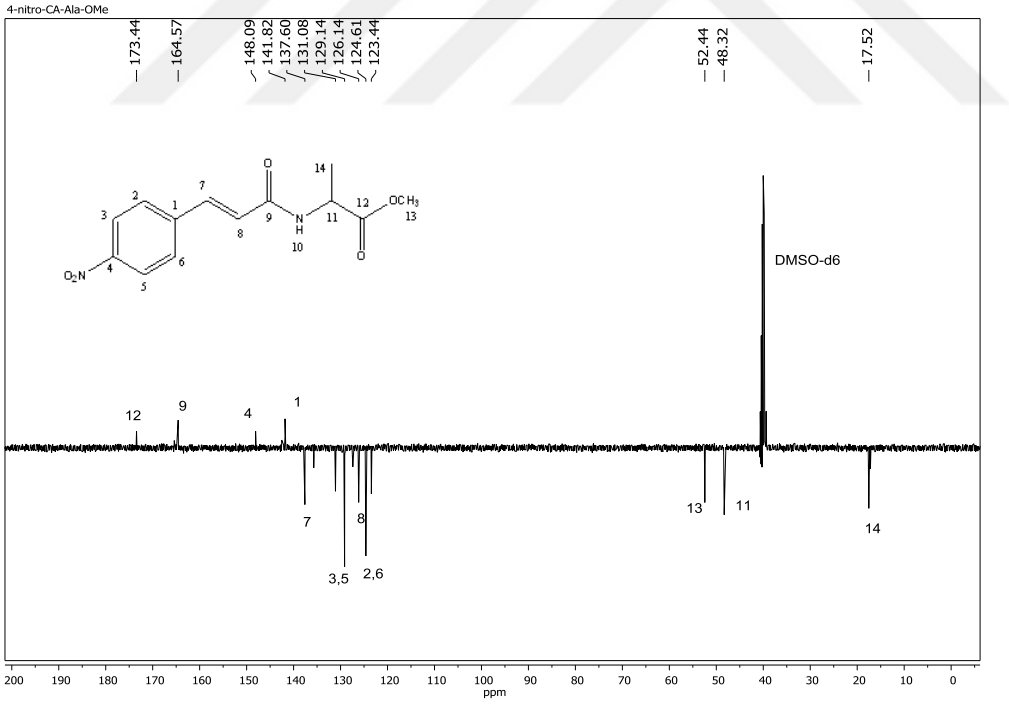

Appx. 1.56. ^{13}C APT NMR spectra of 4-nitro-CA-Ala-OMe

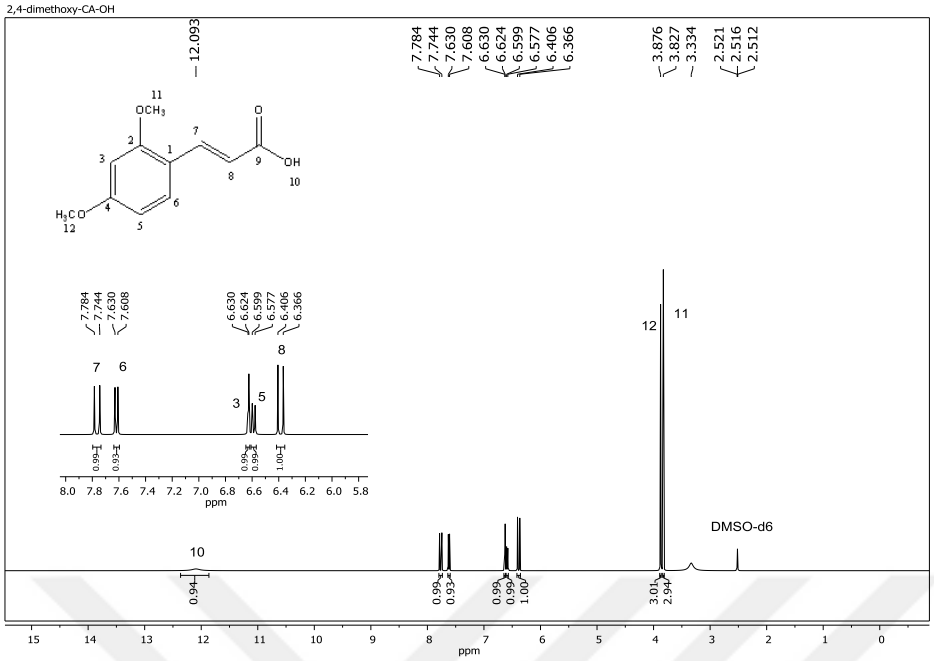

Appx. 1.57. ^{1}H NMR spectra of 2,4-dimethoxy-CA-OH

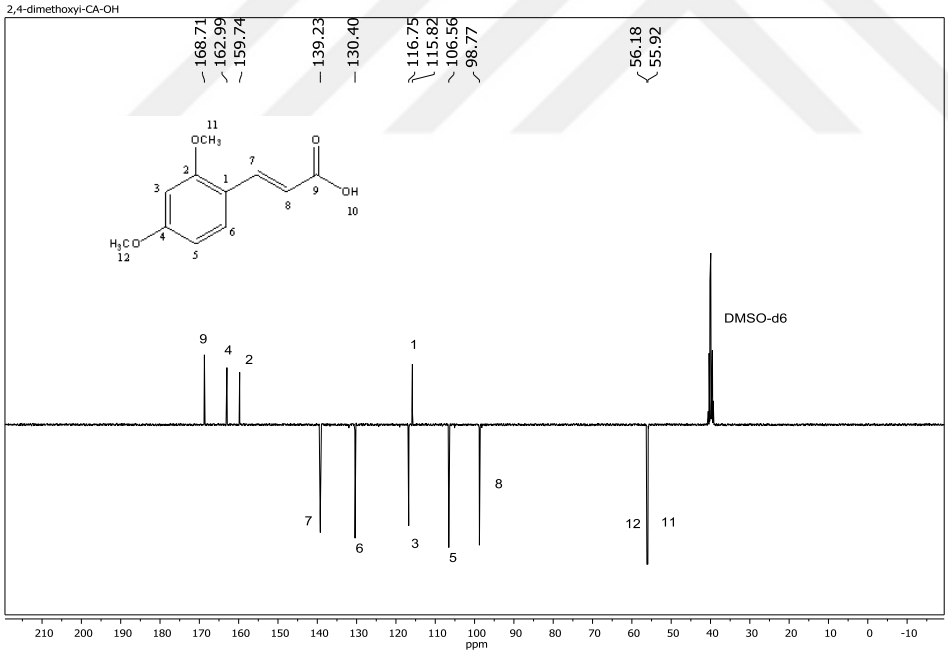

Appx. 1.58. ^{13}C APT NMR spectra of 2,4-dimethoxy-CA-OH

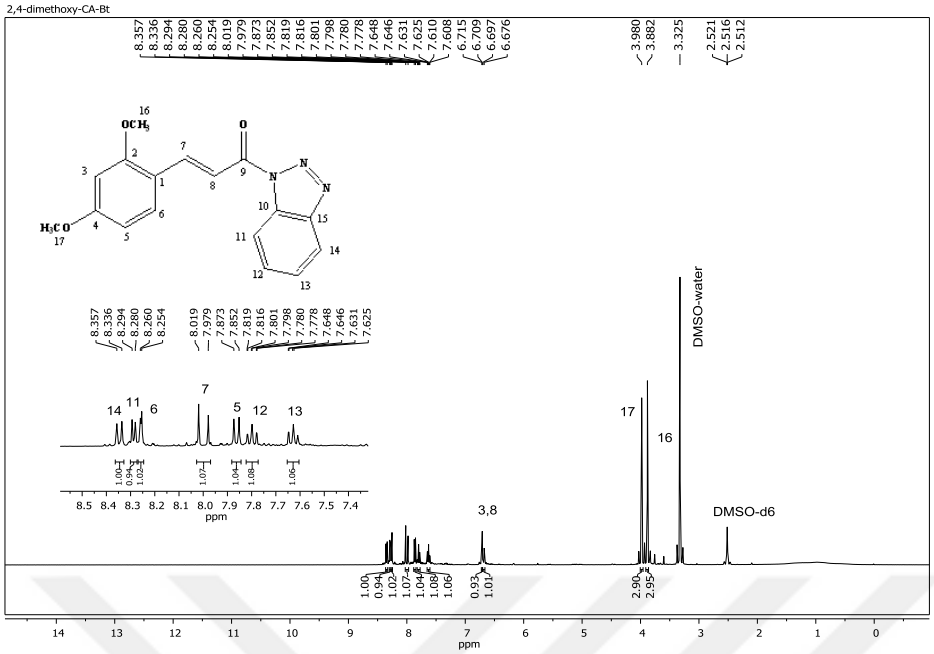

Appx. 1.59. ^{1}H NMR spectra of 2,4-dimethoxy-CA-Bt

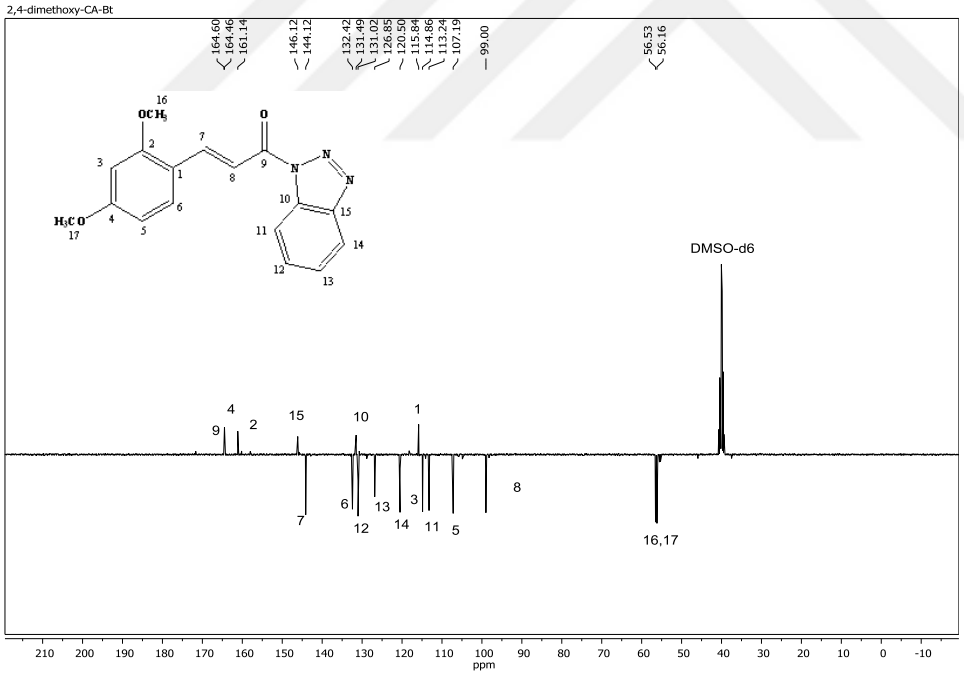

Appx. 1.60. ^{13}C APT NMR spectra of 2,4-dimethoxy-CA-Bt

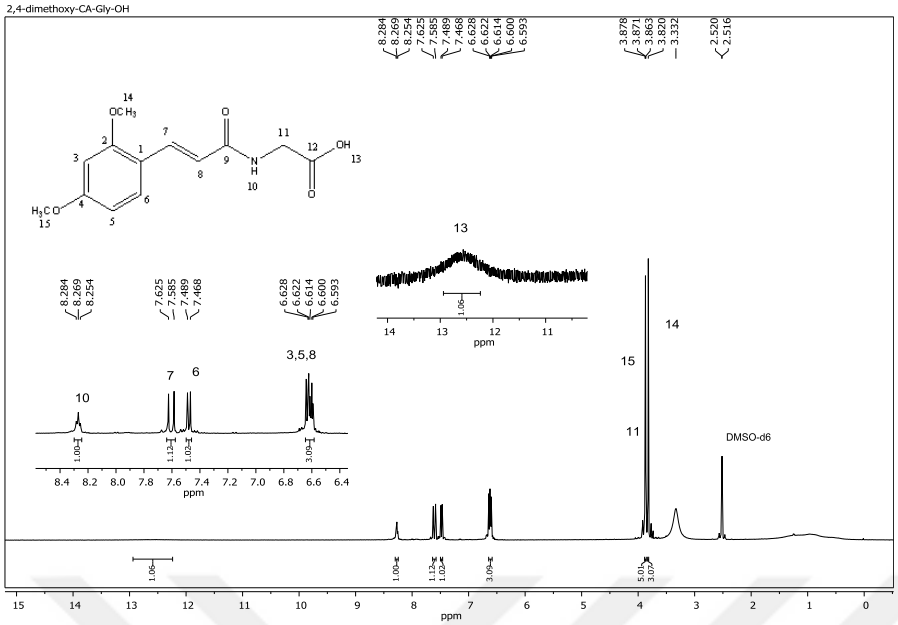

Appx. 1.61. ^{1}H NMR spectra of 2,4-dimethoxy-CA-Gly-OH

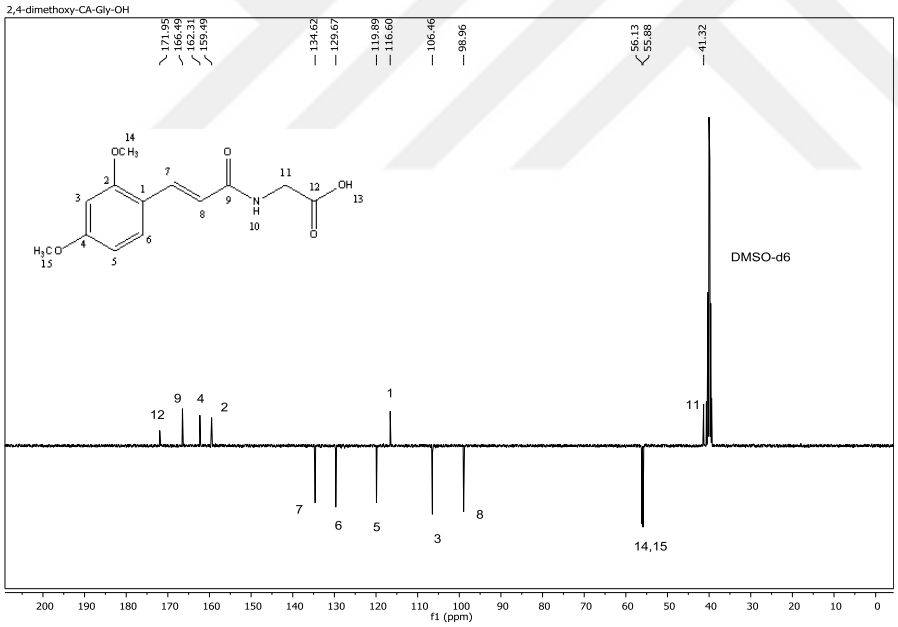

Appx. 1.62. ^{13}C APT NMR spectra of 2,4-dimethoxy-CA-Gly-OH

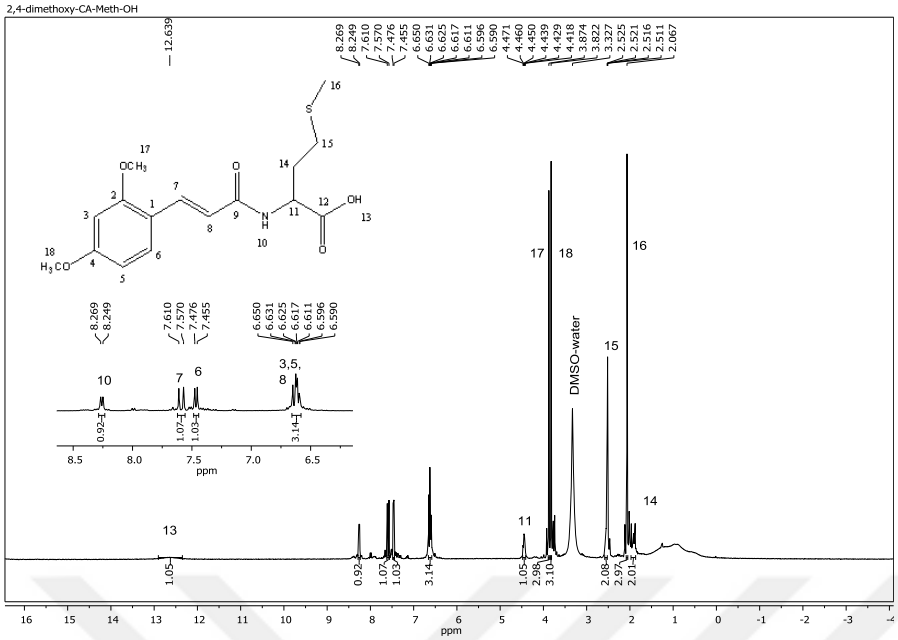

Appx. 1.63. ^{1}H NMR spectra of 2,4-dimethoxy-CA-Meth-OH

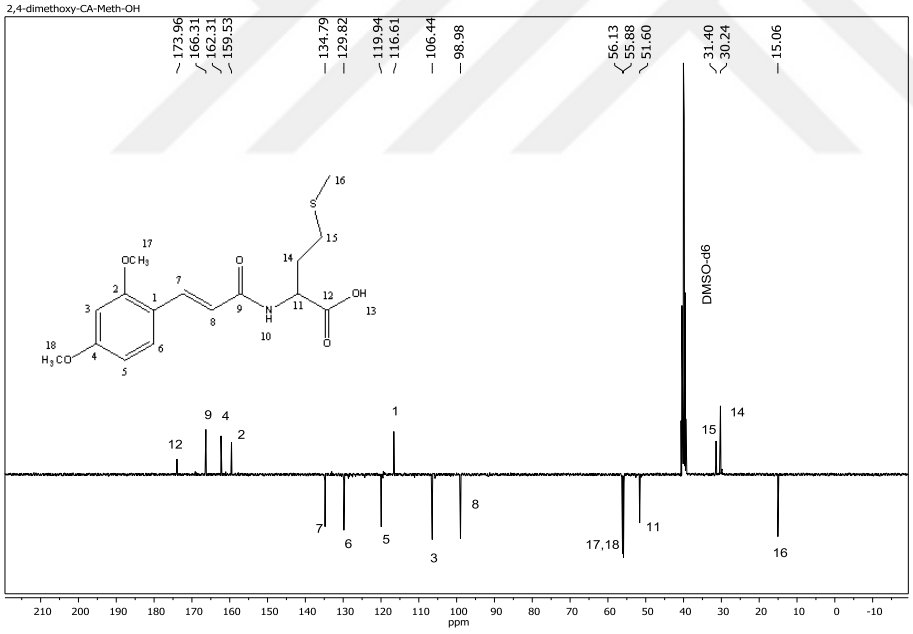

Appx. 1.64. ^{13}C APT NMR spectra of 2,4-dimethoxy-CA-Meth-OH

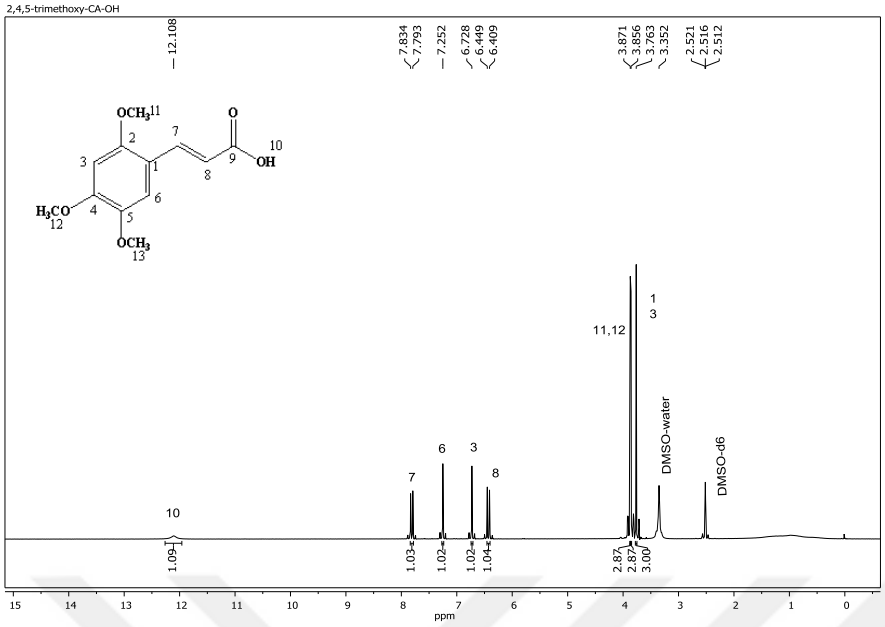

Appx. 1.65. ^{1}H NMR spectra of 2,4,5-trimethoxy-CA-OH

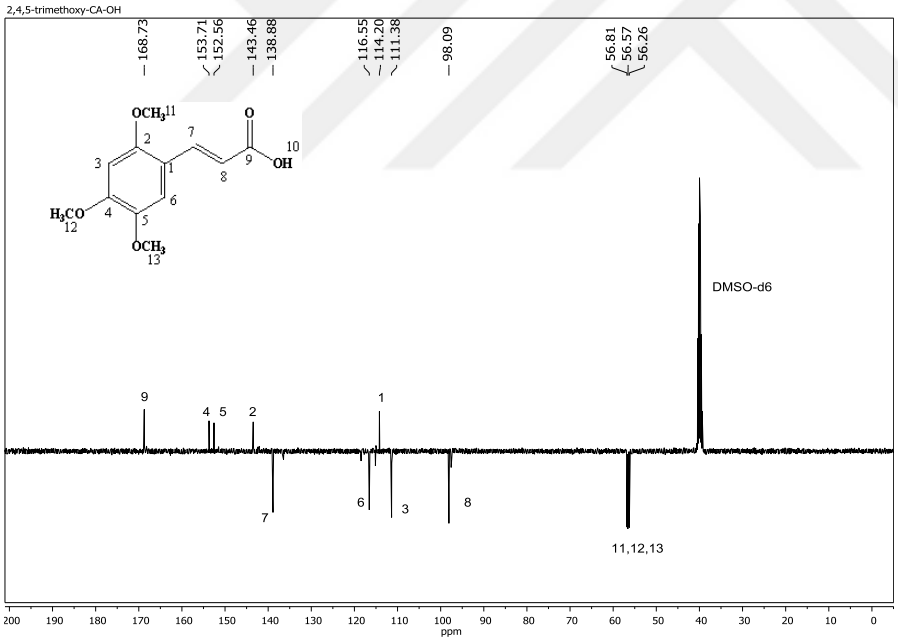

Appx. 1.66. ^{13}C APT NMR spectra of 2,4,5-trimethoxy-CA-OH

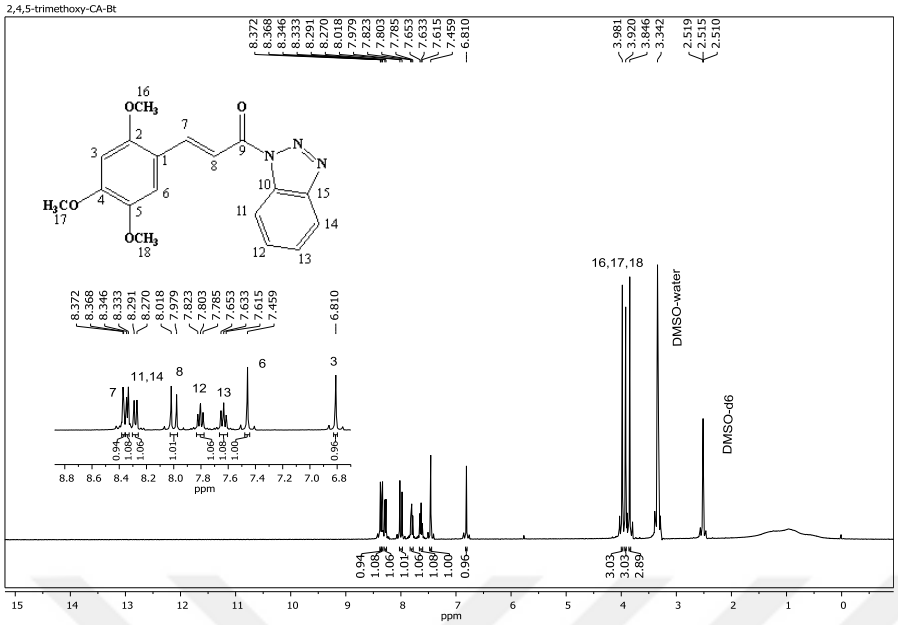

Appx. 1.67. ^{1}H NMR spectra of 2,4,5-trimethoxy-CA-Bt

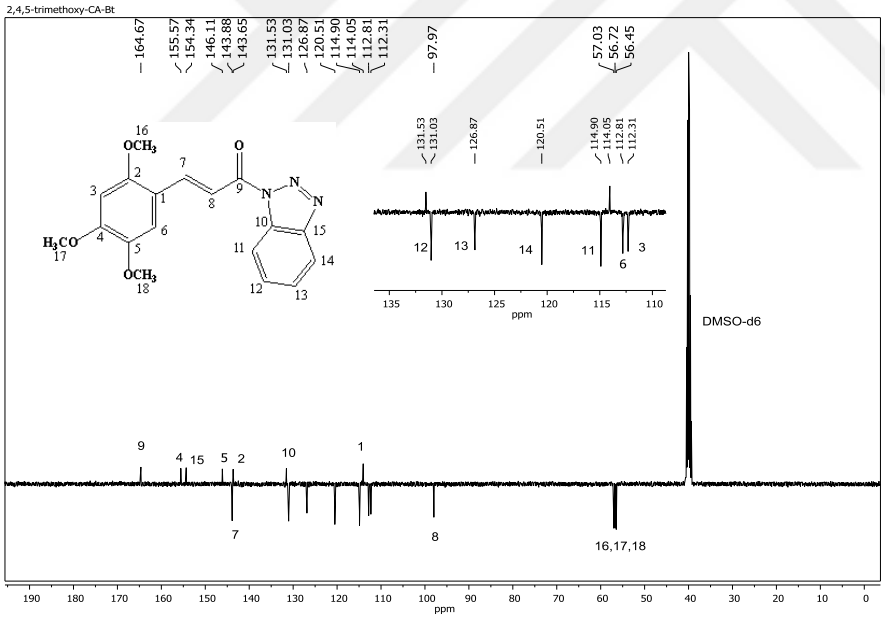

Appx. 1.68. ^{13}C APT NMR spectra of 2,4,5-trimethoxy-CA-Bt

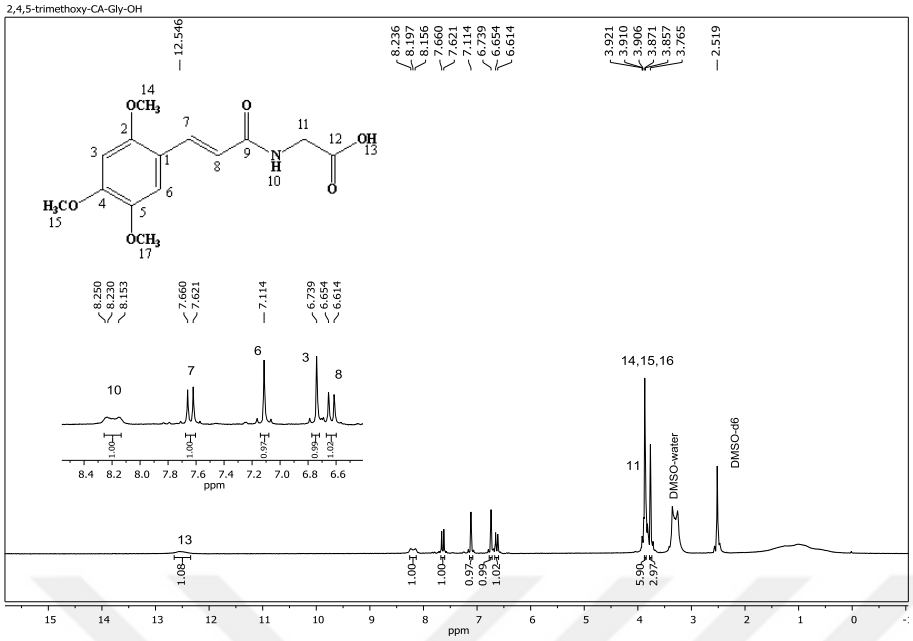

Appx. 1.69. ^{1}H NMR spectra of 2,4,5-trimethoxy-CA-Gly-OH

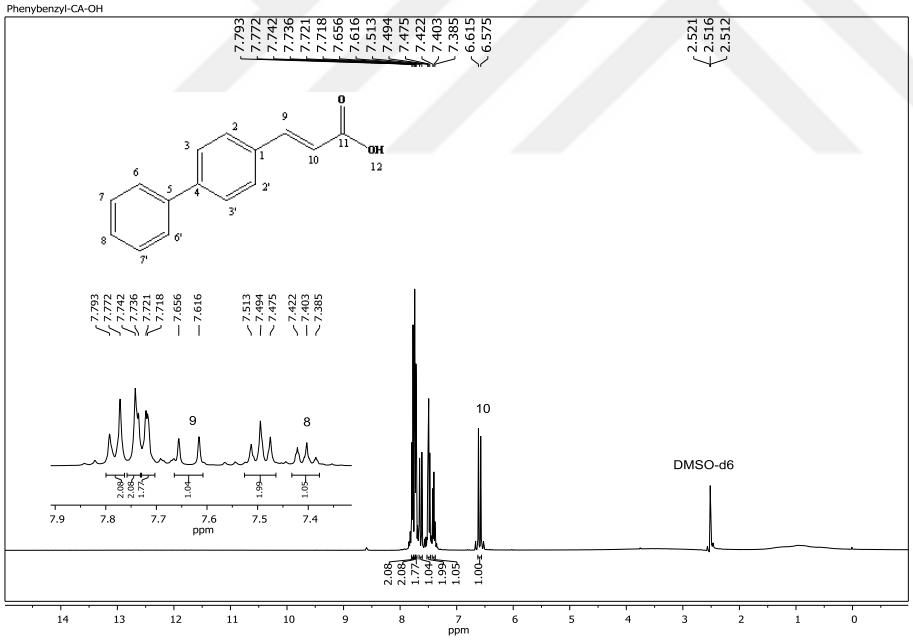

Appx. 1.70. ^{1}H NMR spectra of 4-phenyl-CA-OH

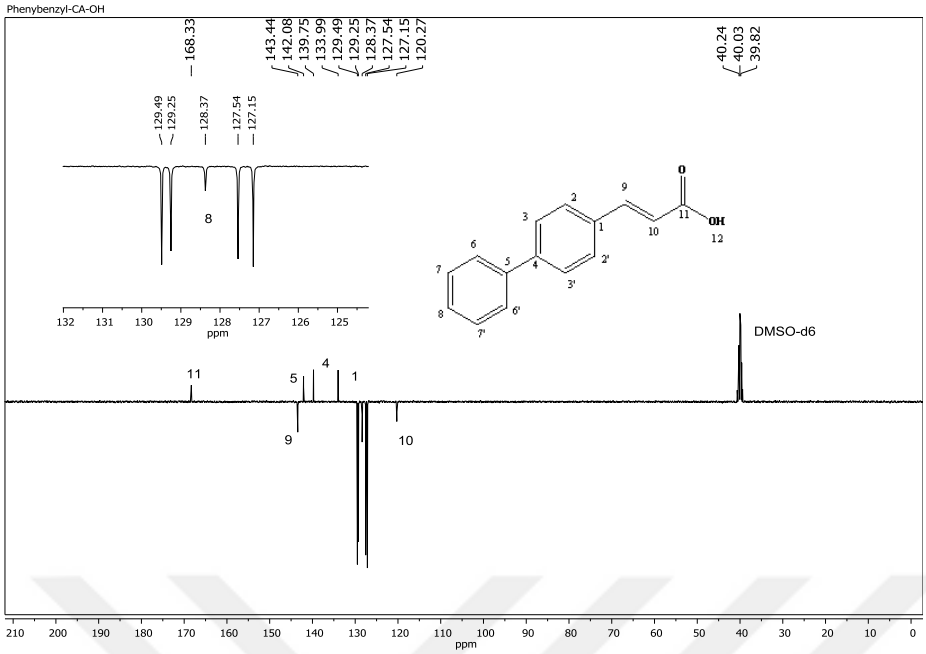

Appx. 1.71. ^{13}C APT NMR spectra of 4-phenyl-CA-OH

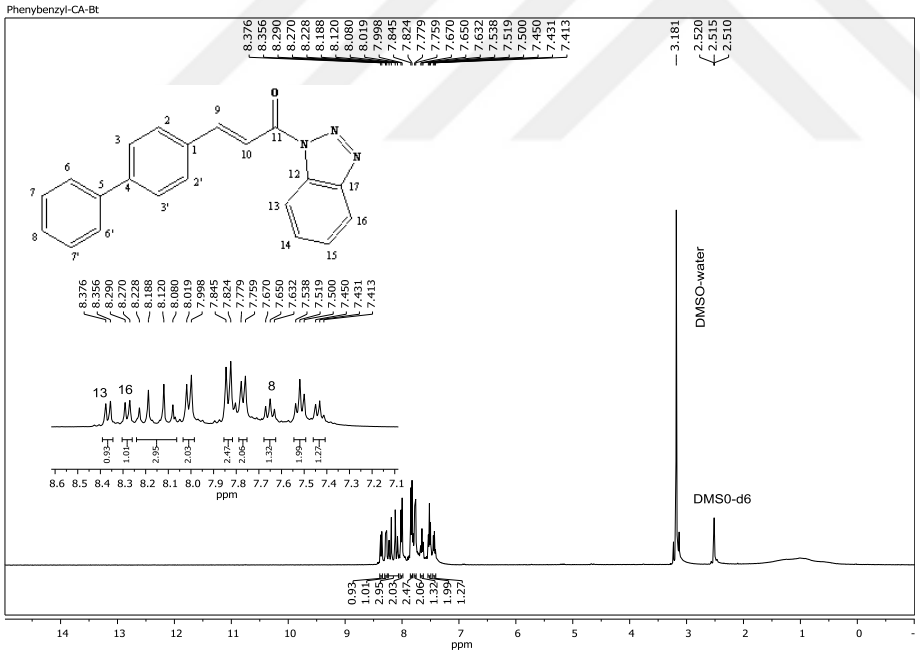

Appx. 1.72. ^{1}H NMR spectra of 4-phenyl-CA-Bt

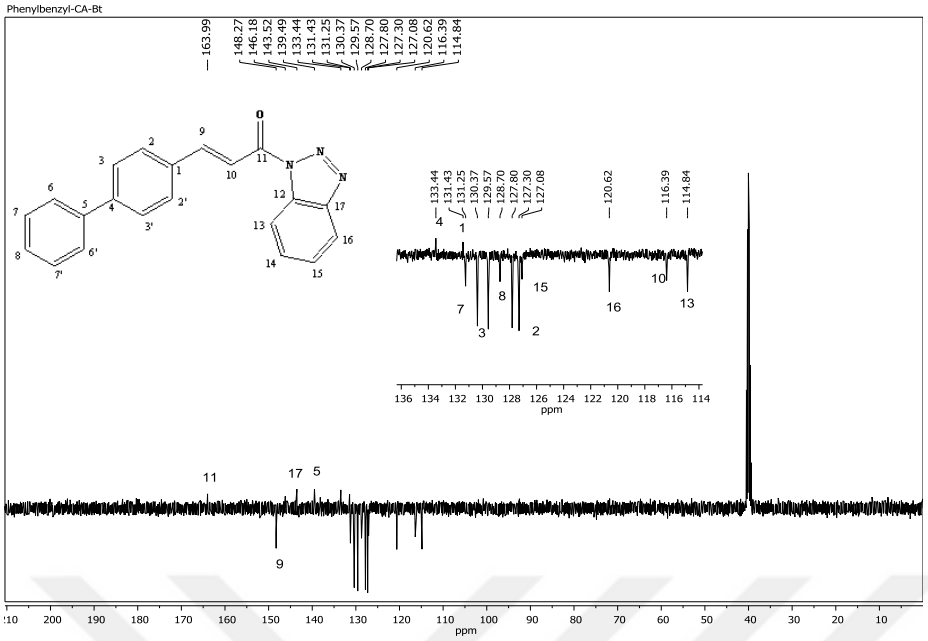

Appx. 1.73. ^{13}C APT NMR spectra of 4-phenyl-CA-Bt

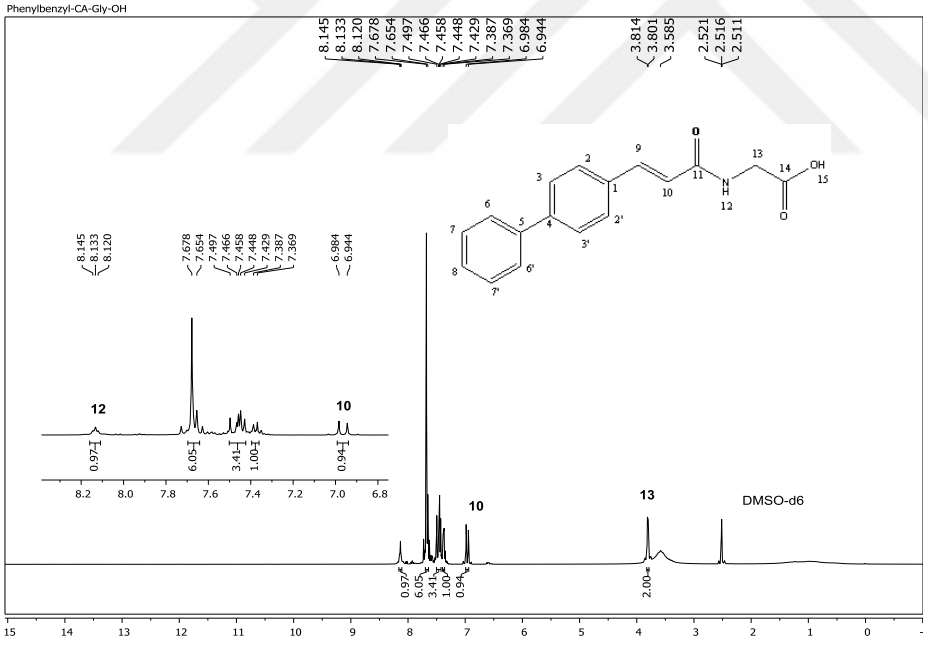

Appx. 1.74. ^{1}H NMR spectra of 4-phenyl-CA-Gly-OH

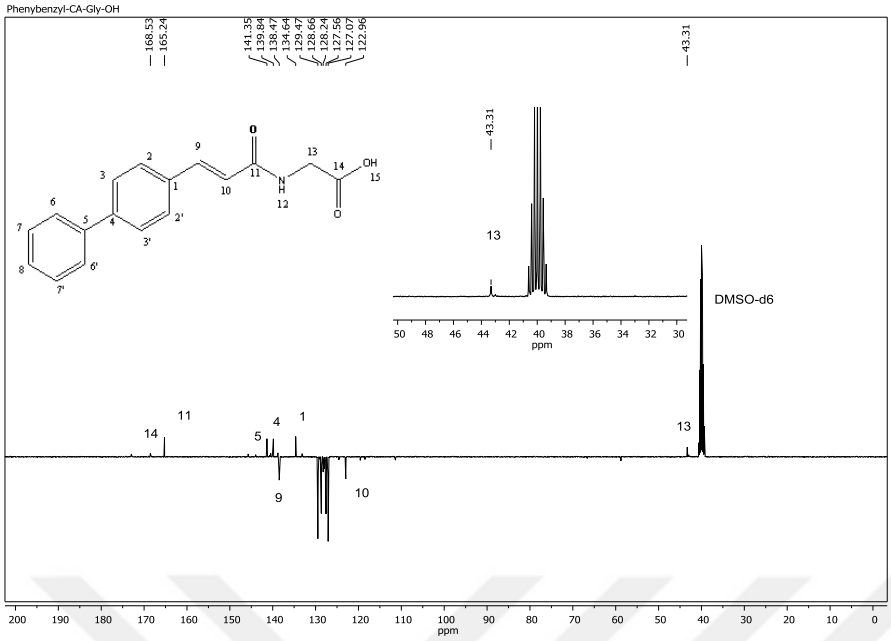

Appx. 1.75. ^{13}C APT NMR spectra of 4-phenyl-CA-Gly-OH

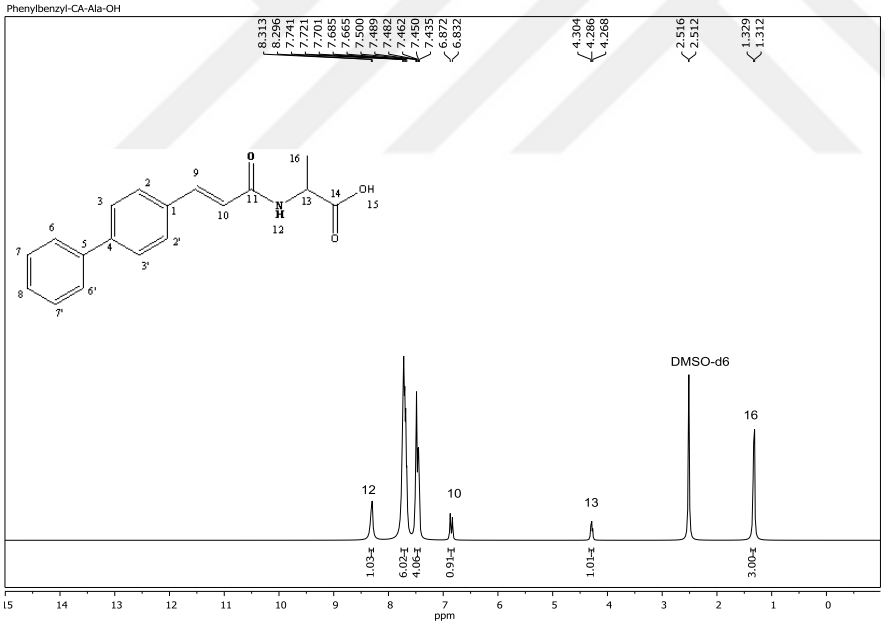

Appx. 1.76. ^{1}H NMR spectra of 4-phenyl-CA-Ala-OH

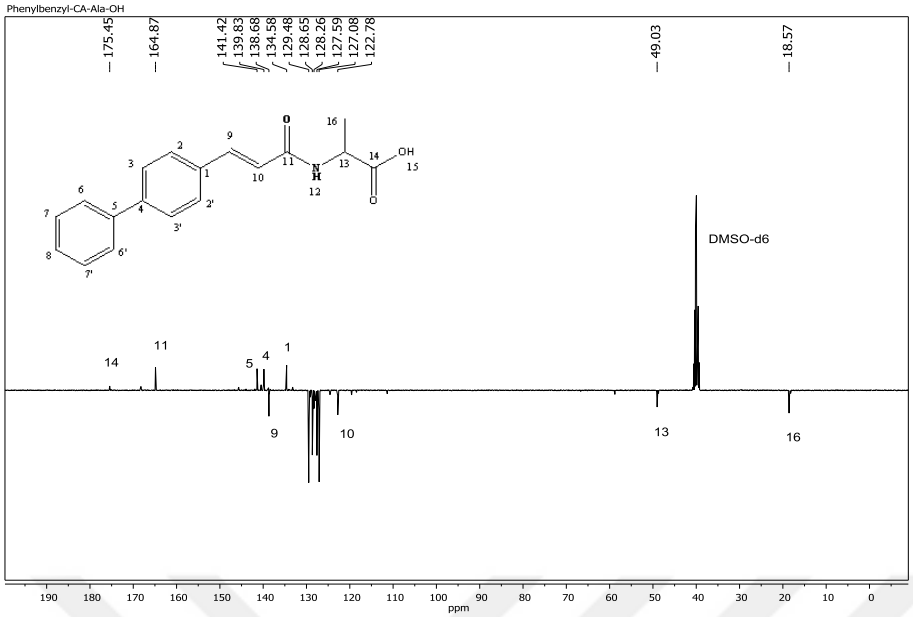

Appx. 1.77. ^{13}C APT NMR spectra of 4-phenyl-CA-Ala-OH

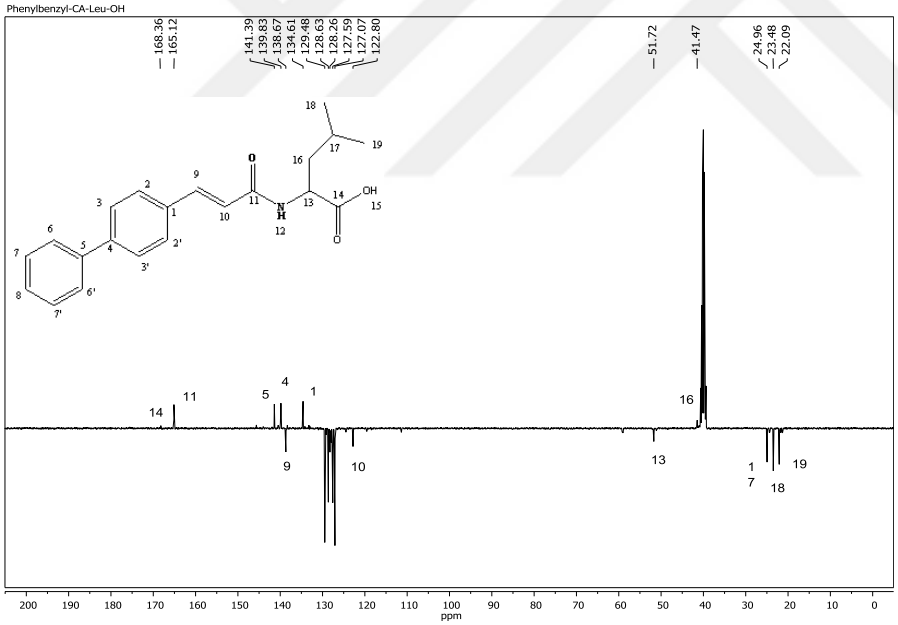

Appx. 1.78. ^{13}C APT NMR spectra of 4-phenyl-CA-Leu-OH

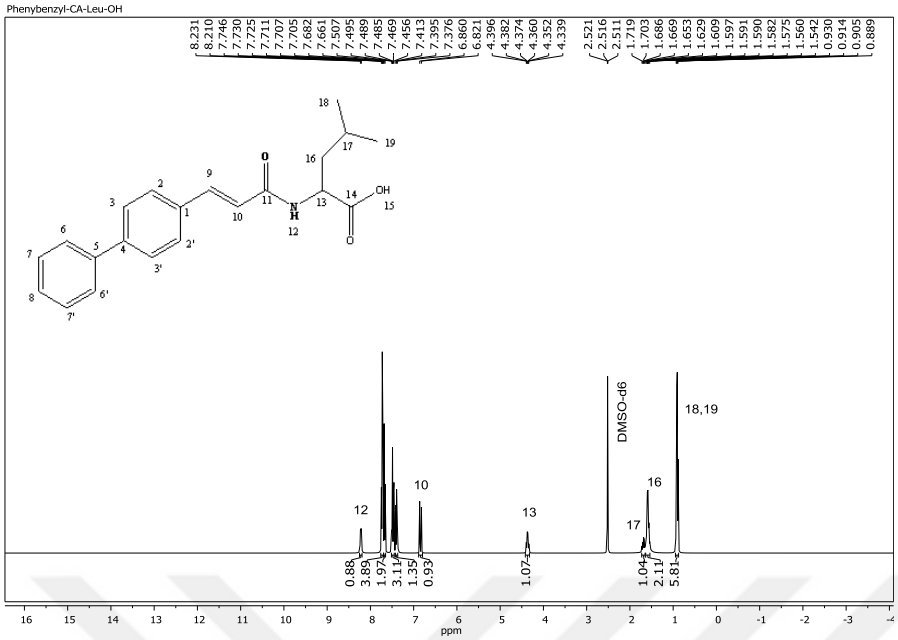

Appx. 1.79. ^{1}H NMR spectra of 4-phenyl-CA-Leu-OH

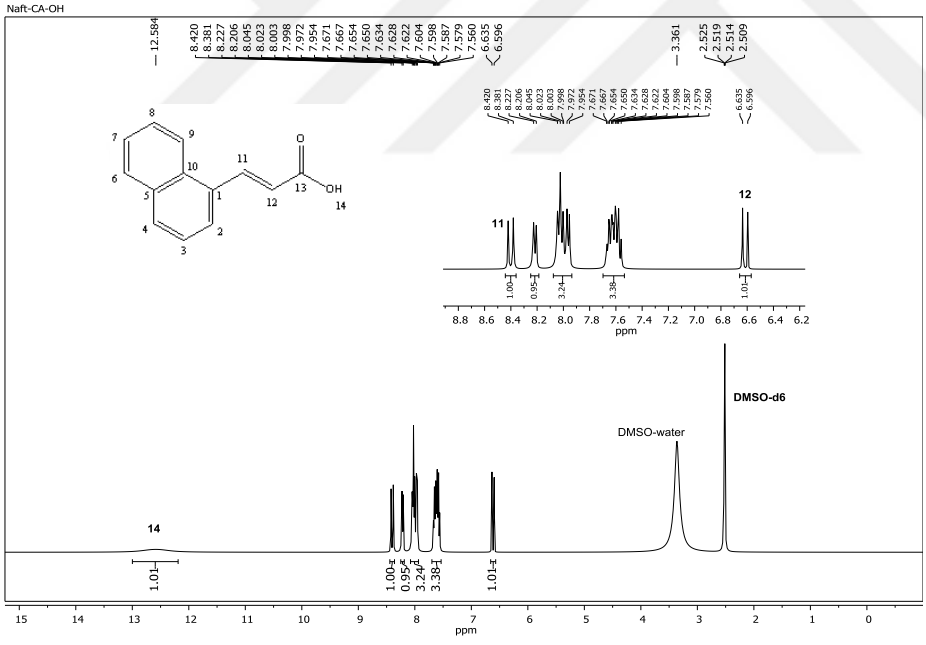

Appx. 1.80. ^{1}H NMR spectra of Naft-CA-OH

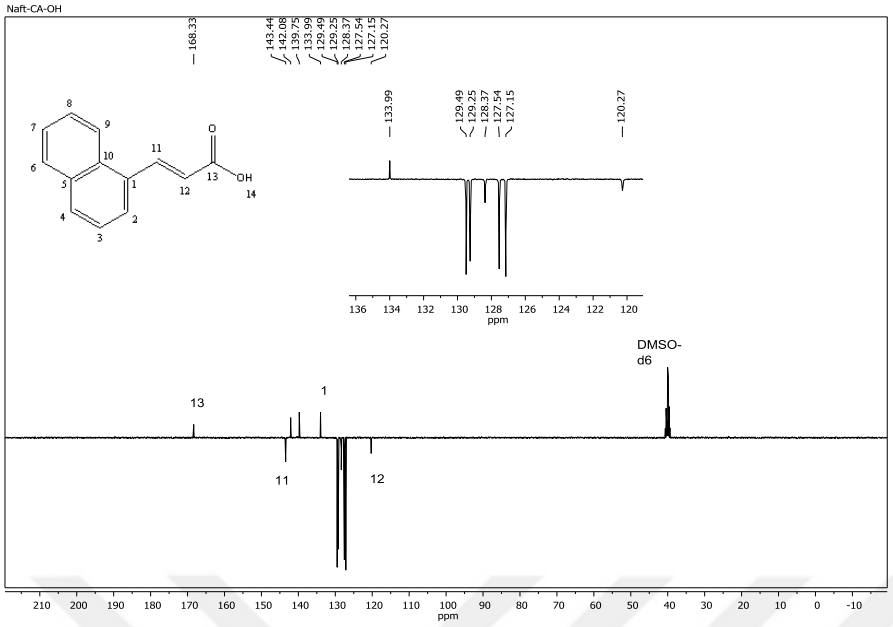

Appx. 1.81. ^{13}C APT NMR spectra of Naft-CA-OH

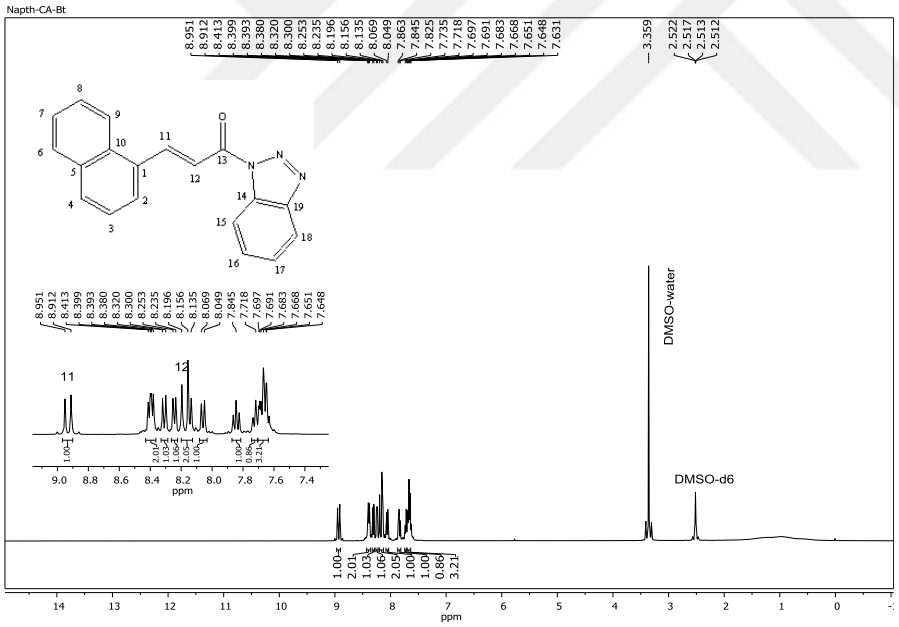

Appx. 1.82. ^{1}H NMR spectra of Naft-CA-Bt

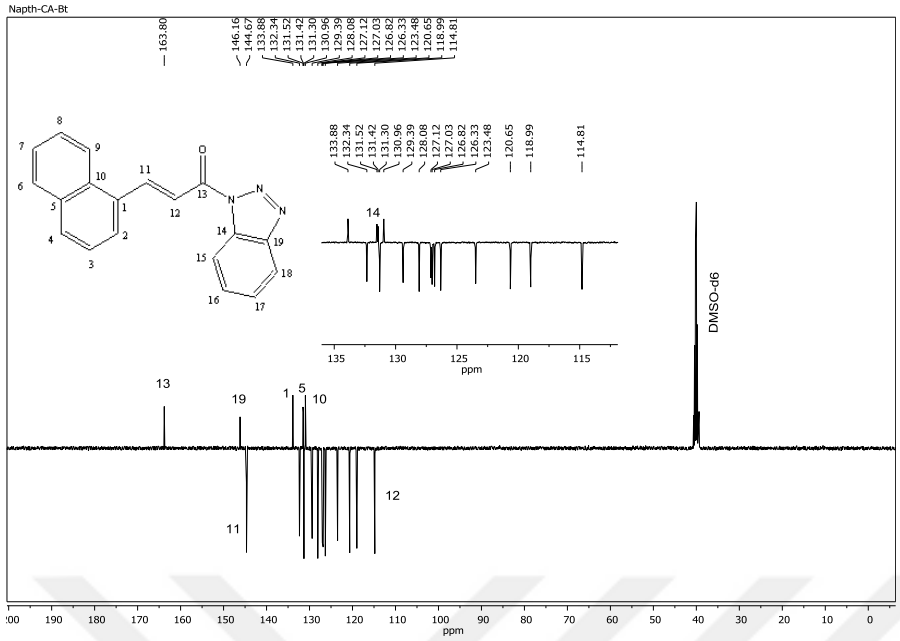

Appx. 1.83. ^{13}C APT NMR spectra of Naft-CA-Bt

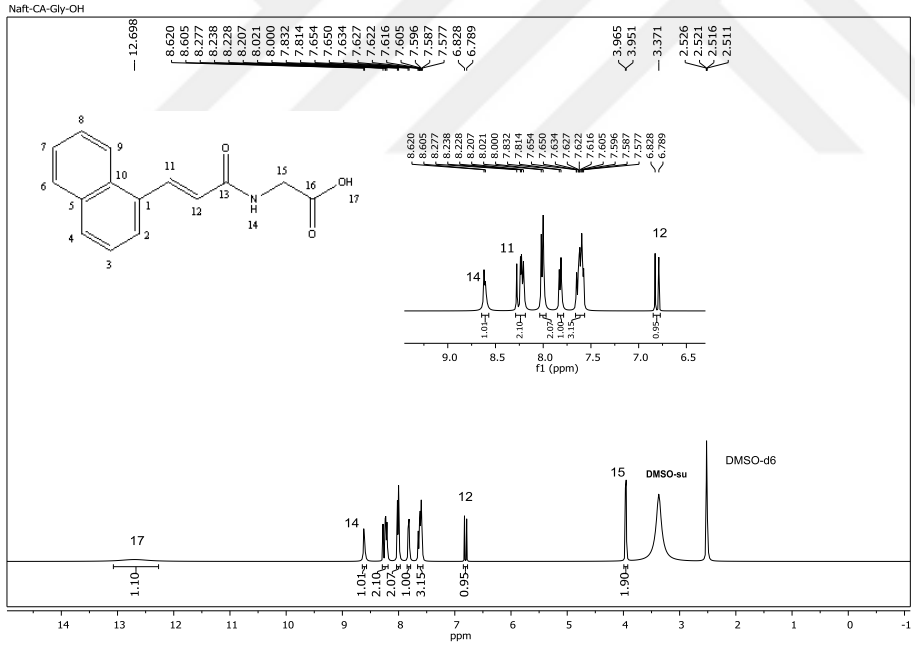

Appx. 1.84. ^{1}H NMR spectra of Naft-CA-Gly-OH

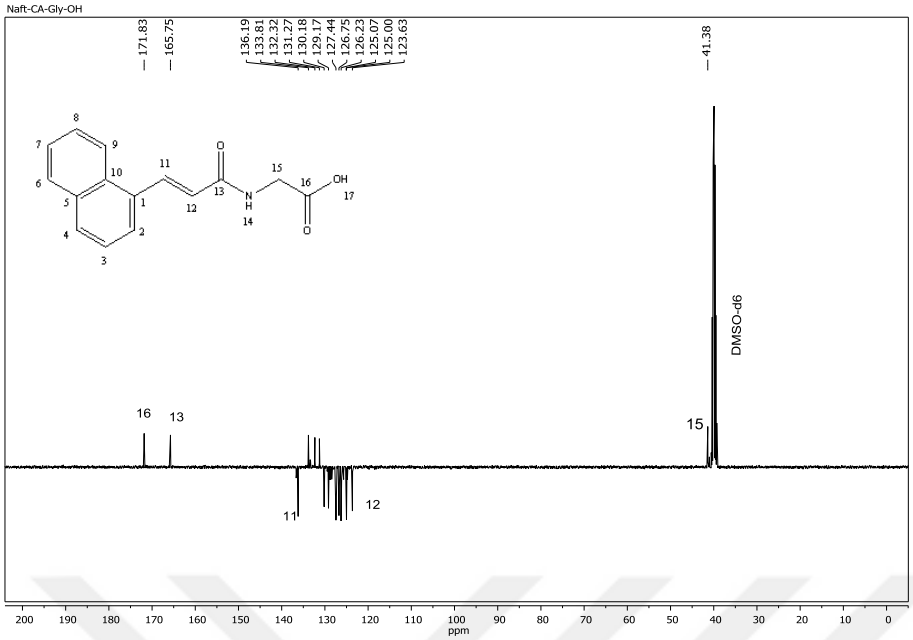

Appx. 1.85. ^{13}C APT NMR spectra of Naft-CA-Gly-OH

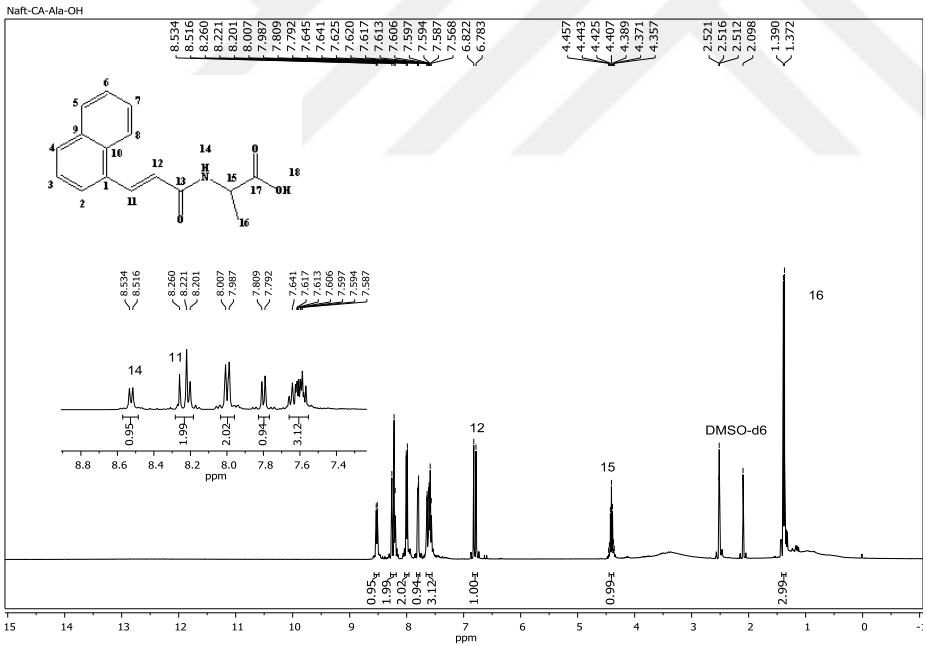

Appx. 1.86. ^{1}H NMR spectra of Naft-CA-Ala-OH

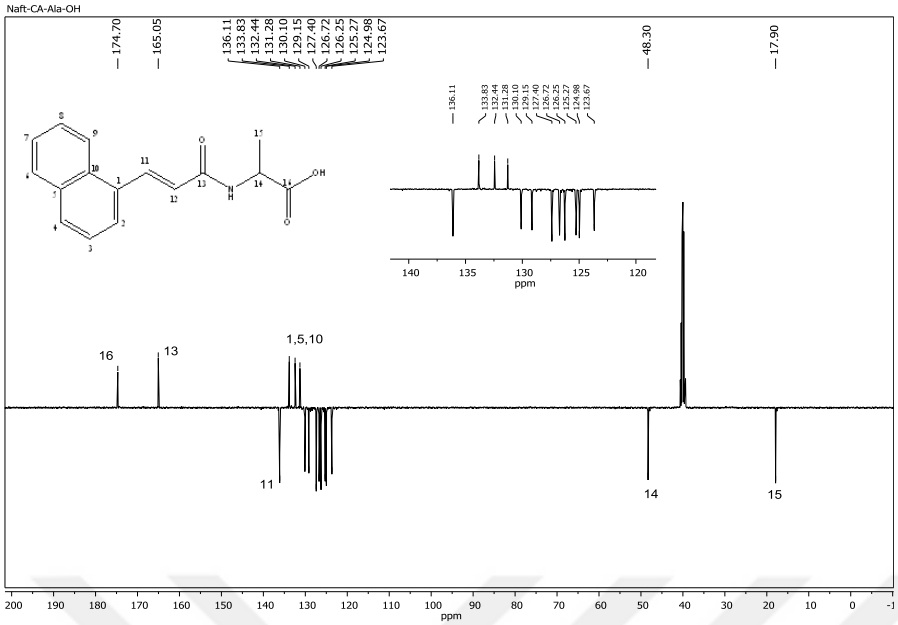

Appx. 1.87. ^{13}C APT NMR spectra of Naft-CA-Ala-OH

Appx. 1.88. ^{1}H NMR spectra of Naft-CA-Meth-OH

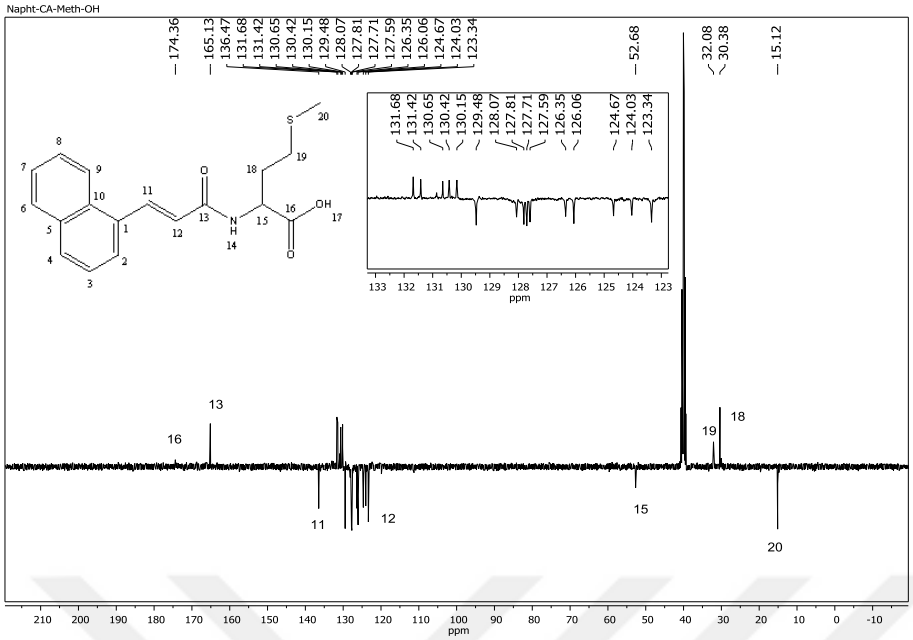

Appx. 1.89. ^{13}C APT NMR spectra of Naft-CA-Meth-OH

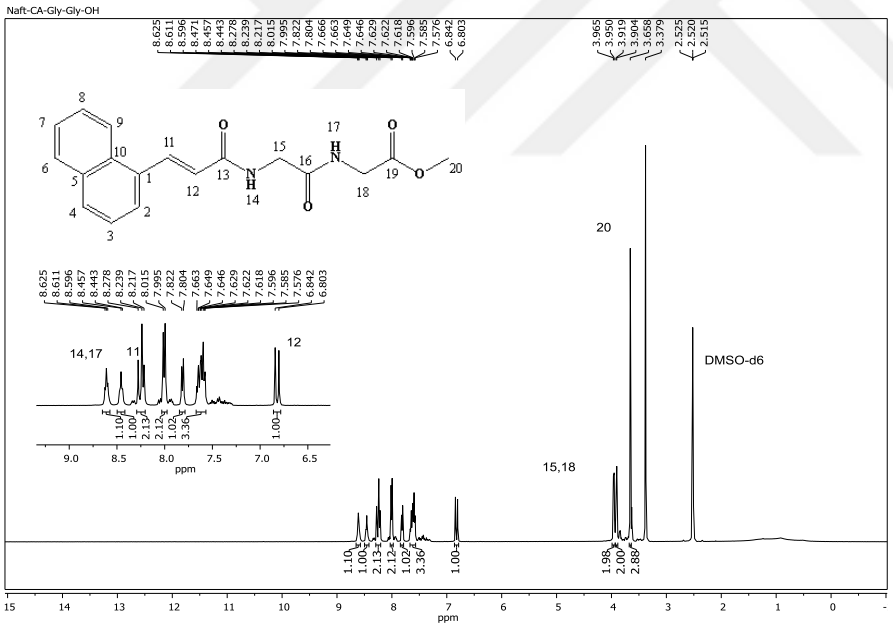

Appx. 1.90. ^{1}H NMR spectra of Naft-CA-Gly-Gly-OMe

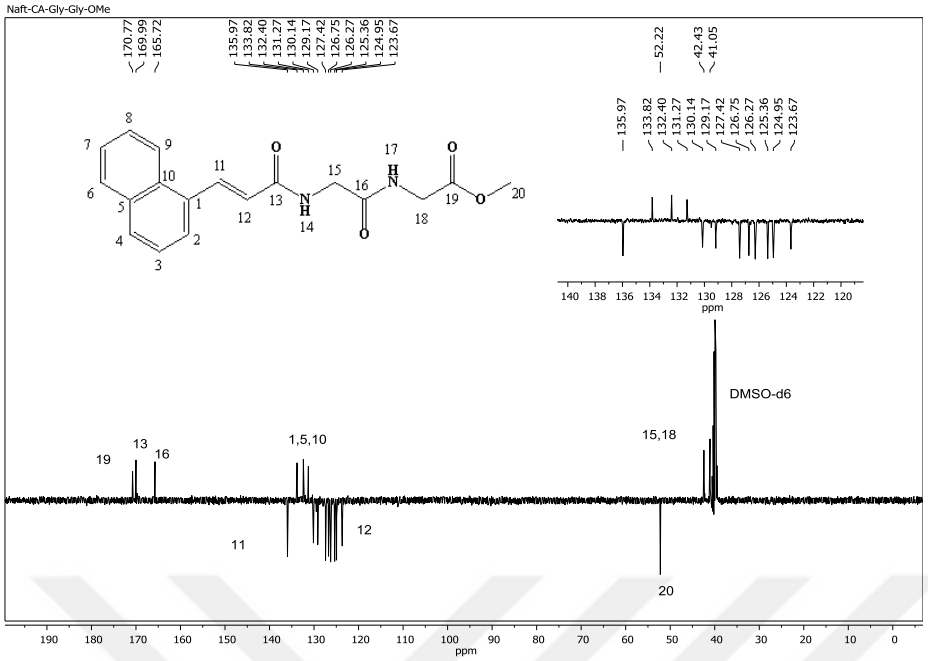

Appx. 1.91. ^{13}C APT NMR spectra of Naft-CA-Gly-Gly-OMe

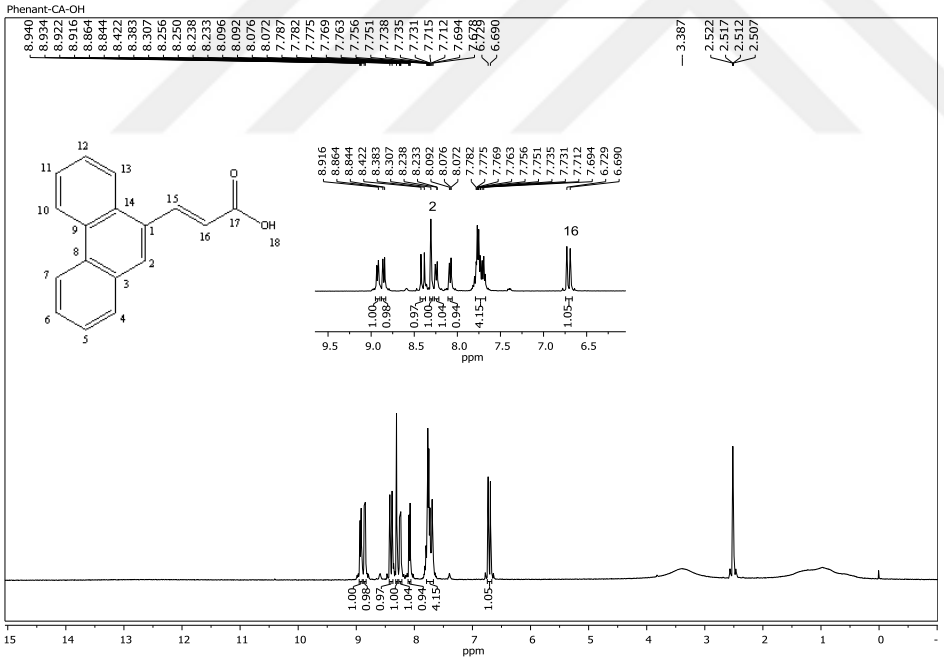

Appx. 1.92. ^{1}H NMR spectra of Phenant-CA-OH

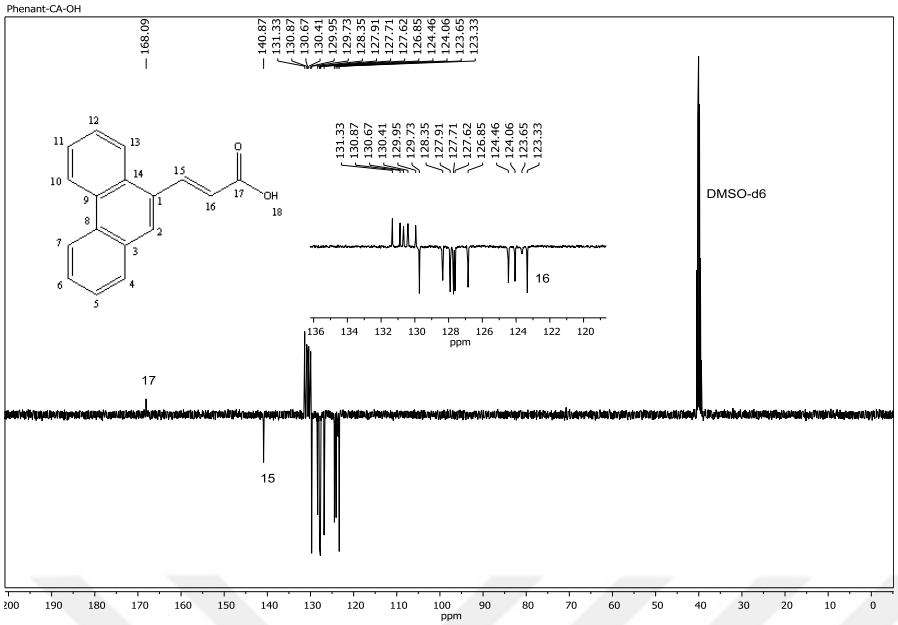

Appx. 1.93. ^{13}C APT NMR spectra of Phenant-CA-OH

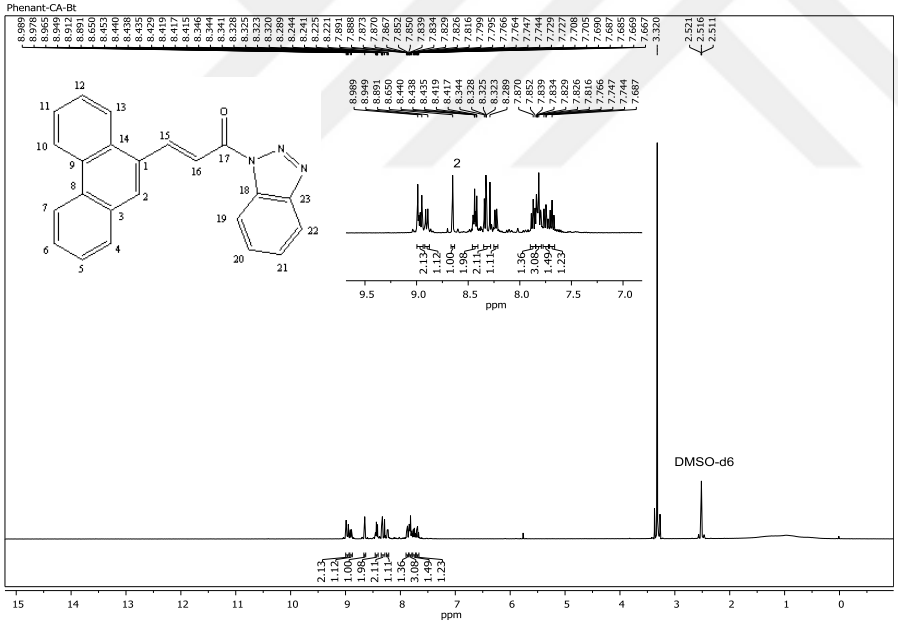

Appx. 1.94. ^{1}H NMR spectra of Phenant-CA-Bt

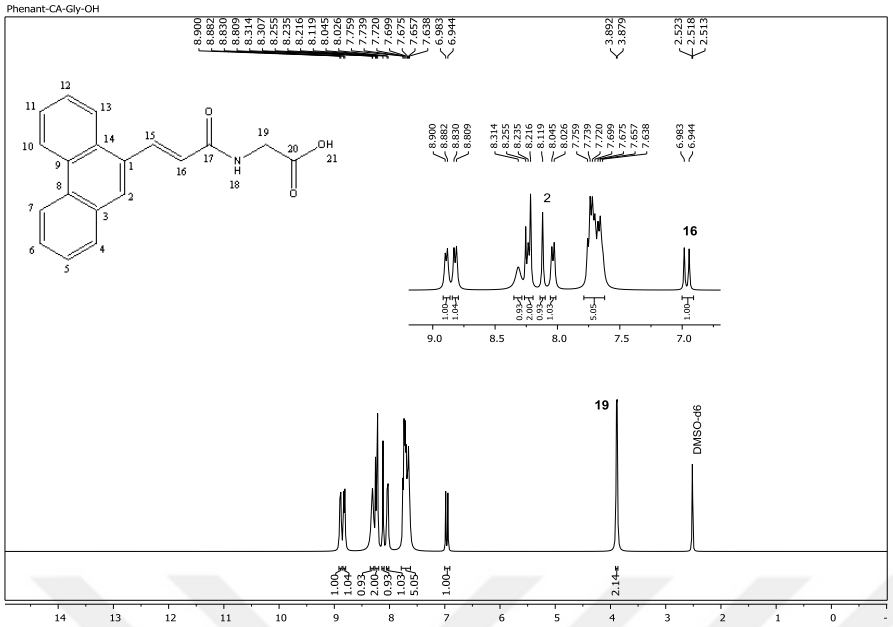

Appx. 1.95. ^{1}H NMR spectra of Phenant-CA-Gly-OH

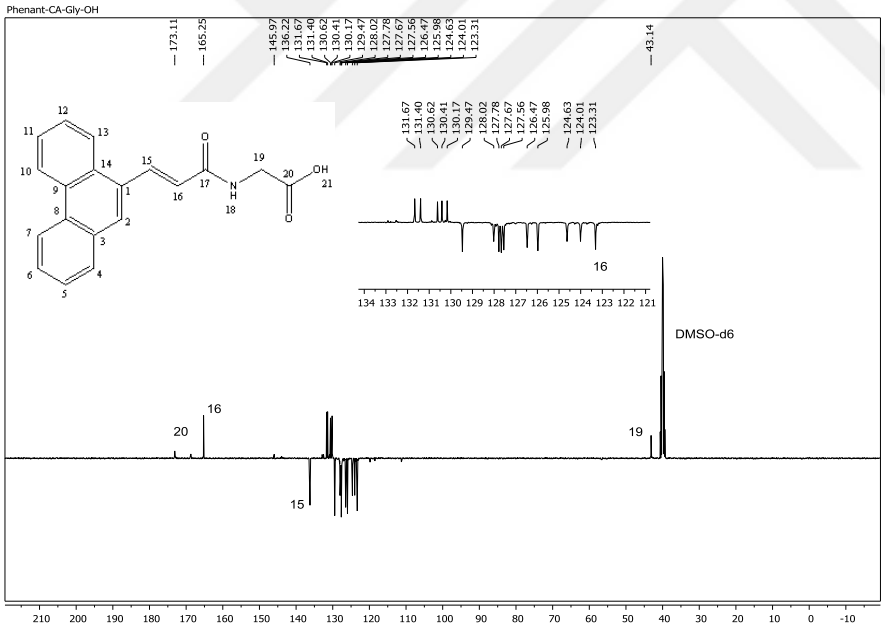

Appx. 1.96. ^{13}C APT NMR spectra of Phenant-CA-Gly-OH

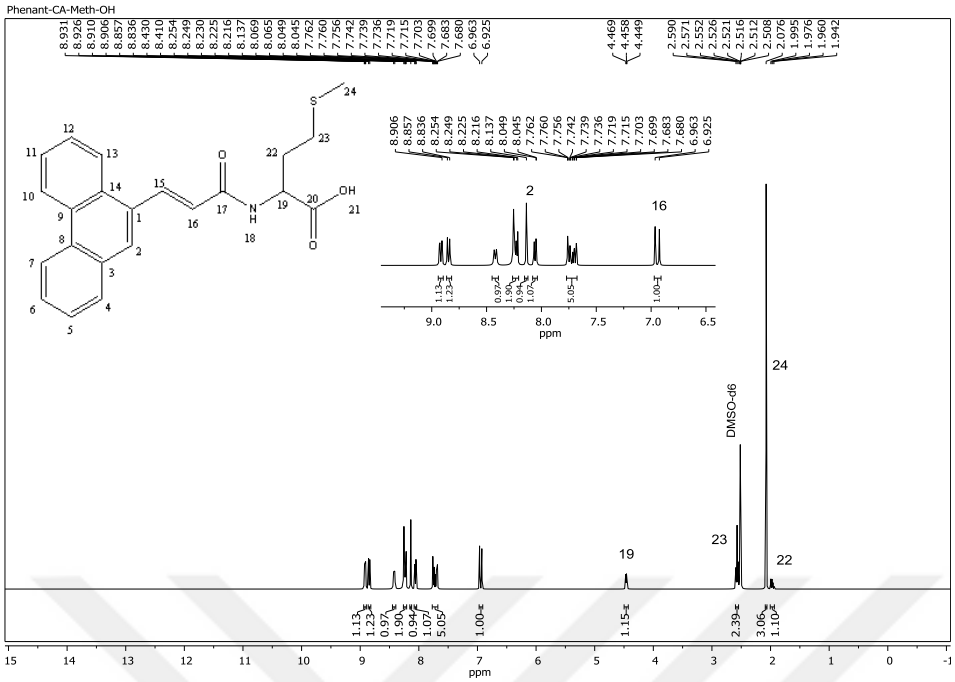

Appx. 1.97. ^{1}H NMR spectra of Phenant-CA-Meth-OH

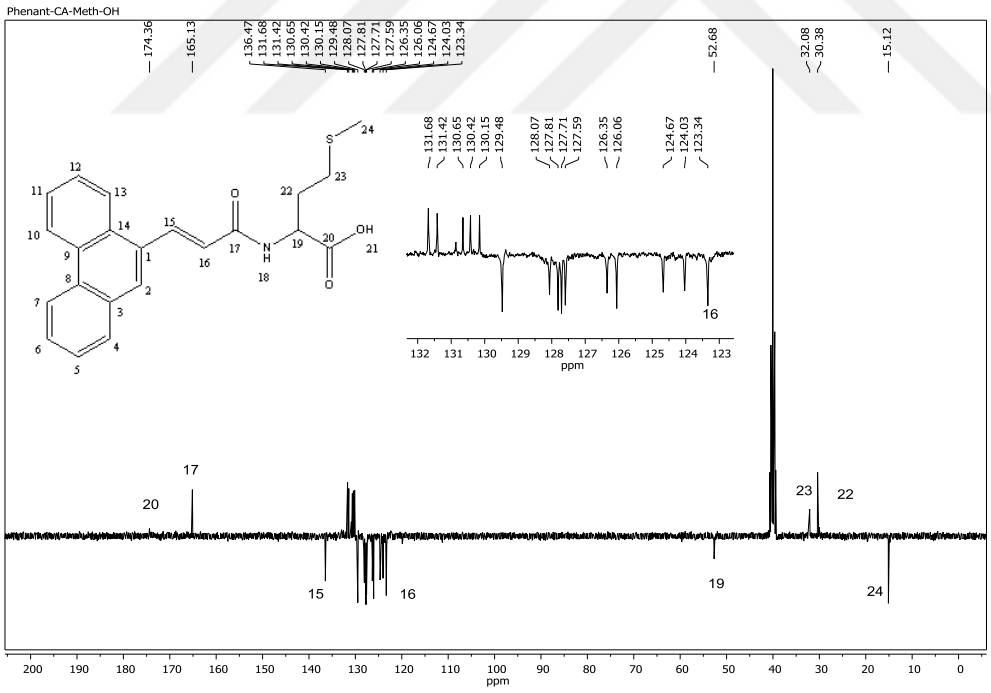

Appx. 1.98. ^{13}C APT NMR spectra of Phenant-CA-Meth-OH

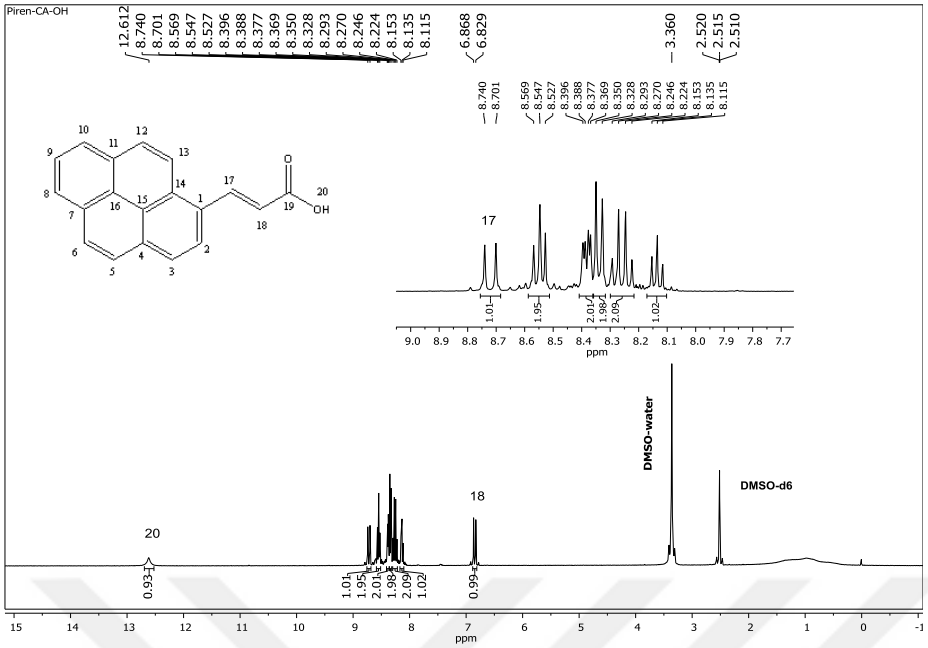

Appx. 1.99. ^{1}H NMR spectra of Pyrene-CA-OH

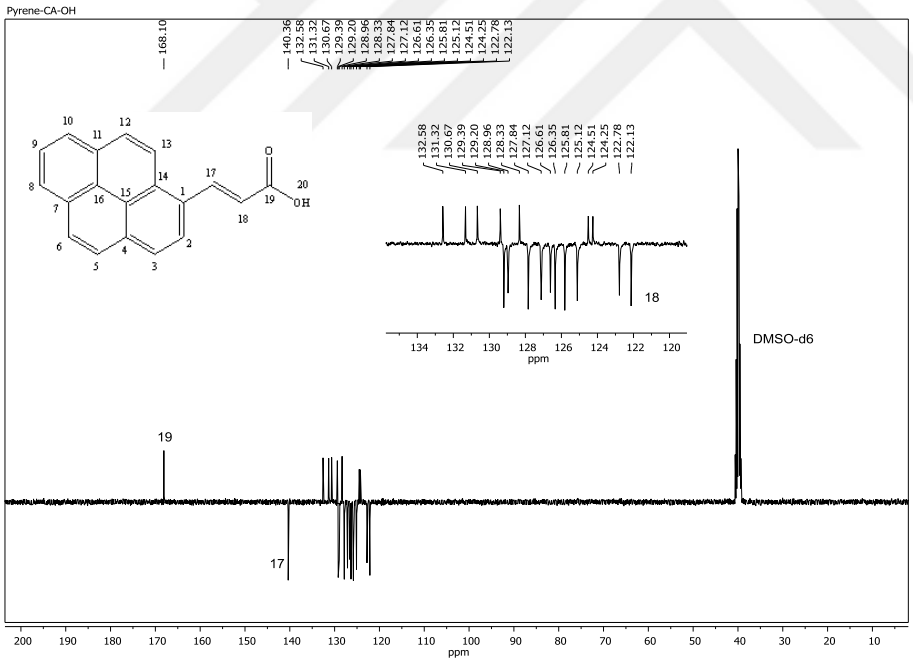

Appx. 1.100. ^{13}C APT NMR spectra of Pyrene-CA-OH

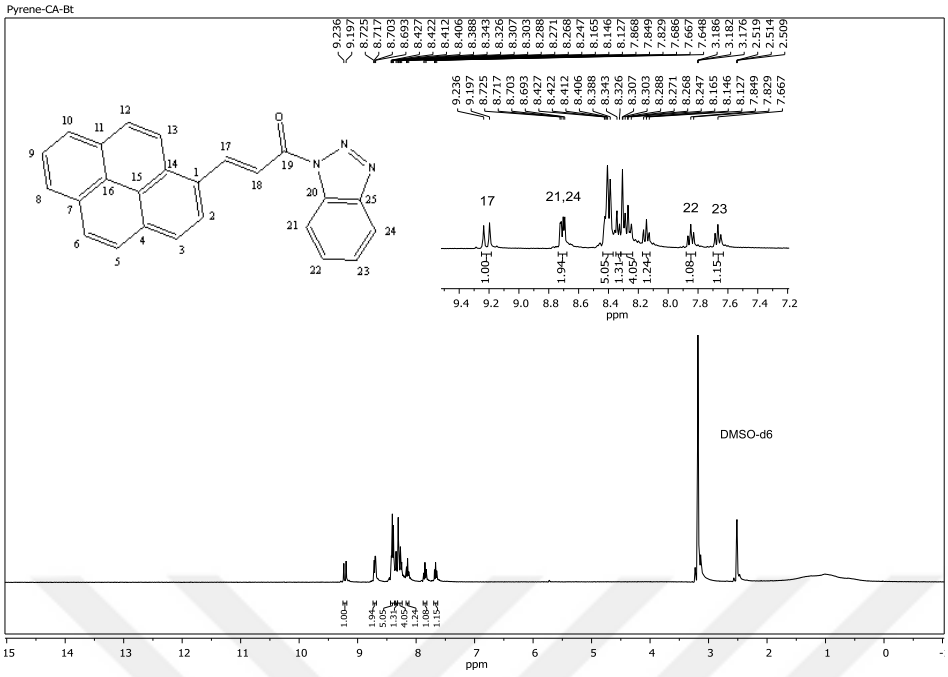

Appx. 1.101. ^{1}H NMR spectra of Pyrene-CA-Bt

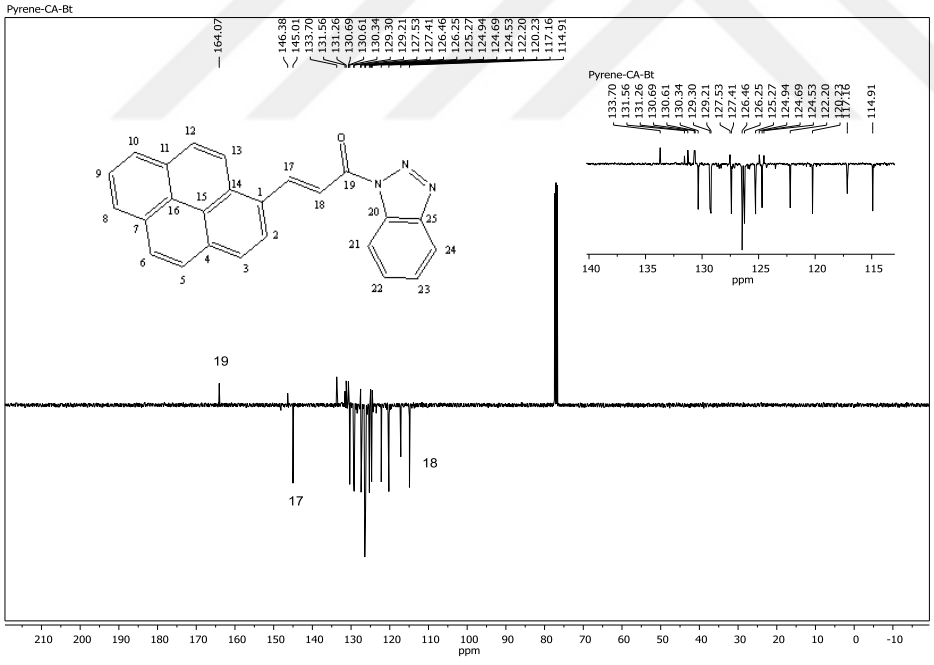

Appx. 1.102. ^{13}C APT NMR spectra of Pyrene-CA-Bt

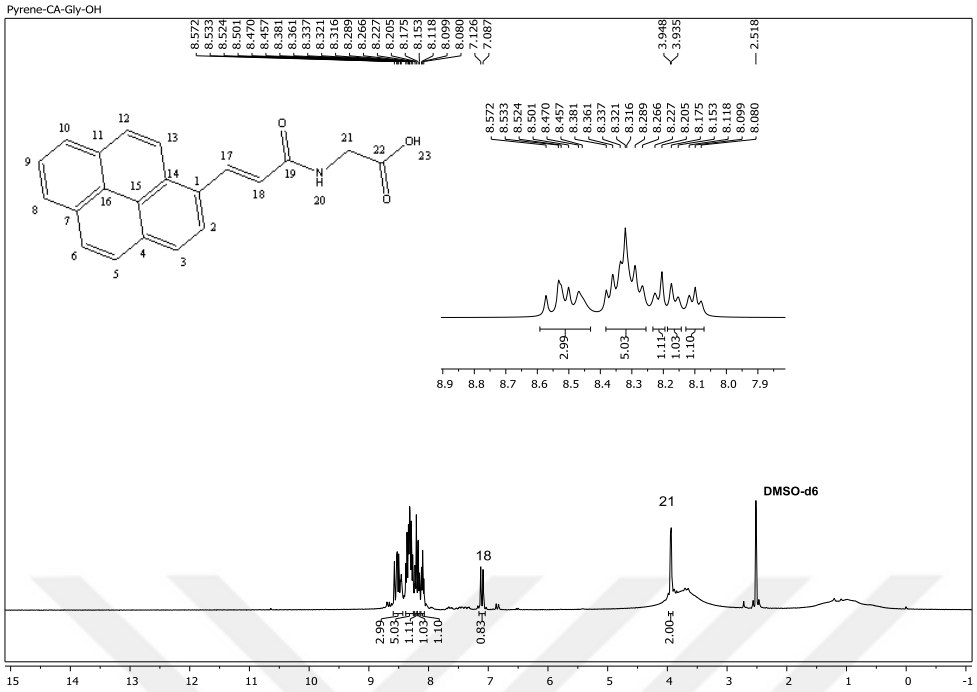

Appx. 1.103. ^{1}H NMR spectra of Pyrene-CA-Gly-OH

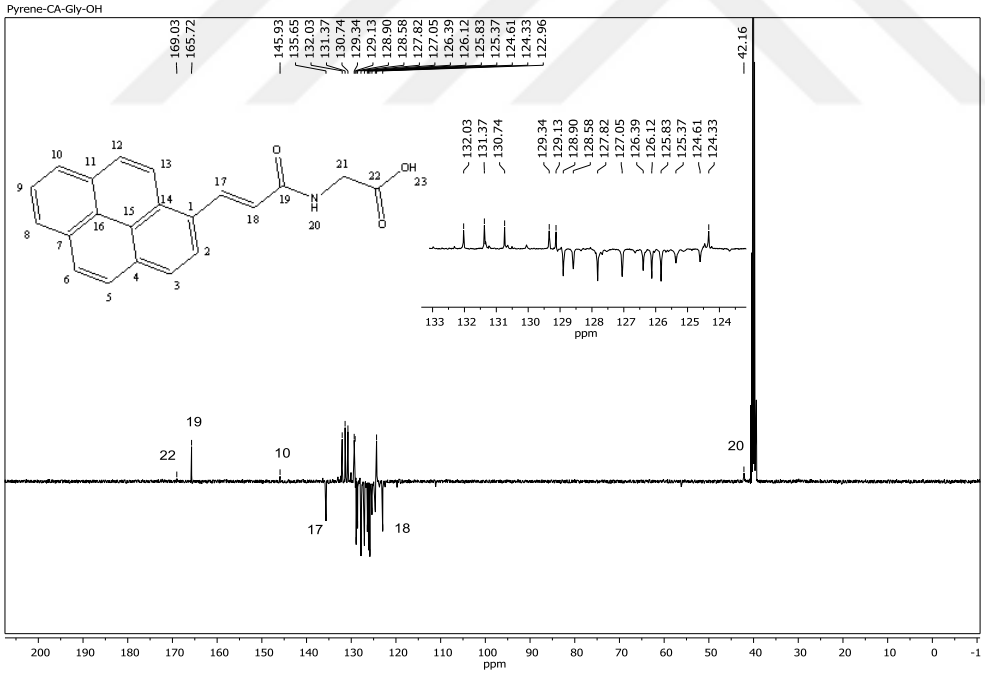

Appx. 1.104. ^{13}C APT NMR spectra of Pyrene-CA-Gly-OH

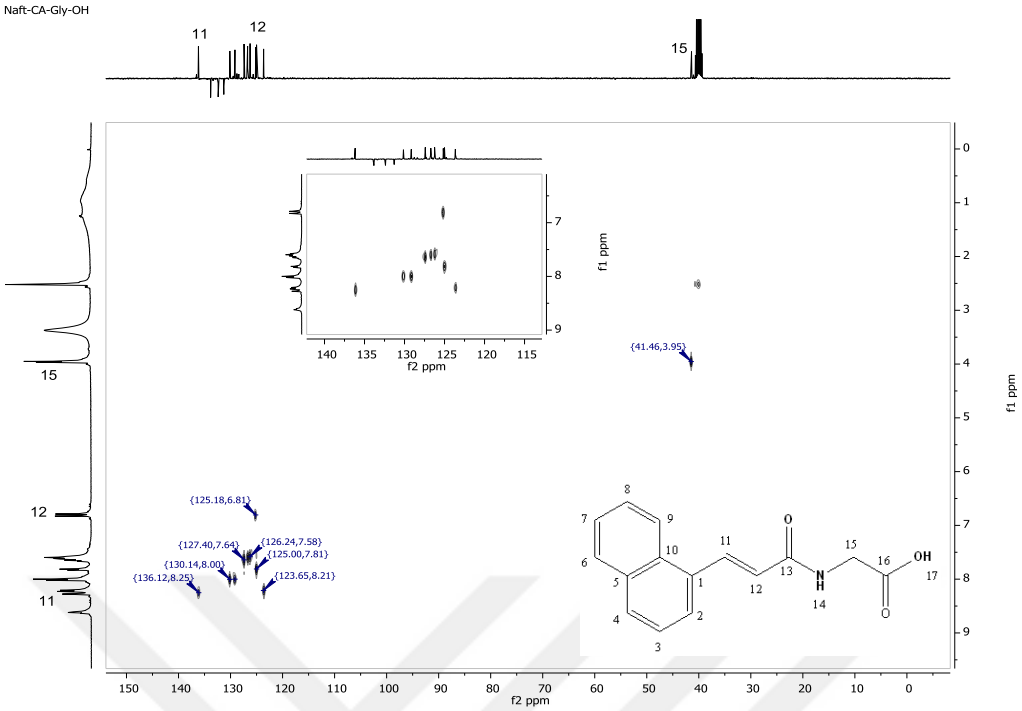

Appx. 1.105. COSY NMR spectrum of Naft-CA-Gly-OH

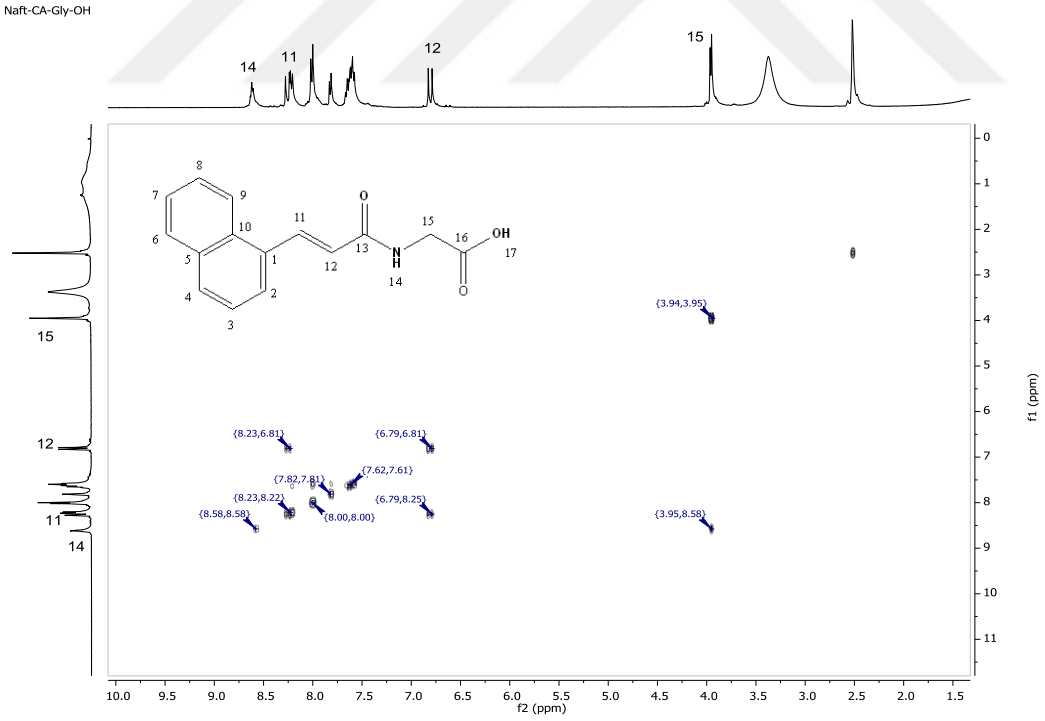

Appx. 1.106. HETCOR NMR spectrum of Naft-CA-Gly-OH

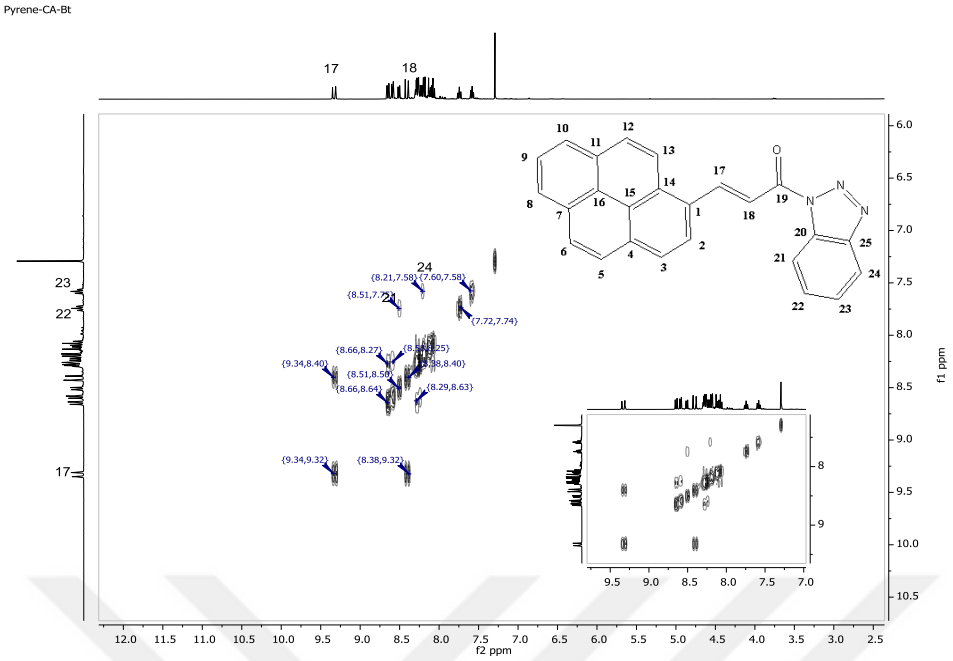

Appx. 1.107. COSY NMR spectrum of Pyrene-CA-Bt

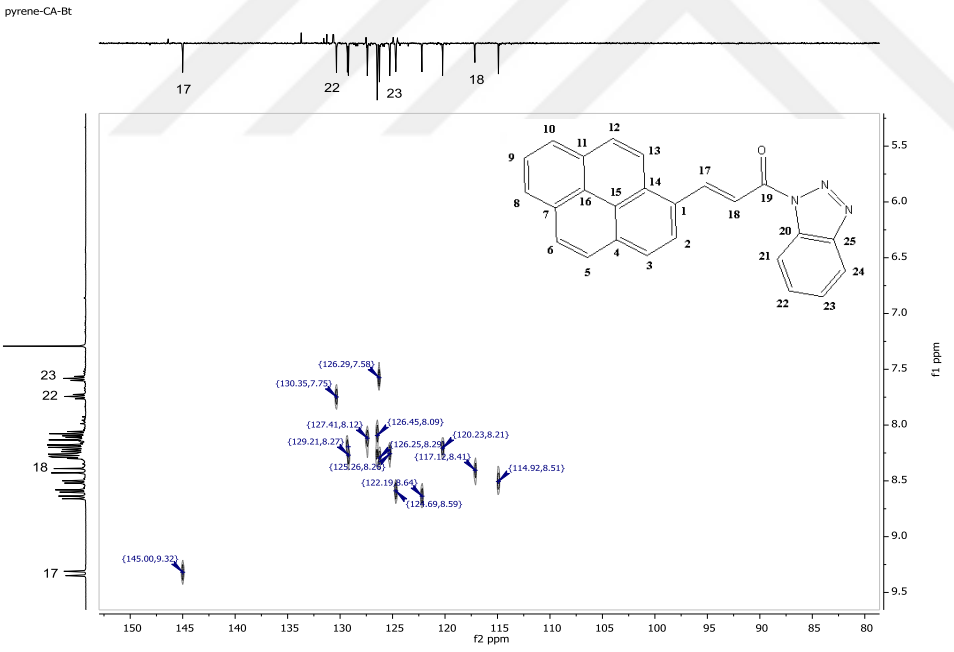

Appx. 1.108. HETCOR NMR spectrum of Pyrene-CA-Bt

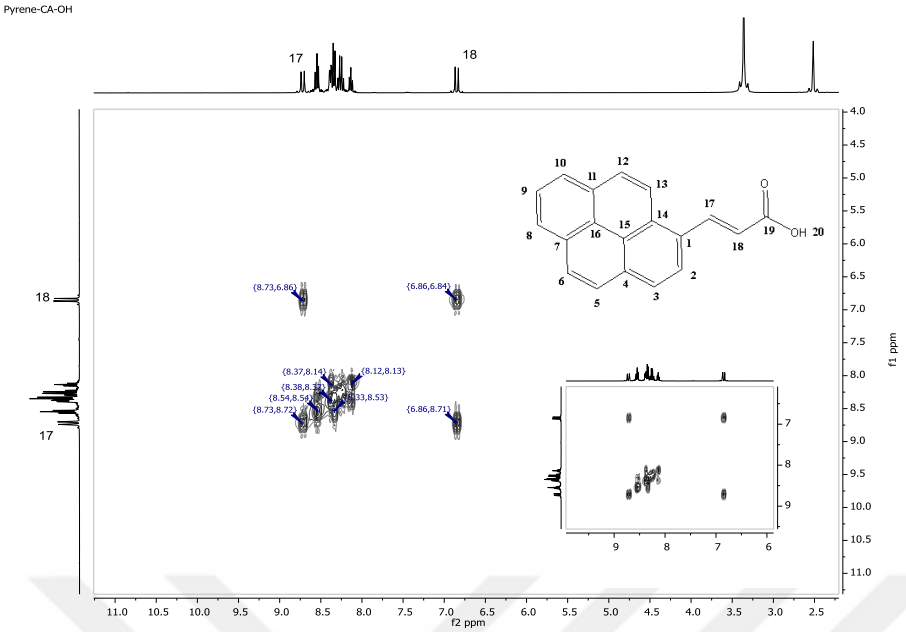

Appx. 1.109. COSY NMR spectrum of Pyrene-CA-OH

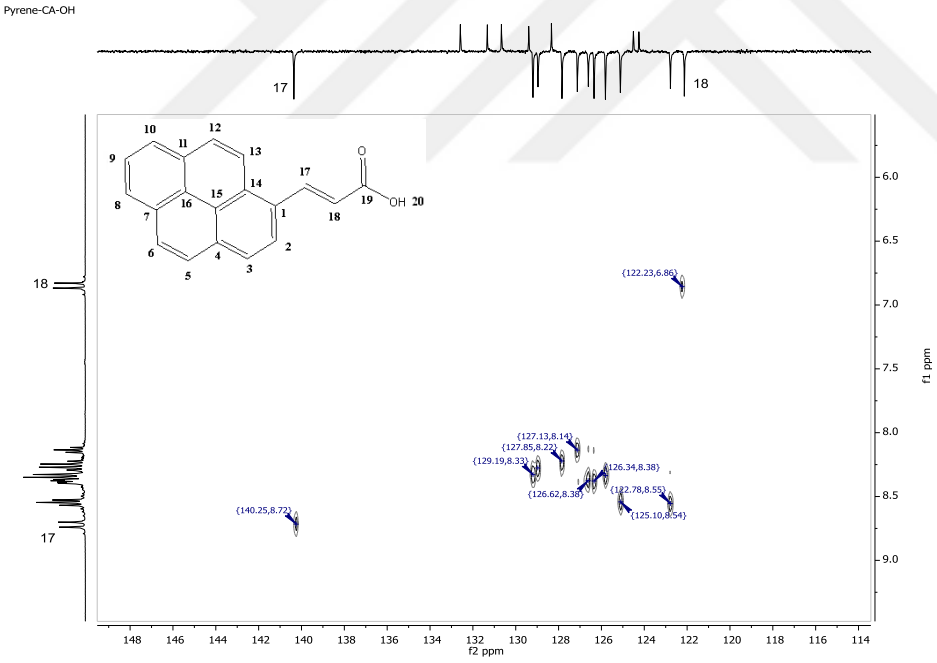

Appx. 1.110. HETCOR NMR spectrum of Pyrene-CA-OH

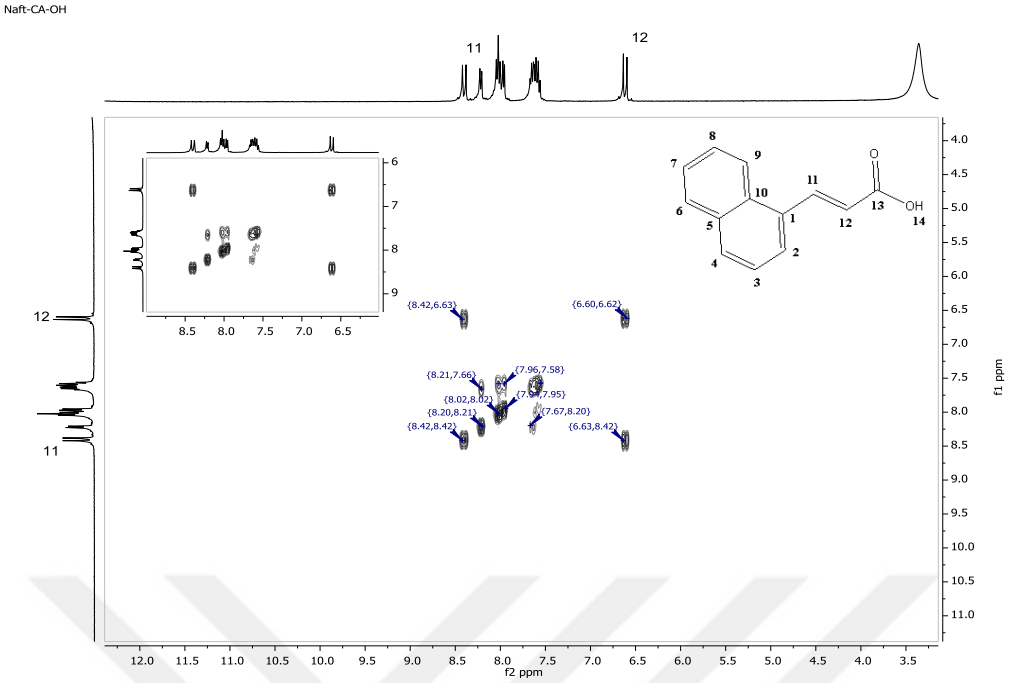

Appx. 1.112. COSY NMR spectrum of Naft-CA-OH

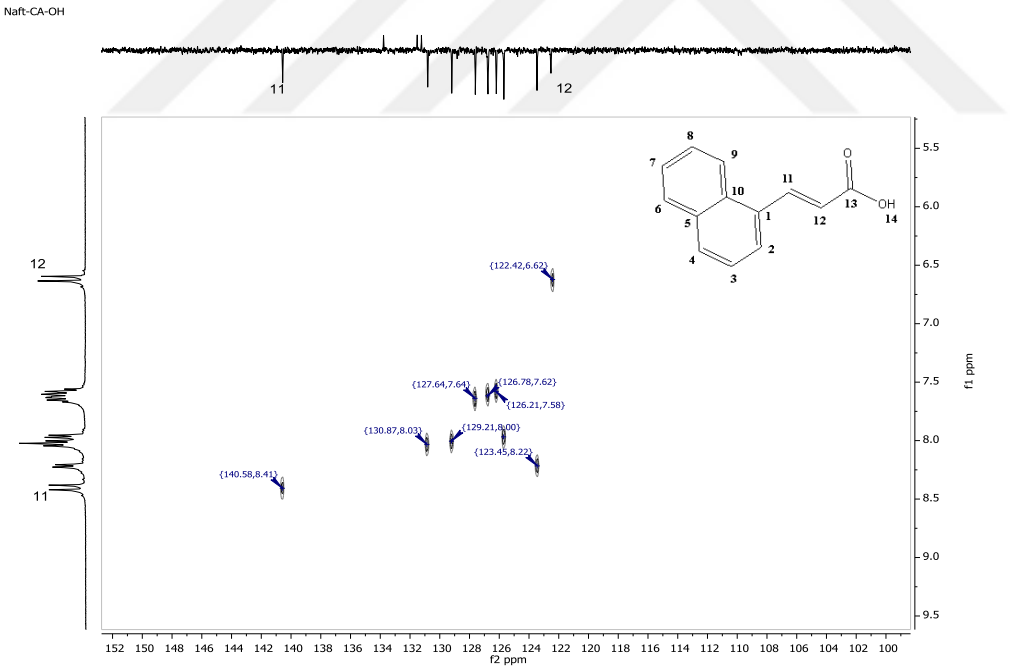

Appx. 1.113. HETCOR NMR spectrum of Naft-CA-OH

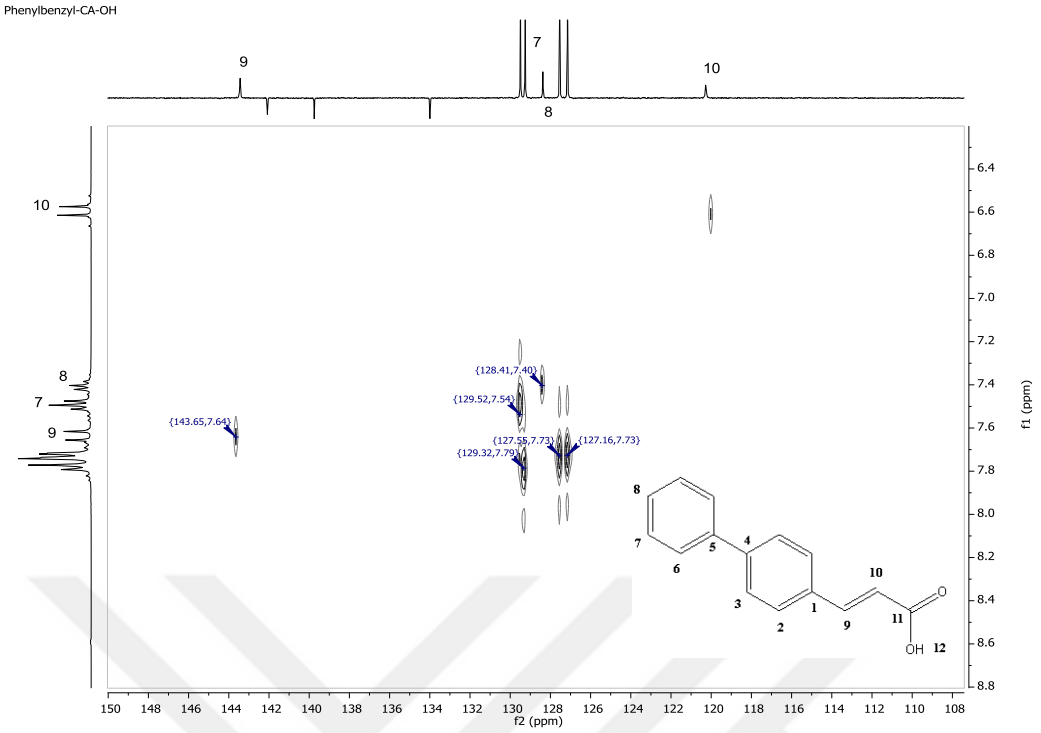

Appx. 1.114. HETCOR NMR spectrum of Phenyl benzyl-CA-OH

A.2. Dielectric measurements of amino acid conjugates

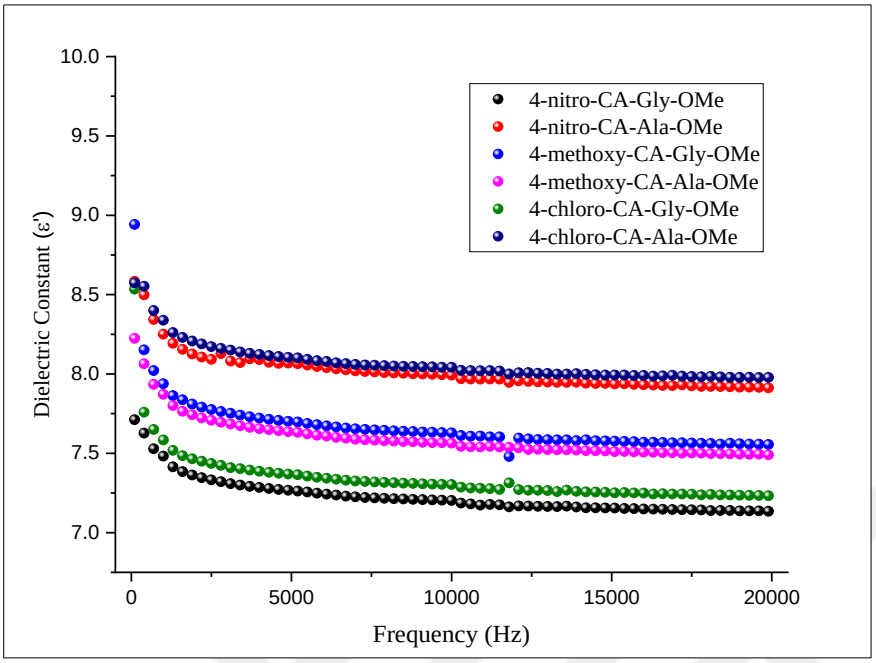

Appx. 2.1. Dielectric constant graph of para substituted conjugates

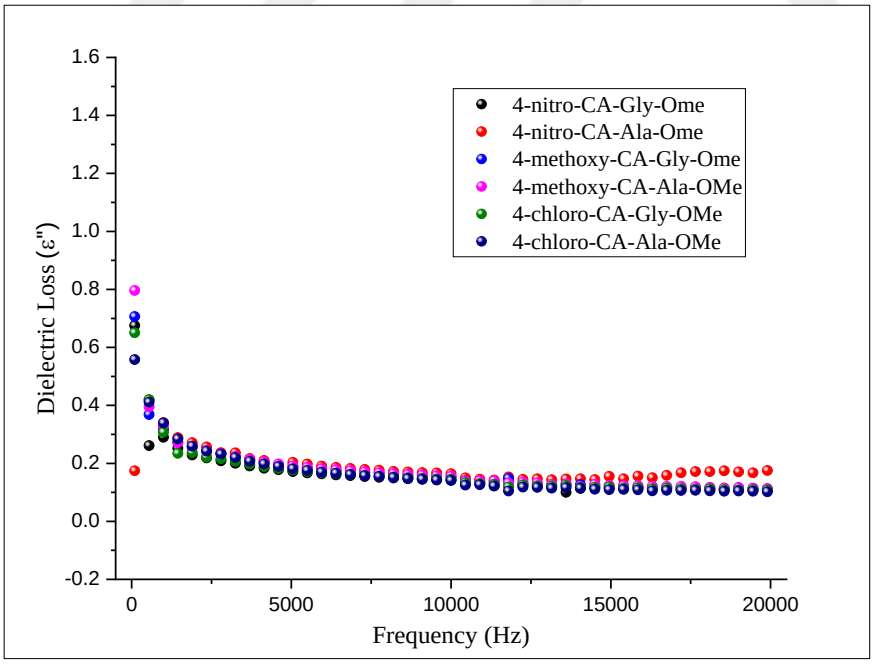

Appx. 2.2. Dielectric loss graph of para substituted conjugates

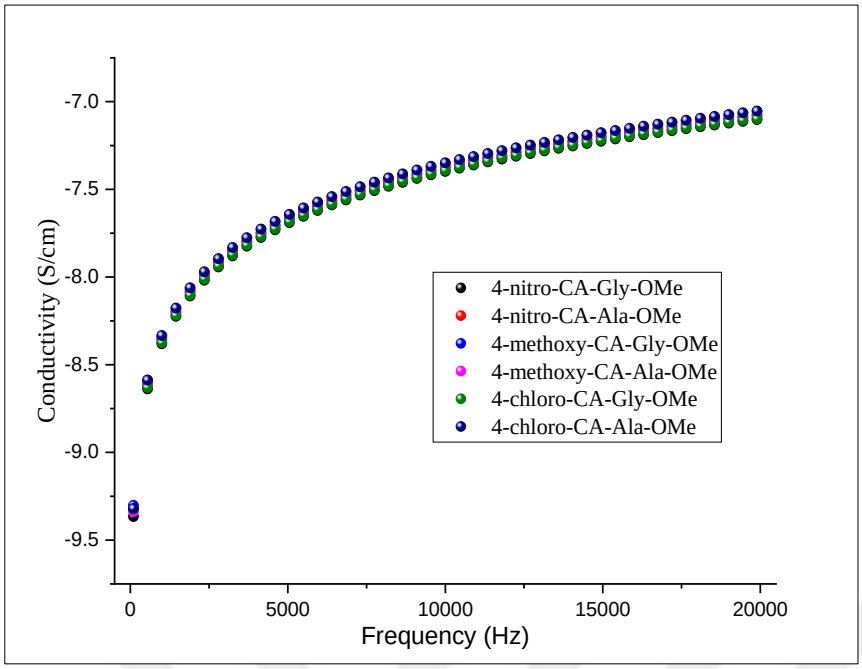

Appx. 2.3. Dielectric loss graph of para substituted conjugates

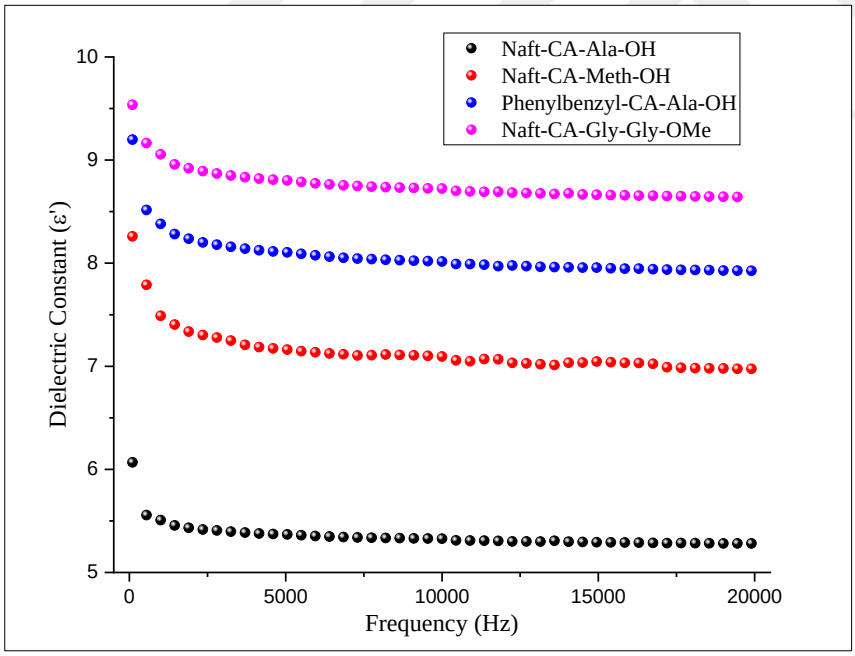

Appx. 2..4. Dielectric constant graph of aromatic ring containing conjugates

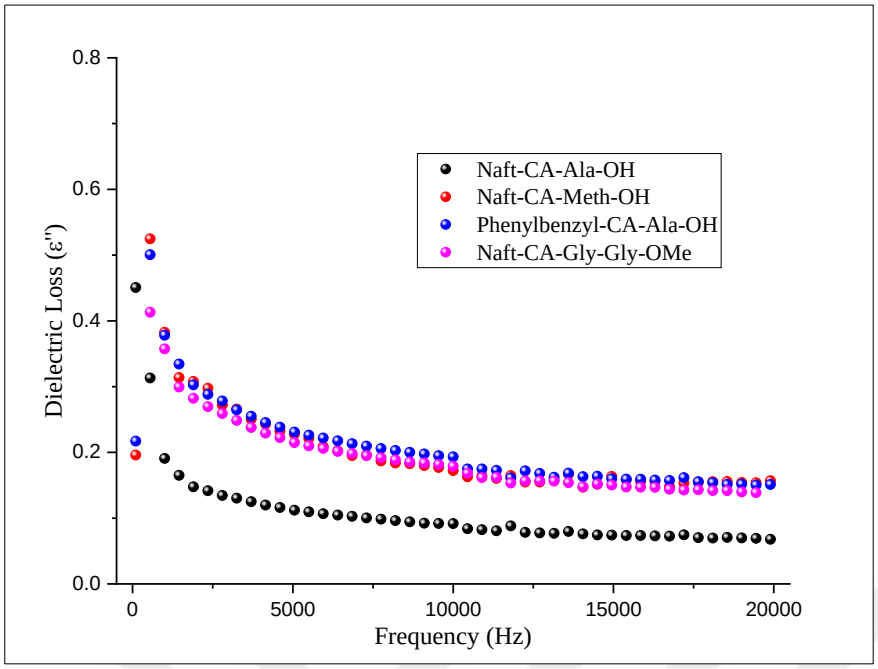

Appx. 2.5. Dielectric loss graph of aromatic ring containing conjugates

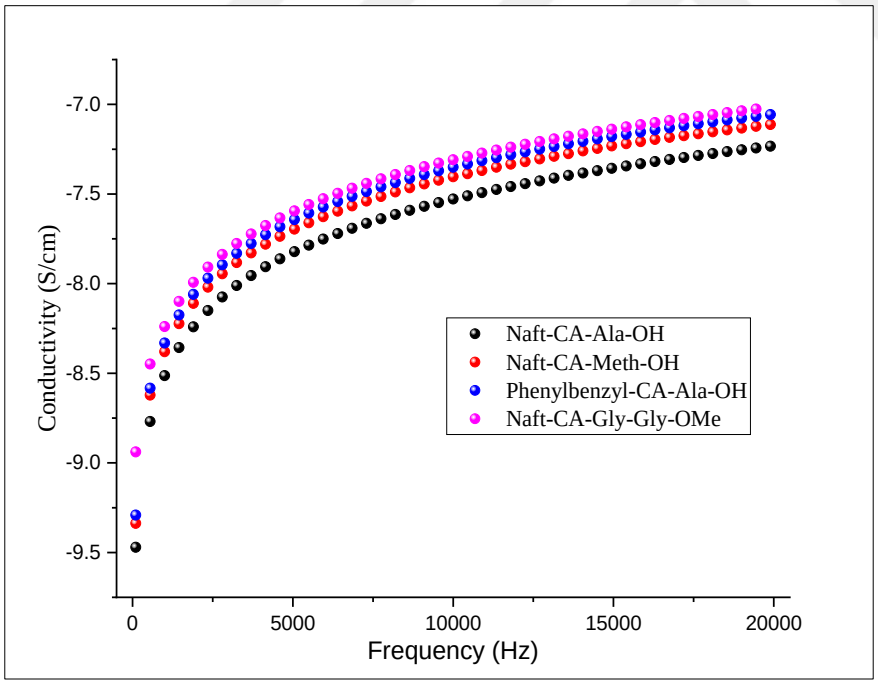

Appx. 2.6. Dielectric loss graph of aromatic ring containing conjugates

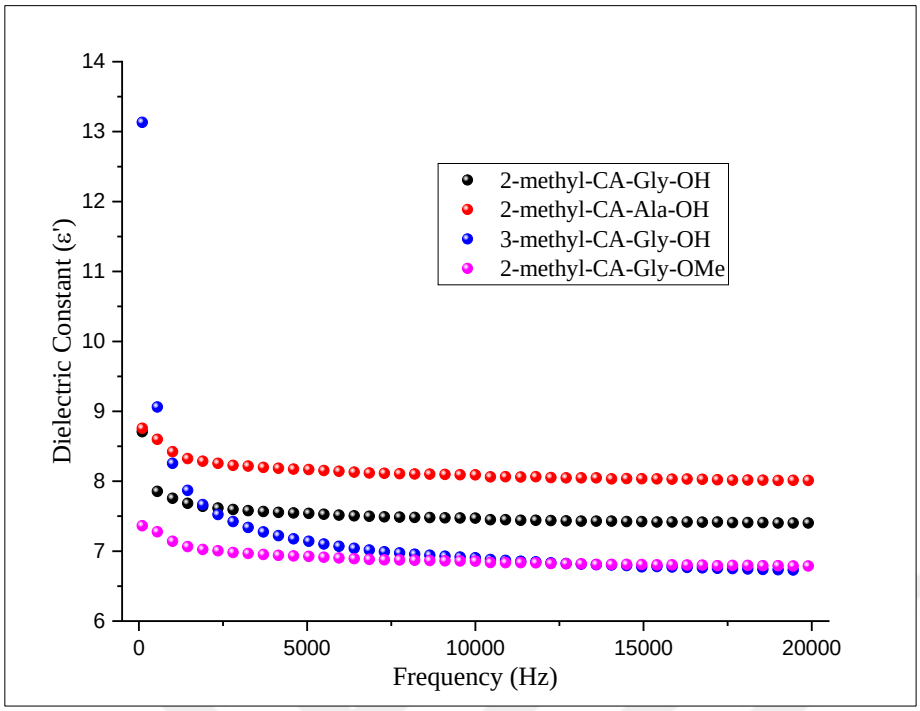

Appx. 2.7. Dielectric constant graph of methyl substituted conjugates

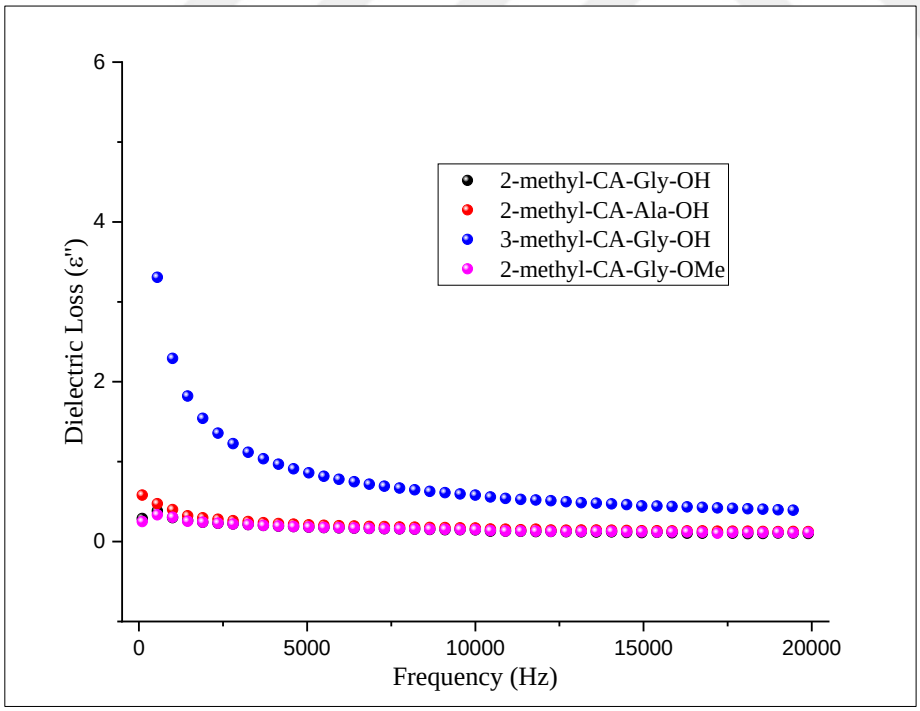

Appx. 2.8. Dielectric loss graph of methyl substituted conjugates

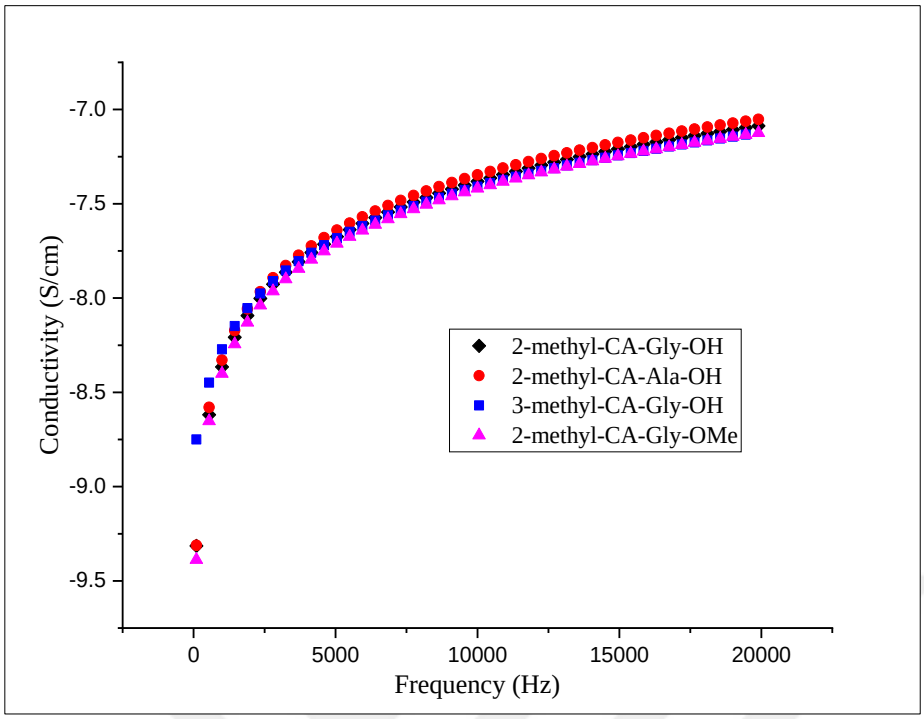

Appx. 2.9. Dielectric loss graph of methyl substituted conjugates

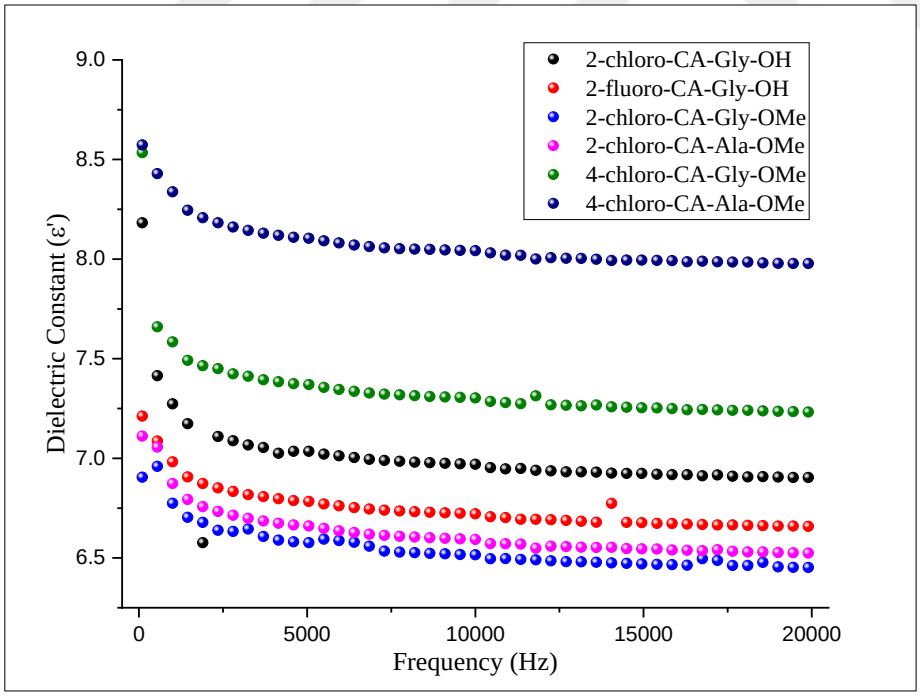

Appx. 2.10. Dielectric constant graph of halogen substituted conjugates

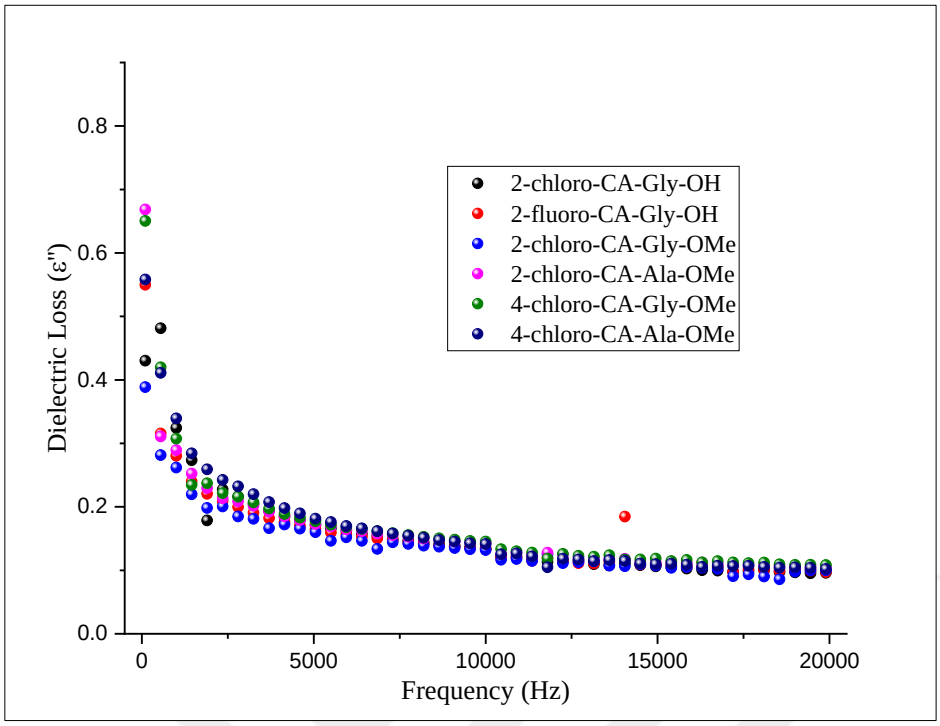

Appx. 2.11. Dielectric loss graph of halogen substituted conjugates

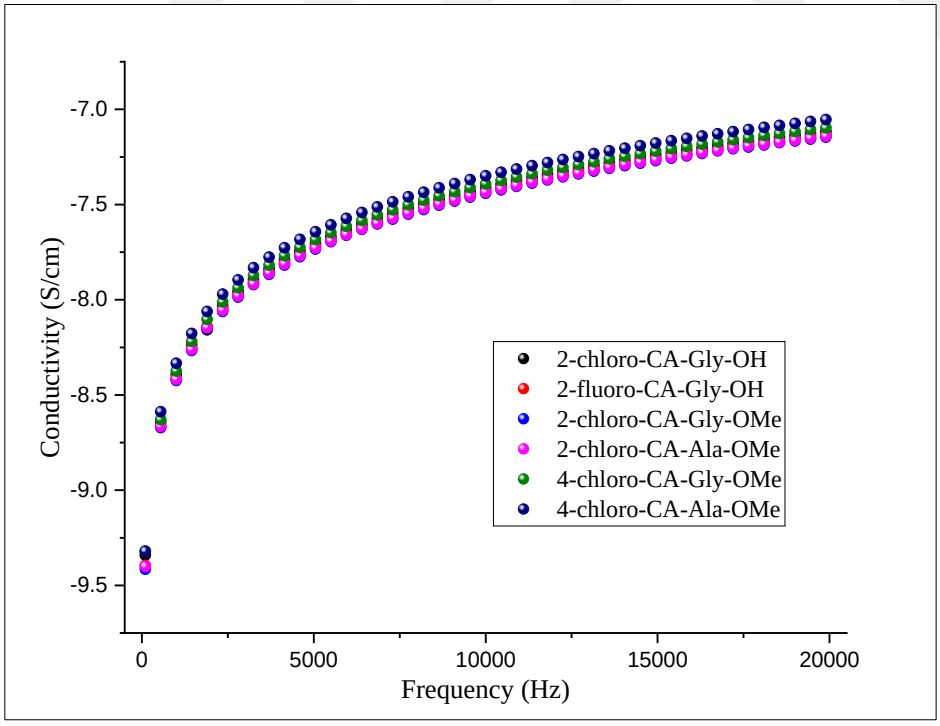

Appx. 2.12. Conductivity graph of halogen substituted conjugates

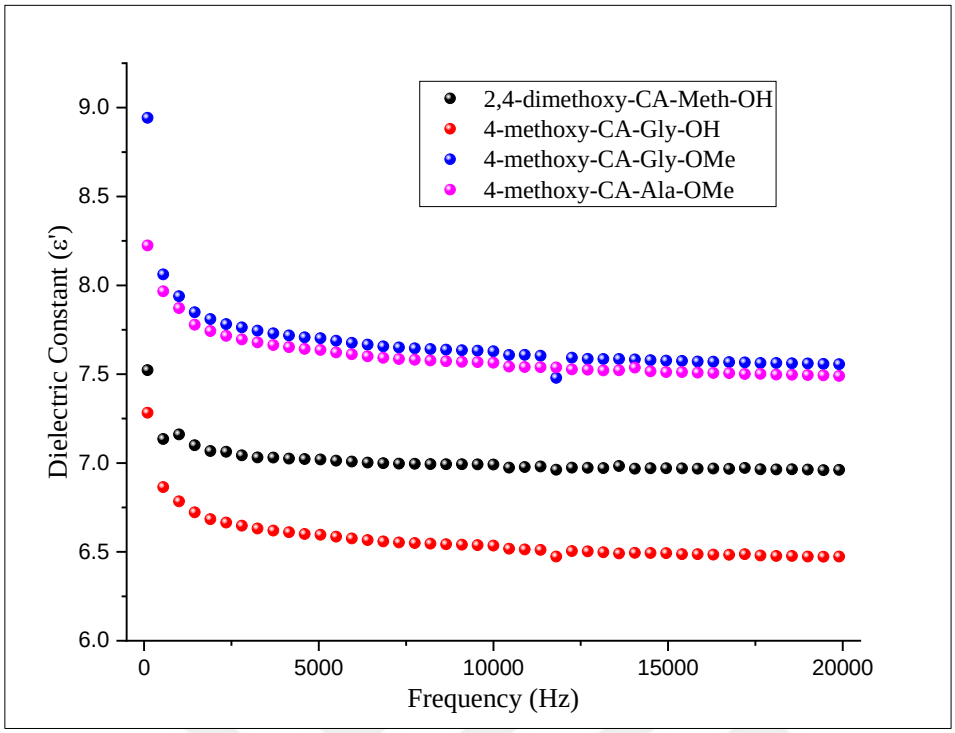

Appx. 2.13. Dielectric constant graph of methoxy substituted conjugates

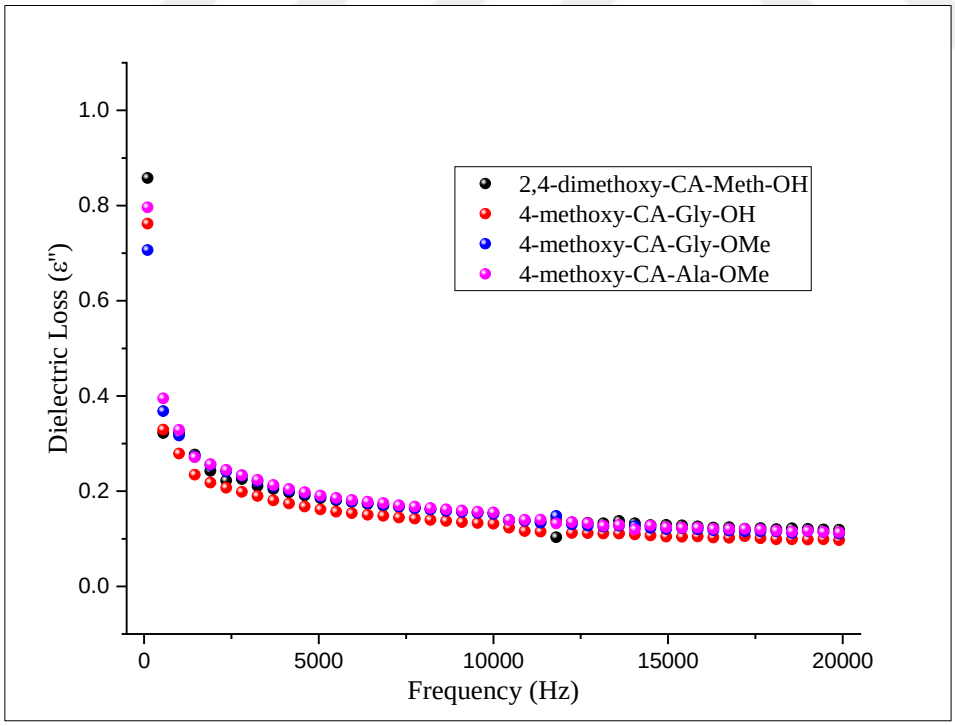

Appx. 2.14. Dielectric loss graph of methoxy substituted conjugates

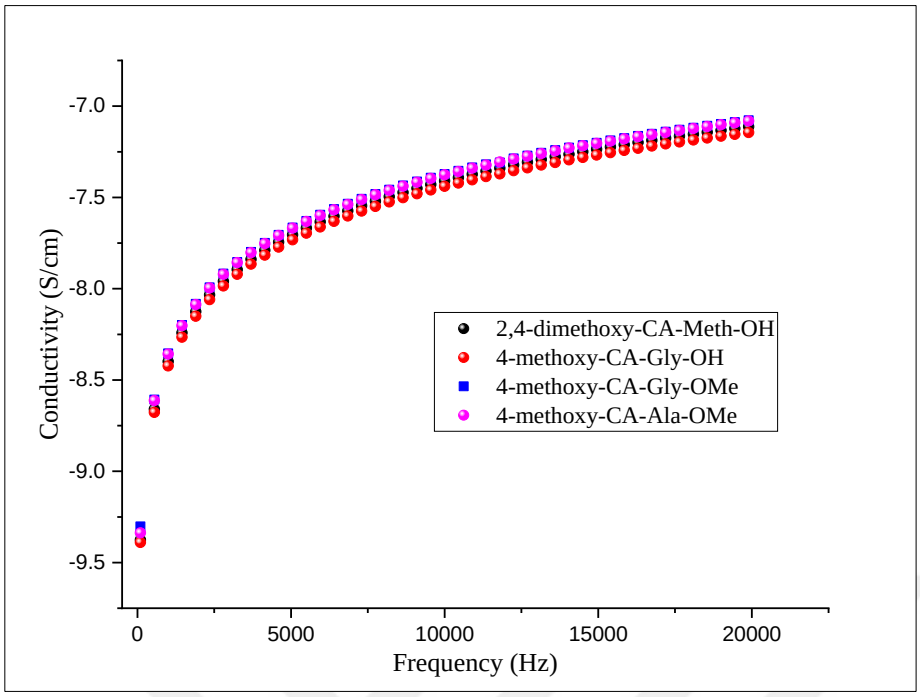

Appx. 2.15. Conductivity graph of methoxy substituted conjugates

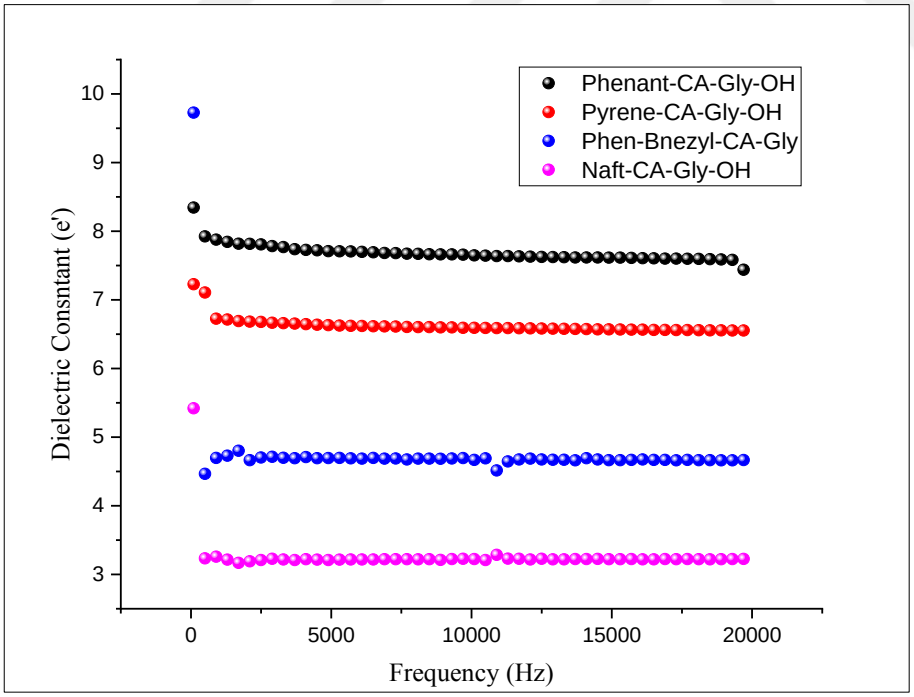

Appx. 2.16. Dielectric constant graph of aromatic ring substituted conjugates

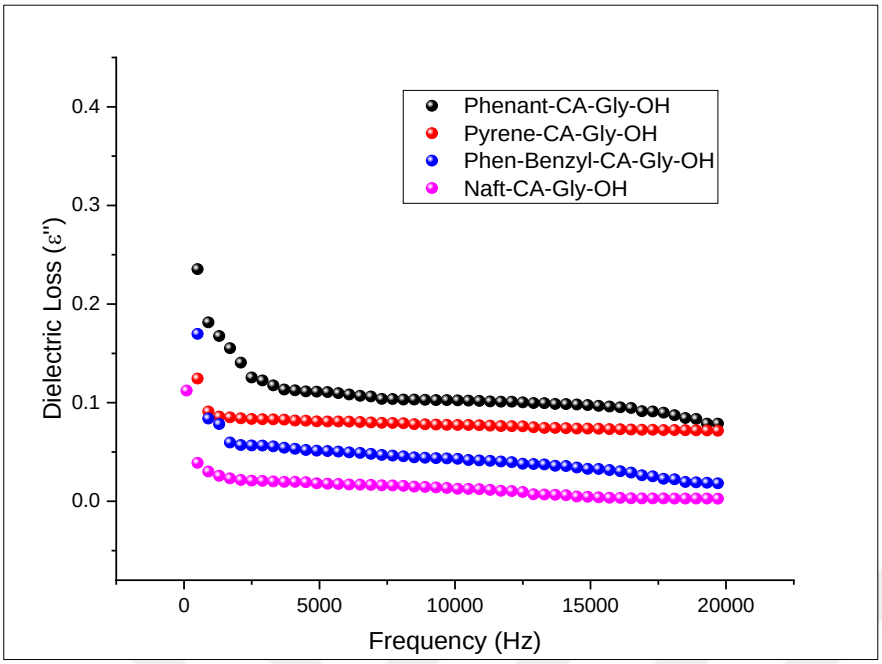

Appx. 2.17. Dielectric loss graph of aromatic ring substituted conjugates

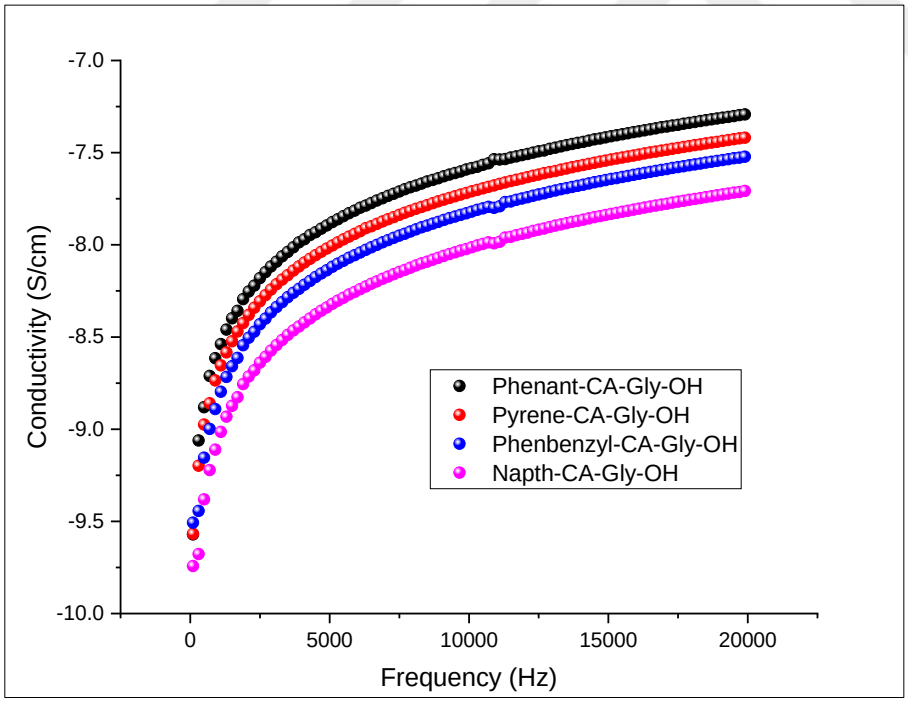

Appx. 2.18. Conductivity graph of aromatic ring substituted conjugates

A.3. FT-IR Spectrum of amino acid conjugates

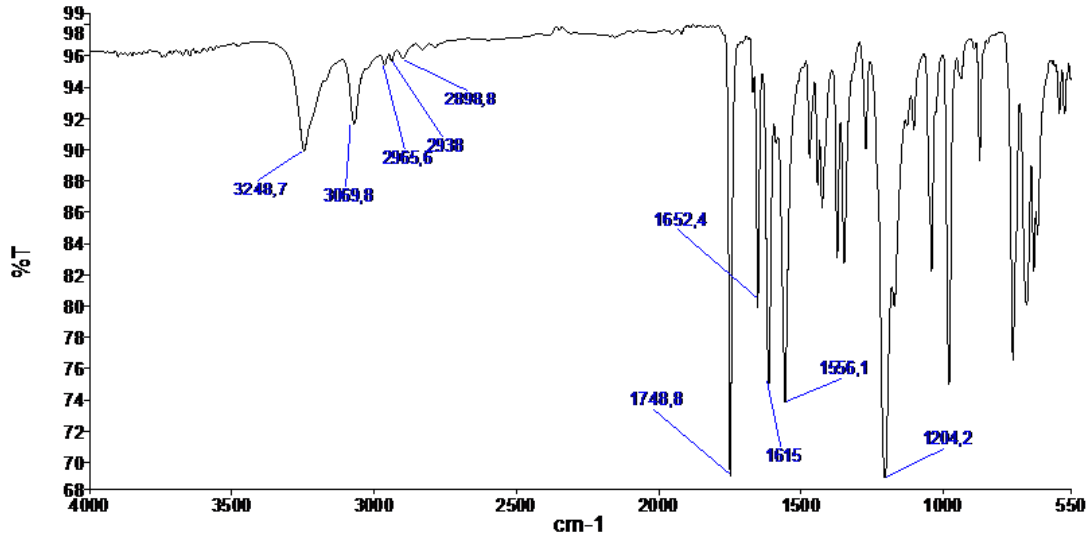

Appx. 3.1. FT-IR Spectra of 2-chloro-CA-Gly-OMe

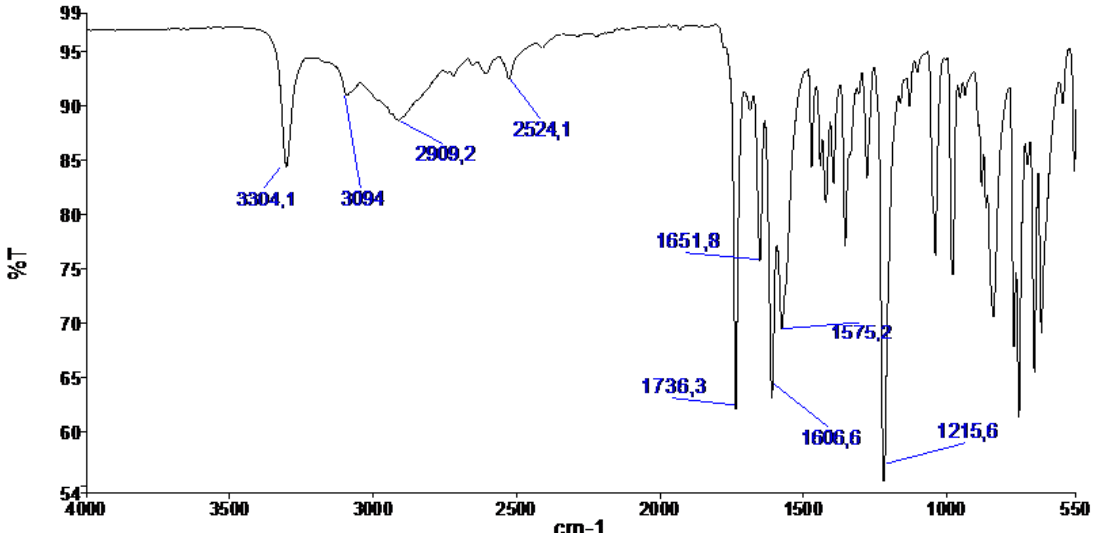

Appx. 3.2. FT-IR Spectra of 2-chloro-CA-Gly-OH

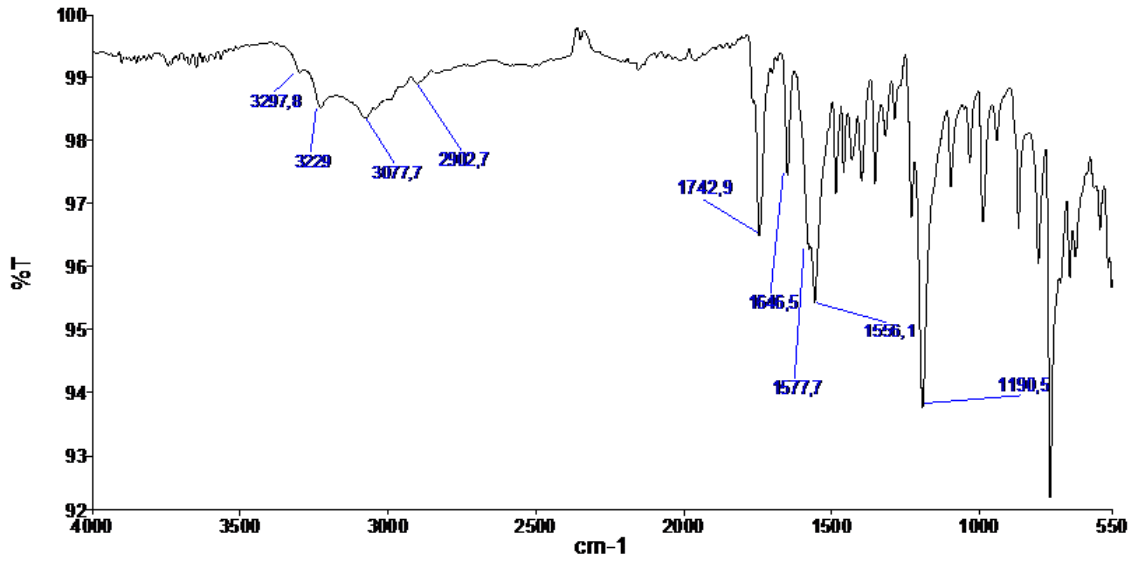

Appx. 3.3. FT-IR Spectra of 2-fluoro-CA-Gly-OH

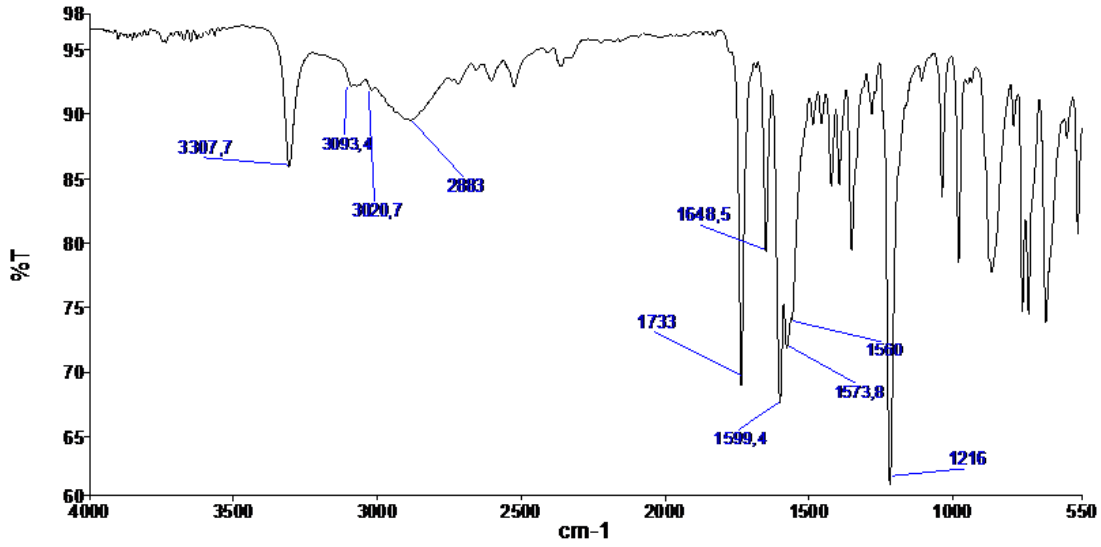

Appx. 3.4. FT-IR Spectra of Pyrene-CA-Gly-OH

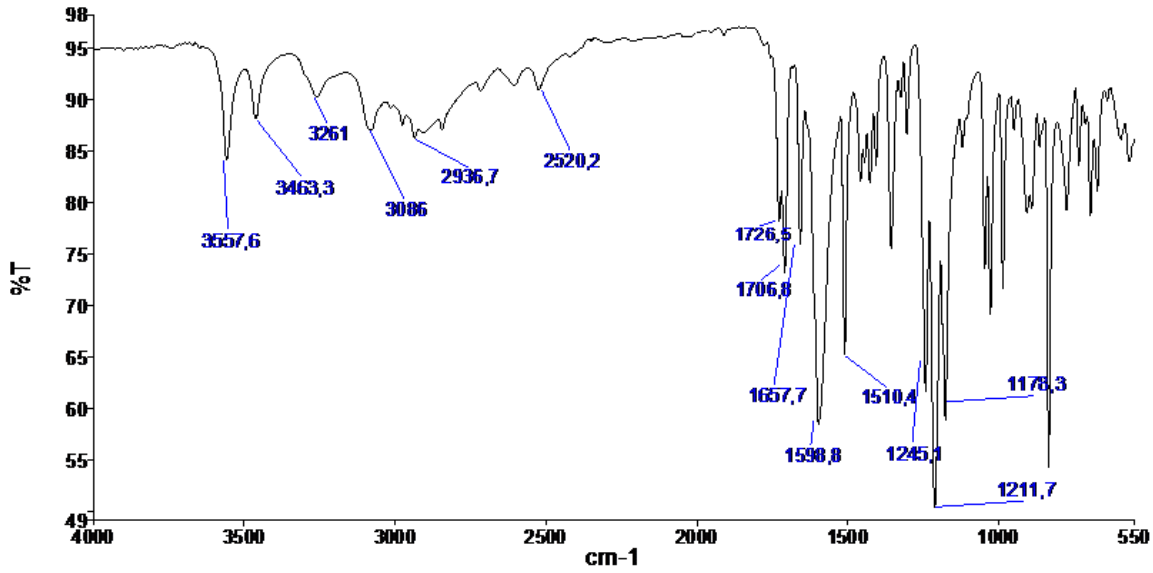

Appx. 3.5. FT-IR Spectra of 4-methoxy-CA-Gly-O

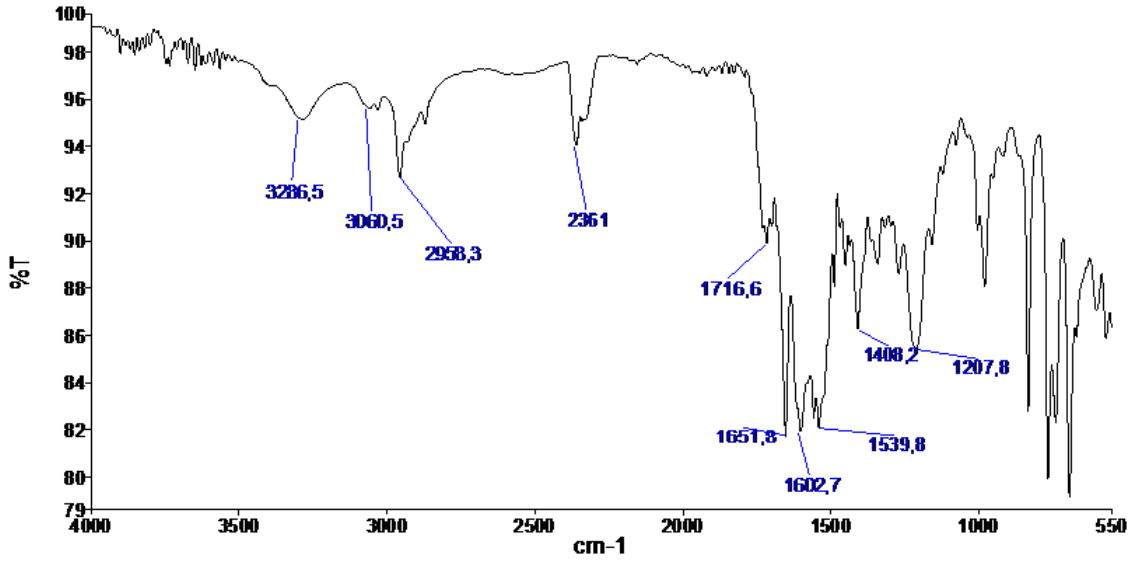

Appx. 3.6. FT-IR Spectra of Phenylbenzyl-CA-Leu-OH

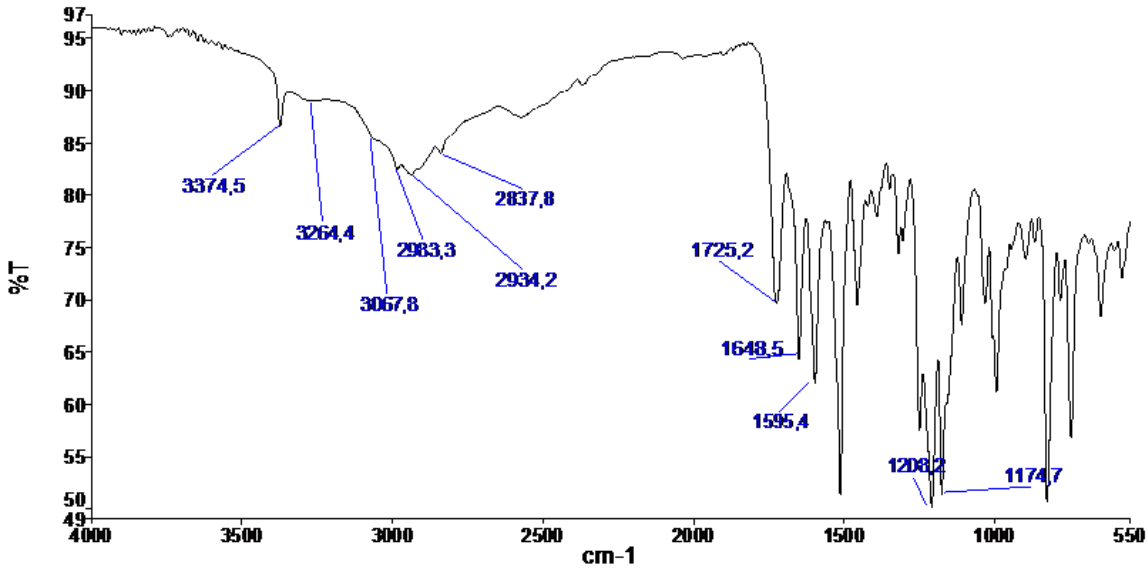

Appx. 3.7. FT-IR Spectra of 4-methoxy-CA-Ala-OH

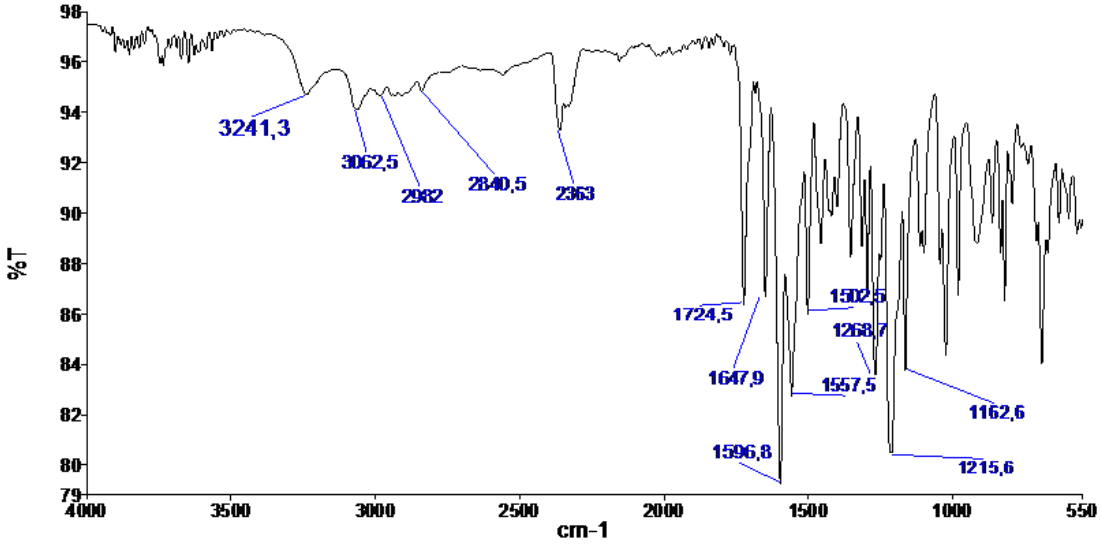

Appx. 3.8. FT-IR Spectra of 2,4-dimethoxy-CA-Gly-OH

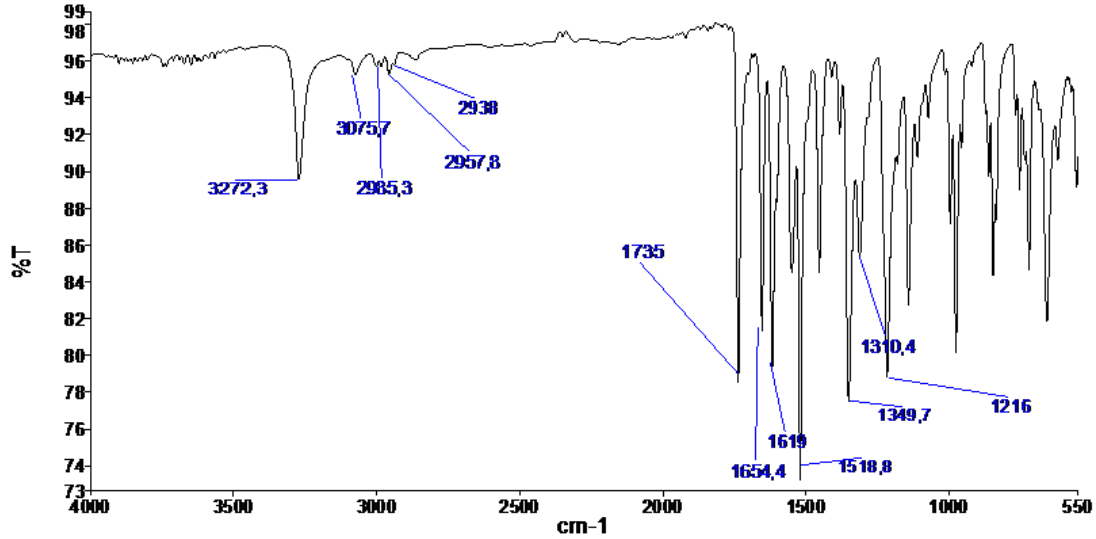

Appx. 3.9. FT-IR Spectra of 4-nitro-CA-Ala-OMe

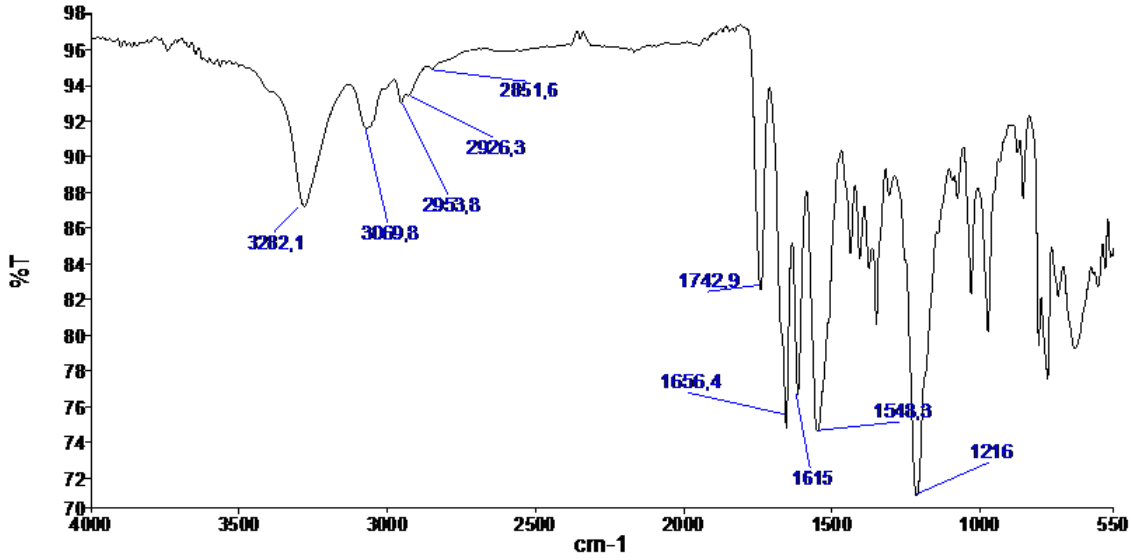

Appx. 3.10. FT-IR Spectra of Naft-CA-Gly-Gly-OMe

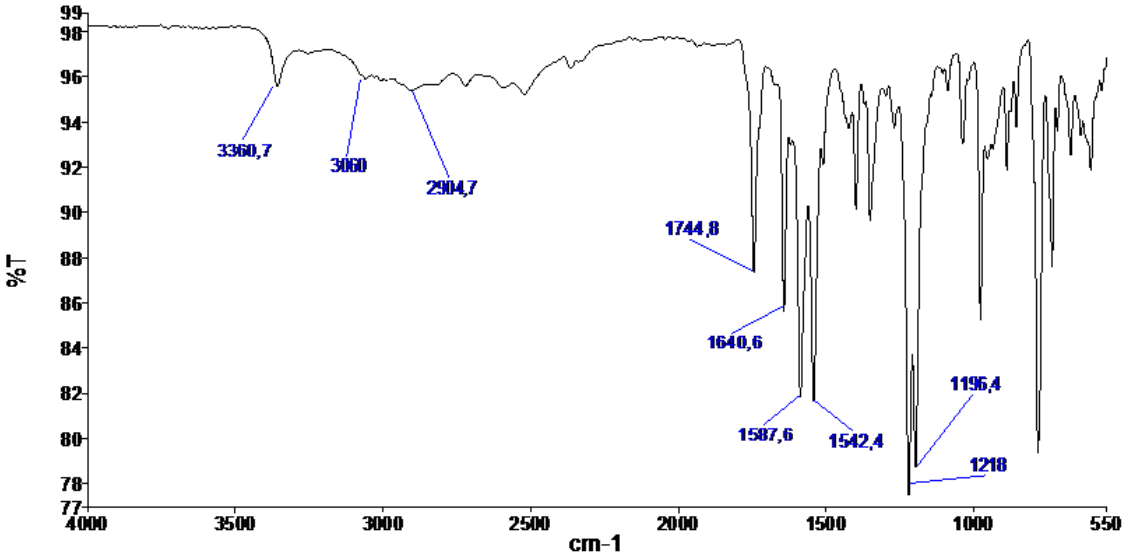

Appx. 3.11. FT-IR Spectra of Naft-CA-Gly-OH

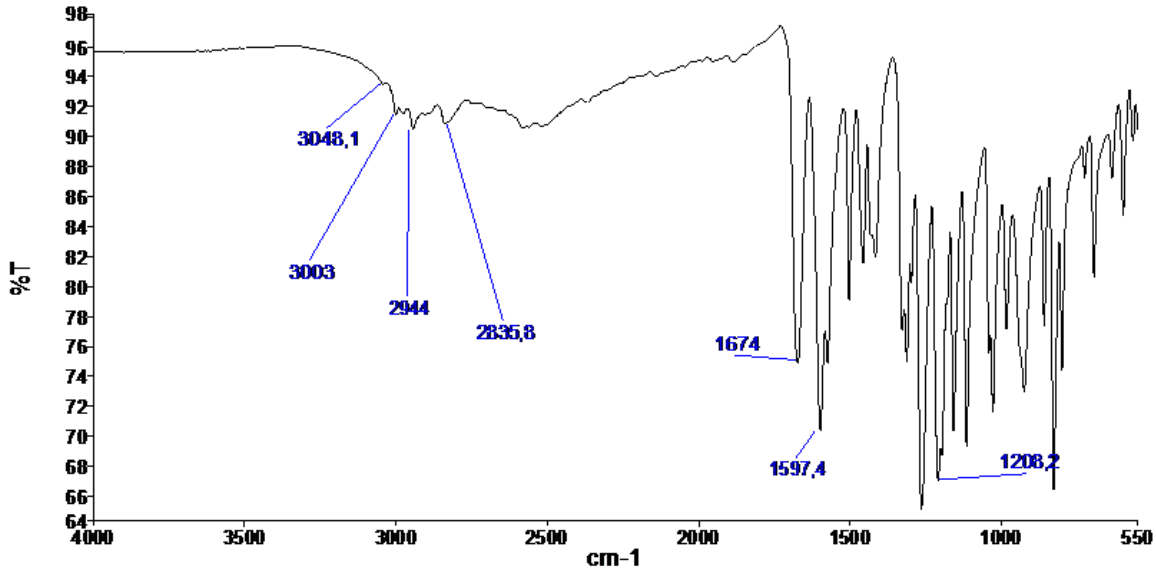

Appx. 3.12. FT-IR Spectra of Naft-CA-OH

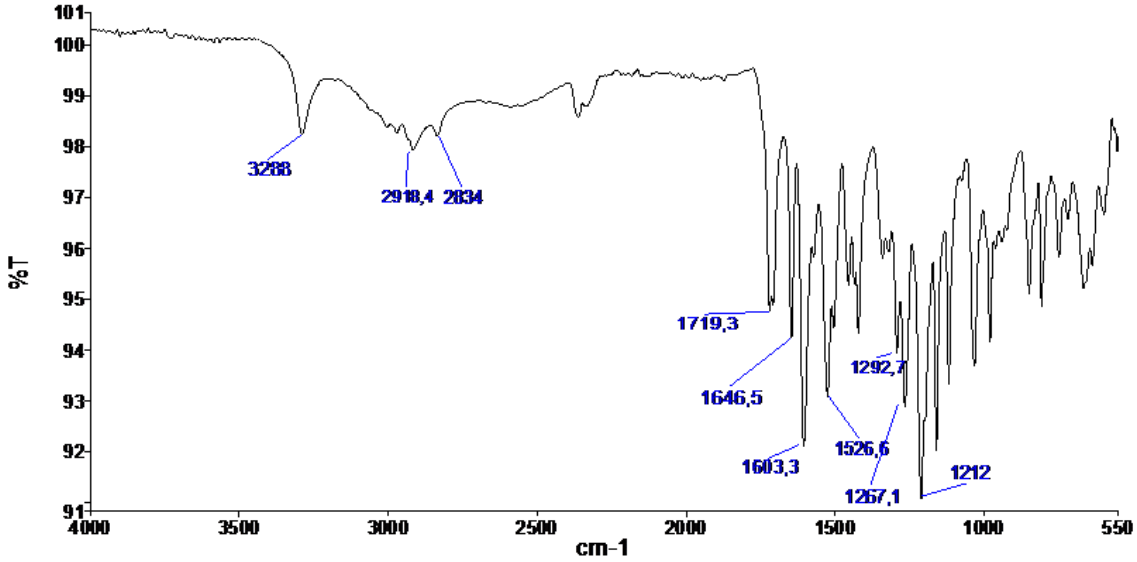

Appx. 3.13. FT-IR Spectra of 2,4-dimethoxy-CA-Meth-OH

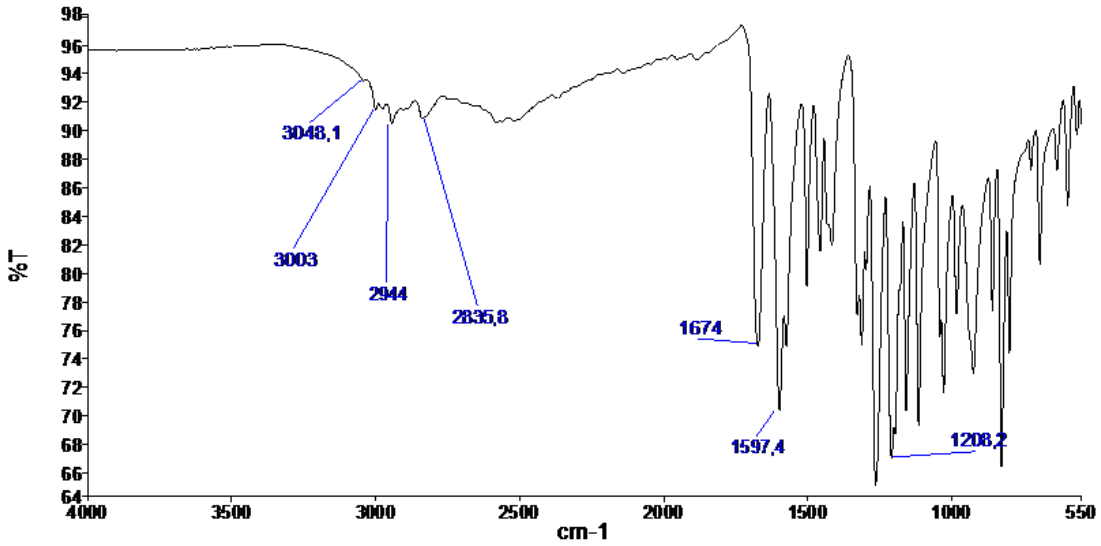

Appx. 3.14. FT-IR Spectra of 2,4-dimethoxy-CA-OH

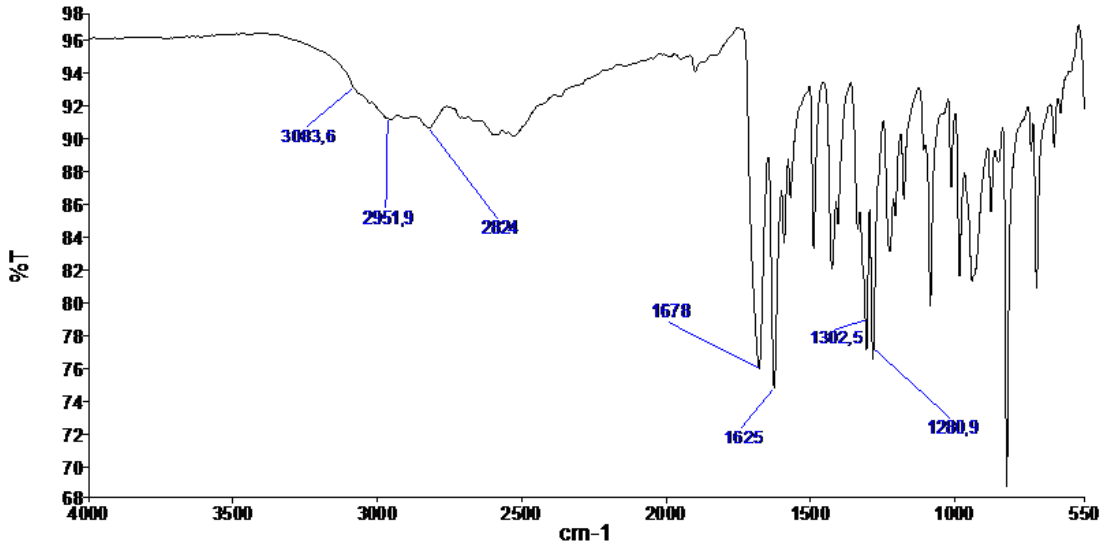

Appx. 3.15. FT-IR Spectra of 2-chloro-CA-OH

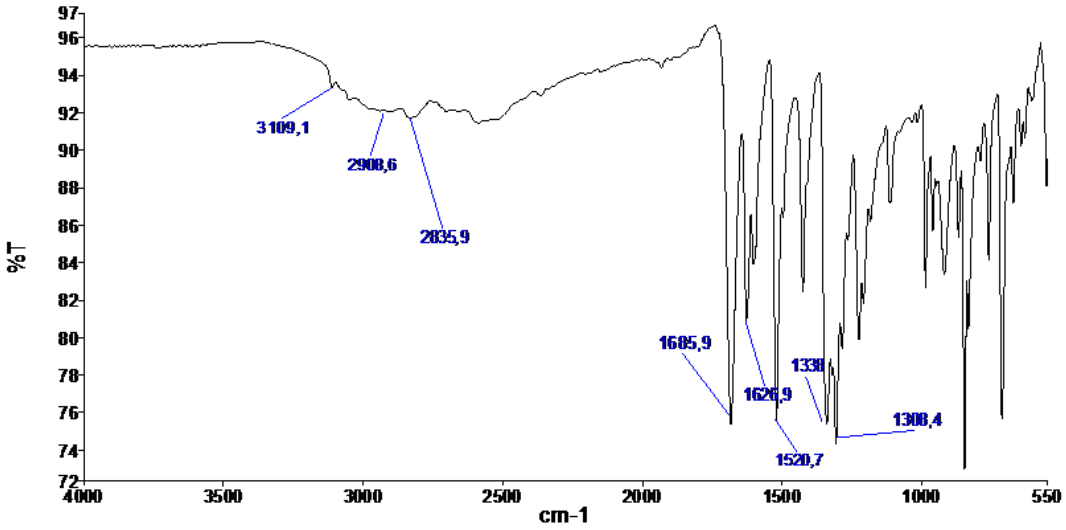

Appx. 3.16. FT-IR Spectra of 4-nitro-CA-OH

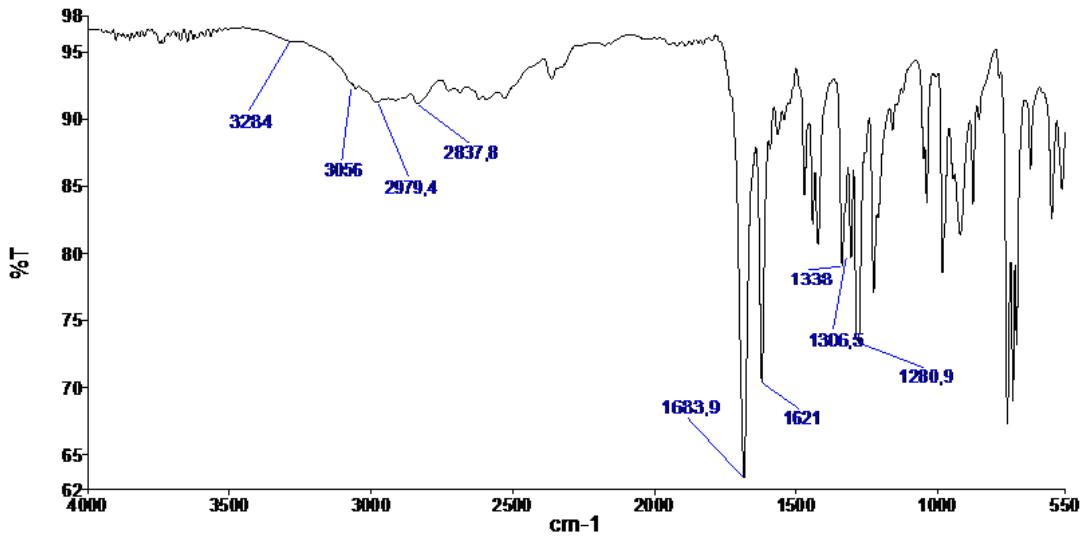

Appx. 3.17. FT-IR Spectra of 2,4,5-trimethoxy-CA-Ala-OH

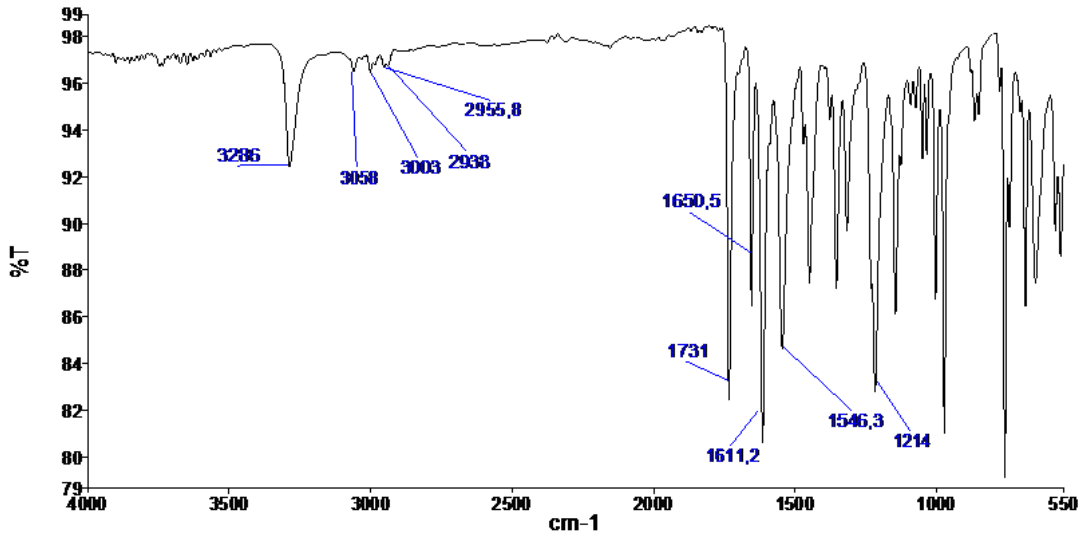

Appx. 3.18. FT-IR Spectra of 2-chloro-Ala-OMe

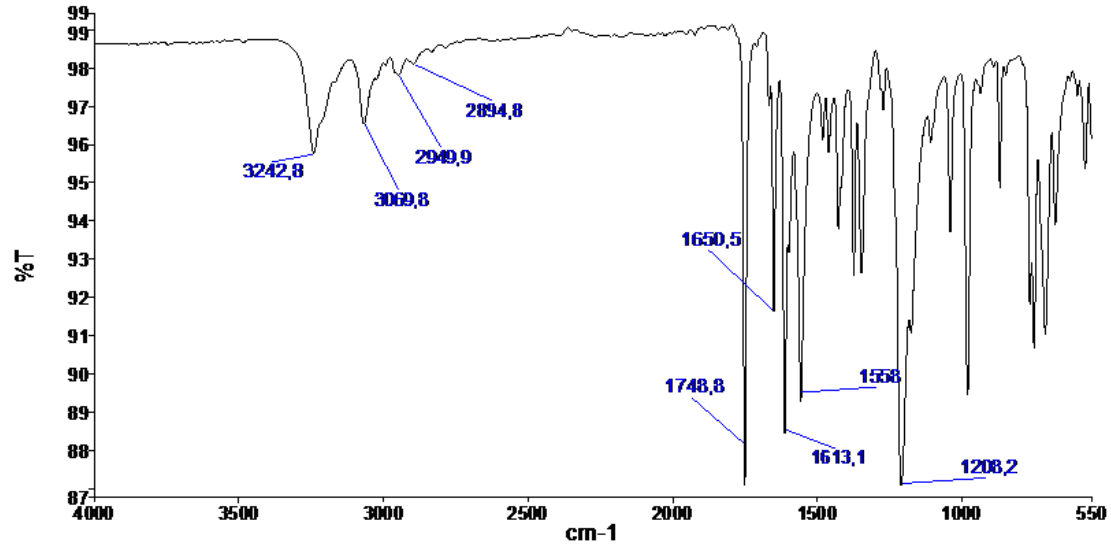

Appx. 3.19. FT-IR Spectra of Phenant-CA-Gly-OH

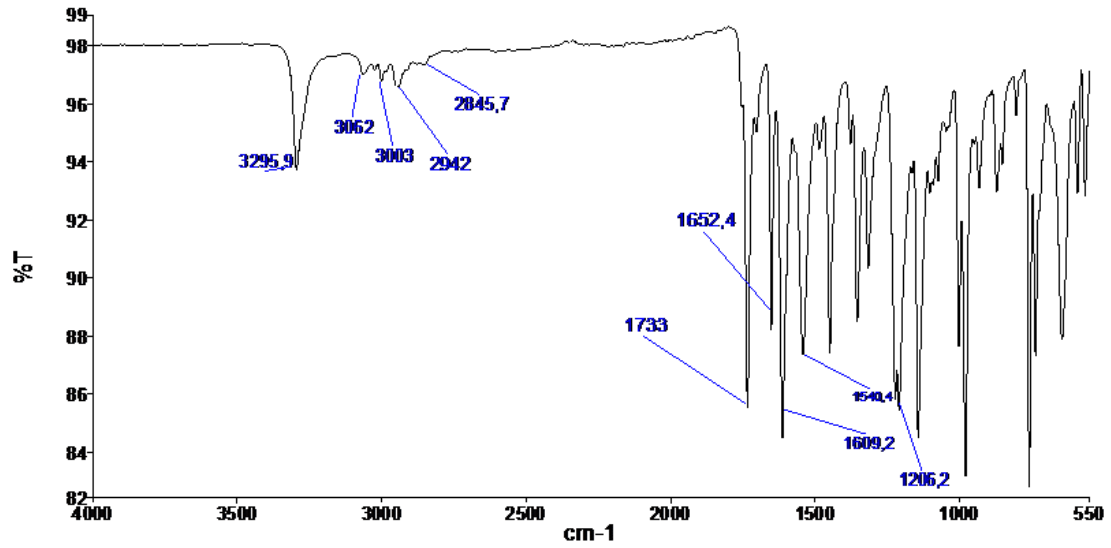

Appx. 3.20. FT-IR Spectra of 2-methyl-CA-Ala-OMe

-

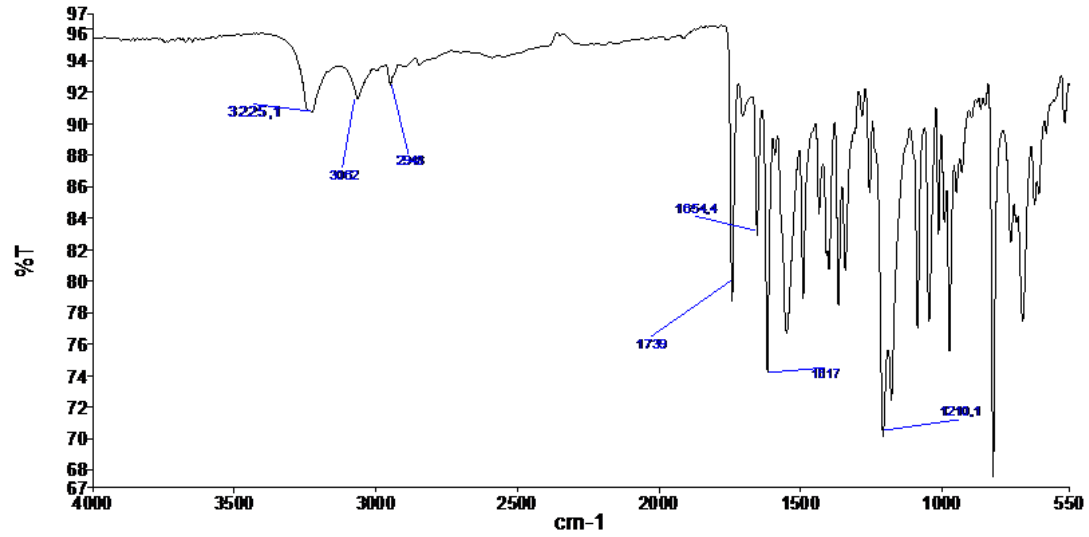

Appx. 3.21. FT-IR Spectra of 4-chloro-Gly-OMe

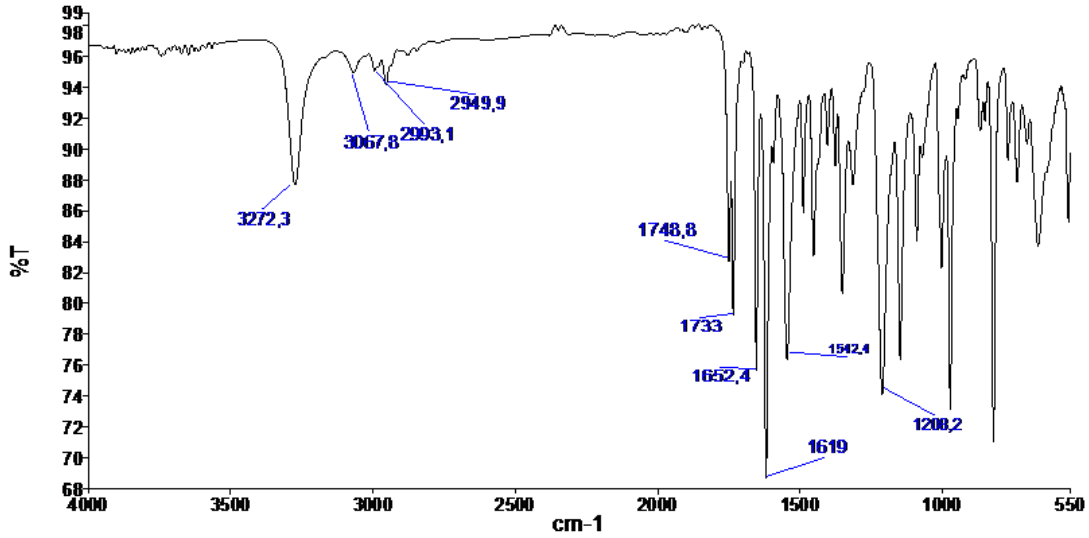

Appx. 3.22. FT-IR Spectra of 4-chloro-CA-Ala-OMe

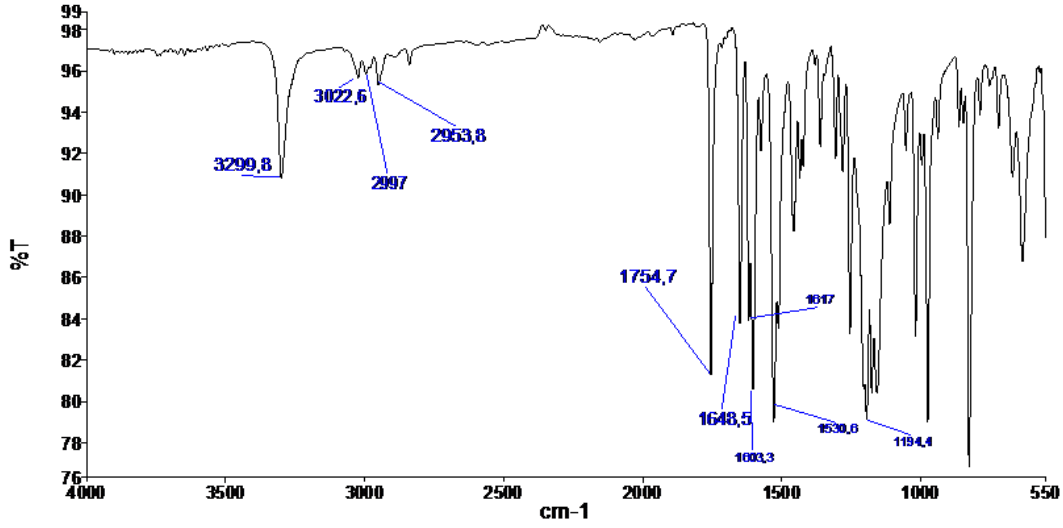

Appx. 3.22. FT-IR Spectra of 4-metoksi-CA-Ala-OMe

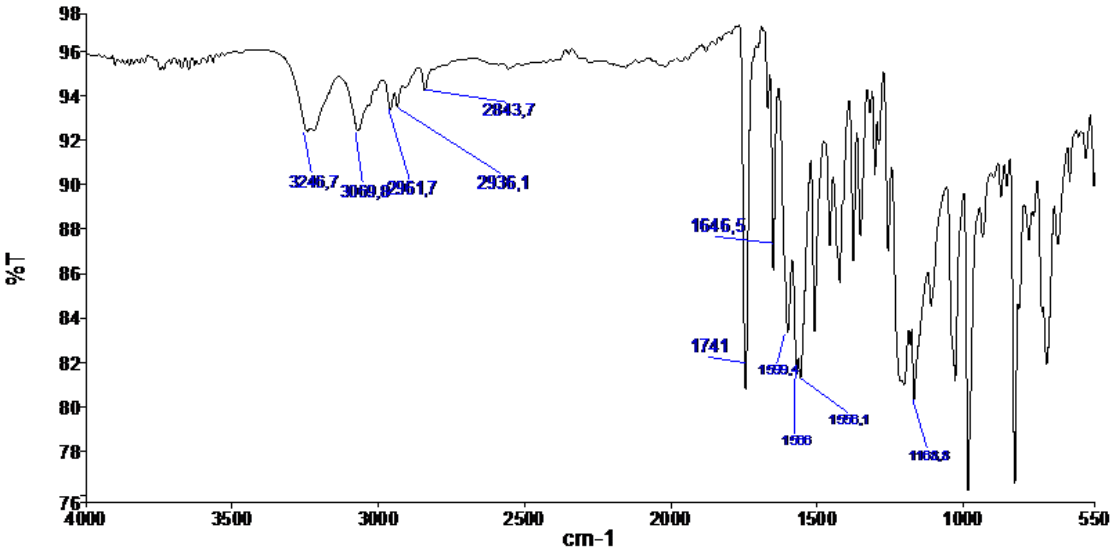

Appx. 3.23. FT-IR Spectra of 4-metoksi-CA-Gly-OMe

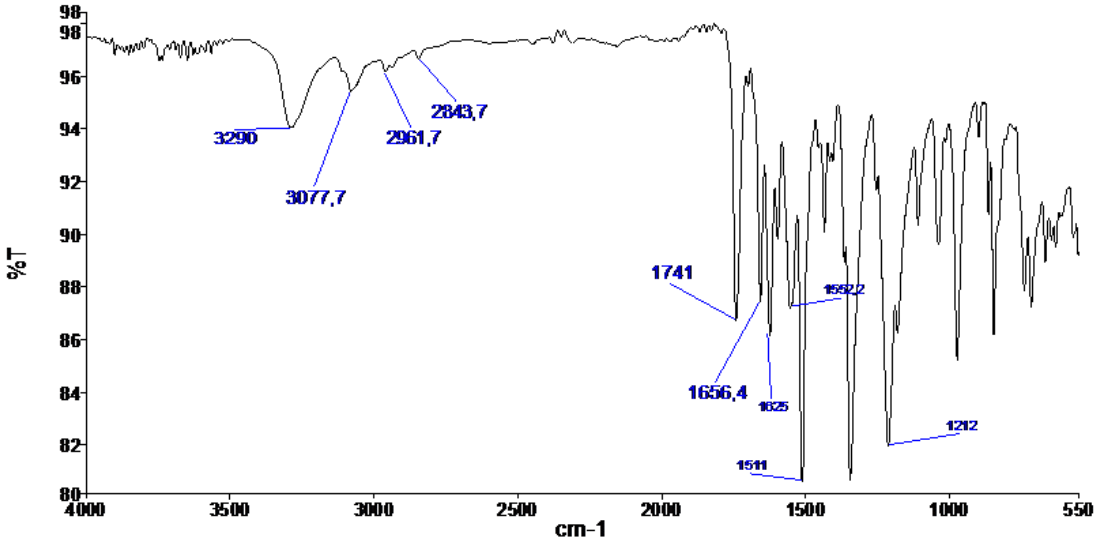

Appx. 3.24. FT-IR Spectra of 4-nitro-Gly-OMe

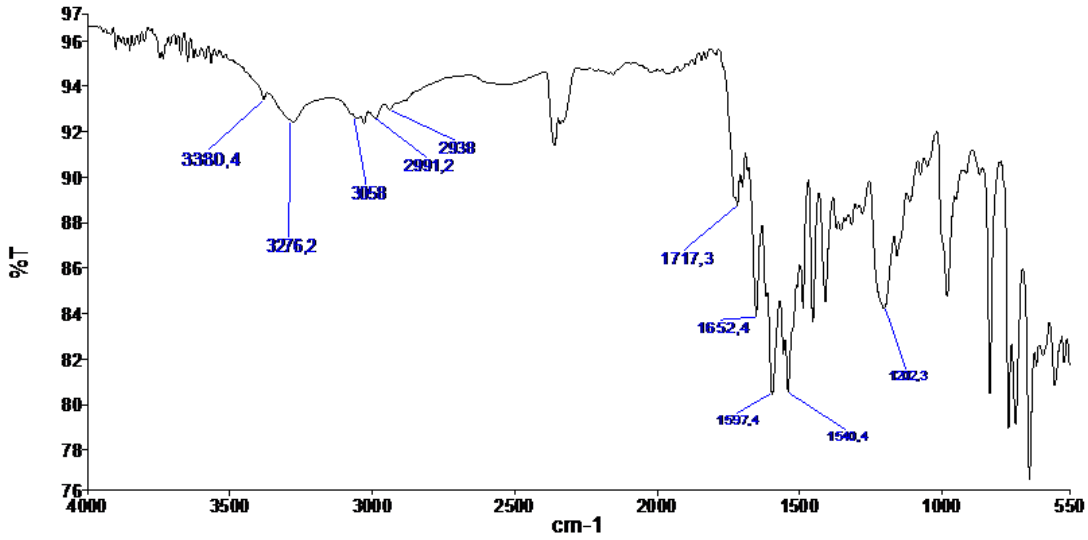

Appx. 3.25. FT-IR Spectra of Phenylbenzyl-CA-Ala-OH

CURRICULUM VITAE

He was born in May 1986 in Elazığ. He completed his primary, high and undergraduate education in Elazığ. He began his undergraduate study at Chemistry Department of Fırat University. After completion of his undergraduate education, he received a fellowship from Ministry of National Education to study abroad. He attended to American Language Program at Columbia University during 2010–2011 educational period. He was admitted to University of Florida Chemistry Department as a master student and joined Kenan Prof. Alan Roy Katritzky's research group. He got MSc degree in 2013 at University of Florida. He was accepted as a PhD student at Bingol University, Institute of Science in 2015 and he simultaneously began as a research assistant at Chemistry Department in Bingol University at 2015.